# Biofilm formation in *Candida glabrata:* the role of the Transcription Factor Tec1

**Diana Gomes Pereira**

Thesis to obtain the Master of Science Degree in

**Biotechnology**

Supervisor(s): Prof. Dr. Miguel Nobre Parreira Cacho Teixeira

## Examination committee

Chairperson: Prof. Dr. Leonilde de Fátima Morais Moreira

Supervisor: Prof. Dr. Miguel Nobre Parreira Cacho Teixeira

Members of the Committee: Dr. Dalila Madeira Nascimento Mil-Homens

**October 2018**

*"O saber não ocupa lugar"*
Avô Manuel Gomes

## Acknowledgments

First of all, I want to specially thank my supervisor **Professor Miguel Nobre Parreira Cacho Teixeira** for giving me the opportunity to develop my thesis in his research team. Thank you for all the times that you put your work aside to help me whenever I knocked your office's door, all the guidance and support made this the most delightful experience.

I also want to thank **Professor Isabel Sá Correia** for my integration in the Biological Sciences Research Group, where I loved to develop my project.

For the collaboration in the transcriptomic analysis herein accomplished, I thank **Professor Geraldine Butler** and her team, from University College of Dublin. For the supply of *Candida glabrata* mutants used in this work, I must thank **Professor Hiroji Chibana**, from University of Chiba, Japan. For the study developed in HPLC analysis of ergosterol levels, I also thank **Professor Nuno Mira** for his availability and assistance. To **Professor Arsénio Fialho, PhD Dalila Mil-Homens** and **Msc Andreia Pimenta**, I must thank the help in the adhesion assays, providing the human vaginal epithelium cells.

**MSc Mafalda Cavalheiro** and **MSc Pedro Pais,** my growth and autonomy in the laboratory relied on your crucial help, thank you for the patient and your amazing friendship.

Also to my colleagues **Raquel Califórnia**, **Susana Vagueiro**, **Rita Simões** and **Romeu Viana**, thank you for the help during the development of this work.

My **family,** specially my father **Aires Pereira** and my aunt **Natalina Gomes**, you boosted my personal fulfillment and seek of knowledge through all the most decisive moments of my life. My twin, **Inês Pereira**, I have not the gift of words like you, but I could not even find a way to describe what you mean to me. I live to be your safe harbor, but no one knows how much I need you and how much I want you to be proud of me.

A special thank you for all my **friends**, who have been the people who support me no matter what and always are behind what makes me smile. **Rute Araújo**, **Melanie Domingues**, **Tânia Ferreira, Lara Alves**, **Sofia Santos**, **Mariana Horta** and **Oumaima Daiboun**, you were particularly closer to me during this step of my life, I owe you every moment of joy.

For all of these people and for the most dedicated, amazing, beautiful, perfect, warrior, loved and missed **mother** of all time, **Adília Pereira**. This was your dream and my goal was to follow it: to study. "Her death the dividing mark: Before and After. And though it's a bleak thing to admit all these years later, still I've never met anyone who made me feel loved the way she did, (...)" The goldfinch, Donna Tartt.

This work was financially supported by Fundação para a Ciência e Tecnologia (FCT), contracts PTDC/BBB-BIO/4004/2014, PTDC/BII-BIO/28216/2017 and UID/BIO/04565/2013, and Programa Operacional Regional de Lisboa 2020, contract LISBOA-01-0145-FEDER-022231.

## Abstract

*C. glabrata* is the second most prevalent cause of human candidiasis. One of the factors underlying the successful colonization and infection by this pathogen is its ability to form resilient biofilms. It is, thus, important to understand the molecular basis behind this phenomenon, in order to guide the design of more successful therapeutic options.

The present work aimed to understand the role and the mechanisms of action of the transcription factor Tec1, encoded by ORF *CAGL0M01716g*, in biofilm formation. Phenotypic analysis showed that Tec1 is intimately involved in biofilm formation, adhesion to biotic surface and pseudohyphal growth. Subcellular localization assessment through fluorescence microscopy demonstrated that nuclear accumulation is not necessary for its activation. Motivated by these findings, the transcriptomic remodeling occurring in *C. glabrata* cells upon 24 h of biofilm formation, and the role of Tec1 in these changes, was analysed through RNA-sequencing. Tec1 was found to control roughly one third of the differentially expressed genes in biofilm cells, including genes related to adhesion, cell wall organization, ergosterol biosynthesis, carbon and nitrogen metabolism and stress and drug resistance. Specifically, Tec1 was found to control the step-wise up-regulation of the adhesin encoding genes *CgAED2*, *CgPWP5* and *CgAWP13*, occurring upon 6 h, 24 h and 48 h of biofilm formation, suggesting a particularly important role in later stages of biofilm formation. Furthermore, Tec1 was shown to indirectly regulate the decrease in ergosterol content registered in biofilm cells, when compared to those growing in planktonic cultivation. Among the identified targets of Tec1, *CgAUR1*, *CgAED2* and *CgSUR2* genes were found to play a role in biofilm formation. Finally, *in silico* analysis revealed the most likely Tec1 recognition sequences “CAATGGBA", “CAMATACA”, “CGATGSCC” and “GCGATGAS”.

Altogether, these results highlight the important role played by the transcription factor Tec1 in *C. glabrata* biofilm formation, making it a promising new target for antifungal therapeutics.



**Keywords:** *Candida glabrata*, *CgTEC1,* biofilm formation, RNA-seq

# Resumo

*C. glabrata* é a segunda causa mais prevalente de candidíase humana. Um dos fatores subjacentes ao sucesso da colonização e infeção por parte deste patógeno é a sua capacidade de formar biofilmes resilientes. É, portanto, importante entender a base molecular por trás deste fenómeno, a fim de orientar a conceção de novas opções terapêuticas mais bem-sucedidas.

O trabalho aqui apresentado destinou-se a estudar o papel e os mecanismos de ação do fator de transcrição Tec1, codificado pela ORF *CAGL0M01716g*, na formação de biofilme. Análises fenotípicas mostraram que o Tec1 está intimamente envolvido na formação de biofilme, adesão a superfícies bióticas e diferenciação de pseudohifas. A observação da localização subcelular do Tec1 feita com microscopia de fluorescência demonstrou que a acumulação no núcleo não é uma característica necessária à ativação deste fator de transcrição. Com base nestas observações, a remodelação transcriptómica que ocorre em células de *C. glabrata* após 24h de formação de biofilme, bem como o papel do Tec1 nestas alterações, foram analisadas com recurso à técnica de sequenciação de RNA. Tec1 revelou controlar cerca de um terço dos genes com expressão alterada em células crescidas em biofilme, os quais estão relacionados com adesão, organização da parede celular, biossíntese de ergosterol e resistência a stress e fármacos. Mais especificamente, o Tec1 mostrou controlar a ativação gradual dos genes *CgAED2*, *CgPWP5* e *CgAWP13*, que codificam adesinas, ao longo de 6 h, 24 h e 48 h de formação de biofilme, sugerindo um papel particularmente importante em estágios mais avançados de desenvolvimento do biofilme. Para além disso, foi demonstrado que a diminuição do conteúdo de ergosterol observada em células de biofilme, quando comparadas com células após crescimento planctónico, é indiretamente regulada pelo Tec1. Dentro dos alvos do Tec1, os genes que indicaram ser relevantes na formação de biofilme *CgAUR1*, *CgAED2* e *CgSUR2.* Por último, uma análise *in silico* revelou que as sequências de reconhecimento do Tec1 mais prováveis são "CAATGGBA", "CAMATACA", "CGATGSCC" e "GCGATGAS".

Todos estes resultados realçam o papel importante que o fator de transcrição Tec1 tem na formação de biofilme, fazendo deste um futuro alvo promissor para aplicações terapêuticas antifúngicas.



**Palavras-chave:** *Candida glabrata*, *CgTEC1*, formação de biofilme, RNA-seq

# Table of contents

# List of Tables

# List of Figures

# List of Abbreviations

**IC** - Invasive candidiasis
**ICUs** - Intensive care units
**ECM** - Extracellular matrix
**NCA** - Non-*Candida albicans*
**VVC** – Vulvovaginal candidiasis
**3D** – 3 dimensional
**EPS** - Extracellular polymeric substances
**GPI** - Glycosyl-phosphatidylinositol
**DNA** - Deoxyribonucleic acid
**eDNA** – Extracellular DNA
**TEM** - Transmission electron microscopy
**SAPs** - Secreted aspartyl proteases
**PKA** - Protein kinase A
**MAPK** - Mitogen-activated protein kinase
**YEPD** - Yeast extract peptone dextrose
**TF** – Transcription factor
**bZIP** - Basic leucine zipper domain
**ROS** - Reactive oxygen species
**bHLH** - Basic helix-loop-helix
**ORF** – Open reading frame
**ABC** - ATP-binding cassette
**MFS** - Major Facilitator Superfamily
**DHA** - drug:H+ antiporter
**GOF** - Gain-Of-Function
**SAGA** - Spt-Ada-Gcn5 acetyltransferase
**Sir** - silent information regulator
**TEA** - Transcriptional enhancer activator
**BSRG** - Biological sciences research group
**RNA** - Ribonucleic acid
**RNA-seq** – RNA-sequencing
**MMG** - Minimal growth medium
**SDB** – Sabouraud's dextrose broth
**RPMI** - Roswell Park Memorial Institute

**EDTA** - Ethylenediamine tetraacetic acid

**CFU** - Colony forming units

**TE** - Tris EDTA

**cDNA** – complementary DNA

**CGD** - Candida genome database

**SGD** - Saccharomyces genome database

**GO** - Gene ontology

**KEGG** - Kyoto gncyclopedia of genes and genomes

**DREME** - Discriminative regular expression motif elicitation

**I-TASSER** - Iterative threading ASSEmbly refinement

**RT-qPCR** - quantitative real time polymerase chain reaction

**DEPC** – diethylpyrocarbonate

**Wt** – Wild-type

**Acetyl-CoA** - acetyl coenzyme A

**PPM** - Phosphopeptidomannan

**PLM** - Phospholipomannan

**B-Mans** - β-mannosides

**MDR** – Multidrug resistance

**IPC** - Inositolphosphorylceramide

**EC** - Enzyme commission

# 1- Introduction

## 1.1- Candidiasis

Invasive fungal infections (pneumocystis, cryptococcosis, mucomycosis, candidiasis) have increased in the past few decades due to advances in the medical field and are known to affect more than 2 million people every year, being associated to up to 50% mortality rates.[1,2,3] Surprisingly, fungal infections are estimated to be more deadly worldwide than tuberculosis or malaria.[1] The host immunity and physiological condition is decisive for the development and clinical manifestation of fungal infections.[2] Immunocompromised patients are the major group of risk, comprising patients with neutropenia, pancreatitis or renal insufficiency, or also those being subjected to treatment with systemic antibiotics, glucocorticosteroids, indwelling medical devices, total parenteral nutrition or major abdominal surgery.[4]

Candidiasis covers a wide range of diseases going from more moderate clinical manifestations (esophageal or oropharyngeal candidiasis) to serious infections, including blood-stream infections and disseminated candidiasis (renal, liver abscess, lung and nervous central system).[2,5] Epidemiological studies have shown that more than 250.000 people worldwide are affected by invasive candidiasis (IC) annually, causing more than 50.000 deaths. Considering the intensive care units (ICUs), candidemia is described as the fourth most common bloodstream infection and this is considered the main manifestation of invasive candidiasis.[7] IC also comprises other severe diseases such as endocarditis, central nervous system infections, endophthalmitis, osteomyelitis and disseminated infections. Although IC is tightly related to the hospital setting and the involvement of invasive interventions and long-term antibiotic use, the community-acquired cases cannot be ignored.[5]

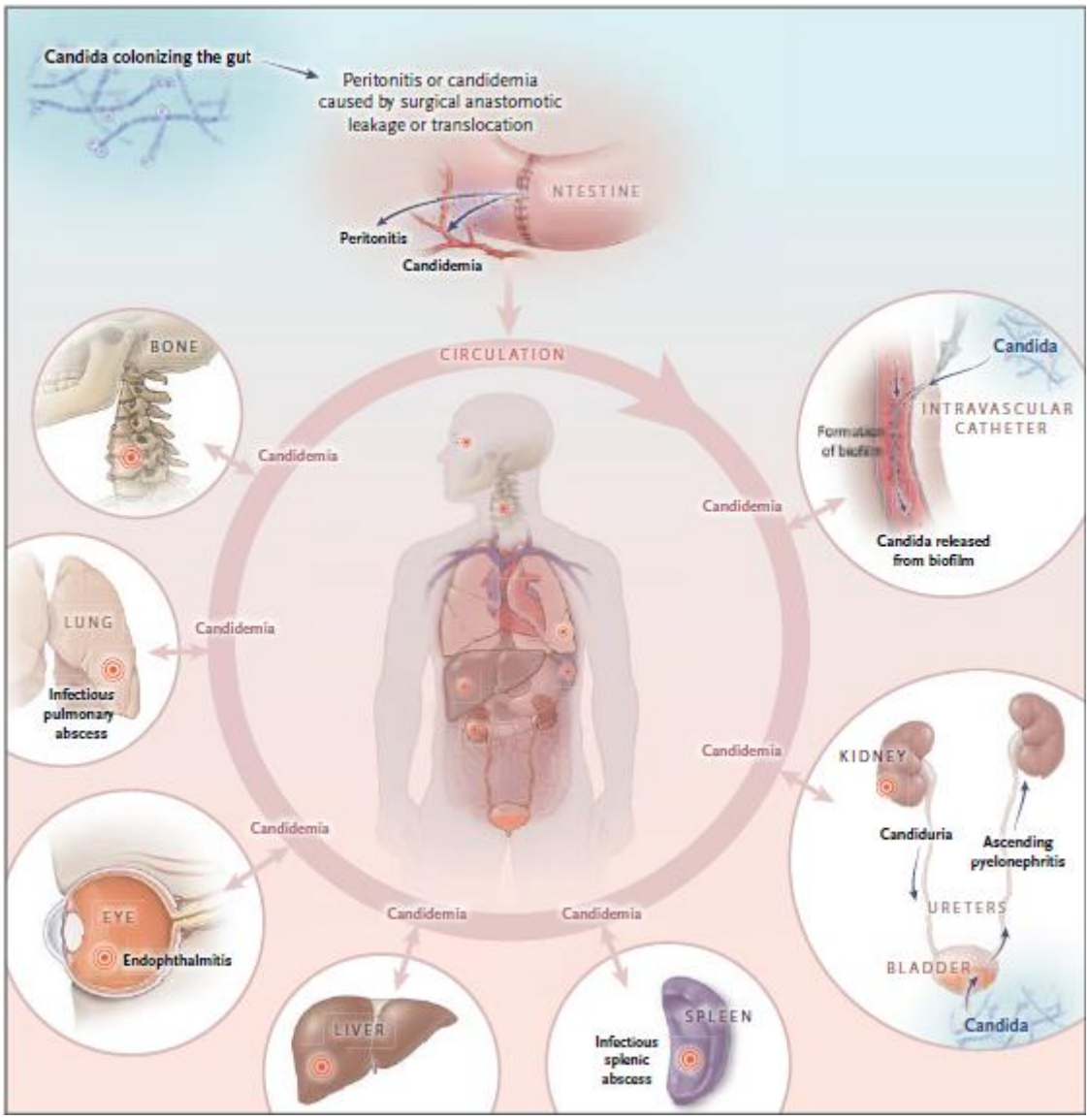


**Figure 1- Pathogenesis of Invasive Candidiasis. (from: Kullberg *et al.* (2015)[6]).**

**Figure 1** presents possible causes and consequences of IC. It could for example start from the gut colonizing *Candida* species, that may invade through translocation or anastomotic leakage after laparotomy, causing either localized, deep-seated infection as peritonitis, or candidemia. Furthermore, when candidemia originates from the gut or the skin, it can lead to the colonization of intravascular catheters in patients and form biofilms. These medical devices boost biofilm proliferation, where *Candida* spp. is most protected by the extracellular matrix (ECM) formed, resisting therapeutics.[7] These also allow the release of the fungi and cause persistent candidemia. With the development of IC, metastatic infections in various organs may be derived and lead to secondary candidemia. Additionally, the fungi in the bloodstream may also enter the urinary tract and cause candiduria.[6]

The majority of the cases of IC are caused by *Candida albicans*, nevertheless there is increasing numbers of infections worldwide caused by non-*Candida albicans* (NCA) species.[8]

## 1.2- *Candida* species

The *Candida* genus comprises over 150 heterogeneous species, but only a few of them can cause human candidiasis. The majority (65%) of *Candida* species are unable to grow at body temperature, 37°C, thus they cannot become pathogens or commensals of humans.[9] Indeed, only 16 species are currently being isolated from patients as infectious agents.[5,9] These species are *Candida albicans*, *Candida glabrata*, *Candida tropicalis*, *Candida parapsilosis*, *Candida krusei*, *Candida guilliermondii*, *Candida lusitaniae*, *Candida dubliniensis*, *Candida pelliculosa*, *Candida kefyr*, *Candida lipolytica*, *Candida famata*, *Candida inconspicua*, *Candida rugosa*, *Candida auris* and *Candida norvegensis*.[5]

*C. albicans* colonizes various regions of the human body, such as the skin, oropharynx, lower respiratory tract, gastrointestinal tract and genitourinary system. This species has been the dominating isolated pathogen, among *Candida* species, but the relative prevalence of the various species is continuously changing, half of the strains currently isolated from candidiasis patients belonging to NCA species. The relative prevalence between *Candida* species also varies considerably with the site of infection and the host.[6] For example *C. parapsilosis* is responsible for 30% of the cases of candidemia in newborns while in adults the percentage decreases to 10% - 15%; while *C. glabrata* infections occur mainly in older and neoplastic patients.[5]

### 1.2.1- *Candida glabrata*

*Candida glabrata* is taxonomically classified as a member of the Nakaseomyces phylome, being phylogenetically much closer to the baking yeast *Saccharomyces cerevisiae* than to *C. albicans*.[11] *C. glabrata* was at first placed in the *Torulopsis* genus as it lacks hyphae formation, which characterizes the *Candida* genera. However, in 1978 it was considered that this is not a definitive distinguishing factor, suggesting that *Torulopsis glabrata* should be classified in the *Candida* genus due to its growing evidence of pathogenicity in humans.[9,10] Among the yeasts of the *Candida* genus, the species *C. glabrata* displays unique features, taking as example its haploid nature, resorting exclusively to asexual reproduction (contrasting with the diploid genome of *C. albicans*). It exists as blastoconidia and are much smaller (1-4 µm) than those of *C. albicans* (4-6 µm).[9,11] Additionally, *C. glabrata* lacks genes related to galactose, phosphate, nitrogen and sulfur metabolism, and genes needed for pyridoxine biosynthesis. These inabilities are generally compensated by the mammalian host environment, that provides for example nicotinic acid, pyridoxine and thiamine.[11] A list of the main features is presented in **Table 1.**

**Table 1- Summary of general features that characterize *Candida glabrata*. (Adapted from: Rodrigues, Célia F. *et al.* (2014)9).**

| Feature | Characteristics |
|---|---|
| Ploidy | Haploid |
| Hyphae | Absent |
| Colonies on SDA | Very small/cream-color |
| Cell size | 1-4 µm |
| Growth on CHROMagar™ | White, pink/purple |
| Biochemical reactions | Ferments and assimilates glucose and trehalose |
| Virulence | Opportunistic pathogen |
| Major sites of infection | Vaginal, oral, disseminated |
| Biofilm formation | Yes |
| Major adhesins | Lectins |
| Mating genes | Present |
| Sexual cycle | Unknown |
| Clonal population structure | Yes |
| Phenotypic switching | Present |
| Auxotrophy | Niacin, thiamine, pyridoxine |
| Mitochondrial function | Petite-positive |
| Epidemiology of infection | Principally nosocomial (except vaginal)<br>(frequently mixed fungal infection)<br>Immunocompromised or debilitated host<br>Specific risk factors: prolonged hospitalization, prior antibiotic use, use of fluconazole, patient exposure, hand carriage by hospital personnel |

*C. glabrata* genome shows high similarity to *S. cerevisiae*, suggesting that these species share the same common ancestor (**Figure 2**).[9,10,12] *S. cerevisiae* is a known food and drink fermenter and it is already known that it shares some features with *C. glabrata*, such as the Flo proteins, responsible for flocculation in beer fermentations, that in *C. glabrata* are closely related to Epa proteins, known to be the main adhesins involved in pathogenesis.[10] On the other hand, *C. glabrata* and *C. albicans* are phylogenetically considerably distinct.[12]

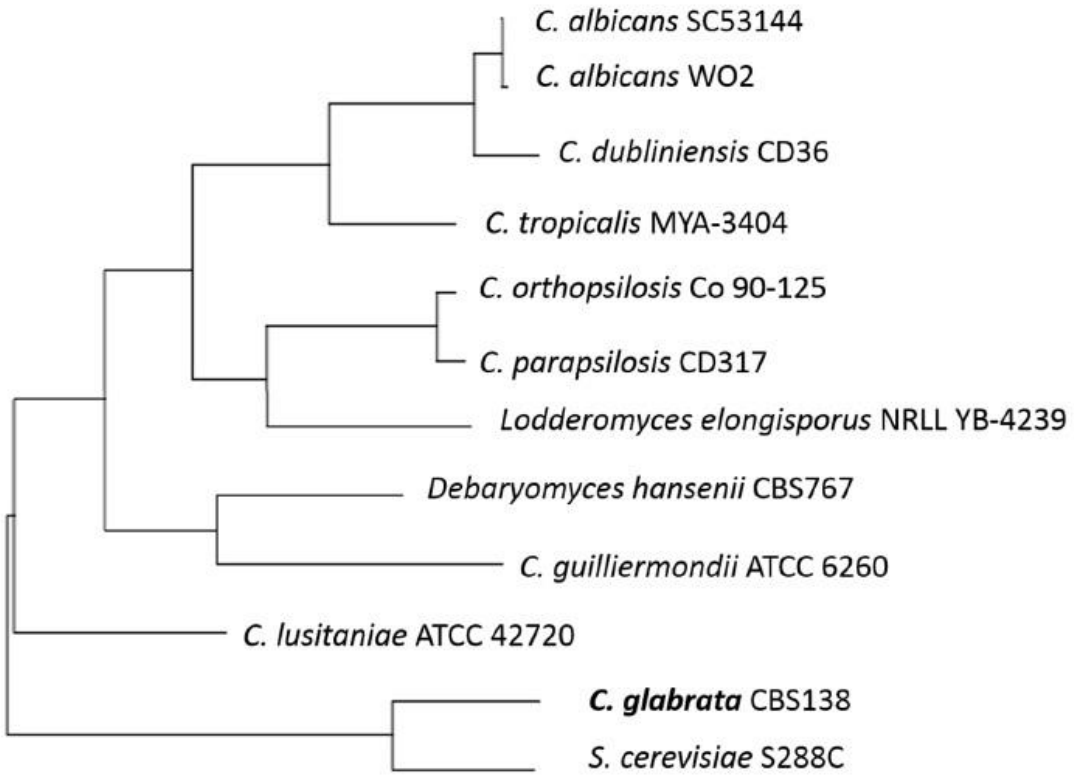


**Figure 2- The phylogenetic tree of some yeast species constructed by comparison of ERG11 sequences. (from: Tam, Phyllix, et al. (2015)[10]).**

*C. glabrata* is a commensal colonist of the intestinal tract in humans, being the second most common cause of vulvovaginal candidiasis (VVC), right next to *C. albicans*. It is also an important agent of candidemia, but due to the absence of the hyphal form, it induces a less intense neutrophil response, when comparing to *C. albicans*.[11]

The mechanisms underlying the pathogenesis of *C. glabrata* are nowadays still a field in discovery.[13] It is already known that it has the ability to survive within macrophages, to synthesize adhesins, to secret phospholipases and, additionally, to limit phagosome maturation in macrophages, thus preventing acidification and limiting hydrolytic attack.[13,14] In fact, *C. glabrata* exhibits an unusual capacity to multiply within phagocytic cells, and is reported to use macrophages as “Trojan-Horses” in order to infiltrate the host.[13] Additionally, it is highly stress tolerant and very robust, since it can not only survive on host tissues but also on inanimate surfaces for more than 5 months and this is due to its capability to form multilayered biofilms.[9,15]

Eradication of *C. glabrata* systemic infections and recurrent candidemia is currently a challenge, and this highlights the imperative need to find more promising strategies to limit biofilm formation or to eradicate mature biofilms. In line with this, there is increasing interest in understanding the transcriptional network mechanisms responsible for regulating this phenomenon, this study being

especially important for the discovery of new drug targets and further drug design in order to better treat infected patients.[16]

## 1.3- Biofilm formation in *Candida* species

Biofilms are organized 3 dimensional (3D) communities of microorganisms that may develop on both living and inert surfaces, inserted in an extracellular matrix synthesized by those microorganisms and with singular biological properties. It is known that 80% of the microorganisms live in biofilms in the environment.[17]

Human infections associated with biofilms are an increasing problem in the clinical setting, being responsible for 65% to 80% of the infections.[17,18] With new microscopy and molecular tools, many studies have reported biofilms as a major cause of persistent human infections.[18] The central significance of biofilms in the context of infections comes from the relationship of biofilms to device-associated infections.[19] Medical devices can be venous and urinary catheters, artificial joints, stents, shunts, implants, endotracheal tubes and pacemakers. The use of these devices is growing, with approximately 10 million new recipients per year.[17] After the infection, the eradication of a biofilm *in vivo* is an indubitable complicated procedure due to the administration of toxic concentrations of antimicrobials and the possible removal of the respective medical device. Besides being difficult, it is also an expensive process that is susceptible to clinical complications for the patient.[18] The study of isolates from infected patient has demonstrated that *Candida* species are among the most common colonizers of implanted devices.[19]

This phenotype has been well characterized for *C. albicans*, being described as a multifactorial process that contains four sequential steps: the first is the adhesion to a foreign surface (the host tissue or a medical device), with following cell proliferation across the substrate surface to form a discrete colony with cell organization. This is followed by the second step, in which there is secretion of extracellular polymeric substances (EPS) by the now well-organized cells. The next step comprises the consequent 3D structure development, with formation of a mature biofilm. The last step is the possible dissemination of progeny biofilm cells, which allow the cells to migrate and form spread biofilms (**Figure 3**).[20,21,22]

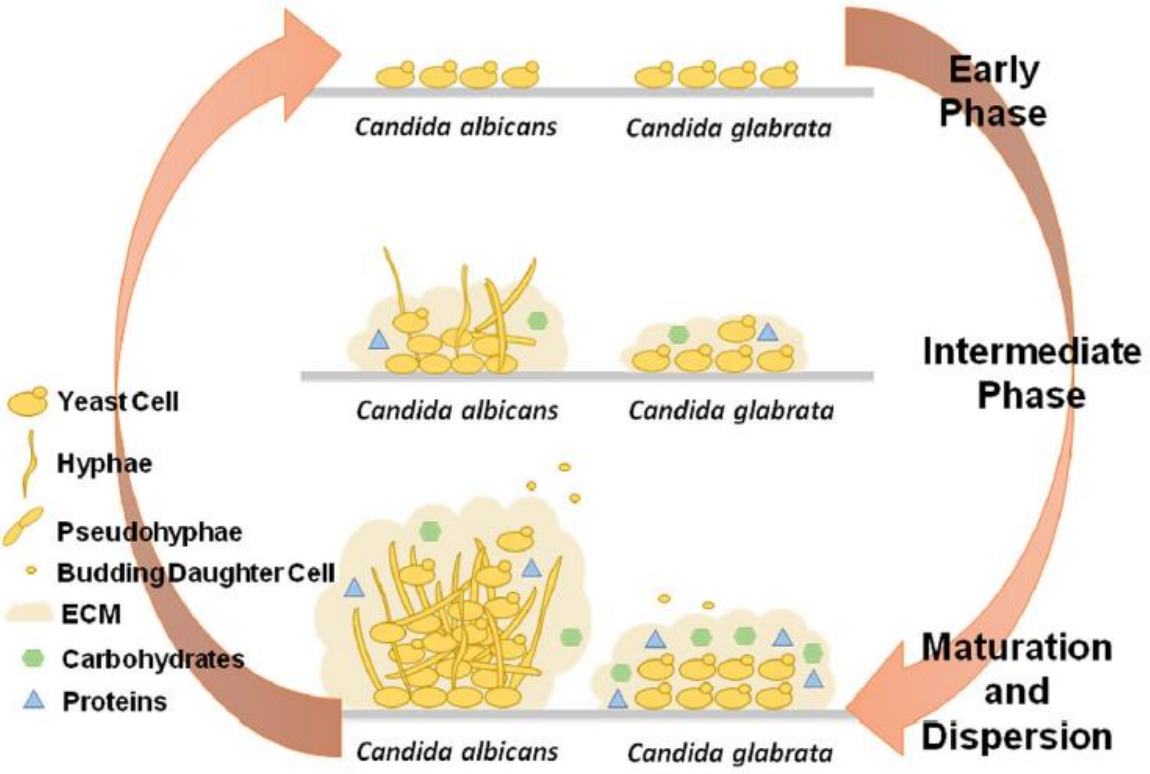


**Figure 3- Overview of the sequence of biofilm development by *Candida albicans* and *Candida glabrata*. (Adapted from: Cavalheiro, M. & Teixeira (2018)[23]).**

Naturally, there are larger numbers of studies approaching biofilm formation in *in vitro* models. *C. albicans* biofilms have been described on polymethylmethacrylate strips as having three main phases: an early phase (0 to 11 h), which is characterized by the adherence and development of blastospores into distinct microcolonies; intermediate (12 to 30 h), being distinguished by the organized biofilm cells with a structure in bilayer and production of EPS; and the maturation (30 to 72 h), in which the biofilm is composed of a dense network of yeasts, pseudohyphae and hyphae cells embedded in a thick EPS layer.[22] On the other hand, it was shown by Andes *et al*. (2004) that *Candida* biofilms' *in vivo* models follow the same sequence with some different features: the maturation phase occurs faster (24 h) and the thickness is greater.[24] Considering *C. glabrata,* the early phase was similar between *in vivo* and *in vitro* conditions, but after 24 h, *in vitro* biofilms presented a confluent layer of yeast cells while *in vivo* biofilms only exhibited patches of yeast cells aggregated. Finally, the maturation phase was observed at 48 h in serum-coated triple-lumen catheters in a rat subcutaneous model. Regarding the thickness, *C. glabrata* biofilms were found to have approximately half of the thickness of those formed by *C. albicans*.[25]

Rajendran, Ranjith, *et al*. (2016) studied particularly the impact of biofilm formation in patient mortality and reported that biofilm-forming ability was significantly associated with *C. albicans* mortality (34 of 157 patients).[26] In *C. albicans,* hyphal differentiation is a critical feature in biofilm formation, playing roles on

its structure and function, but *C. glabrata* lacks this ability, being reported to form pseudo-hyphae, but, even so, not during biofilm formation. This aspect raises the question of the mechanistic similarities and peculiarities in biofilm formation between these two species.[17]

## 1.4- The process of biofilm formation in *Candida glabrata*

Biofilm formation in *C. glabrata* enables it to survive as commensal and pathogen and tolerate the competition from other microorganisms. Hence it represents an ecological advantage for *C. glabrata*.[9] As an example, biofilm formation protects *C. glabrata* from detachment by salivary flow or by physical forces and consequent removal in denture and oral apparatus.[10]

An important initial step in the establishment of a biofilm is the adherence of yeast cells to the host epithelial tissue or to an abiotic medical device.[12,15,27] The so-called adhesins are a group of specialized cell wall proteins that enable cells to adhere to surfaces and to other cells, crucial for the development of a layered, differentiated biofilm.[21,22,27,28] The process of adhesion takes 1 to 2 hours and is, at first, mediated by non-specific interactions with the substratum and then, adhesins facilitate stronger adhesion.[22]

Adhesins are generally glycosyl-phosphatidylinositol (GPI)-cell wall proteins, comprising three domains: a hydrophobic C-terminal containing a GPI anchor addition site, which binds the adhesin to the cell wall; the N-terminal is usually composed by carbohydrates or a peptide binding domain; lastly, serine- and threonine-rich repeats that compose the larger middle domain, serving as the factor of variability between adhesins.[28,29]

In *C. glabrata*, the epithelial adhesin (Epa) family of adhesins is crucial for adhesion. The role of the Epa adhesins in *C. glabrata* is similar to that of the Als proteins in *C. albicans* biofilm formation.[9,10,28,30] The *CgEPA* family is composed of 17 to 23 genes (**Figure 4**) depending on the strain, from which the most relevant and best studied are *CgEPA1*, *CgEPA6*, and *CgEPA7*.[30,31,32] These three proteins have been reported to play roles in mediating adherence to human epithelial and endothelial cells.[31]

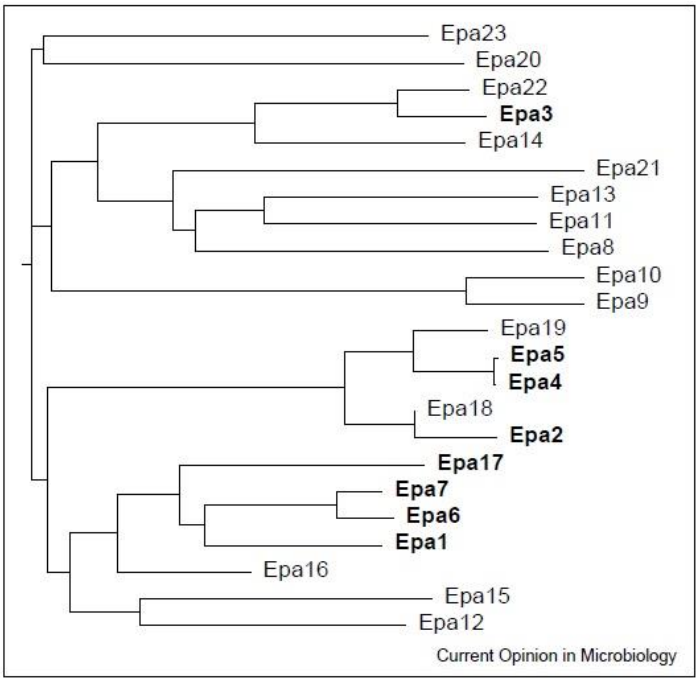


**Figure 4- Dendrogram that shows the relationships between *EPA*-related sequences in the *C. glabrata* genome. All sequences are taken from strain BG2.** The dendrogram is constructed from the amino acid sequence of the N-terminal ligand-binding domains using neighbor-joining methodology (MacVector). In bold are 8 *EPA* genes that are known to correspond to GPI-CWPs; for the others, the sequence of the full-length gene has not been completed in strain BG2. (from: Kaur, Rupinder, *et al.* (2005)[12]).

Despite recognizing a terminal galactose residue, Epa1, Epa6 and Epa7 adhesins bind to different specific glycan ligands, with Epa6 having the larger specificity range.[19] Epa1 is a $Ca^{2+}$-dependent lectin, presenting similarities with the Flo1 flocculin of *S. cerevisiae* and was shown to recognize host encoded N-acetyl-lactosamine-containing glycoconjugates and lactose.[29,33] Furthermore, a fuller picture of the ligands recognized by Epa1 was obtained by resorting to a printed slide glycan microarray containing over 260 different glycans, covalently immobilized, which revealed that this adhesin also binds to glycans with a terminal galactose residue, glucose, N-acetylgalactosamine and N-acetylglucosamine.[34] The deletion of *CgEPA1* alone was demonstrated to significantly reduce *in vitro* adherence to human epithelial cells.[29,31,32] Epa1 was also shown to govern binding to innate immune cells.[31] However, despite proof of Epa1 effective adherence, studies revealed that in murine vaginal and stomach tissues, this adhesin is not necessary for infection to occur. This may be because in these models the high affinity ligands were not exposed to the surface of host cells or the adhesion was mediated by other adhesins.[33] Epa6 is reported to be the main adhesin contributing for biofilm formation.[15] *CgEPA6* gene showed evidence of being transcribed during adherence to uroepithelial cells *in vitro* and during bladder colonization in a mouse urinary tract infection model.[27] Regarding biofilm formation, both *CgEPA6* and *CgEPA7* appear to be predominantly expressed in stationary phase cells, which are more prone to develop a biofilm, and upon biofilm formation, apart from *CgEPA1*, that is essentially expressed during the exponential phase of cell growth.[19] Another adhesin known to be involved in adhesion to epithelial

cells and biofilm formation is Epa3, since the expression of its encoding gene was found to be up-regulated in *C. glabrata* biofilm cells.[19,27] Furthermore, Epa2 was found to be related to oxidative stress response.[19]

Along with the Epa family, there are other predicted adhesins that seem to be involved in biofilm formation, associated with changes in *C. glabrata* cell wall, such as the Pwp subfamily. This family is composed of seven members that present high similarities between their N-terminal effector domain with the ones of Epa and Flo (from *S.cerevisiae*) families.[19,31] Pwp proteins have other features as lectins, being related to aggregation processes, including host binding and biofilm formation.[31] Desai *et al.* (2011) characterized the interaction of Pwp7 and Aed1 adhesins with human umbilical vein endothelial cells, coming to the observation of a significant reduction in adhesion to the host cells when compared with the wild type. Additionally, these adhesins are predominantly expressed in stationary phase of cell growth.[35] Furthermore, the expression of some *CgAWP* genes (encoding non-Epa adhesin-like cell wall proteins) was shown to be altered during adherence and biofilm formation both *in vitro* and in animal models.[19]

As already referred, after the first step of biofilm formation (adhesion), morphologic modifications then occur, together with increase in cell number and production of EPS, which are determinants of the final biofilm architecture. The multilayer composition of *C. glabrata*'s biofilm includes intimate packing of blastoconidia.[12,36] In fact, this is a much deeply studied topic in *C. albicans*, where morphological differentiation to produce hyphae plays an important role in biofilm maturation and virulence of this species.[21]

Hyphae and pseudohyphae can be distinguished by their shape, for instance, a hyphae that develops from a bastospore does not present constriction at the neck of the mother cell and have parallel sides along their entire length, as depicted in **Figure 5** (right). On the other hand, pseudohyphae displays constriction at the neck of the mother cell and the bud, as well as in every subsequent septal junction. The left side of **Figure 5** represents the cell cycles 2 to 4 of pseudohyphae, after re-inoculation of unbudded yeast cells, where the synchrony of budding in the pseudohyphal mycelium can be noted. It must be considered that the structures shown in cycles 3 and 4 are unlikely to be observed when cultured in liquid due to the shear forces that ends up fragmenting longer filaments.[37]

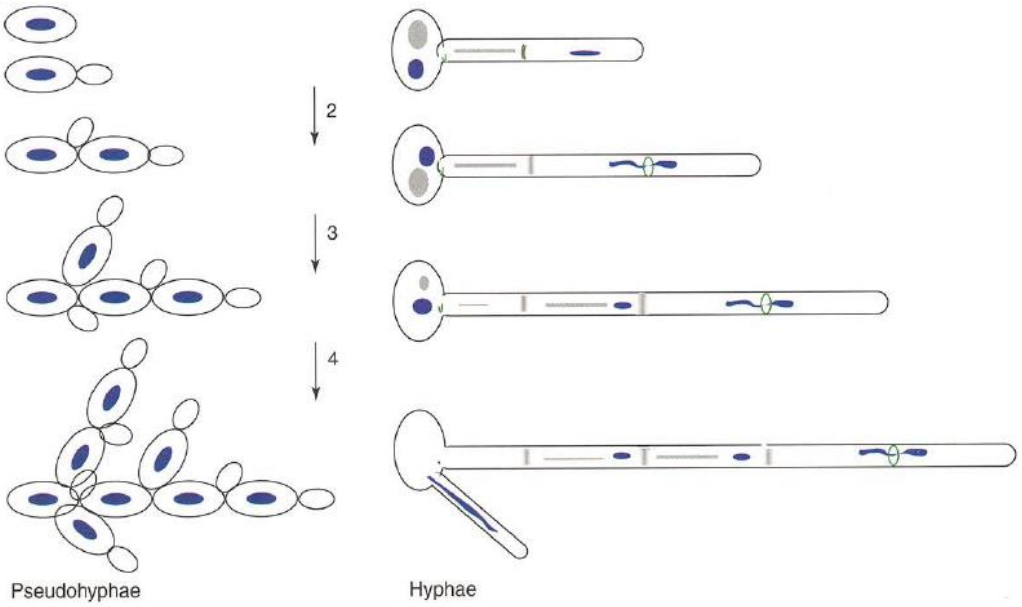


**Figure 5- Representation of the development of pseudohyphae (left) and hyphae (right). (from: Sudbery, Peter, Neil Gow, and Judith Berman (2004)[37]).**

*S. cerevisiae* can undergo the morphological change from yeast to the filamentous invasive/pseudohyphal form, when starved for nitrogen.[38] This is hypothesized to be an adaptation mechanism that allows *S. cerevisiae* to search for nutrient-rich and therefore more optimal growth substrates. In response to nutrient deprivation, both the cAMP-protein kinase A (PKA) pathway and of the mating pheromone-responsive mitogen-activated protein kinase (MAPK) cascade were shown to be required for the establishment of the pseudohyphae phenotype.[39] This phenomenon can be induced by a number of environmental signals, which include nitrogen starvation, growth on a poor nitrogen source or growth in the presence of low concentrations (0.1–1%) of fusel alcohols. Fusel alcohols, such as isoamyl alcohol, are the products of the breakdown of essential amino acids, accumulating when nutrients become limiting. This is enough to induce filamentation in yeast cells even when grown in nutrient-rich yeast extract peptone dextrose (YEPD) medium.[40]

In *C. albicans* both morphological change from yeast to hyphal or pseudohyphal growth happen in response to a wide variety of conditions, including nitrogen starvation and shifts in extracellular pH.[38] Additionally, during the establishment of a biofilm, cells use quorum sensing as intercellular communication, which is an essential mechanism of control of cell growth and dispersion. The main messenger molecules that modulate this phenomenon are tyrosol and farnesol, which play distinct roles: tyrosol acts in the initial stage of biofilm formation, promoting growth and hyphae formation; otherwise farnesol prevents the excessive growth of the biofilm and inhibits hyphal differentiation, promoting the dispersion of cells from the biofilm to other sites in the host body.[41]

In the case of *C. glabrata*, this species does indeed produce invasive pseudohyphae under nitrogen limiting conditions on solid media and it can also form invasive yeast cells on the same media supplemented with ammonium sulfate.[38] Additionally, *C. glabrata* was already observed to switch to pseudohyphal form in the host, as reported by Vandeputte *et al.* (2007), that studied a clinical isolate of *C. glabrata* with poor susceptibility to polyenes, recovered from a patient treated with amphotericin B. The cells were found to differentiate in pseudohyphae in different culture media and presented lack of ergosterol and an accumulation of late sterol intermediates, which was then related to a mutation in the *CgERG6* gene.[42]

At this stage, the key mechanism for the development of a mature biofilm is the production of the ECM.[36] The matrix is essential as it protects *Candida* cells from phagocytic cells and also acts as a barrier to drugs and toxic substances.[43] *Candida* biofilm ECM is enriched in carbohydrates and proteins, consisting primarily of exopolysaccharides, with β-glucans as the main one. These are D-glucose-based polysaccharides with different types of glycosidic bonds, that are composed by β-D-glucose units linked to form linear chains (homoglucans), which can extend both from carbon 1 to carbon 3 (β 1→3) and from carbon 1 to carbon 6 (β 1→6).[22,32,44] Formed biofilms are also dependent on the EPS that are produced in biofilm formation step 3, which give a gel-like hydrated 3D structure to the biofilm. EPS play important roles in the defense against phagocytosis, scaffold for biofilm integrity and prevention of drug diffusion.[45] The production of EPS is reported to vary according to some factors, such as species/strain, available carbon source and the flow rate of the medium.[22] Moreover, the ECM also includes extracellular deoxyribonucleic acid (eDNA). eDNA is reported as an important component of fungal and also bacterial biofilm ECMs, playing roles in structural integrity and stability through the promotion of adhesion and binding to other biopolymers. In these biofilms there are low oxygen regions that support anaerobic growth due to the extracellular matrix.[36]
Zarnowski. *et al.* (2014) studied the composition of the matrix of *C. albicans* through transmission electron microscopy (TEM) and biochemical assays, which proposed the following components: 55% of proteins, 25% of carbohydrates, 15% of lipids and 5% of noncoding DNA. This study went further by revealing that the major polysaccharide present on the matrix was a mannan-glycosyl complex. Other minor ECM components, but also important for its structure, are β-1,3-glucan and β-1,6-glucan.[46] In general *C. glabrata* biofilms present less total biomass yet relatively higher production of proteins and carbohydrates (*C. tropicalis* and *C. parapsilosis*)[47]. The production of phospholipases contributes to host cell membrane damage as they hydrolyze phospholipids into fatty acids, promoting cell damage or exposition of receptors that facilitate adherence. Compared to *C. albicans*, which is known to hold ten genes encoding for lipases, *C. glabrata* has only been found to produce two, suggesting that phospholipase production is less important to *C. glabrata*'s pathogenicity.[9,10]

After colonization on host cells, the last step of a biofilm formation cycle is the dissemination of *Candida* cells. *C. glabrata*'s invasive growth starts with the destruction of the host tissue by the secretion of

proteases, as the secreted aspartyl proteases (Saps) and phospholipases.[48] The extracellular glycosylphosphatidylinositol (GPI)-linked aspartyl proteases family (Yps proteases) also plays a role in *C. glabrata* virulence, being related to its survival within macrophages.[48,49] Besides virulence, these proteases are important for the cell wall integrity maintenance and adherence. This is due to the processing of the GPI-linked adhesin, Epa1, which results in cell wall remodeling by removal and release of GPI-anchored cell wall proteins.[49]

As mentioned above, the phenotype switching ability in *C. albicans* is considered crucial for virulence, as hyphae and pseudohyphae could allow tissue penetration during early stages of infection and boost the dissemination of the yeast cells in the bloodstream.[37] However a study conducted with *C. glabrata* reported that this species alone cannot easily invade the human vaginal-epithelium, unless there is a first colonization by *C. albicans* and tissue invasion mediated by its pseudohyphae and hyphae that would, then, allow *C. glabrata* cells to penetrate and disseminate in the bloodstream, promoting prolonged systemic infection.[50]

When comparing the metabolic activity in *C. glabrata* biofilms with other *Candida* species, *C. glabrata* displays the lowest levels, even though it has the highest number of biofilm cultivable cells.[9,10,36]. *C. glabrata* was observed to develop the thickest slim layer on acrylic resins strip when compared to other *Candida* species, including *C. albicans*. Additionally, the biofilm formation ability was also higher for *C. glabrata*.[51]

## 1.5- The complex transcriptional regulation of biofilm formation in *C. albicans* and *C. glabrata*

Biofilm formation includes several stages of development, as addressed before. This process has been viewed from the perspective of how gene expression is altered from that in free-living planktonic cells. Taking into account all different steps of biofilm formation, each one of them is tightly regulated at the molecular level. The study of these mechanisms of regulation is expected to lead to the discovery of good drug targets that would limit biofilm development in the host. However, this phenomenon is better understood in *C. albicans* than in *C. glabrata*. It is important to highlight that *C. albicans* biofilms differ considerably from *C. glabrata*'s, as it is composed by a mixed population of budding yeast and hyphae, mainly because of the formation of a sexual biofilm, while no filamentation has been yet observed in *C. glabrata* biofilms[38].

### 1.5.1- Regulation of the adhesion process

In *C. glabrata,* the regulation of the expression of many adhesins is intimately involved in biofilm formation, as already referred, being dependent on both environmental conditions and growth phase.[27] About two-thirds of the adhesin genes are located at sub-telomeric loci, that contains the coding regions of *CgEPA1-7*, which are regulated by transcriptional silencing.[12,27,31] It is interesting to note that silencing

at sub-telomeres harboring *CgEPA* genes appears to vary from cell to cell as indicated by variation in the expression of the *CgURA3* gene inserted at different location in the sub-telomeric *CgEPA1-3, CgEPA4-5* and *CgEPA6* loci.[19]

Silencing depends on many of the orthologs of the trans-acting factors that are implicated in sub-telomeric silencing in *S. cerevisiae*, including silent information regulator (Sir) Sir2, Sir3 and Sir4, Rap1 and Rif1 (involved in telomere length, which affects indirectly the sub-telomeric silencing and regulation of biofilm formation).[12,52] Sub-telomeric silencing is initiated by Rap1p binding to the telomeric repeats and subsequent recruitment of the Sir complex by protein–protein interactions, starting with Sir2 (a $NAD^+$-dependent histone deacetylase) that provides high affinity binding sites for Sir3 and Sir4.[12,29] The binding of the Sir complex to hypoacetylated histones allows for the spread of the Sir complex from the telomere itself across the sub-telomeric region.[12] *CgEPA6* and *CgEPA7* were shown to be negatively regulated by Sir4 and Rif1 and induction of these genes upon biofilm growth to be dependent on the presence of an intact sub-telomeric silencing machinery.[19,53] Furthermore, cells with silencing mutations apparently are hyper-adherent to various epithelial cell lines *in vitro*.[12] This suggests that *C. glabrata* biofilm formation requires the negative regulation of sub-telomeric silencing that in turns allows expression of the Epa6 and Epa7 adhesins.

The Yak1 kinase/Sir2-4 pathway was found to be an important intervenient in biofilm formation, similar to the role played by the orthologous pathway in the regulation of the *ScFLO* genes in *S. cerevisiae*. It was demonstrated that *CgEPA6* expression is regulated by Yak1, a kinase that controls Sir4 and Rif1-dependent sub-telomeric silencing.[15,19] Also related with regulation of adhesion is the *C. glabrata* Cst6 transcription factor (TF), a basic Leucine Zipper Domain (bZIP) domain-containing protein involved in the negative regulation of *CgEPA6*, possibly intervening in chromosome stability and telomere maintenance and its deletion limits the development of biofilm.[10,15,48] It has been proposed that Yak1 and Cst6 control *CgEPA6* expression, and consequently biofilm formation, independently.[19]

The Swi/Snf chromatin remodeling complex is yet another player in biofilm formation. Indeed, an insertion mutation near the *CgSNF6* gene was found to result in decreased biofilm formation and *CgEPA6* expression and a similar phenotype was observed upon deletion of *CgSNF2* gene encoding another component of the Swi/Snf complex. The Swi/Snf complex is involved in chromatin remodeling by destabilizing histone-DNA interactions, thereby modulating gene expression of a large number of genes in a positive or negative manner. Recruitment of the complex at specific sites is mediated by interaction with transcription activators and repressors. As the function of the Swi/Snf complex in biofilm formation is only observed when sub-telomeric silencing is intact, this complex must negatively modulate sub-telomeric silencing either through interaction with components of the silencing machinery or TFs necessary for the activation of *CgEPA6*. Interestingly, the Swi/Snf complex does not appear to impact *CgEPA1* expression.[15,19]

Both Swi/Snf and Sir complexes appear to underlie the regulation of biofilm formation and these are specific of *C. glabrata*, when compared to other *Candida* species.[23] A schematic representation of the transcriptional regulation of *CgEPA6* and *CgEPA7* genes is presented in **Figure 6**.

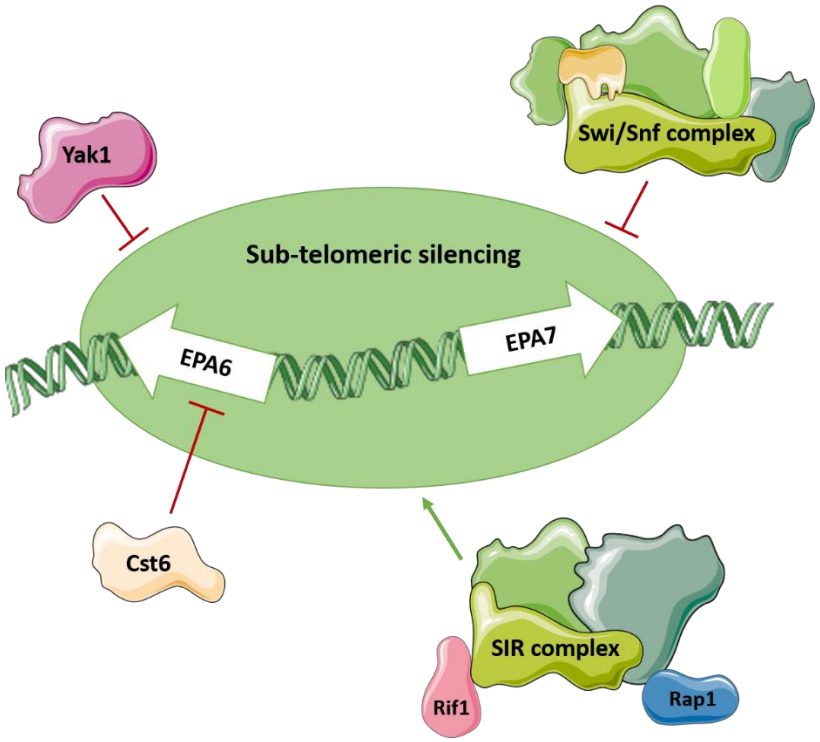


**Figure 6- *CgEPA6* and *CgEPA7* genes encoding important adhesins in *Candida glabrata*'s biofilm formation and its transcriptional regulation.**

### 1.5.2- Ability of to undergo phenotypic switching from budding yeast to pseudohyphae

In *C. albicans*, filamentous growth is a determinant feature of biofilm formation, leading to hyphal differentiation. There is a great number of TFs regulating biofilm formation that are known to be involved in filamentation, as represented in **Figure 7**, considering that hyphal differentiation occurs during biofilm development.[23] Current knowledge identifies at least five distinct signaling pathways activating hyphal development in *C. albicans*, and these are tightly controlled by an array of TFs, as the positive regulators Cph1 (also known as Acpr), Efg1, Rim101, Tec1, Cph2 and Czf1, and the negative regulators Tup1, Nrg1 and Rfg1.[54,55]

The positive regulators Efg1 and Cph1 mainly regulate cell wall and adhesion-related genes, which include *CaECE1*, *CaHYR1*, *CaHWP1,* and *CaALS3*.[16,23] This can be explained by the morphological alterations inherent to the yeast to hyphae transition that require cell wall remodeling.

One of the signaling cascades that regulate morphogenesis in *C. albicans* is the Cek1-mediated MAP kinase pathway. Cph1 is the terminal TF of this pathway, belonging to the STE-like TF family.[23,54] Cph1 TF can act as both positive or negative regulator depending on the morphological state and physiological conditions, with a feedback regulation. Moreover, this TF was reported to mediate cellular reactive oxygen species (ROS) homeostasis and control morphogenesis under stressful conditions.[55]

The ortholog of *C. albicans* Cph1 in *S. cerevisiae* and *C. glabrata* is the Ste12 TF. In haploid *S. cerevisiae* strains Ste12 - activated by a MAPK pathway - is known to regulate the response to mating pheromone and the invasive growth phenotype whereas in diploid cells it is involved in filamentous growth, in response to nitrogen starvation.[56]

Ste12 in *C. glabrata* plays a role in the regulation of filamentation induced by nitrogen starvation as well.[23,56] Moreover, a study that used a murine model of *C. glabrata* systemic infection demonstrated that *Δste12* mutants show attenuated virulence when compared to *CgSTE12* reconstituted strains.[56] This TF plays an important role in cell wall structural components, regulating negatively the expression of *CgTIP1* and *CgCIS3* genes, which encode structural components of the cell wall in *C. glabrata* and *S. cerevisiae*.[10]

Cph1 may act together with the TF Efg1 in regulating morphogenesis in *C. albicans*. Efg1 is a basic helix-loop-helix (bHLH) TF that is crucial for Ras-cAMP signaling pathway regulation, in response to nutrient deprivation or serum.[55] Efg1 not only regulates the yeast-to-hyphae transition but is also required for the generation of chlamydospores and determination of cell shape during white-opaque switching.[57] Both the double *Δefg1Δcph1* and the *Δefg1 C. albicans* deletion mutants display severe morphological defects *in vitro* and can only grew to form a monolayer of adherent elongated cells.[23,54] Additionally, the *Δefg1Δcph1* displayed highly attenuated virulence in a mouse model systemic infection, which was related to the inactivation of both Ras-cAMP and MAP kinase pathways.[54]

Efg1 has two homologs in *C. glabrata*, encoded by the *CAGL0L01771g* and *CAGL0M07634g* open reading frame (ORF), however these remain uncharacterized.[23] Together with Efg1, Efh1 regulates genes known to be involved in filamentation.[57]

### 1.5.3- Production of extracellular polymeric substances

Transcriptional regulators involved in biofilm matrix biogenesis in *C. albicans* include Rlm1 and Zap1 (also known as Csr1). Deletion of *CaRLM1* gene results in reduced matrix formation, potentially through downregulation of the Gsc1 β-1,3-glucan synthase subunit, which catalyzes the formation of β-1,3-glucan.[58] Csr1 regulates adhesion and ECM development in *C. albicans* biofilms. Deletion of *CaCSR1* leads to increased matrix formation, which can be explained by the negative control of β-1,3-glucan present in the matrix by this TF, potentially through downregulation of *CaGCA1,* Ca*GCA2* and *CaADH5* genes, related to the conversion of long-chain polysaccharides into smaller-chain polysaccharides, and upregulation of *CaCSH1* and *CaIFD6*. Moreover, the deletion of the genes *CaALG11, CaMNN4-4, CaMNN9, CaMNN1, CaPMR1, CaVAN1* and Ca*VRG4* involved in mannan synthesis, *CaBIG1* and *CaKRE5* involved in β-1,6-glucan synthesis, and *CaGSC1* involved in β-1,3-glucan synthesis was shown to negatively impact matrix synthesis. Additionally, Csr1 has also been related to the control of filamentous growth.[51,56]

*C. glabrata* carries a Csr1 homologue, Zap1, that remains uncharacterized.

### 1.5.4- Additional biofilm-related transcription factors

Schwarzmuller *et al*. (2014) studied biofilm formation adopting a large-scale reverse genetics approach with 619 *C. glabrata* deletion mutants. The TF Ace2 was found to decrease significantly *C. glabrata*'s virulence, being known to regulate genes involved in cell separation and biofilm formation processes, such as *CgCTS1*, *CgEGT2*, *CgTAL1* and *CgTDH3* genes.[16] Moreover, Ace2 mutants showed to be hypervirulent in a murine model of candidiasis, causing much earlier mortality, comparing with the wild-type. This demonstrates that Ace2 plays a critical role in mediating the host-*Candida* interaction.[59] In *C. albicans,* an Ace2 TF was also found, conserving the C2H2 zinc finger domain.[16] It has been shown to be required for biofilm formation in normoxia conditions[60] and filamentous growth under hypoxic conditions.[61]

Interestingly, the lack of Mig1 (a TF mediating glucose repression) results in increased biofilm development in *C. glabrata*. It is tempting to speculate that nutrient deprivation may to some extent favor biofilm formation, in line with the idea that this process constitutes a mean for this species to survive hostile environments.[19]

Lastly, deletion of the *CgMED12*, *CgMED13* and *CgMED15* genes encoding components of the Mediator complex has been shown to lead to increased biofilm formation.[62] The Mediator complex connects specific transcription regulators and the general TFs. Specifically, Med15 (Gal11) is a component of the tail domain of Mediator involved in the interaction with several TFs while Med12 (Ssn8) and Med13 (Ssn2) are components of the kinase module. When this kinase module is lacking, it can provoke positive and negative effects on expression of genes induced by nutrient deprivation, which may explain the associated increase in biofilm formation in *C. glabrata,* as discussed above.[19]

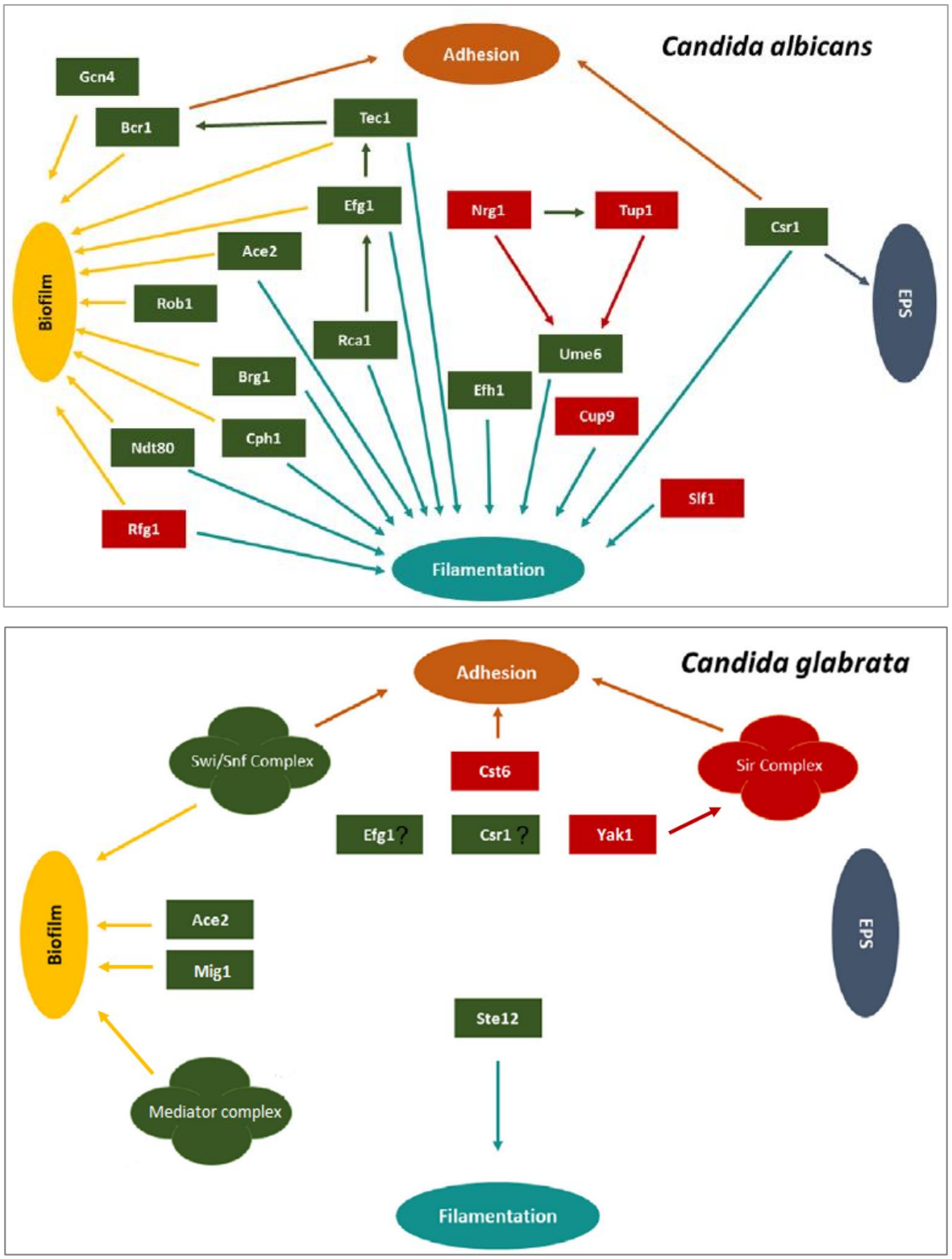


**Figure 7- Transcription factors described to be involved in biofilm formation processes and its' regulatory networks, highlighting the difference between the current knowledge in *Candida albicans* (up image) and *Candida glabrata* species (down image).** Green boxes indicate activators and red boxes indicate repressors. Participation of each transcription factor in these processes is indicated by the colored arrows: brown arrows correspond to adhesion, dark blue arrows correspond to EPS, light blue arrows correspond to filamentation, and yellow arrows correspond to biofilm formation. (from: Cavalheiro, M. & Teixeira (2018)[23]).

### 1.5.5- Biofilm formation boosts antifungal resistance

Currently, there are efforts to decrease the mortality associated with *Candida* species, namely through prophylactic or empirical antifungal treatments administered to ICU patients without documented candidiasis. This has boosted the use of antifungal drugs, as triazoles and echinocandins, leading to an increase in the selective pressure for drug resistant strains. However, cases of therapeutic failure are expanding due to resistance to these drugs, which is alarming considering the limited number of drug classes, that target different fungal components, available for clinical use.[22] The major classes of antifungals used are azoles, echinocandins and polyenes, which are categorized based on their mechanism of action on the yeast pathogen. Cells grown as biofilm exhibit typically lower susceptibility to antimicrobial agents, when compared to planktonic cells, and this is also the case with *C. glabrata.*[10] The biofilm structure results in resistant cells to one or several antifungals. Different mechanisms of resistance vary among drugs, typically because of the mode of action of each class of antifungal. Azoles are known to have fungistatic activity, targeting the ergosterol biosynthetic pathway, by binding to the Cyp51 family of cytochrome P450, the 14-α sterol demethylases that are encoded by *CgERG11* leading to changes in membrane fluidity.[20,32] The polyenes bind to the membrane ergosterol provoking transmembrane aggregates and pores, which lead to osmotic imbalance. Finally the echinocandins target the cell wall synthesis by inhibiting β-1,3-glucan synthesis, interfering with cell wall integrity.[32] Biofilm drug resistance in *C. glabrata* holds various general mechanisms, such as the up-regulation of efflux pumps, changes in cell wall composition, presence of an extracellular matrix, adhesion and activation of stress response genes.

Drug extrusion mediated by membrane transporters has been strongly associated with both ATP-binding cassette (ABC) and Major Facilitator Superfamily (MFS) transporters, playing a determinant role in cellular drug resistance. Overexpression of the efflux pump genes *CgCDR1*, *CgCDR2* and *CgTPO1_2*, encoding multidrug resistance transporters, as well as the multidrug resistance zinc cluster-containing TF, encoded by the gene *CgPDR1*, have been observed in *C. glabrata* biofilms, and are thought to be one of the key causes of antifungal drug resistance in biofilm cells during early-phase of biofilm development.[63,64] Tpo1_2 is a drug:H+ antiporter (DHA) belonging to the MFS that is not only related to antifungal resistance, but is also necessary for the normal expression of *CgALS1*, *CgEAP1* and *CgEPA1* genes involved in adhesion.[13,65]

Fluconazole resistance in *C. glabrata* is thought to be almost exclusively caused by Gain-Of-Function (GOF) mutations in the *CgPDR1* gene, resulting in upregulation of the ABC transporter genes *CgCDR1, CgPDH1*, and *CgSNQ2* responsible for increased fluconazole efflux.[66] Recent studies have provided new insights into the regulation of Pdr1. Site-directed mutagenesis of Pdr1 binding sites in the *CgPDR1* promoter demonstrated that autoregulation of *CgPDR1* is required for its normal function.[64] Moreover, Jjj1 was shown to be a negative regulator of fluconazole resistance in *C. glabrata* acting through

inhibition of the TF Pdr1, which turns into a decreased expression of the ABC transporter gene *CgCDR1*.[66]

Studies have shown that in early-phase biofilms, efflux pumps contributed to antifungal resistance, as mentioned above, while in intermediate and mature phase biofilms azole resistance was associated with changes in the levels of ergosterol biosynthesis intermediates.[20,22] Taking the target of azole molecules, it is expected that the genes involved in ergosterol biosynthesis are up-regulated upon its presence. These include *CgERG1, CgERG3, CgERG6, CgERG7, CgERG9* and especially Cg*ERG11*, whose product is the direct target of azole drugs and converts lanosterol into 4,4-dimethylcolesta-8,14,24-trienol, as can be seen in **Figure 8**.[9] Depletion of the ergosterol content in a *CgERG1* mutant was shown to increase the levels of susceptibility to azoles and further complementation of the *CgERG1* mutation restored drug sensitivity to wild-type levels.[67] Additionally, Ada2, a component of the Spt-Ada-Gcn5 acetyltransferase (SAGA) complex, appears to mediate antifungal drug tolerance and cell wall integrity through the control of its downstream target *CgERG6*, that encodes a C24 sterol methyltransferase involved in ergosterol biosynthesis, as its deletion increases echinocandin susceptibility similar to *CgADA2* mutants.[48]

It was shown that progression of drug resistance in *Candida* biofilms was associated with parallel increase in metabolic activity of the developing biofilm. This observation came to confirm that increased drug resistance is not because of lower metabolic activity of cells in maturing biofilms, but is more related to the maturation process.[22] By isolation of membrane sterols from biofilms and analysis through gas liquid chromatography, it was shown that ergosterol levels of biofilms grown to the intermediate and mature phases were reduced by 41% and 50%, respectively, in *C. glabrata* when compared to *C. albicans.* During *C. albicans* biofilm formation the levels of sterols is modulated, contributing to drug resistance in a phase-specific manner.[20]

A developed biofilm is also implicated in prevention of antifungal drug penetration through formation of the ECM, which acts as a diffusion barrier.[32] β-1,3-glucans are present in *C. glabrata* matrices, similarly to *C. albicans,* functioning to secure biofilm cells to a surface and enabling the development of antifungal drug resistance.[68] The expression of various genes associated with matrix production (*CgBGL2*, *CgXOG1*, *CgFKS1*, *CgFKS2*, *CgGAS2*, *CgKNH1*, *CgUGP1* and *CgMNN2*) was analyzed in presence of fluconazole, amphotericin B, caspofungin, or micafungin. Among these, *CgBGL2*, *CgXOG1*, *CgGAS2* genes, related to production of β-1,3-glucans, showed the highest expression levels induced by micafungin.[68] There is also evidence that β-1,3-glucans can bind specifically to amphotericin B, giving the biofilm the ability to sequester this drug.[32]

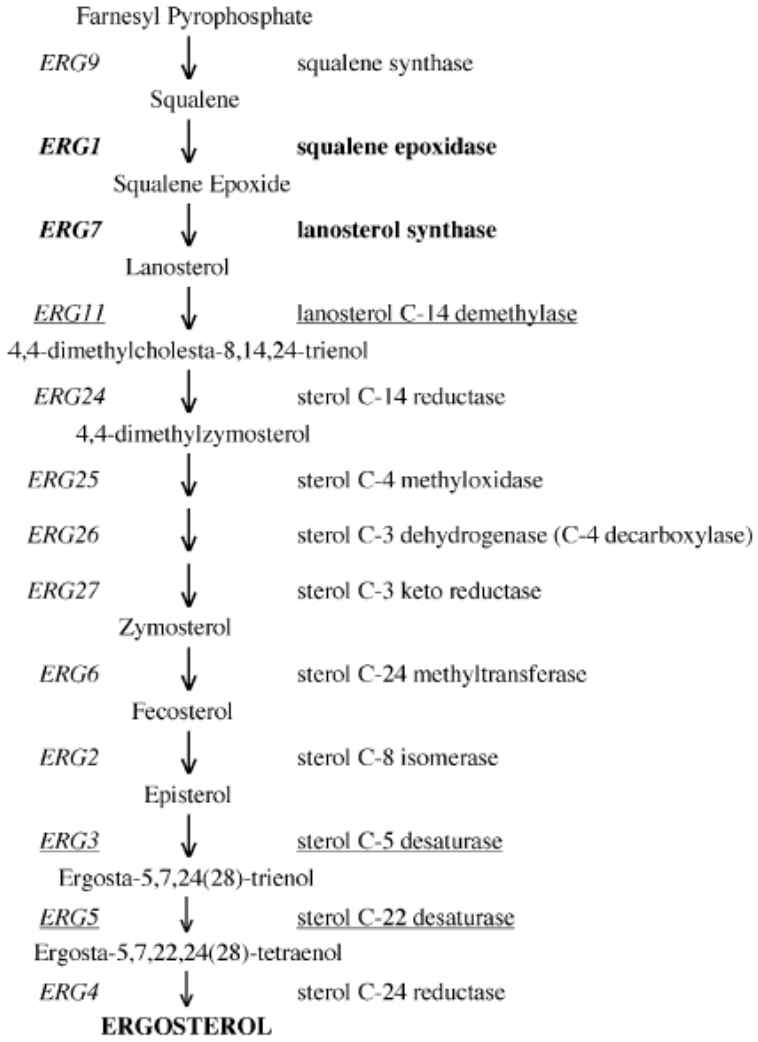


**Figure 8- The ergosterol biosynthetic pathway. (from M. Brad *et al.* (2005)[69]).**

Other specific genes up-regulated during biofilm formation are also important in stress response: peroxisomal catalase (*CgCTA1*), tyrosine biosynthetic genes (*CgARO*), the muscle creatine kinase (*Cg*MSK), the heat shock protein 90 (*CgHSP90*), the sphingolipid biosynthesis genes (*CgSKN1* and *CgKRE1*), SIR and telomere-binding protein (RIF), both involved in telomeric silencing, and the ECM regulators: zinc regulated genes (*ZAP1*), g-carbonic anhydrase (*CgGCAL1*), alcohol dehydrogenase (*CgADH5*), and also cell surface hydrophobicity (*CgCSH1*).[32] Some of these alterations were linked to modifications in the structure of *C. glabrata* biofilms by creating cell clusters, which could be a possible mechanism of biofilm tolerance to the antifungal fluconazole.[32,70]

## 1.6- The predicted role of the Tec1 transcription factors in biofilm formation

Biofilm formation is a highly regulated phenomenon, where various TFs play an important role in activating biofilm-related genes as well as interacting with other TFs, as a complex regulatory network. Nobile *et al.* carried out a study with a collection of *C. albicans* deletion mutants where nine regulators were identified as essential for biofilm development both *in vitro* on polystyrene plates and on silicone squares, and *in vivo* in rat catheter and denture models: Bcr1, Brg1, Efg1, Flo8, Gal4, Ndt80, Rob1, Rfx2 and Tec1. All these mutants were shown to form defective biofilms. Resorting to chromatin Immunoprecipitation assays it was possible to conclude that these regulators form a transcriptional network (**Figure 9**), affecting the expression of each other, along with approximately 1000 target genes.[43,58,71]

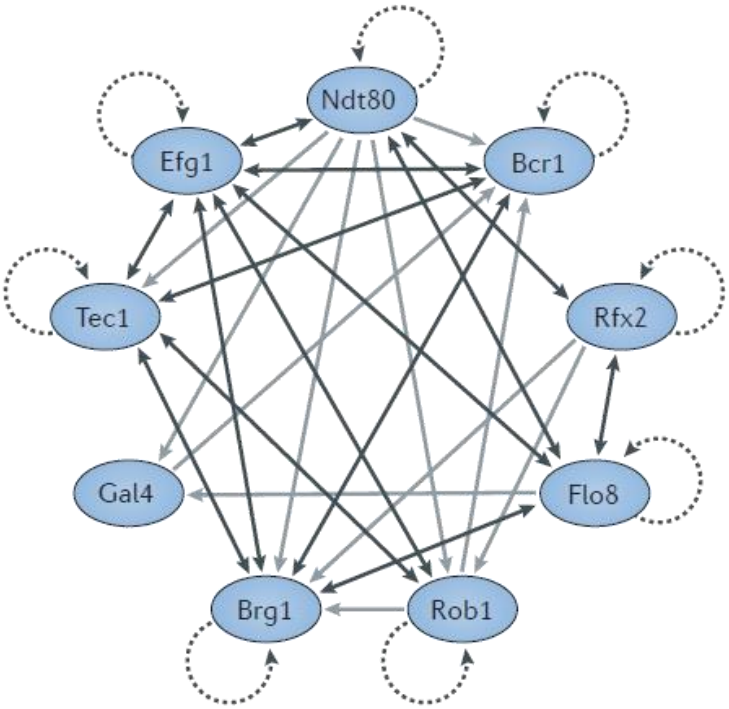


**Figure 9- Transcriptional network controlling biofilm formation in *Candida albicans.*** Autoregulation is indicated by dotted arrows, direct binding interactions between two regulators that each regulate the activity of the other are indicated by double-headed dark grey arrows, and direct binding interactions where one regulator controls another regulator are indicated by single-headed light grey arrows. (from: Lohse, Matthew B., *et al*. (2018)[58]).

Tec1 is a member of the transcriptional enhancer activators (TEA/ATTS) family of TFs that was shown to be a positive regulator of morphogenesis upon serum induction, macrophage evasion and expression of aspartyl proteinase genes, required for hyphal formation and virulence in *C. albicans*.[16,43,23] The DNA-binding region is contained in 66–76 conserved amino acids in the N-terminus.[43]

Tec1 is involved in the regulation of hyphal growth in planktonic cells, together with some of the previously mentioned core regulators of biofilm formation, such as Efg1, Ndt80 and Rob1. The deletion

of any one of these genes implicated a significant reduction of hyphae development.[58] Depending on the environmental cues and cell type, the MAPK signal activates filamentation programs transduced by Tec1.[72]

By resorting to ChIP-chip, it was possible to infer a statistically significant motif for Tec1 (RCATTCY), which is identical to that determined for its homolog, Tec1, in *S. cerevisiae*. This motif differs from the one previously reported in the white-specific pheromone response element, AAAAAAAAAAGAAAG in *C. albicans*.[71]

A study carried by Daniels, Karla J., *et al.* (2015) intended to analyze the role of *C. albicans* Tec1 by comparing the effects of deleting *CgTEC1* gene on initial adhesion to silicone elastomer, high-resolution confocal microscopy assessments of the stages and cellular phenotypes during the 48 h of a *MTL*-homozygous mature sexual biofilm development, human white cell penetration, and integrity of the biofilms. The results showed that Tec1 plays a minor role in initial adhesion to silicone elastomer but to be relevant in the growth of the basal yeast cell polylayer, vertical extension of hyphae and matrix deposition in the upper portion of the biofilm, final biofilm thickness, penetrability of human white blood cells, and final biofilm integrity.[73]

There are a modest number of studies that aimed to disclose Tec1 transcriptional networks in *C. albicans*. One was performed by Sahni, Nidhi, *et al.* (2010) using the increase in adhesion associated with white cell pheromone response as an assay, that demonstrated that Tec1 was the only factor among 107 TFs to induce adhesion when overexpressed in the absence of pheromone. Tec1 revealed to be the TF regulated by the MAP kinase cascade in the white cell pheromone response pathway and was shown to belong to an ancestral filamentation pathway, taking its conserved role in both *C. albicans* and *S. cerevisiae* filamentation. Tec1 binds selectively to WPRE-containing promoters of the genes up-regulated by α-pheromone in white cells (*CaCSH1*, *CaPBR1*, *CaRBT5*, *CaWH11*, *CaSTE2* and *CaRBT1*).[74]

Tec1 expression is directly regulated by Efg1 and Cph2 TFs, functioning to mediate hyphal gene transcription in *C. albicans.* [16,43,23] Furthermore, Bcr1 is positively regulated by Tec1 and was predicted to have a role in hyphal development. Bcr1 is a C2H2 zinc finger transcriptional activator of cell-surface protein and adhesion genes such as *CaECE1*, *CaALS3*, *CaHWP1,* and *CaHYR1.*[16]

Glazier, V. E. *et al.* (2017) study adressed the functional consequences of the integration of the TFs in *C. albicans* biofilm network (composed of Bcr1, Brg1, Efg1, Ndt80, Rob1, and Tec1) and the identities of pairs of TFs that functionally interact. This TF network revealed to be efficient, but not robust, in relation to Tec1 expression regulation. The deletion of each of the regulator genes, except for *CaNDT80*, led to a decrease in *CaTEC1* expression, indicating that this TF is an important output of the network and highly connected to its functional state. The importance of Tec1 to the function of the newtwork was highlited in this study, which discloses that a significant portion of biofilm formation reduction is due to the reduced network mediated *CaTEC1* expression in the deletion mutants. This shows the ability of this transcriptional network to answer to small perturbations at a number of nodes by communicating to regulate the expression of a functionally important member of the network.

If the biofilm network functioned in a robust manner, the *CaTEC1* expression would be less susceptible to small changes in the network instead of provoking significant changes in phenotype.[75]
Moreover, *Δtec1* deletion mutant also displayed a significant reduction in acetylation-stimulating protein protein production, which is a major component of the ECM of *C. albicans* biofilms, as was observed for *Δefg1* deletion mutants as well.[76]
Considering *S. cerevisiae*, van der Felden, Julia, *et al.* (2014) studied the mechanisms by which Tec1 and Ste12 confer promoter-specific transcriptional control. Tec1, together with Ste12 TF, controls development, including cell adhesion and biofilm/filament formation. Tec1-Ste12 complexes control target genes through Tec1 binding sites (TEA consensus sequences) that can be further combined with Ste12 binding sites (pheromone response elements) for cooperative DNA binding. The activity of Tec1-Ste12 complexes is known to be negatively controlled by Dig1 and Dig2 transcriptional corepressors, that confer regulation by upstream signaling pathways. This complex was shown to associate *in vitro* and *in vivo* with the regulatory proteins Msa1 and Msa2, which were previously found to interact with cell cycle-related TFs (Swi4 and Mbp1). Tec1-Ste12-Msa1-Msa2 complexes activate a subset of genes involved in adhesion and biofilm/filament formation. Msb2 and Tec1, together with Msa proteins, are proposed to form a positive-feedback loop that controls the activity of the invasive/filamentous MAPK cascade, which helps to stably maintain cells in an invasive or filamentous growth mode under stress conditions, such as lack of nutrients.[77]
Additionally, Zhang, Qiuyu, *et al.* (2016) identified about 20 enhancers and 20 repressors of filamentation that included Tec1 between a number of highly conserved TFs, in *C. tropicalis.* This was performed by screened an overexpression library of 156 TFs. Most of the regulators (e.g., Tec1, Gat2, Nrg1, Sfl1, Sfl2 and Ash1) were demonstrated to have a conserved role in the regulation of filamentation, as in *C. albicans* or *S. cerevisiae*, but some TFs (e.g., Wor1, Bcr1, Stp4, Efh1, Csr1 and Zcf17) were found to play a specific role in *C.tropicalis* filamentation process only.[78]
In *C. parapsilosis*, *TEC1* gene seems not to play the same role as in *C. albicans*, since biofilm formation was not significantly reduced in the case of *C. parapsilosis Δtec1* mutant.[43] Nevertheless, it is an important transcription regulator promoting filamentation in this species.[23]
Despite this knowledge, little is known about the influence of the predicted Tec1 homolog, Tec1 TF (encoded by ORF *CAGL0M01716g*) in biofilm formation, in the case of *C. glabrata*.[43]

The transcriptional network found to control biofilm formation in *Candida albicans*, by Nobile, Clarissa J., *et al.* (2012), motivated our research group to find if these TFs were also related to biofilm formation in *C. glabrata.* Based on sequence homology, the *CgTEC1*, *CgTEC2*, *CgBCR1* and *CgNDT80* genes were found in *C. glabrata*, as homologues of the *C. albicans CaTEC1*, *CaBCR1* and *CaNDT80* genes. The possible involvement of these TFs in *C. glabrata* biofilm development on polystyrene wells was demonstrated. The deletion of *CgTEC1* was shown to affect biofilm formation the most (Santos *et al*., unpublished results).

A Blast analysis was performed using the Candida Genome Database (CGD) and two homologous of the *CaTEC1* gene were found: was named *CgTEC1* (ORF *CAGL0M01716*) with 44.6% of identity and the second with 46.5% identity was named *CgTEC2* (ORF *CAGL0F04081*), which despite having shown a minor impact in biofilm formation, it was the one displaying the highest identity score.

### 1.7- Thesis outline and motivation

*C. glabrata* is a commensal colonist of the intestinal tract in humans, being an opportunistic pathogen. Biofilm formation ability contributes to *C. glabrata* persistence and results in a low therapeutic response and serious recurrent candidiasis. For their complex organization, biofilms are very resistant to antifungal treatment. Additionally, *C. glabrata* is a high stress tolerant and very robust species, since it can not only survive on host tissues but also on inanimate surfaces for more than 5 months and this is due to its capability to form multilayered biofilms. Even though there is a high amount of information available regarding the mechanisms that control biofilm formation in *C. albicans*, scarce information is available for *C. glabrata*.

The *C. albicans* TF Tec1 is a positive regulator of morphogenesis, required for hyphal differentiation and also an important regulator of biofilm formation, recently considered a member of the TEA/ATTS family of TFs. Contrasting with the knowledge on the biological roles played by *C. albicans* Tec1 TF, in *C. glabrata* the biological functions of its predicted orthologs Tec1 and Tec2 remain unclear. However, preliminary unpublished results suggest that Tec1 is also related to biofilm formation in *C. glabrata.* Motivated by this hypothesis, this dissertation was outlined in order to clarify and improve the knowledge about the role and the mechanisms of action of the *C. glabrata* Tec1 TF in its ability to form stable biofilms and to unveil possible targets for the future development of strategies to prevent biofilm-based pathogenicity by *C. glabrata*.

This thesis starts with a first chapter introducing the main topics addressed in this study, such as the increasing relevance of *C. glabrata* as an opportunistic pathogen and its main features. A description of known biofilm formation mechanisms is given, comprising each stage of development. The importance of biofilm formation for virulence in *Candida* species is also addressed, giving special attention to the transcriptional control underlying this phenomenon. Lastly, the role of the transcription regulatory network controlling biofilm formation in *C. albicans* and other related yeast species, including the Tec1 TFs in particular, is overviewed, highlighting the lack of knowledge on the transcriptional control of biofilm formation in *C. glabrata*.

The second chapter presents the materials and methods required for the development of this work.

The third chapter describes the results and discussion of the functional characterization of the *C. glabrata* TF Tec1. This functional characterization encompasses biofilm formation and adhesion assays

to polystyrene surfaces and human vaginal epithelium cells, respectively, where the behavior of a wild-type (wt) is compared to *Δtec1* deletion mutant or the *CgTEC1* overexpressing strain. The subcellular localization of Tec1 was assessed, as well as its involvement in pseudohyphal differentiation. To understand the role of Tec1 in *C. glabrata* biofilm formation, when compared to planktonic growth, ribonucleic acid (RNA)-sequencing (RNA-seq) analysis of the effect of deletion of the *CgTEC1* gene on the transcriptome in both conditions is presented. Based on the indications obtained from the transcriptomics analysis, some adhesion-related genes were studied in relation to their relevance in biofilm formation. The deletion of 9 genes found to be upregulated by Tec1 during biofilm development on polystyrene surface was evaluated along with 3 other genes up-regulated in biofilm cells. This chapter also includes the study of the effect of deleting the *CgTEC1* gene in the concentration of ergosterol present in *C. glabrata* cells grown under biofilm and planktonic conditions. At last, an *in silico* prediction of the Tec1 binding sequences, structure and conserved domains was performed and presented. The obtained results are discussed in comparison with current knowledge in other species.

The thesis ends with the fourth section, Final Discussion, focusing on the most significant aspects of our findings. Some final remarks and future perspectives are also discussed.

# 2- Experimental Procedures

## 2.1- Cell cultures

### 2.1.1- Strains

The parental strain *C. glabrata* KUE100 and derived single deletion mutants: *Δtec1, Δpup1, Δaur1, Δaed2, Δpwp5, Δbmt1, Δbmt7*, *Δawp13* and were kindly provided by Prof. Hiroji Chibana, Medical Mycology Research Center, Chiba University, Chiba, Japan. *C. glabrata* L5U1 strain (*Δcgura3Δcgleu2*) was kindly provided by John Bennett[79] of the National Institute of Allergy and Infectious Diseases, NIH, Bethesda, MD. Additionally, the CBS138 *C. glabrata* strain, whose genome sequence was released in 2004, was used in this study for gene amplification purposes. The plasmid pGREG576 was obtained from the Drag & Drop collection (**Figure A1**)[80].

### 2.1.2- Growth media

*C. glabrata* cells were batch-cultured at 30ºC with orbital agitation (250 rpm) in different growth media according to the following protocols:

- The yeast extract peptone dextrose (YEPD) growth media was used as a rich medium, with the following composition (per liter): 20 g glucose (Merck), 10 g yeast extract (HIMEDIA) and 20 g bacterial-peptone (Dickson).
- The minimal growth medium (MMG) used contained per liter: 20 g glucose (Merck); 2.7 g $(NH_4)_2SO_4$ (Merck); 1.7 g yeast nitrogen base without amino acids and $(NH_4)_2SO_4$ (Difco).
- Also used was Sabouraud's dextrose broth (SDB) pH 5.6 containing 40 g glucose (Merck) and 10 g peptone (LioChem) per liter.
- Roswell Park Memorial Institute (RPMI) 1640 growth medium pH 4 contained per 600 mL: 6.24 g RPMI 1640 (Sigma); 20.72 g 3-(N-morpholino) propanesulfonic acid (MOPS) (Sigma); 10.8 g glucose (Merck).

### 2.1.3- Human epithelium cell line for adhesion assays

The VK2/E6E7 human epithelium cell line ATCC® CRL-2616™, used for adhesion assays, is derived from the vaginal mucosa of a healthy premenopausal female submitted to vaginal repair surgery. VK2/E6E7 cell maintenance was achieved with Keratinocyte-Serum Free medium, containing 0.1 ng/mL human recombinant EGF, 0.05 mg/mL bovine pituitary extract and additional 44.1 mg/L calcium chloride. Subculturing of cells was performed using 75 $cm^2$ flasks, beginning with the removal of the culture medium, rinsing the cell layer with 0.25% (w/v) Trypsin-0.03% (w/v) Ethylenediamine tetraacetic acid (EDTA) solution to remove all traces of serum that contains trypsin inhibitor. Afterwards, 3.0 ml of Trypsin-EDTA solution was added to the flask, following observation of cells under an inverted microscope until the cell layer was dispersed. Trypsin was neutralized by adding 8.0 mL of a 1:1 mixture of Dulbecco's modified Eagle's medium and Ham's F12 medium (DMEM:F-12), containing 10% fetal

bovine serum. Subsequently, cells were aspirated and transfer to a centrifuge tube, for centrifugation at 125 x g for 10 min. Cells were resuspended in fresh serum-free growth medium and divided in aliquots to add to new culture vessels, which were incubated at 37°C, with 95% air and 5% $CO_2$.

### 2.2- Quantification of Biofilm Formation

In order to assess the capacity of biofilm formation of *C. glabrata* cells, the Presto Blue assay (**Figure A2**) was used. Cells were grown in SDB medium or MMG-U medium (composed of minimal medium supplemented with 60 mg/L Leucine) and collected at mid-exponential phase. A cell suspension was prepared with an $OD_{600}$ of 0.1. Cells were then inoculated in 96-well polystyrene titter plates (Greiner), which were previously filled with the appropriated medium, SDB at pH 5.6 or RPMI at pH 4, in order to have an initial $OD_{600nm}$ = 0.05±0.005. Afterwards, cells were sealed with a membrane (Greiner Bio-One) and cultivated at mild orbital shaking (70 rpm), for 24h, at 30ºC. Subsequently, each well was washed two times with 100 µL of sterile PBS pH 7.4 [PBS contained per liter: 8 g NaCl (Panreac), 0.2 g KCl (Panreac), 1.81 g $NaH_2PO_4.H_2O$ (Merck), and 0.24 g $KH_2PO_4$ (Panreac)] to remove the cells that were not attached to the formed biofilm. After washing, Presto Blue reagent was prepared in a 1:10 solution in the medium used for biofilm formation, adding 100 µL of the solution to each well. Plates were incubated at 37ºC for 30 min. Afterwards, absorbance reading was determined in a microplate reader (SPECTROstar Nano, BMG Labtech) at the wavelength of 570 nm and 600 nm for reference.

### 2.3- Adhesion to human vaginal epithelium cells assay

For the epithelium adhesion assays, VK2/E6E7 human epithelium cells were grown adhered to an abiotic surface and further detached in order to be inoculated in 24-well polystyrene plates (Greiner) with a density of $2.5x10^5$ cell/mL. Additionally, *Candida glabrata* cells were inoculated with an initial $OD_{600nm}$ = 0.05±0.005, cultivated at 30 ºC, during 16±0.5 h, with orbital shaking (250 rpm). In order to initiate the assay, the culture medium of mammalian cells was removed and substituted by new culture medium, in each well, and, subsequently, *C. glabrata* cells were added to each well, with a density of $12.5x10^5$ CFU/well. The plate was centrifuged for 1 min at 1000 rpm and room temperature. Then, cells were incubated at 37°C, 5% $CO_2$, for 30 min. Afterwards, each well was washed 3 times with 500 µL of PBS pH 7.4, following the addition of 500 µL of Triton X-100 0.5% (v/v) and incubation at room temperature for 15 min. The cell suspension in each well was then recovered and spread onto agar plates to determine Colony Forming Units (CFU) count, which represent the proportion of adherent cells to the human epithelium.

### 2.4- *C. glabrata* transformation

For transformation purposes, cells were batch-cultured at 30°C, with orbital agitation (250 rpm) in liquid rich medium YEPD.

All transformation reactions were performed using the Alkali-Cation Yeast Transformation Kit (MP Biomedicals), according to the manufacturer's instructions. Mid-exponential *C. glabrata* L5U1 cells were batch-cultured at 30ºC with orbital shaking (250 rpm) in YEPD liquid medium until a standard $OD_{600nm}$ 0.4 ± 0.04 was reached. The cells were harvested by centrifugation at 7 000 rpm for 5 min at 4ºC and the resulting pellets were resuspended in 2.7 mL of Tris EDTA (TE) buffer, pH 7.5. After a second centrifugation step, the cells were harvested and rinsed with 1.5 mL of 0.15 M Lithium Acetate solution and shaken gently (100 rpm) at 30ºC for 25 min. Cells were harvested by centrifugation (7 000 rpm, 5 min, 4 ºC) and resuspended in 300 µL TE buffer, pH 7.5. Cells were then transferred to microcentrifuge tubes, combining: 100 µL yeast cells, 5 µL Carrier DNA, 5 µL Histamine Solution and 100-200 ng plasmid DNA. Cells were gently mixed and incubated at room temperature for 15 min. A mixture of 0.8 mL PEG and 0.2 mL TE/Cation MIXX solution was added to each transformation reaction, followed by 10 min incubation at 30 ºC and heat shock at 42ºC for 10 min. Cells were then pelleted in a microcentrifuge and resuspended in 100 µL YEPD liquid medium before plating in appropriate medium agar plates.

## 2.5- RNA-sequencing analysis

### 2.5.1- Total RNA extraction

Cells for RNA-seq analysis were grown in SDB medium. Planktonic cells were cultured at 30ºC with orbital agitation (250 rpm), while biofilm cells were cultured at 30ºC, in square Petri dishes, with orbital agitation (70 rpm). Three independent total RNA isolates were extracted from wild type and single deletion mutant cells during planktonic exponential growth and upon 24h of biofilm growth. Total RNA was isolated using an Ambion Ribopure-Yeast RNA kit, according to manufacturer's instructions.
Cell cultures and RNA extraction were performed by Mafalda Cavalheiro.

### 2.5.2- Library preparation and RNA-sequencing

Strand specific RNA-seq library preparation and sequencing was carried out as a paid service by the NGS core from Oklahoma Medical Research Foundation, Oklahoma City, Oklahoma, USA. Prior to RNA-seq analysis quality control measures was implemented. Concentration of RNA was ascertained via fluorometric analysis on a Thermo Fisher Qubit fluorometer. Overall quality of RNA was verified using an Agilent Tapestation instrument. Following initial QC steps sequencing libraries were generated using the Illumina Truseq Stranded Total RNA library prep kit with ribosomal depletion via RiboZero Gold according to the manufacturer's protocol. Briefly, ribosomal RNA was depleted via pull down with bead-bound ribosomal-RNA complementary oligomers. The RNA molecules were then chemically fragmented and the first strand of (cDNA) was generated using random primers. Following RNase digestion, the second strand of cDNA was generated replacing dTTP in the reaction mix with dUTP. Double stranded cDNA then underwent adenylation of 3' ends following ligation of Illumina-specific adapter sequences. Subsequent PCR enrichment of ligated products further selected for those strands

not incorporating dUTP, leading to strand-specific sequencing libraries. Final libraries for each sample were assayed on the Agilent Tapestation for appropriate size and quantity. These libraries were then pooled in equimolar amounts as ascertained via fluorometric analyses. Final pools were absolutely quantified using qPCR on a Roche LightCycler 480 instrument with Kapa Biosystems Illumina Library Quantification reagents. Sequencing was performed on an Illumina HiSeq 3000, producing 2x150 bp paired-end reads, 2 gigabases (GB) clean data, yielding 52 million reads per sample.

### 2.5.3- Computational analysis

Paired-end reads were obtained from wild type (*C. glabrata* KUE100) and correspondent deletion mutant strain (*CAGL0M01716g*). Two replicates of each sample were obtained from three independent RNA isolations, subsequently pooled together. Samples reads were trimmed using Skewer[81] and aligned to the *C. glabrata* CBS138 reference genome, obtained from the *Candida* Genome Database (CGD)[82], using TopHat. HTSeq[83] was used to count mapped reads per gene. Differentially expressed genes were identified using DESeq2[84] with an adjusted *P*-value threshold of 0.01 and a log2 fold change threshold of -1.0 and 1.0. Default parameters in DESeq2 were used. Significantly differentially expressed genes were clustered using hierarchical clustering in R[85]. *Candida albicans* and *Saccharomyces cerevisiae* homologs were obtained from the CGD and Saccharomyces Genome Database (SGD)[86], respectively. Raw data pre-treatment was performed by Pedro Pais, in collaboration with Geraldine Butler, University College Dublin.

## 2.6- Transcriptomic data analysis

The RNA-sequencing analysis provided two datasets: wild type vs *Δtec1* deletion mutant in planktonic growth and wild type planktonic vs wild type biofilm growth. The genes of each dataset were submitted to several analysis using different databases and bioinformatic tools, so they could be grouped according to their biological functions. This was accomplished mainly by resorting to the description of the *C. glabrata* genes found on the CGD (http://www.candidagenome.org/). The uncharacterized genes were clustered based on the description of ortholog genes in *S. cerevisiae* or in *C. albicans*, according to the SGD or in CGD, respectively. Go-Stats from GoToolBox web server[87] allowed the determination of the main Gene Ontology (GO) terms to which the genes were related. The bioinformatic tool Kyoto Encyclopedia of Genes and Genomes (KEGG) Mapper[88] was used to analyze the main metabolic pathways to which the genes were related to. The KEGG organism code chosen was “cgr” for *C. glabrata.* The functional protein association networks tool, STRING[89], helped to understand the protein-protein interactions and its cellular functions. From this organization, several genes related to cell adhesion were chosen for the following gene expression analysis.

For the analysis of the possible Tec1 recognition sequences, a search for consensus sequences in the upstream regions of each positively regulated gene in biofilm was performed. By resorting to

PathoYeastract[90] database, these upstream regions were obtained and then, these were used in DREME (Discriminative Regular Expression Motif Elicitation)[91] informatic tool.

I-TASSER (Iterative Threading ASSEmbly Refinement)[92] approach was used for Tec1 structure and ligand binding residues prediction. The InterPro[93] database was used to search for conserved domains in Tec1 and Clustal Omega[94] program (https://www.ebi.ac.uk/Tools/msa/clustalo/) allowed the multiple alignment of the three *TEC1* orthologs from *C. albicans, S. ceresiviae* and *C. glabrata*.

## 2.7- Gene expression analysis

The quantitative Real Time Polymerase Chain Reaction (RT-qPCR) technique was used in order to estimate the expression levels of *CgPWP5, CgAED2* and *CgAWP13* genes encoding adhesins, by visualizing the abundance of mRNA transcripts in each sample.

For the planktonic growth condition, *C. glabrata* KUE100 and *Δtec1* single deletion mutant strains were grown in YEPD medium, at 30 ºC, with an orbital agitation of 250 rpm until an $OD_{600nm}$ of 0.8±0.08 was achieved. For the biofilm growth condition, the same strains were grown in SDB medium and collected at mid-exponential phase. Cells were then inoculated in square polystyrene titter plates filled with 40 mL of SDB medium at pH 5.6, to have an initial $OD_{600nm}$ = 0,05±0.005. Afterwards, cells were cultivated at mild orbital shaking (70 rpm), for 24 h and 48 h, at 30ºC. The cultures were conducted in triplicates. Afterwards, the planktonic cells were harvested with a centrifugation of 7000 rpm, at 4ºC for 7 min, obtaining the desired pellets. Then, the pellets were resuspended in 1 mL of supernatant and centrifuged at 9000 rpm for 2 min. The pellets obtained were stored at -80ºC until further use. Biofilm cells were harvested by discarding the medium, leaving only biofilm cells in the plates, then 3 mL of sterile water were added and the plate was scraped. The resultant suspension of cells was transferred to a centrifuge tube. This process was repeated and the suspension was centrifuged at 7000 rpm, at 4 ºC for 5 min, obtaining the desired pellets. Then, the pellets were resuspended in 1 mL of supernatant and centrifuged at 13500 rpm for 2 min. The pellets obtained were stored at -80 ºC until further use.

### 2.7.1- Total RNA extraction and quantification

The total RNA extraction was performed for *C. glabrata* KUE100 and *Δtec1* single deletion mutant strains cells grown in planktonic and biofilm growth conditions, according to the Hot-phenol method described by Kohrer & Domdey[95]. For the first step of this method, the pellets were resuspended in 900 µL of AE buffer (50 mM NaAc (Sigma), 10mM EDTA (Aldritch), pH=5.3; 0.1% (v/v) diethylpyrocarbonate (DEPC) treated). Afterwards, it was added 90 µL of SDS 10% (w/v) (Sigma) and 800 µL of phenol, following a short vortex of 5 sec. Then, samples were incubated at 65 ºC for 4 min and transferred into dry ice until the formation of crystals was identified. The mixtures were centrifuged at 15000 rpm, at 4 ºC for 5 min. The upper phase was collected to new microcentrifuge tubes. Subsequently, a two-step extraction with phenol was performed where for each step 400 µL of a 25:24:1 phenol/chloroform/isoamilic acid solution (Sigma) was added. A short vortex was carried out, following

a centrifugation at 15000 rpm, at 4 ºC for 5 min. The top phase was collected to new microcentrifuge tubes. Then, a final extraction was performed, using 800 µL of 24:1 chloroform/isoamilic acid solution (Sigma), following vortex and centrifugation in the same conditions, finishing with the collection of the top phase.

After this stage, a 1/10 of the final volume of the mixture obtained by centrifugation of sodium acetate 3 M (Merck, pH=5.3, 0.1% DEPC treated) was added. Then a purification step was performed by adding 1 mL of cold ethanol 100%. After a short vortex, the samples were stored in -20˚C for 20 min. Then, a prolonged centrifugation was carried out at 15000 rpm, at 4ºC for 20 min. The liquid phase was discarded and the remaining precipitates were washed with 750 µL of cold ethanol 70% (v/v) and centrifuged at 15000 rpm, at 4 ºC for 20 min. The liquid phase was carefully discarded, and afterwards, in order to preserve the formed precipitates, a drying step at Speed Vacuum Concentrator Plus (Eppendorf) was performed for 15 min. Then, the material was resuspended in 50 µL of sterile deionized water 0.1% (v/v) DEPC treated and the volume was divided by two aliquots of 10 µL and 40 µL. The aliquots of 10 µL were used to assess the purity and quantify total RNA concentration in a NanoDrop ND-1000 spectrophotometer (NanoDrop Technologies).

At last, the samples were diluted in order to have a concentration of 500 ng/µL for the real time RT-PCR.

### 2.7.2- Real Time RT-PCR

The SYBR® Green fluorescence is detected by the 7500 Real-Time PCR Systems (Applied Biosystems®), following the registration performed by the software 7500 Systems SDS Software from Applied Biosystems in the amplification plot. The detection is considered at a threshold level when the signal is slightly greater than the background. The purpose is to find the number of cycles (Ct) necessary to achieve a given level of fluorescence above the threshold[96].

Therefore, the signal level is registered in an amplification plot, from which Ct is estimated by the intersection between exponential phase curve and threshold line. The normalization of the Ct values is performed using an internal control as shown in **Equation 1**.

$$\Delta C_t = C_t(target) - C_t(control) \qquad \textbf{Equation 1}$$

Afterwards, each normalized value correspondent to each gene is compared with the physiological calibrator considered, as demonstrated in **Equation 2**.

$$\Delta\Delta C_t = \Delta C_t(sample) - \Delta C_t(calibrator) \qquad \textbf{Equation 2}$$

Then, the gene expression level can be estimated using the **Equation 3**.

$2^{-\Delta\Delta Ct}$ **Equation 3**

In order to start this technique, it is necessary to synthesize cDNA from the total RNA extracted from *C. glabrata* strains. In this first step of the procedure, a reaction using MultiScribeTM reverse transcriptase according to the mixture present in **Table 2** was performed in the conditions described in **Table 3**.

**Table 2- Reaction mixture for the first step of the real time RT-PCR (Applied biosystems).**

| Component | Volume per reaction (µL) |
|---|---|
| TaqMan RT buffer (10x) | 1.0 |
| $MgCl_2$ (25 mM) | 2.2 |
| dNTPs (2.5 mM) | 2.0 |
| Random hexamers (50 µLM) | 0.5 |
| RNAse inhibitor (20 U/L) | 0.2 |
| MultiScribe™ reverse transcriptase (50 U/L) | 0.25 |
| RNA sample (50 ng/µL) | 2.0 |
| $ddH_2O$ DEPC treated | 1.85 |
| Total | 10.0 |

**Table 3- Thermal cycling parameters for the first step of the real time RT-PCR (Applied biosystems).**

| Step | Time (min) | Temperature (ºC) |
|---|---|---|
| Incubation | 10 | 25 |
| Reverse transcription | 30 | 48 |
| Reverse transcriptase inactivation | 5 | 95 |

After the first step was completed, the cDNA samples were stored at -20ºC. Afterwards, each sample was diluted 1:4.

For the second step of RT-PCR, it is necessary to consider a housekeeping gene like *CgACT1,* which encodes actin, in order to have an internal control. For the preparation of this second step, a mixture for each reaction was prepared according to the internal control and *CgAED2, CgPWP5 and CgAWP13* genes (See **Table 4**).

**Table 4- Reaction mixture for the second step of real time RT-PCR (Applied Biosystems).**

| Component | Volume per reaction (µL) |
|---|---|
| SYBR®Green PCR Master Mix (2x) | 12.5 |
| Foward Primer (4 pmol/µL) | 2.5 |
| Reverse Primer (4 pmol/µL) | 2.5 |
| cDNA sample | 2.5 |
| $ddH_2O$ | 5.0 |
| Total | 25.0 |

Each reaction of the second step was performed in a thermal cycler block (7500 Real-Time PCR System – Applied Biosystems), according to the parameters present in **Table 5**.

**Table 5- Thermal cycling parameters for the second step of the real time RT-PCR (Applied Biosystems).**

| Step | | Time | Temperature (ºC) |
|---|---|---|---|
| AmpliTaq gold® DNA polymerase activation | | 10 min | 95 |
| PCR (40 cycles) | Reverse transcription | 15 sec | 95 |
| | Reverse transcription inactivation | 1 min | 60 |

The primers used in the second step of RT-PCR are present in **Table 6**.

**Table 6- Primers for *CgACT1, CgAED2, CgPWP5* and *CgAWP13* genes.**

| Gene | Primer | Sequence |
|---|---|---|
| *CgACT1* | Forward | 5'-AGAGCCGTCTTCCCTTCCAT-3' |
| | Reverse | 5'-TTGACCCATACCGACCATGA-3' |
| *CgAED2* | Forward | 5'-AAAGCCTCAATGGTATGACAGAAGAC-3' |
| | Reverse | 5'-CAGATGAATTTTGGAATGGGAAA-3' |
| *CgPWP5* | Forward | 5'-GGCTGGCTTTCGTGCAATA-3' |
| | Reverse | 5'-CGACGGACCCTTGTAAGATTGT-3' |
| *CgAWP13* | Forward | 5'-TTAATATCTTGCTGGGCTTTTGG-3' |
| | Reverse | 5'-AGCGTAGCACTGTCTATGATTATTTCTT-3' |

## 2.8- Quantification of total cellular ergosterol

Total ergosterol content was extracted from *C. glabrata* KUE100 and *Δtec1* single deletion mutant cells using the method of physical disruption[97] with some adjustments. Planktonic growth condition cells were cultivated in 100 mL of YEPD and with an orbital agitation of 250 rpm until stationary phase was reached. Biofilm growth condition cells were grown in SDB medium and collected at mid-exponential phase. Cells

were then inoculated in square polystyrene titter plates filled with 40 mL of SDB medium at pH 5.6, to have an initial $OD_{600nm}$ = 0,05±0.005. Afterwards, cells were cultivated at mild orbital shaking (70 rpm), for 24h, at 30ºC. The cultures were conducted in triplicates. Planktonic cells were harvested by centrifugation and ressuspended in 5 mL of methanol and biofilm cells were harvested by discarding the medium, leaving only biofilm cells in the plates, then 3 mL of sterile water were added and the plate was scraped. The resultant suspension of cells was transferred to a centrifuge tube. This process was repeated and the suspension was centrifuged and and ressuspended in 5 mL of methanol. The Cholesterol, used as an internal standard to allow quantification of the yield of ergosterol extraction, was added in order to have a final concentration of 1 mg/mL in each sample. Afterwards, glass beads were added approximately in the same weight as the cell pellet. Then, each sample was homogenized in 30 sec, following an orbital agitation of 320 rpm for 1 h. The samples were centrifuged at 8000 rpm for 7 min at 4ºC. 1.7 mL of supernatant was extracted to an eppendorf, following another centrifugation at 11000 rpm for 10 min at 4ºC. 1 mL of the supernatant was then collected and stored until analysis.

The extracts obtained were analyzed by High Pressure Liquid Chromatography with a 250 mm x 4 mm C18 column (LiChroCART Purospher STAR RP-18 end- capped 5 mm) at 30ºC. The samples were eluted in 100% methanol at a flow rate of 1 mL methanol per min. Cholesterol was detected at 210 nm corresponding to a retention time of 14.08±0.21 min. Ergosterol was detected at 282 nm with a retention time of 11.71±0.17 min.

The corresponding results are presented as the ratio between the average concentration of ergosterol of the KUE100 strain or *Δtec1*, according to each case, and the concentration of the other samples tested.

### 2.9- Tec1 Subcellular localization assessment

The subcellular localization of the Tec1 protein was determined based on the observation of L5U1 *C. glabrata* cells transformed with the pGREG576-Pdc1-*CgTEC1* and pGREG576 (for control) plasmids. The cells transformed with the first, express the *CgTEC1_GFP* fusion protein, whose localization may be determined using fluorescence microscopy.

*C. glabrata* cells were grown at 30ºC, with an orbital agitation of 250 rpm, until to mid-exponential phase in minimal growth medium, and then inoculated to the same medium to have an initial $OD_{600nm}$ = 0.02±0.005, for planktonic growth condition. For biofilm growth condition, cells were inoculated in square polystyrene titter plates filled with 40 mL of SDB medium at pH 5.6, to have an initial $OD_{600nm}$ = 0,05±0.005. Afterwards, biofilm cells were cultivated at mild orbital shaking (70 rpm), for 6h and 24h, at 30ºC. After around 22 hours, the distribution of *CgTEC1_GFP* in planktonic living cells was inspected through fluorescence microscopy in a Zeiss Axioplan microscope (Carl Zeiss MicroImaging, Oberkochen, Germany), using excitation and emission wavelength of 395 and 509 nm, respectively. Fluorescence images were captured using an Axiocam 503 Color (Zeiss). The same was executed after 6 and 24 hours of biofilm growth.

## 2.10- Pseudohyphal growth induction

Filamentation of the *Candida glabrata* KUE100 and *Δtec1* deletion mutant strains was achieved by incorporating 0.5% (v/v) of isoamyl alcohol (Sigma) to the growth media, following what had already been described in *Saccharomyces cerevisiae*[98]. Cells grew overnight in YEPD without isoamyl alcohol. The inoculum was made to an initial $OD_{600nm}$=0.1±0.01 in YEPD supplemented with 0.5% (v/v) of isoamyl alcohol, and cells grew at 30ºC with orbital agitation (250 rpm) for 48 hours. After the 48 h of incubation 7 µL of the cell suspension was observed by optical microscopy (Zeiss Axioplan Microscope, Carl Zeiss Microimaging). Pictures were captured using a Axiocam 503 Color (Zeiss) and cells and filaments were counted with Fiji Is Just ImageJ tool.

## 2.11- Statistical analysis

Statistical analysis of all data was performed using Graphpad Prism Software version 6.0 (La Jolla, CA, USA). *P*-values were calculated performing one-way ANOVA tests on Microsoft® EXEL 2016. *P*-values equal or inferior to 0,05 were considered statistically significant.

# 3- Results and Discussion

## 3.1- Tec1 is a determinant of biofilm formation in polystyrene surface

Based on the observation that the Tec1 TF is a key regulator of biofilm formation in *Candida albicans*[71] a similar role for the homologous *C. glabrata* TFs, Tec1 (ORF *CAGL0M01716*) and Tec2 (ORF *CAGL0F04081*), was investigated. Preliminary results from our group had hinted that the deletion of *CgT*s to decreased biofilm formation on polystyrene wells, using the crystal-violet method. (Santos *et al*., unpublished results).

To consolidate the previous observations, quantification of biofilm formation in polystyrene surface upon the deletion mutant *Δtec1* was performed using the PrestoBlue cell viability assay, in both SDB and RPMI media. The deletion of this TF in *C. glabrata* was found to reduce biofilm formation in 30% or 10%, in cells cultivated in SDB or RPMI media, respectively (**Figure 10**).

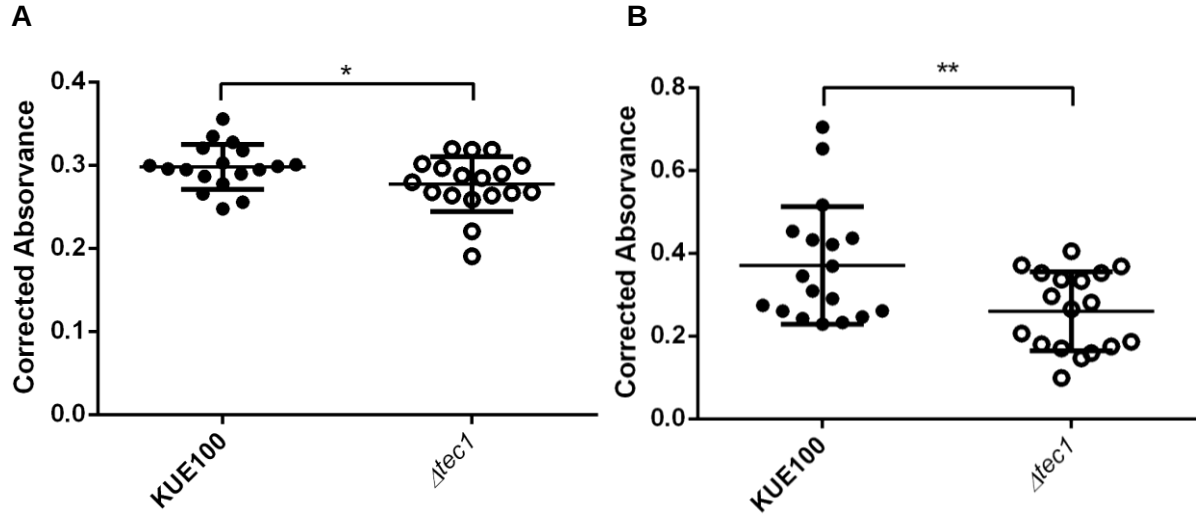


**Figure 10- Biofilm formation followed by Presto Blue Cell Viability Assay and measurements of absorbance at 570 nm and 600 nm for reference for the *C. glabrata* KUE100 and *Δtec1* strains**. Cells were grown for 24 h and the experiment was performed in RPMI medium pH 4 (A) and SDB medium pH 5.6 (B). In the scatter dot plot represented each dot corresponds to the level of biofilm formed in each sample. The indicated values are averages of at least three independent experiments. Error bars represent the corresponding standard deviations. ** *P*<0,01; * *P*<0,05.

To further assess if the over-expression of the *CgTEC1* gene would lead to an increase in biofilm formation on polystyrene surface, the quantification of biofilm formation was performed using the L5U1+vv (*C. glabrata* L5U1 cells transformed with the pGREG576 plasmid) and L5U1+*CgTEC1* (*C. glabrata* L5U1 cells transformed with the pGREG576 plasmid containing *PDC1* promotor and *CgTEC1* gene) strains, through the Presto Blue assay. The overexpression of *CgTEC1* resulted in a significant increase in biofilm formation in both media, 73% in SDB and 28% in RPMI, when compared to the parental strain, harboring the empty vector pGREG576 (**Figure 11**).

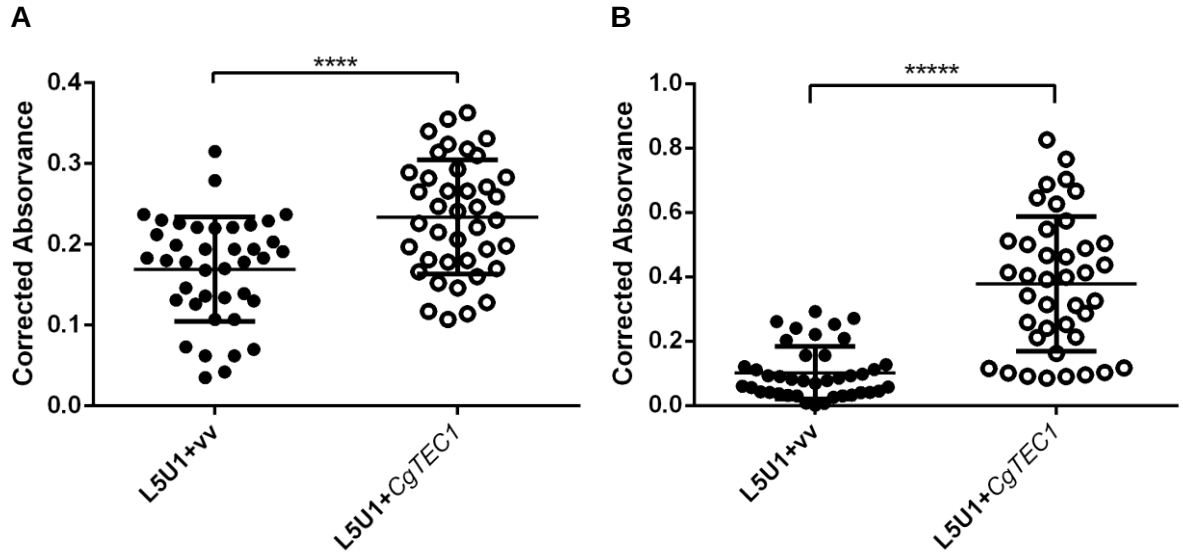


**Figure 11- Biofilm formation followed by Presto Blue Cell Viability Assay and measurements of absorbance at 570 nm and 600 nm for reference for the *C. glabrata* L5U1+vv and L5U1+*CgTEC1* strains**. Cells were grown for 24 h and the experiment was performed in RPMI medium pH 4 (A) SDB medium pH 5.6 (B). In the scatter dot plot represented each dot corresponds to the level of biofilm formed in each sample. The indicated values are averages of at least three independent experiments. Error bars represent the corresponding standard deviations. (A ) ***** *P*<0,00001; (B) **** *P*<0,0001.

Both experiments reinforce the notion that Tec1 is a key player in *C. glabrata* biofilm formation.

### 3.2- Tec1 is required for *C. glabrata* adhesion to human vaginal epithelium cells

Recently, *C. glabrata* biofilms have also been implicated in VVC, particularly in the setting of treatment failure and recurrence.[99]

As an attempt to understand the impact of Tec1 on the capacity of *C. glabrata* cells to adhere to the human vaginal epithelium cells, *C. glabrata* KUE100 and *Δtec1* deletion mutant strains were cultivated at 30 ºC, during 16±0.5 h, with orbital shaking (250 rpm). These cell suspentions were added, with a density of $12.5x10^5$ CFU/well, to VK2/E6E7 human epithelium cells previously inoculated in 24-well polystyrene plates with a density of $2.5x10^5$ cell/mL. The percentage of adhesion was then calculated for each replicate, representing the percentage of adhered *C. glabrata* cells, by the ratio between the CFU/ml recovered after incubation with the epithelial cells and the initial CFU/ml for each suspension (**Figure 12 A**). The further assessment of the effect of over-expressing the *CgTEC1* gene on adhesion to human vaginal epithelium cells was performed with the L5U1+vv (*C. glabrata* L5U1 cells transformed with the pGREG576 plasmid) and L5U1+*CgTEC1* strains (*C. glabrata* L5U1 cells transformed with the pGREG576 plasmid containing *PDC1* promotor and *CgTEC1* gene) (**Figure 12 B**).

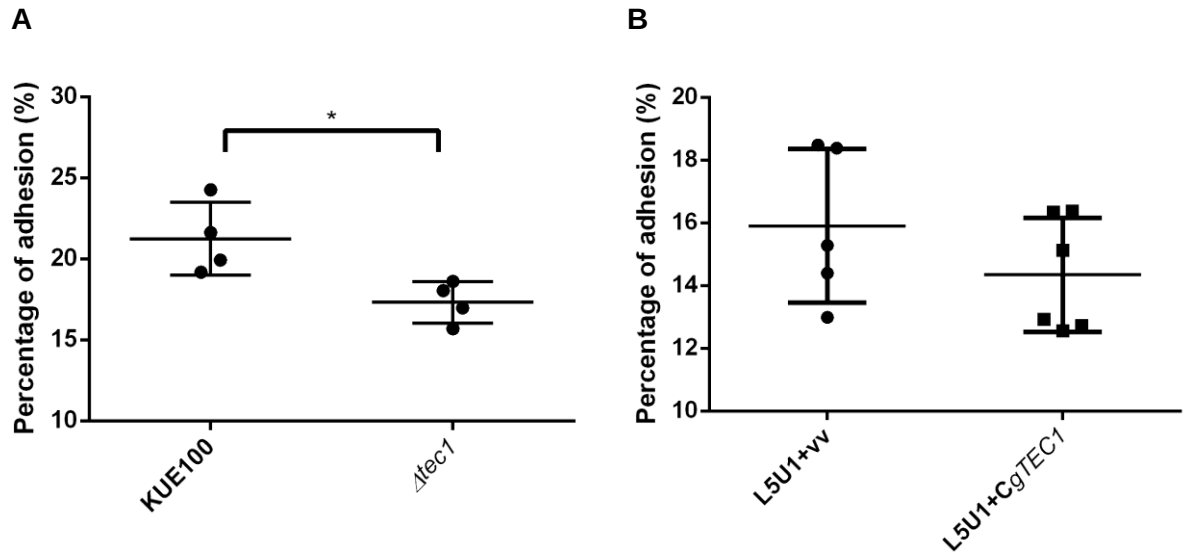


**Figure 12- Adhesion capacity to the human vaginal epithelium cells for the KUE100 and Δ*tec1* strains (A) and L5U1+vv and L5U1+*CgTEC1* (B).** Cells were cultivated for 16±0.5 h in YEPD medium. *C. glabrata* cells were added to the human cells and incubated at 37°C, 5 % $CO_2$, for 30 min. The cell suspension in each well was then recovered and spread onto agar plates to determine CFU count. In the scatter dot plot represented each dot corresponds to the proportion of adherent cells to the human epithelium. The indicated values are averages of at least three independent experiments. Error bars represent the corresponding standard deviations. **P*<0.05.

The deletion of *CgTEC1* was found to lead to a 18% reduction in the biofilm formed on top of the epithelial cell layer. This highlights the importance of the TF Tec1 in regulating cell adhesion, even to biotic surfaces. On the other hand, the over-expression of *CgTEC1* gene did not led to an increase in adhesion of cells to the human vaginal epithelium cells.

In the first part of this work, Tec1 was confirmed to be a determinant of biofilm formation in *C. glabrata* and shown to be required for biofilm formation in abiotic surfaces, but also to favor adhesion to epithelial cells.

### 3.3- Is Tec1 relevant in pseudohyphae differentiation by *C. glabrata* cells?

*C. albicans* ability to form hyphal cells both in planktonic cultures and during the maturation step of biofilm formation is well documented,[100] but although the pseudohyphal differentiation phenomenon has already been reported to happen in *C. glabrata*, this field remains scarcely explored.

Tec1 has been linked to the formation of pseudohyphae in *C. albicans* along with other transcriptional regulators. Therefore, this motivated an assay to find whether Tec1 is controlling pseudohyphal differentiation of *C. glabrata cells*. Similarly to the adopted procedure for pseudohyphae formation induction in *S. cerevisiae*[101], KUE100 and *Δtec1* cells were cultivated in rich YEPD medium supplemented with 0.5 % (v/v) of isoamyl alcohol. After 48 h of growth with this fusel alcohol, 7 µL of the suspensions were observed under the microscope, and the desired differentiation was observed (**Figure 13**).

A B

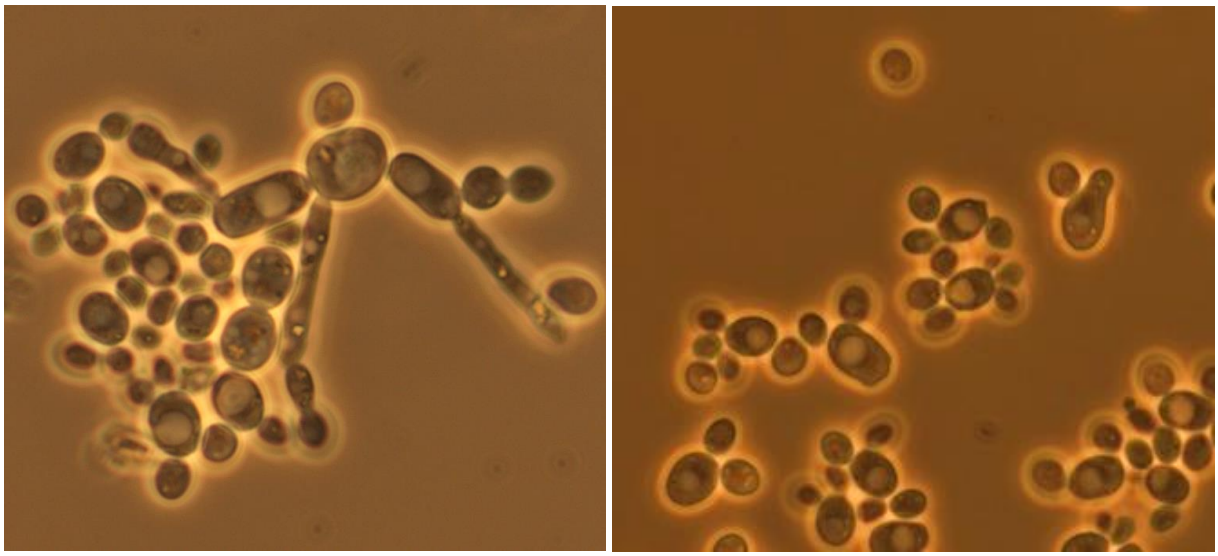

**Figure 13- The deletion mutant *Δtec1* (B) displays reduced pseudohyphae differentiation than *C. glabrata* KUE100 strain (A) when stimulated with 0.5% of isoamyl alcohol.** The bright field images were taken after 48 h of cellular growth in medium supplemented with 0.5% (v/v) isoamyl alcohol. The image represents the observed reduction of pseudohyphal cell number.

**Figure 13** illustrates what could be observed for both strains. From the wild type image (A), the different shapes that cells may adopt in a pseudohyphal state can also be highlighted, including polar and axial growth.

A total of 10018 cells from the wild type strain and 15204 cells from the *Δtec1* strain were analyzed. For each isolated assay, the percentage of pseudohyphal cells was computed for each strain, by counting the number of cells contained in each filament. The deletion of *CgTEC1* gene was shown to results in a 72% decrease in the percentage of pseudohyphae cells in the overall population (**Figure 14**). Despite these observations, pseudohyphal differentiation was not yet reported as required for development of *C. glabrata* biofilms, as it is for *C. albicans*.

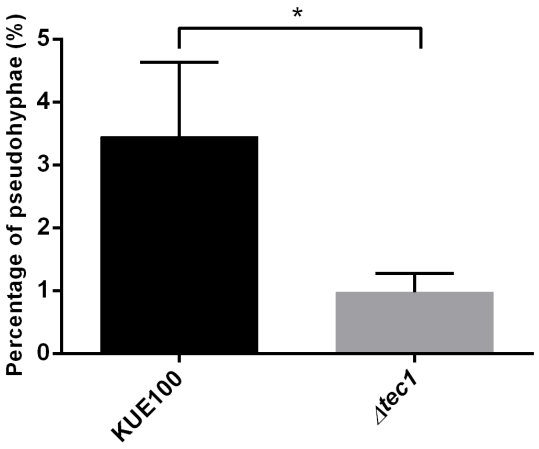


**Figure 14- The transcription factor Tec1 plays a role in pseudohyphae differentiation in *C. glabrata* cells. Average percentage of pseudohyphal formation by *C. glabrata* KUE100 and Δtec1 after 48 h of cellular growth in medium supplemented with 0.5 % (v/v) isoamyl alcohol.** The displayed pseudohyphal percentage was calculated by the average of pseudohyphal cells of four independent experiments in relation to the total cells observed in each experiment, standard deviation being represented by the error bars. *$P$<0,05.

### 3.4- Nuclear accumulation is not an activation mechanism of Tec1 transcription factor

One of the activation mechanisms known to modulate the activity of TFs is its accumulation to the nucleus where it can bind to the target genes, in response to some condition.[102] To evaluate if this could be one of the mechanisms of activation of Tec1 its subcellular localization was assessed, using a GFP fusion. *C. glabrata* cells expressing the *CgTEC1_GFP* fusion gene were evaluated under control conditions, that is in planktonic cultivation, when compared to the expected activating conditions, that is during biofilm development.

To observe the subcellular localization of the TF Tec1, *C. glabrata* cells harboring the pGREG576 plasmid (L5U1+vv) and cells harboring pGREG576_*PDC1_CgTEC1* plasmid (L5U1+*CgTEC1*) were grown in SDB medium and subcellular localization was assessed in planktonic cultivation, and during the early stage (6 h) and the mature phase (24 h) of biofilm formation. *C. glabrata* cells expressing Tec1_GFP fusion protein were observed by fluorescence microscopy. **Figure 15** represents the cells that could be observed under the microscope, as 6 h biofilms did not present significative changes in fluorescence of the cells, these are not shown in the figure.

.

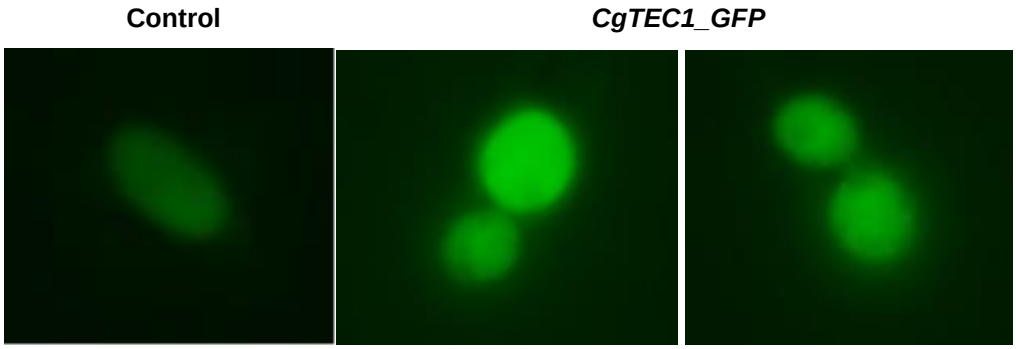


**Figure 15- The transcription factor Tec1 does not accumulates in the nucleus upon 24 hours of biofilm formation.** Fluorescence of exponential-phase *C. glabrata* L5U1 cells harboring either the cloning vector pGREG576 (control) or the pGREG576_*PDC1_CgTEC1* (*CgTEC1_GFP*) after 24 h of recombinant protein production in biofilm growth. The results indicate that the *CgTEC1-GFP* fusion protein localizes to the whole *C. glabrata* cells.

The GFP fluorescence is observed to fill the entire cell in all tested conditions, suggesting that Tec1 activation does not involve nuclear accumulation.

## 3.5- Transcriptomics analysis of the role of Tec1 in biofilm formation

Herein, the effect of *Δtec1* deletion in the transcriptome-wide response of *C. glabrata* cells to biofilm growth was assessed through RNA-sequencing. The RNA-seq analysis started with the global gene expression changes observed in cells cultivated as biofilm for 24 h, when compared to the gene expression profile of planktonic cultivation. This was followed by the analysis of the genes whose expression was found to be controlled by Tec1 in biofilm cells. The most significant differentially expressed genes in the wild-type strain grown in biofilm relatively to planktonic growth are displayed in **Table A1**, while those differentially expressed in the *Δtec1* mutant relatively to the wild-type strain in biofilm growth are displayed in **Table A2**. The complete datasets are provided in supplementary material.

### 3.5.1- Transcriptome-wide changes occurring upon 24 h of biofilm formation: general features

RNA-seq analysis was used for the comparison of the transcriptome of biofilm cells, cultivated in SDB medium for 24 h in polystyrene dishes, in relation to the same cells grown in planktonic conditions, in the same medium.

A total of 3070 genes were found to have altered expression levels. Among these, 1565 were found to be up-regulated and 1505 down-regulated upon 24 hours of biofilm formation. Since the C. glabrata genome includes 5293 identified ORFs, these numbers highlight the tremendous changes that *C. glabrata* cells must undergo during biofilm development, suggesting also a high degree of transcription regulation complexity.

In order to uncover the main biological processes underlying biofilm formation, the up- and down-regulated genes were clustered by biological function. This was performed based on the description of the *C. glabrata* genes, found on CGD and, for the large number of uncharacterized genes, based on the description of ortholog genes in *S. cerevisiae* or in *C. albicans*, as registered in SGD or in CGD, respectively. This strategy was adopted due to the lack of specific enriched GO terms, given by the Gene Ontology term enrichment analysis, using the Gene Ontology (GO) term finder from CGD. The retrieved GO terms involved mostly processes related to "RNA metabolic process", but also other general processes as "transport" or "regulation of biological process". The poor GO term enrichment results are likely due to the large number of genes under analysis, which are related to many pathways linked to the different biological functions present in a living cell.

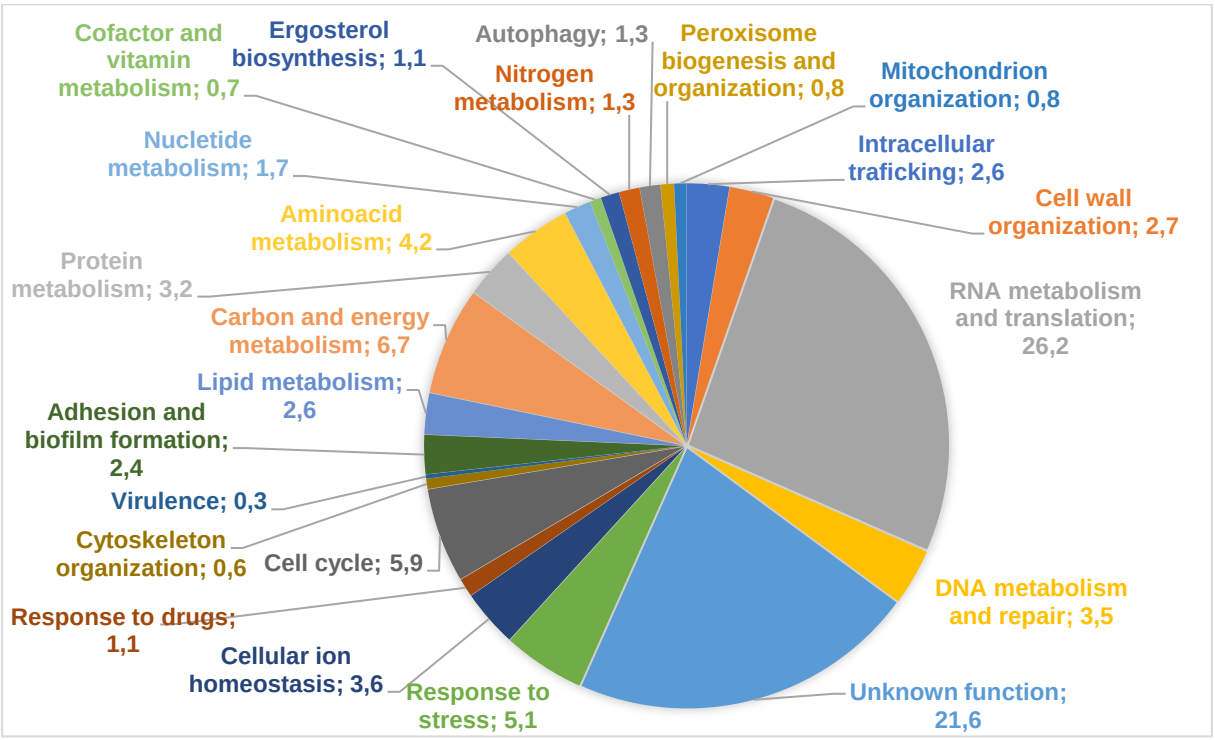


**Figure 16- Categorization and frequency of the genes up-regulated in *C. glabrata* cells upon 24 hours of biofilm growth, given by the wild-type cells grown in biofilm in relation to wild-type cells grown in planktonic conditions, based on the biological process taxonomy of gene ontology (*P*-value<0.05).**

**Figure 16** displays the main biological functions of the 1565 up-regulated genes, which were: "RNA metabolism and translation" (26.2%), "Unknown function" (21.6%), "Carbon and energy metabolism" (6.7%), "Cell cycle" (5.1%) and "Response to stress" (5.1%). Among the 1505 down-regulated genes, the more enriched were: "RNA metabolism and translation" (13.5%), "Unknown function" (12.8%), "Cell cycle" (12.2%), "Intracellular trafficking" (9.6 %), "DNA metabolism and repair" (9%), "Carbon and energy metabolism" (7.4%) and "Protein metabolism" (7.5%) (**Figure 17**).

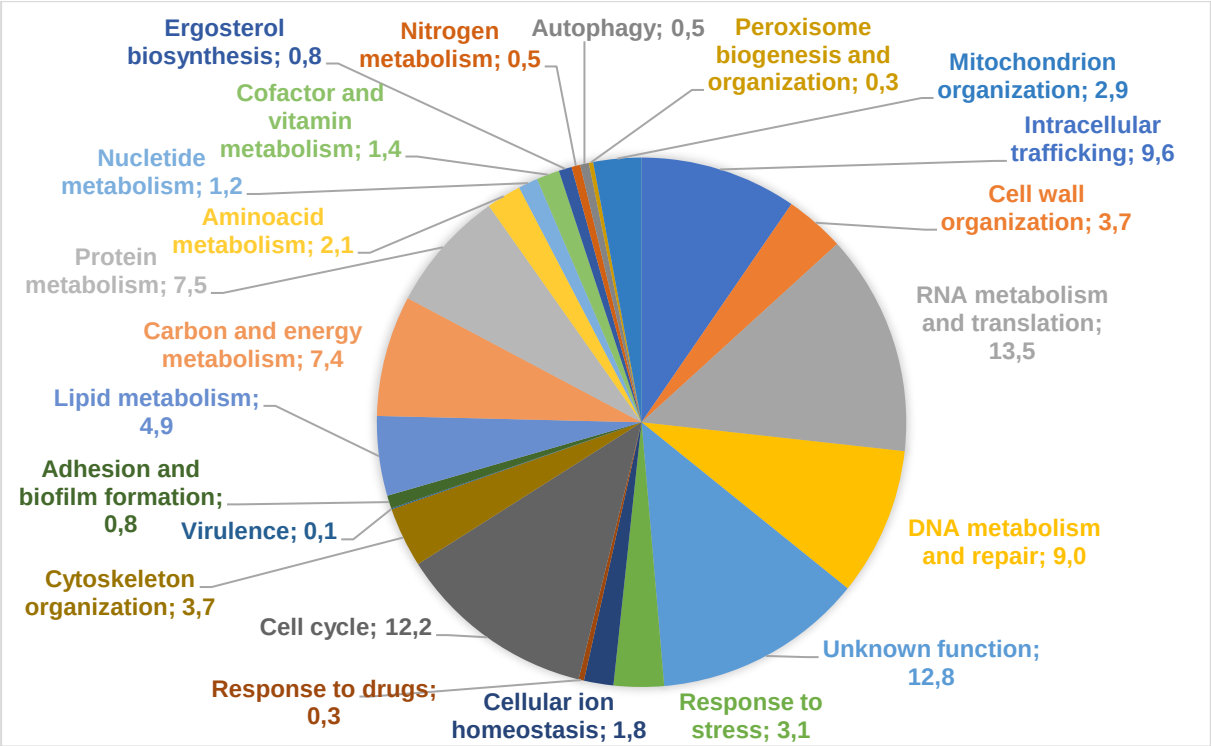


**Figure 17- Categorization and frequency of the genes down-regulated in *C. glabrata* cells upon 24 hours of biofilm growth, given by the wild-type cells grown in biofilm in relation to wild-type cells grown in planktonic conditions, based on the biological process taxonomy of gene ontology (*P*-value<0.05).**

An initial investigation into the transcription profiles of *C. albicans* biofilms grown in plastic surfaces was performed by García-Sánchez *et al.* (2004)[103] which revealed gene expression in biofilm cells significantly differ from gene expression in planktonically grown cells. This study was performed with different biofilm-forming conditions, including 72 h of biofilm formation in microtiter plates. Transcriptome profiles were determined using macroarrays with probes for 2002 ORFs randomly chosen as representing the whole genome of *C. albicans*. The authors found a 325 genes, within a total of 1850 tested. These genes were then assigned to 25 functional groups based on homology to *S. cerevisiae* genes. Among these, the most relevant functional groups were found to be “Amino acid metabolism”, “Nucleotide metabolism”, “Lipid, fatty acid, and isoprenoid metabolism”, “Transcription”, “Protein synthesis”, “Cell fate”, “Control of cellular organization”, “Subcellular localization” and “Unclassified”. Considering our RNA-seq results, the functional groups that we found to be more enriched in both up and down-regulated genes were “RNA metabolism and translation” and “Unknown function”, which is consistent with what was observed by García-Sánchez *et al*. Nevertheless, our findings differ in the most important groups, concerning “Cell cycle”, “Intracellular trafficking”, “DNA metabolism and repair”, “Carbon and energy metabolism” and “Response to stress”, which can be explained by the variance between species, the large number of 741 genes that were not distributed by having no homology to *S. cerevisiae*, and at last the number of genes under study only comprised roughly 1/3 of *C. albicans*

genome, which may have influenced the overall perception of the transcriptional behavior of the biofilm cells.

A more recent investigation on the transcriptional consequences of biofilm formation in *C. albicans* conducted by Nett *et al.* (2009)[104] was carried out with an *in vivo* central venous catheter model at two time points, 12 and 24 hours of biofilm formation. Oligo microarrays and RT-PCR were used to measure RNA abundance, and these were compared with the ones obtained with *in vitro* grown planktonic cells. Since our RNA-seq analysis was carried out with a mature biofilm stage (24 h), the following comparison will focus on the 24 hours' results. Among all the 6354 genes under study, the results obtained with the 24 hours biofilms revealed that 1034 transcripts (16.3%) were differentially regulated, including 523 up-regulated and 511 down-regulated genes. The functional groups found to be enriched in the up-regulated gene list were "Unknown function", "Transcription and protein synthesis", followed by "Energy and metabolism", "Transport", "DNA/cell cycle", and "Carbohydrate processing". Again, the abundancy of genes related to RNA metabolism in our study is in agreement with Nett *et al.* (2009) findings. Additionally, there were many genes with no attributed function. Other consistent up-regulated gene clusters were related to cell cycle and energy and carbohydrate metabolism. The up-regulation of carbohydrate metabolism might not only serve for energy purposes but also for EPS biosynthesis, which is corroborated by the extensive accumulation of ECM material already observed to be characteristic of the final maturation step of *Candida* biofilms.[105] However, we have found stress response as one of the most important biological functions attributed to a large number of up-regulated genes in biofilm, and the same did not happen in Nett *et al.* study. Considering that *C. glabrata* biofilms are characterized by having about half of the thickness of *C. albicans* biofilms, these might be more easily exposed to stress conditions induced by fluctuations in the surrounding environment, leading to a stronger defense mechanism that requires the activation of stress response-related genes.

Lastly, Nett *et al.* (2009) described "Unknown function", "Transcription and protein synthesis", "DNA/cell cycle" and "Transport" as the most down-regulated genes enriched functional groups, as observation which is in agreement with our observations. It is important to highlight the huge number of genes with no attributed biological function present in both the discussed studies and our work. This can be explained by the lack of homology with *S. cerevisiae* or *C. albicans* genes and by the very high number of genes that remain uncharacterized, in both *C. albicans* (70%) and *C. glabrata* (95%) genomes.

The following section will focus on the analysis of selected gene clusters, based on their foreseen importance in biofilm formation.

3.5.1.1- Up-regulation of adhesion-related genes in biofilm cells

One of the most important *C. glabrata* biofilm-establishment factors is its capacity to adhere to a host surface or abiotic medical device and the subsequent formation of a biofilm.[27] Such properties were expected to be found in the present transcriptomic analysis, where a significant number of adhesion-related genes were up-regulated in biofilm cells. These comprised genes encoding members of cluster I Epa adhesins: *CgEPA1*, *CgEPA2*, *CgEPA3*, *CgEPA9*, *CgEPA10*, *CgEPA12*, *CgEPA20*, *CgEPA23*; followed by cluster II Pwp adhesins: *CgPWP1*, *CgPWP2*, *CgPWP3*, *CgPWP5*; cluster III adhesins: *CgAED1* and *CgAED2*; and cluster IV Awp adhesins: *CgAWP1*, *CgAWP3*, *CgAWP4*, *CgAWP6*, *CgAWP13*. Other important up-regulated genes are *SNF2* encoding a component of the chromatin remodeling Swi/Snf complex, and *CgCST6* encoding a bZIP domain-containing protein involved in the negative regulation of *CgEPA6*.

Kraneveld *et al*. (2011)[27] conducted a study that aimed to disclose the level of gene expression and cell wall incorporation of adhesins in *C. glabrata* biofilm cells with 24 hours of biofilm development, in comparison to planktonically grown cells. In this study, tandem mass spectrometry allowed the identification of six adhesins in *C. glabrata* cell walls: Awp2, Awp4-6, Epa3 and Epa6. Then, expression levels of these and other relevant adhesins (*CgEPA1, CgEPA3, CgEPA6, CgEPA7, CgEPA22, CgAWP1, CgAWP2, CgAWP3, CgAWP4, CgAWP5, CgAWP6, CgAWP7*) were investigated through real-time qPCR analysis. The results showed a significant up-regulation of most adhesin genes, except for *CgEPA6* and *CgAWP2*, which were shown to be abundantly present in planktonic cultures as well. This is consistent with our transcriptomic data, where *EPA6* and *AWP2* genes appear not to suffer changes in expression.

As already discussed in the Introduction section of the thesis, Swi/snf complex negatively modulates sub-telomeric gene expression either through interaction with components of the silencing machinery or TFs necessary for the activation of *CgEPA* genes. The up-regulation of the Swi/Snf complex component *CgSNF2* gene is explained here as many of the adhesin genes analyzed in this study are located at sub-telomeric loci and thus possibly subjected to transcriptional regulation by this complex. On the other hand, the *CgCST6* gene up-regulation might act to moderate *CgEPA6* gene transcription, since it was observed not to follow the increase of other adhesins expression on 24 h biofilms.

Two other ORFs with a predicted role in adhesion, *CAGL0M01716g* and *CAGL0M07634g*, were found to be up-regulated. They encode, respectively, the predicted *C. albicans* Tec1 and Efg1 orthologs. These are known TFs recently found to incorporate the biofilm formation transcriptional network in *C. albicans*.[58] The *CgTEC1* (ORF *CAGL0M01716g*) gene holds the first place of the most up-regulated genes in the ”Adhesion and biofilm formation” cluster, while the expression of its predicted paralog encoded by ORF *CAGL0F04081* (*CgTEC2* gene) remained constant. This is consistent with the results obtained in our group, which revealed no significant decrease in biofilm formation upon *CgTEC2* deletion. A similar observation was made regarding the *CaEFG1* orthologs in *C. glabrata*. *CgEFG1* (*CAGL0M07634g*) was demonstrated to be up-regulated in biofilm cells and required for its formation,

while *CgEFG2* (*CAGL0L01771g)* showed no role in biofilm formation and no change in expression in biofilm cells.

3.5.1.2- Amino acid and nitrogen metabolism genes are differentially expressed in biofilm cells

The expression of 127 genes related to amino acid and nitrogen metabolism were found to be changed in cells undergoing biofilm formation, when compared to planktonic cells, including 86 up-regulated and 41 down-regulated genes. In order to understand the role of these gene expression changes in the biofilm development context, KEGG PATHWAY tool (https://www.genome.jp/kegg/pathway.html) was used (**Figure 18**). The up-regulated genes (represented by the green and yellow arrows in **Figure 18**) are mostly involved in the biosynthesis of positively charged histidine and arginine amino acids, but also phenylalanine, threonine and aspartate. Additionally, there seems to be up-regulation of some deamination steps that lead to the formation of pyruvate from alanine, glutamate from glutamine, 2-oxoglutarate, 2-oxoisovalerate and 3-methyl-2-oxopentanoate. Interestingly, these α-oxoacids and other intermediates might be accumulating since its conversion to the respective amino acid (amination steps) is down-regulated, as for example valine, leucine, isoleucine and proline. Other down-regulated genes interfere with the biosynthesis of the sulfur-containing amino acids cystein and methionine, along with lysine and glycine. Overall, these results suggest that biofilm cells might be experiencing lack of available nutrients within the biofilm, including to nitrogen limitation/starvation. This is likely a consequence of the thick cell layers and ECM that characterize biofilms, leaving at least the most inner cells with decreased access to the nutrients in the media. As a consequence, cells might be going through a metabolic shift that favors the energetic metabolism instead of the biosynthesis of amino acids.

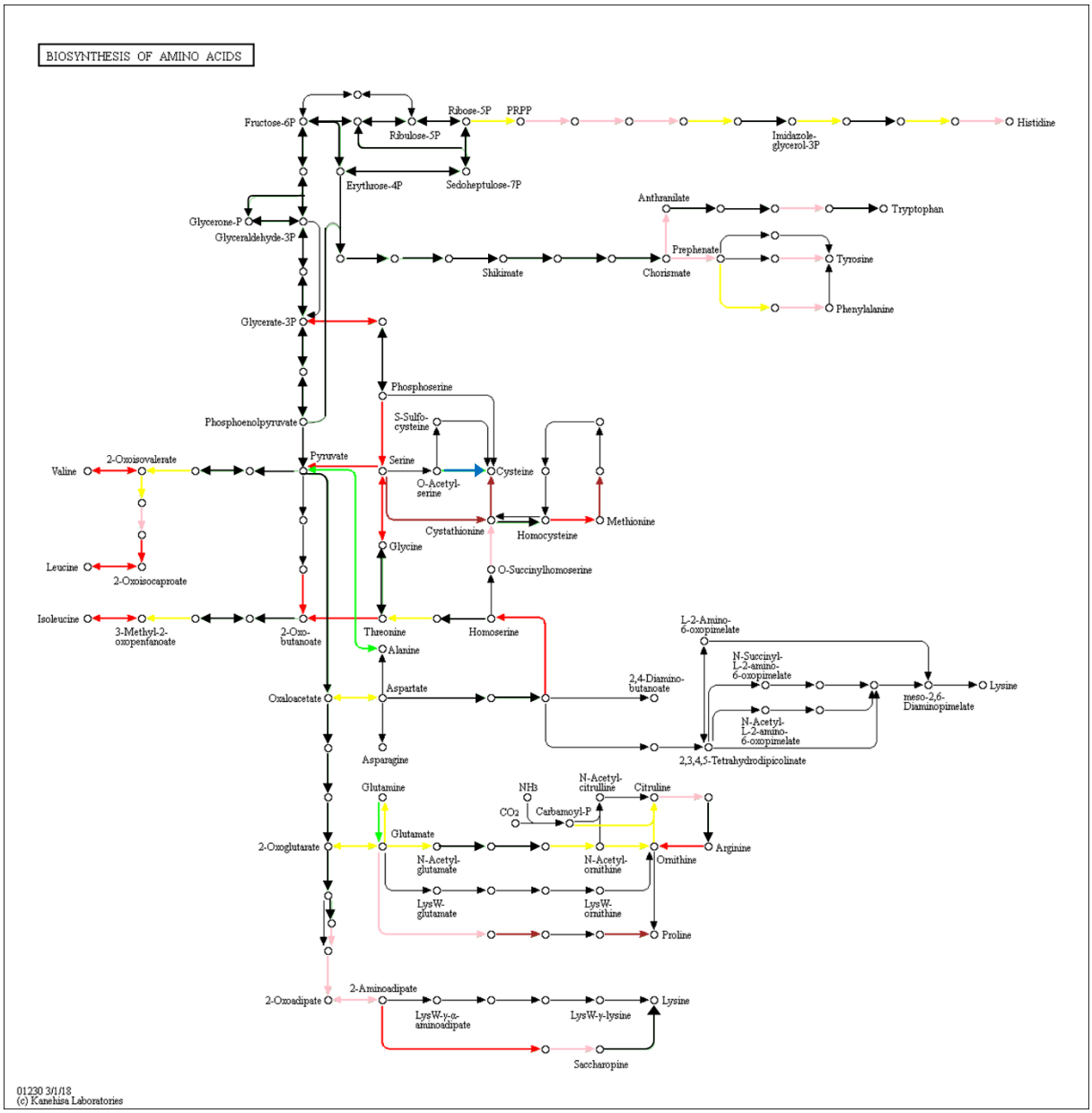


**Figure 18- Distribution of differently expressed genes in wild-type biofilm vs planktonic growth and *Δtec1* vs wild-type biofilm cells, identified by RNA-seq analysis to be related to amino acid biosynthesis.** Green and red arrows: genes found, respectively, up- and down-regulated in both wild-type biofilm vs planktonic growth and *Δtec1* vs wild-type biofilm cells datasets; yellow and brown arrows: genes found, respectively, up- and down-regulated in the wild-type biofilm vs planktonic growth dataset; blue and pink arrows: genes found, respectively, up- and down-regulated in the *Δtec1* vs wild-type biofilm cells dataset. The image was retrieved in https://www.genome.jp/kegg/pathway.html.

A very interesting study by Rajendran *et al*. (2016)[107] describes the central metabolic pathways driving biofilm heterogeneity, through a RNA-seq analysis to 24 h grown biofilms of high and low biofilm forming isolates. By resorting to an integrated KEGG pathway analysis, the authors identified amino acid, pyruvate and fatty acid metabolism pathways to be crucial in high biofilm forming isolates. Genes related to arginine, proline, purine, alanine, aspartate and glutamate metabolism were shown to be up-regulated. Except for proline, this goes in agreement with our obtained results. The exact mechanisms

regulating this amino acid metabolism are not clear yet, nevertheless, the general amino acid control response transcription factor Gcn4 is known to be activated upon amino acid starvation, and this is required for normal biofilm formation in *C. albicans* and *S. cerevisiae.* Although *CgGCN4* gene remains uncharacterized, this is found up-regulated in *C. glabrata* biofilm cells in the present study.

Furthermore, a study carried out by Yeater *et al*. (2007) intended to identify the changes in gene expression in three *C. albicans* biofilm developmental phases: early (6 h), intermediate (12 h), and mature (48 h).[108] Similar to the studies of García-Sánchez *et al.* (2004) and Murillo *et al*. (2005), the authors report differential regulation of genes involved in the synthesis of branched-chain amino acids, glutamate and glycine. According to our data, the glutamate biosynthetic pathway from glutamine is up-regulated, but the glycine biosynthesis is down-regulated. Additionally, biosynthesis of the branched-chain amino acids valine, leucine and isoleucine is down-regulated in our data. Interestingly, these down-regulated genes are all involved in amination steps of the respective α-oxoacid precursors, which is consistent with the hypothesis of nitrogen starvation experience.

Lastly, considering the *in vivo* study carried out with *C. albicans* biofilms by Nett *et al.* (2009), changes in expression of genes involved in methionine and cysteine biosynthesis were predominant in early and intermediate stages of biofilm growth, but not in mature biofilms. Instead of these, mature biofilms were found to activate genes encoding amino acid permeases, such as *CaDAO2, CaDIP5, CaGAP6,* and *CaGNP1*. In our RNA-seq data, only the *C. glabrata* ortholog *CgDIP5* is present, and found up-regulated. However, from a total of 66 up-regulated genes related to amino acid metabolism, 22% codify for amino acid transporters: *CAGL0L07546g, CAGL0B04455g, CAGL0J08162g, CAGL0D02178g, CgDIP5, CAGL0A02508g, CAGL0J08184g, CAGL0I07689g, CAGL0K05753g, CgCYN1, CAGL0L06710g, CgGAP1, CAGL0E05632g, CAGL0K10362g, and CAGL0H08393g*. The idea that increased intracellular levels of pyruvate, pentoses and amino acids in early biofilms contributes to increased biomass in maturation phase is consistent with Yeater *et al*. (2007) and Nett *et al.* (2009) findings.[107,108]

The functional group of “Nitrogen metabolism” comprise 20 up-regulated genes from a total of 28 genes found to be differentially expressed under biofilm growth conditions. The activated genes are mainly composed of ammonium and polyamine encoded transporters. *CgDUR3*, CAGL0H09152g, and *CgDUR31* genes are related to polyamine transport and the up-regulated genes that are involved in the ammonium transport are *CAGL0M03465g* (*ATO2*), *CAGL0A03212g* (*ScATO3*), *CAGL0I10747g* (*ScMPE1*)*, CgMEP2* and *CAGL0D04928g* (*Sc*). Altogether, our results from amino acid and nitrogen metabolism strongly suggest that *C. glabrata* is exposed to nitrogen limitation in mature biofilms.

3.5.1.3- Changes in carbon and energy metabolism gene expression during biofilm formation

As metabolic adaptation is a key process for biofilm cells[107], we wanted to investigate the transcriptional changes of genes related to carbon and energy metabolism. For this, KEGG PATHWAY tool (https://www.genome.jp/kegg/pathway.html) was again used to better understand the distribution of these genes on carbon metabolism pathways. **Figure 19** highlights the up-regulation of genes encoding glyoxylate cycle enzymes, and down-regulation of some glycolytic pathway related genes. This leads us to speculate that biofilm cells are suffering glucose deprivation and trying to use alternative carbon sources, such as the final products of β-oxidation.[104] β-oxidation is a multistep process in which fatty acid molecules are broken down by removing two-carbon units from the carboxyl-end of a fatty acid molecule to produce acetyl coenzyme A (acetyl-CoA). In fact, Nett *et al.* (2009) also noted an up-regulation of the glyoxylate cycle, specially the transcripts of *CaMLS1* and *CaICL1* genes, encoding respectively for malate synthase and isocitrate lyase enzymes. These were found 2.4- and 2.3-fold more abundant in mature biofilms. Our *C. glabrata* biofilm cells showed the orthologs of these genes *CAGL0L03982g* and *CAGL0J03058g* had its expression increased in 5.2- and 5.0-fold, comparing to cells grown in planktonic conditions.

As fatty acids are important constituents of lipids, they play diverse functions in the cells, from integrity and dynamics of cell membrane and adhesion to host cells, to energy storage.[107] To further investigate if biofilm cells are using fatty acids as an alternative to produce energy, the genes found to be associated to lipid metabolism were inserted in KEGG PATHWAY tool (**Figure 20**). Every step of long-chain fatty acid production was found to be down-regulated in biofilm cells, while the pathway leading to fatty acid degradation is up-regulated. The products of fatty acid β-oxidation can enter the glyoxylate cycle, thus supporting our hypothesis about the need of biofilm cells to use alternative carbon sources for energy purposes.

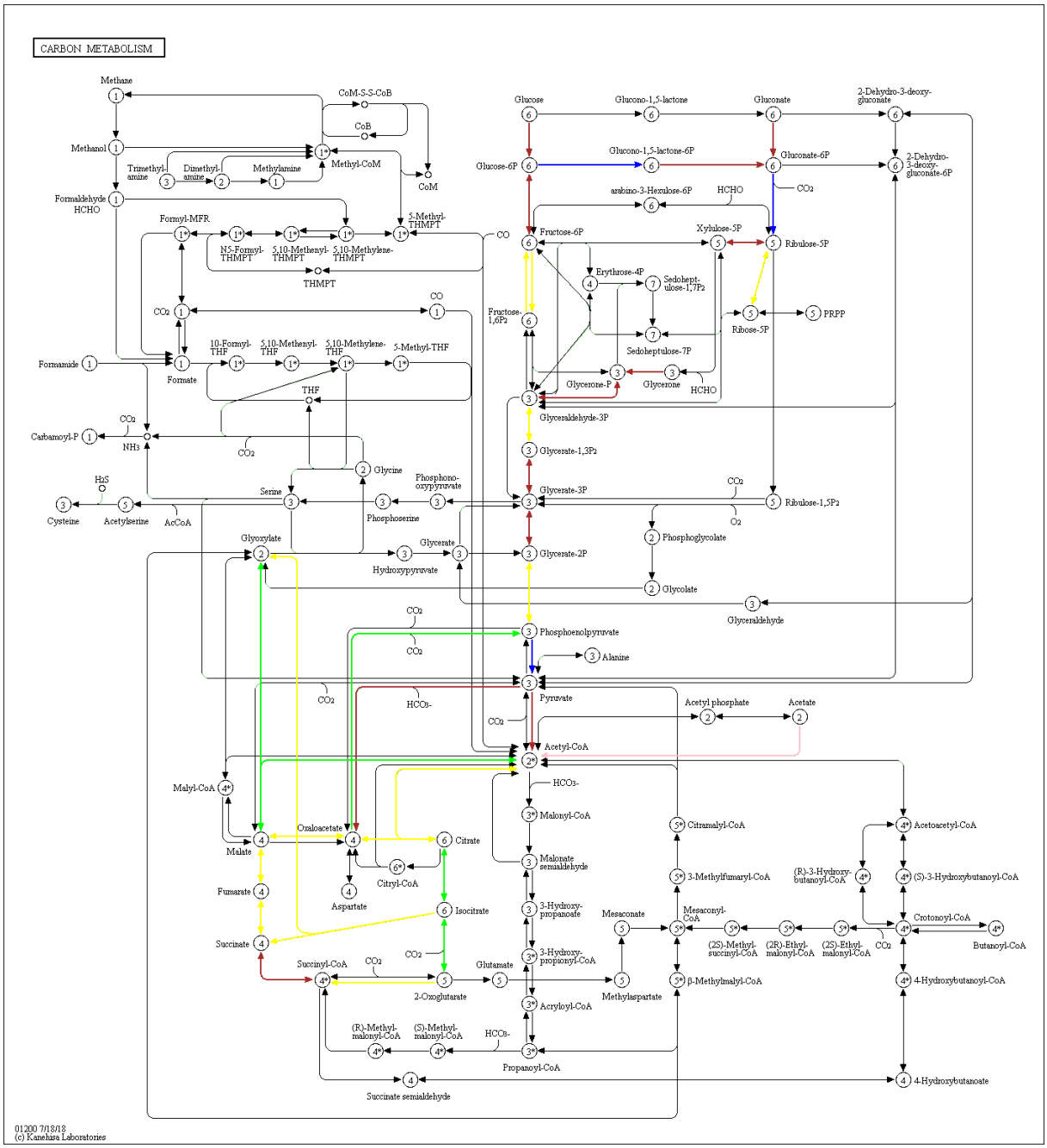


**Figure 19- Distribution of differently expressed genes in wild-type biofilm vs planktonic growth and *Δtec1* vs wild-type biofilm cells, identified by RNA-seq analysis to be related to carbon metabolism.** Green and red arrows: genes found, respectively, up- and down-regulated in both wild-type biofilm vs planktonic growth and *Δtec1* vs wild-type biofilm cells datasets; yellow and brown arrows: genes found, respectively, up- and down-regulated in the wild-type biofilm vs planktonic growth dataset; blue and pink arrows: genes found, respectively, up- and down-regulated in the *Δtec1* vs wild-type biofilm cells dataset. The image was retrieved in https://www.genome.jp/kegg/pathway.html.

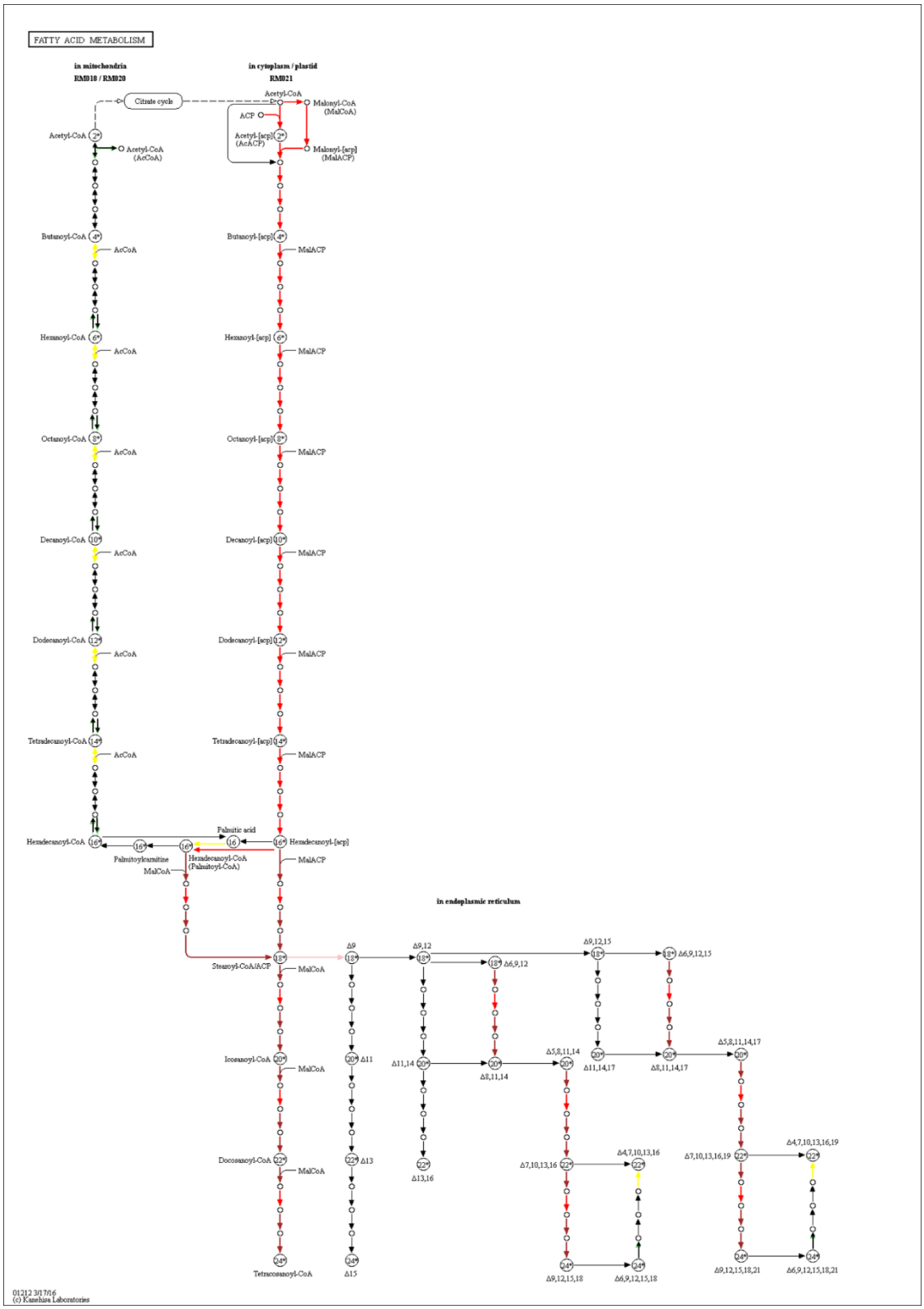


**Figure 20- Distribution of differently expressed genes in wild-type biofilm vs planktonic growth and *Δtec1* vs wild-type biofilm cells, identified by RNA-seq analysis to be related to fatty acid metabolism.** Green and red arrows: genes found, respectively, up- and down-regulated in both wild-type biofilm vs planktonic growth and *Δtec1* vs wild-type biofilm cells datasets; yellow and brown arrows: genes found, respectively, up- and down-regulated in the wild-type biofilm vs planktonic growth dataset; blue and pink arrows: genes found, respectively, up- and down-regulated in the *Δtec1* vs wild-type biofilm cells dataset. The image was retrieved in https://www.genome.jp/kegg/pathway.html.

Significantly, 13 out of the 18 genes required for the biogenesis of peroxisomes (the organelles where fatty-acid β-oxidation takes place), namely *CgPEX3, CgPEX5, CgPEX6, CgPEX10, CgPEX12, CgPEX21, CgPEX21B, CgPEX24, CgPEX25, CgPEX32, CAGL0D00352g, CAGL0M02387g, and CAGL0M03245g*, were found to be up-regulated in biofilm cells.

3.5.1.4- Genes related to ergosterol biosynthesis are found to be differentially expressed in biofilm cells

A total of 30 ergosterol biosynthesis-related genes were found to be differentially expressed in biofilm cells, including 18 up- and 12 down-regulated genes. These included mainly genes from the ERG gene family: *CgERG1*, *CgERG3*, *CgERG11*, *CAGL0F03861g* (ortholog of *CaERG12*) and *CAGL0K04477g* (ortholog of *CaERG25*) among the up-regulated, and *CgERG2*, *CgERG4*, *CgERG8*, *CgERG9*, *CAGL0L12364g* (ortholog of *CaERG10*), *CAGL0I02970g* (ortholog of *CaERG24*) and *CAGL0M11506g* (ortholog of *CaERG27*) among the down-regulated. Figure 21 schematically presents the distribution of the enzymes encoded by these genes in the ergosterol biosynthetic pathway (colored boxes). Biofilm growth appears to induce the transcription of some genes related to ergosterol biosynthesis, but on the other hand, other genes are down-regulated in these conditions. This prevented us from reaching a clear conclusion about the ergosterol content regulation in biofilm cells, when compared to cells grown in planktonic conditions.

In addition to ERG gene family, *CgAUS1* gene can also be found among the up-regulated genes in this dataset. *CgAUS1* gene encodes a plasma membrane sterol transporter of the ABC family of transporters. This is required for uptake of exogenous sterols and their incorporation into the plasma membrane. Furthermore, sterol uptake is required for the cell to grow in anaerobic conditions[67], since sterol biosynthesis requires oxygen. Therefore, the up-regulation of *CgAUS1* is in agreement with the idea that the most internal biofilm cells are subjected to low oxygen availability.

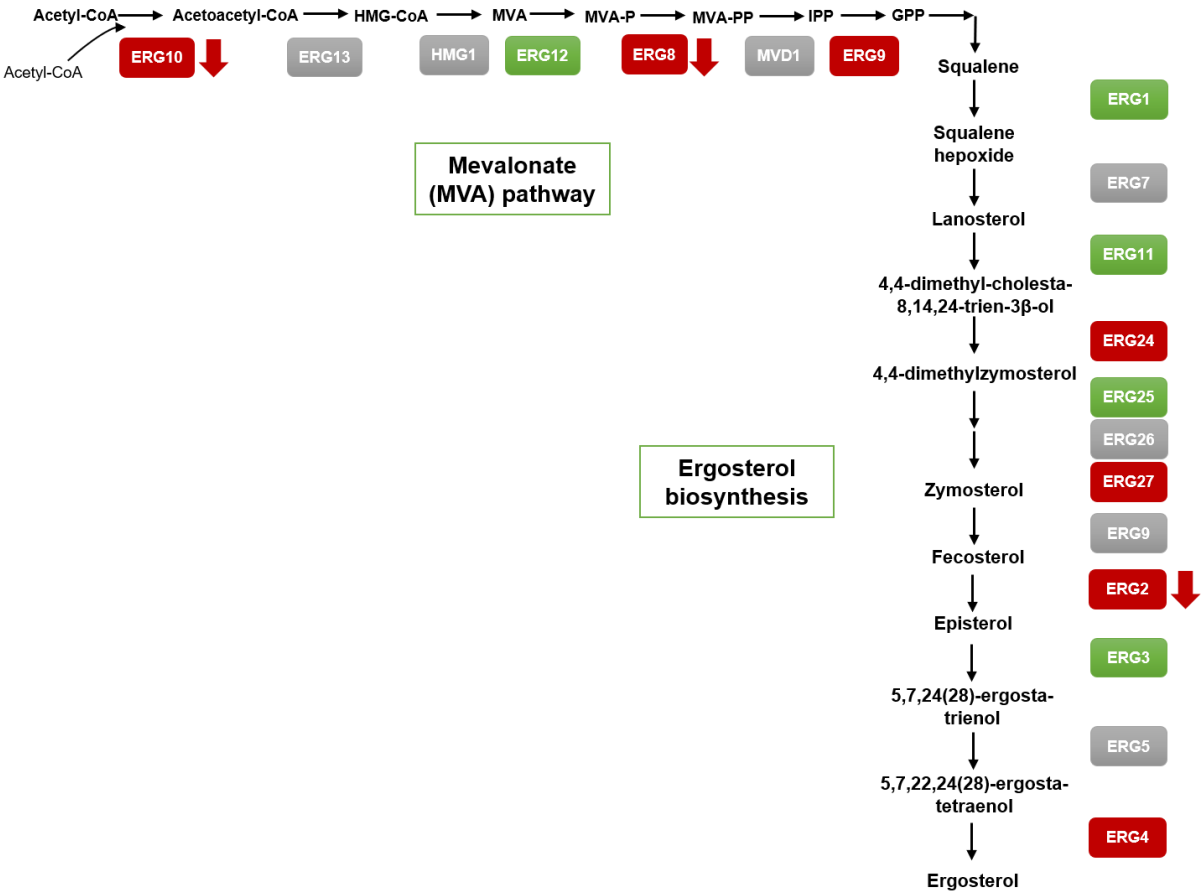


**Figure 21- Distribution of differently expressed genes in wild-type biofilm vs planktonic growth and *Δtec1* vs wild-type biofilm cells, identified by RNA-seq analysis to be related to ergosterol biosynthesis.** The genes found in the wild-type biofilm vs planktonic growth dataset are represented by the green (up-regulated) and red (down-regulated) boxes. The genes found in the *Δtec1* vs wild-type biofilm cells dataset are represented by the green (up-regulated) and red (down-regulated) arrows.

Some of the observations made in other studies with *C. albicans* are consistent with what we describe in this study relatively to ergosterol biosynthesis-related gene expression in biofilm cells. García-Sánchez *et al.* (2004) reported overexpression of *CaERG16* and *CaERG25* genes in 72 h *C. albicans* biofilms, whose orthologs in *C. glabrata* are *CgERG11* and *CAGL0K04477g*, both up-regulated in our dataset. Furthermore, Nett *et al.* (2009) also identified altered regulation of ergosterol and β-glucan pathways associated with *in vivo C. albicans* biofilm growth at both intermediate and mature phases. They found *CaERG25* gene to be up-regulated in the mentioned conditions, but down-regulation of *CaERG7* gene. *Ca*ERG7 ortholog in *C. glabrata CAGL0J10824g* was found to have no altered expression in 24 h biofilms, when compared to planktonic growth. The *C. glabrata* ortholog of *CaERG25*, *CAGL0K04477g* is a putative C-4 methyl sterol oxidase with a role in C4-demethylation of ergosterol biosynthesis intermediates. In fact, the up-regulation of genes intervening in intermediate steps of ergosterol biosynthesis is observed, which could lead to an accumulation of intermediate compounds. The authors proposed that *CaERG25* up-regulation may allow for increased conversion of lanosterol to nonergosterol intermediates, such as eburicol and 14-methyl fecosterol. However, there is still no attributed role for these intermediates.

3.5.1.5- Genes belonging to the functional group of cell wall metabolism present differential expression pattern

Fungal biofilm formation implies some structural changes at the cell wall level in order to allow cell-substrate and cell-cell adhesion. In this study, *C. glabrata* cells were found to change the expression of 98 genes related to cell wall organization during biofilm formation. These were used in KEGG PATHWAY tool to get further clues on their activity, and a pathway that stood out was the biosynthesis of GPI-anchor.

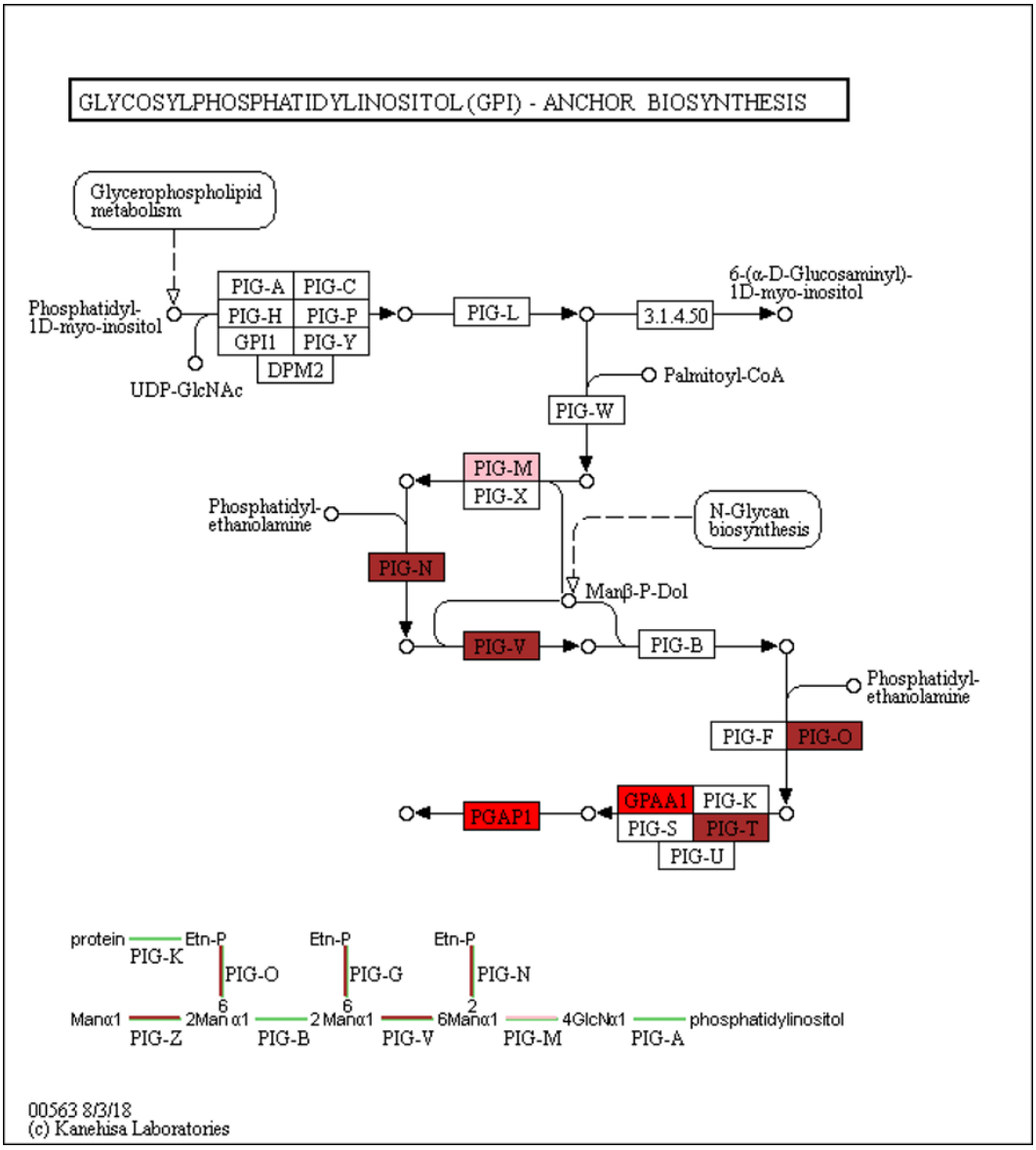


**Figure 22- Distribution of differently expressed genes in wild-type biofilm vs planktonic growth and Δtec1 vs wild-type biofilm cells, identified by RNA-seq analysis to be related to GPI-anchor biosynthesis.** Green and red arrows: genes found, respectively, up- and down-regulated in both wild-type biofilm vs planktonic growth and Δtec1 vs wild-type biofilm cells datasets; yellow and brown arrows: genes found, respectively, up- and down-regulated in the wild-type biofilm vs planktonic growth dataset; blue and pink arrows: genes found, respectively, up- and down-regulated in the Δtec1 vs wild-type biofilm cells dataset. The image was retrieved in https://www.genome.jp/kegg/pathway.html.

Significantly, all the differentially expressed genes involved in GPI-anchor biosynthesis are down-regulated in biofilm cells (**Figure 22**). Nett *et al*. (2009) also identified genes related to cell wall organization in both 12 h and 24 h *in vivo C. albicans* biofilms, however, only one was found to be involved in GPI-anchor biosynthesis, *CaCWH43*, which despite being found down-regulated in their study, in our data this gene was not differentially expressed. Moreover, Yeater *et al*. (2007) reported many GPI-linked cell wall protein genes among the up-regulated genes at both 6 h and 12 h time points of *C. albicans* biofilm formation. Considering these results, it leads us to speculate that GPI-anchor biosynthesis might be phase-specific, being required for the cell at earlier stages of biofilm formation, when cells need to adhere to a surface and to other cells. As biofilms develop, it might be advantageous for cells to be released and start colonizing other places, being associated to the final dispersal phase.

Another set of genes found in the cell wall metabolism cluster is composed of β-mannosyltransferase-encoding genes, such as *CgBMT1-4*, *CgBMT6* and *CgBMT7*. These enzymes were recently identified in several yeast species, including *C. albicans*, *C. glabrata* and *C. tropicalis*.[109] The central core of their cell walls is composed of branched β-(1,3)-, β-(1,6)-glucan linked to chitin via a β-(1,4)-glucan linkage. This structure is found close to the cell membrane, with chitin as the innermost element, and the β-(1,6)-glucan structure displayed outwards and being a linker to a mannose-rich glycoconjugate outer layer composed of PPM (phosphopeptidomannan, or just 'mannan'), mannoproteins and PLM (phospholipomannan). *N*- and *O*-linked mannans and the presence of β-mannosides (β-Mans) are major pathogen-associated molecular features and, along with β-glucans, are important for triggering host innate immunity.[110,111] *C. albicans* β-mannosyltransferases have been more extensively studied, being involved in transferring β-(1,2)-linked mannose units to β-(1,2) linkage-containing side chains, or attach β-(1,2)-linked mannose units to β-linked mannooligosaccharides. These enzymes were found to be encoded by nine *BMT* genes in this species.[112] From these, six were phenotypically analyzed and it was found that *CaBMT1* and *CaBMT3* act on the acid-stable moiety of PPM, *CaBMT2–4* on the acid-labile moiety of PPM, and *CaBMT5* and *CaBMT6* act on PLM.[111]

Jawhara, S. *et al.* (2012)[112] aimed to understand the role of β-Mans in *C. glabrata* colonization and virulence in a murine model of dextran sulfate sodium induced colitis, using *C. glabrata* strains deficient in five genes encoding β-mannosyltransferases. A western blot experiment showed a significant reduction in of β-(1,2)-mannoside residues in *Δbmt2-bmt6* cluster deletion mutant. Furthermore, *C. glabrata* wild-type strain in colitis mice models led to reduced survival rates, when compared to those infected with the mutant stain. Additionally, after 7 days of infection, lower numbers of colonies of *Δbmt2–6* cells were recovered from stools. Based on these observations, the authors report that these enzymes are determinant for *C. glabrata*'s capacity of gastrointestinal tract colonization. Overall, β-Mans were proposed to play an important role in colonization and virulence of *C. glabrata* cells. Besides these results, no studies have been yet conducted in order to disclose the possible involvement of *BMT* genes

in biofilm formation. However, it can be proposed a role in the a role in host recognition and adhesion process.

3.5.1.6- Activation of multiple stress-responsive genes during biofilm development

The expression of 80 genes related to stress response was found to be up-regulated in biofilm cells, when compared to those cultivated planktonically. These comprise diverse classes of stress response genes, including those encoding for heat-shock proteins, as *CgHSP12*, *CgSSA3, CgSSB2, CgPDR13* and *CgSSE*, and other chaperones, required for the response to protein denaturation and aggregation. A number of oxidative stress response genes (11 genes), such as two superoxide dismutase encoding genes, *CgSOD1* and the ortholog to *C. albicans CaSOD2* encoded in ORF *CAGL0E04356g*, and other genes responsible for maintaining the redox balance in the cell, as for example *CgTSA1*, *CgGSH1*, the ortholog of *C. albicans CaGRX3* encoded by the ORF *CAGL0G08151g* and *CgTRR1* genes, were also found to be up-regulated in biofilm cells. The up-regulation of these genes is consistent with the up-regulation of known stress response TFs, as Yap6, Yap7, Cad1 and Ap1, responsible for oxidative and metal stress response, Msn1 and Msn4, regulators of the general stress response, Rim101, Haa1, War1, involved in the response to acid/alkaline stress, Hac1, controlling the unfolded protein response and Hot1, regulator of the osmotic stress response.
From the observations of Nett *et all.* (2009), stress-responsive genes were also found to be up-regulated in both intermediate (12 h) and mature (24 h) biofilms. Several stress-responsive genes were also found to be up-regulated in biofilm cells by Yeater *et al*. (2007). Overall, the up-regulation of a large array of stress responsive gene suggest that *C. glabrata* biofilm cells, are either sensing environmental stress conditions, or, at least, prepared to deal with it, if it comes.

3.5.1.7- Genes encoding multidrug resistance proteins are up-regulated during biofilm formation

In this transcriptomic analysis some of multidrug resistance (MDR)-related genes were found to be up-regulated upon biofilm formation, namely some genes belonging to the Major Facilitator Superfamily (MFS) of MDR transporters that include *CgQDR2*[113], *CgAQR1*[114], *CgTPO1_2*[13] and *CgTPO3*[115], already described as being determinant of fungal drug resistance in *C. glabrata*, and two uncharacterized ORFs *CAGL0B02343g* (*ScATR1* homolog) and *CAGL0J00363g* (*ScYHK8* homolog) predicted to belong to this family of transporters. It is important to highlight that Tpo1_2 multidrug transporter was found to play a role in biofilm formation, as its deletion impaired *C. glabrata* biofilm development, although the underlying molecular connection is unclear.[13]
Among the down-regulated genes *CgCDR1* gene deserves particular attention. This gene encodes a major ATP binding cassette (ABC) drug efflux pump involved in azole resistance and it was reported in *C. glabrata* (similar to what was observed in *C. albicans*) to exhibit time-dependent increase on its

expression in biofilm cells. For instance, the levels of expression of this gene were investigated during the early (6 h), intermediate (15 h), and mature (48 h) phases of biofilm development. At 6 h and 15 h, the biofilms exhibited approximately 1.5- and 3.3-fold upregulation of *CgCDR1* when compared to planktonic cells.[63,104,116]

Nett *et al.* (2009) also reported the up-regulation of drug resistance-related genes in *in vivo C. albicans* biofilms. The authors report the up-regulation of *CaCDR2* at 12 h of biofilm formation, and of *MDR1* at both 12 h and 24 h. Interestingly, Mdr1 belongs to the Drug:H+ Antiporter family, displaying homology to the above referred MFS MDR transporters, whose gene expression was found to be up-regulated in *C. glabrata* biofilm cells. Moreover, Yeater *et al.* (2007) study highlights some genes encoding efflux pumps which were found differently expressed throughout the development of *C. albicans* biofilm, namely *CaQDR1,* which is the ortholog of *C. glabrata*'s *CgQDR2* up-regulated in our dataset; *CaNAG3/MDR97* and *CaCDR4*, both with no described orthologs in *C. glabrata.*

However, the reason why biofilm cells display increased expression of multidrug transporters in the absence of drug exposure is still unknown.

### 3.5.2- What is the role of the transcription factor Tec1 on *Candida glabrata* biofilm formation?

Given the importance of Tec1 in biofilm formation, the transcriptomic changes occurring during planktonic growth and after 24 hours of biofilm formation upon the deletion of *CgTEC1* were analyzed. The expression of a total of 417 or 1082 genes is affected by Tec1 in planktonic cultivation or in 24 h biofilm cells, respectively. Considering biofilm cells alone, 487 genes were found to be activated, while 595 genes were repressed by Tec1. Further grouping of the Tec1 regulated genes by its biological function allowed the construction of **Figures 23** and **24**. The most enriched groups among the up-regulated genes were: "Unknown function" (28%), "Response to stress" (8%), "Protein metabolism" (6%), "Cell cycle" (6%), "Carbon and energy metabolism" (6%) and "Cell wall organization" (5%) (**Figure 23**).

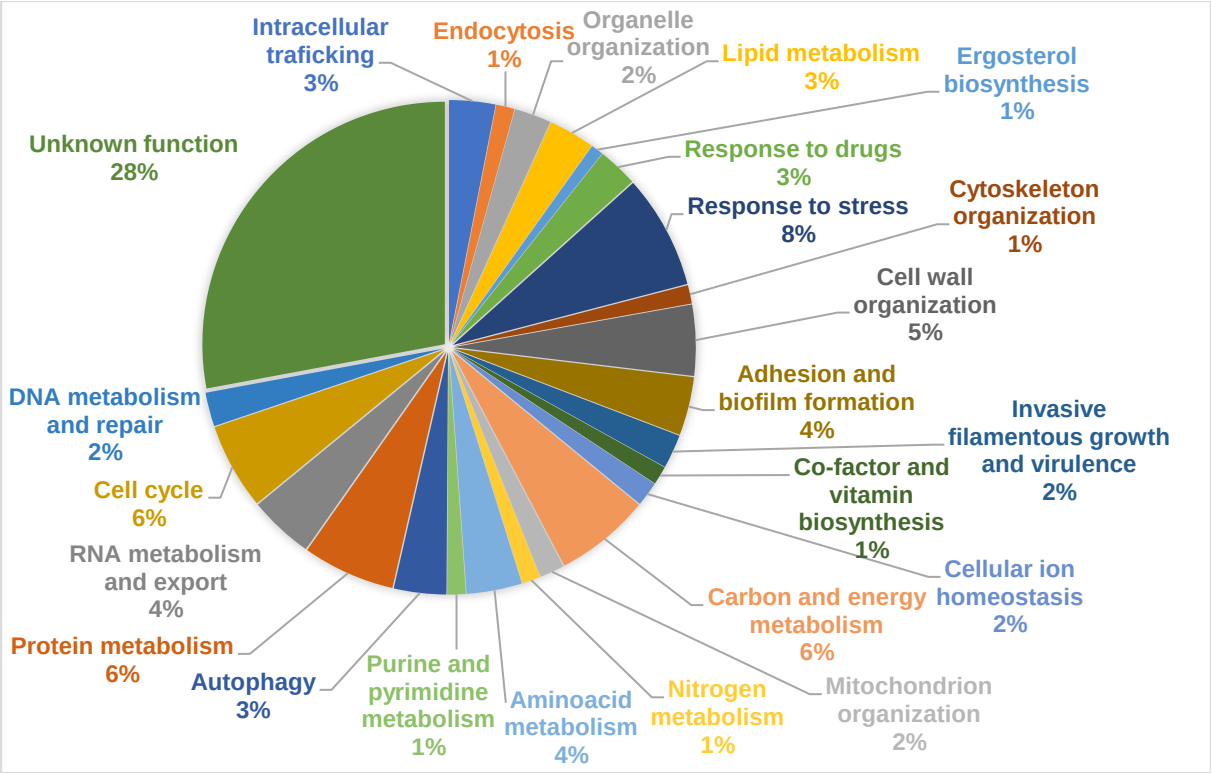


**Figure 23- Categorization and frequency of the genes up-regulated by Tec1 upon biofilm growth in *C. glabrata*, given by the *Δtec1 deletion mutant* cells in relation to wild-type cells grown in biofilm, based on the biological process taxonomy of gene ontology (*P*-value<0.05).**

The most represented biological functions among the down-regulated genes are: “Cell cycle” (15 %), “Unknown function” (12 %), “DNA metabolism and repair” (11%), “RNA metabolism and export” (8 %), “Amino acid metabolism” (7 %) and “Protein metabolism” (6%) (**Figure 24**).

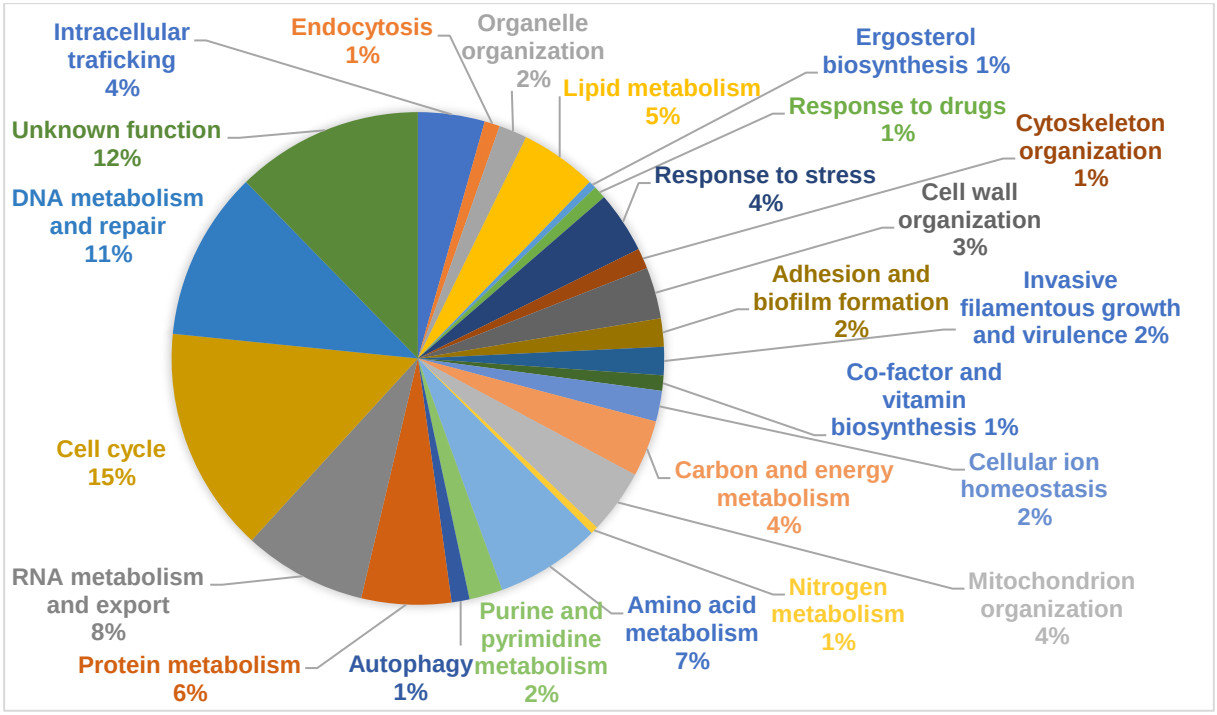


**Figure 24- Categorization and frequency of the genes down-regulated by Tec1 upon biofilm growth in *C. glabrata*, given by the *Δtec1 deletion mutant* cells in relation to wild-type cells grown in biofilm, based on the biological process taxonomy of gene ontology (*P*-value<0.05).**

Furthermore, it is important to evaluate especially whether Tec1 is responsible for activating the expression of genes found to be up-regulated in biofilm cells (**Figure 25**). From this analysis, it was possible to conclude that this TF contributes to the transcriptional remodeling of biofilm cells by positively regulating the expression of 389 out of the 1565 genes up-regulated in wild-type cells after 24h of biofilm formation. These 389 genes correspond to ¾ the total Tec1 up-regulated genes and about ¼ of the up-regulated genes in biofilm cells, highlighting the relevance of Tec1 in biofilm formation in *C. glabrata*. As expected, it can also be noted that Tec1 is responsible for the activation of much more genes in biofilm, than in planktonic growth.

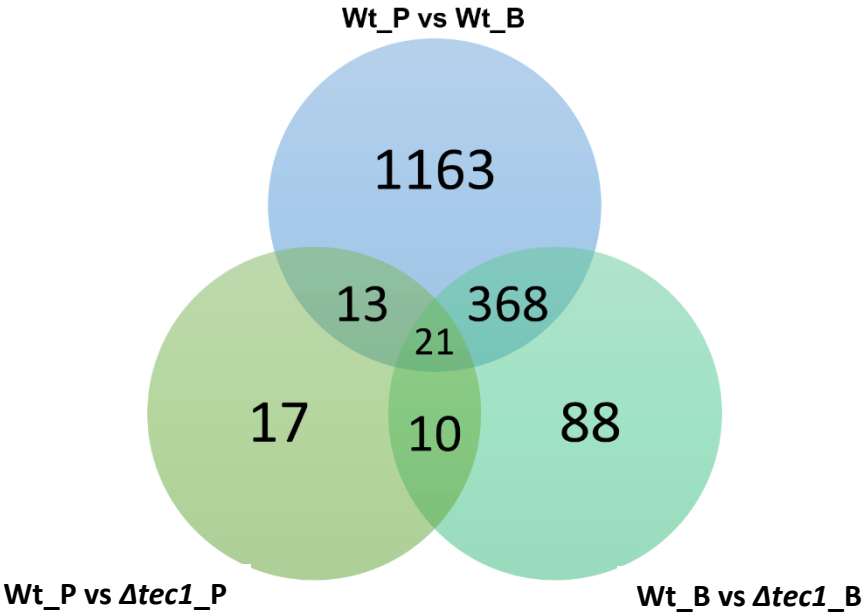


**Figure 25- Venn diagram exhibiting the intersection of the number of up-regulated genes from the three datasets under study.**

The 389 Tec1 activated genes found to up-regulated in wild-type cells grown in biofilm, when compared to planktonic growth, were then clustered according to their biological functions (**Figure 26**). The most relevant categories were found to be: “Unknown function” (30%), “Response to stress” (8%), “Protein metabolism” (6%), “Cell cycle” (6%) and “Carbon and energy metabolism” (6%).

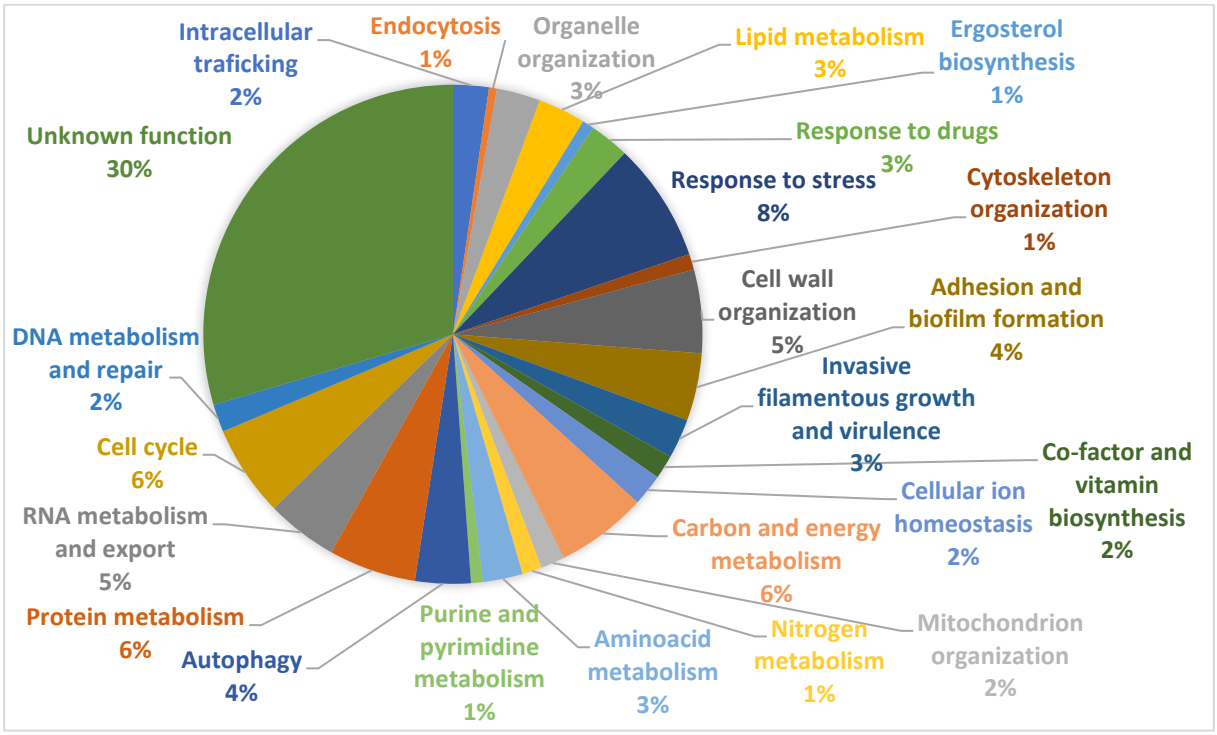


**Figure 26- Categorization and frequency of the Tec1 up-regulated genes in biofilm and up-regulated in cells under biofilm growth conditions, based on the biological process taxonomy of gene ontology (*P*-value<0.05).**

Altogether, the results suggest that the most important mechanisms underlying biofilm formation by the TF Tec1 *in C.* glabrata are mainly related to adhesion, amino acid and nitrogen metabolism, carbon source and energy metabolism, ergosterol biosynthesis, cell wall organization, stress response and multidrug resistance. In the next section, these selected functional groups are discussed in the context of their role in biofilm formation.

3.5.2.1- Tec1 controls the expression of adhesion related genes at different biofilm formation stages.

Among the 19 adhesion-related genes found to be activated by Tec1 during biofilm formation, there are six adhesin encoding genes: *CgAED1*, *CgAED2*, *CgAWP13*, *CgEPA9*, Cg*EPA10* and *CgPWP5.* Interestingly, Tec1 was also found to control the expression of the TF encoding gene *CgEFG1,* another key biofilm formation regulator in *C. glabrata*[117]. This complex regulatory association controlling biofilm formation seems to be similar to what was reported in *C. albicans*, where Tec1 and Efg1 were shown to be mutually controlling each other's expression during biofilm development.[71]

Biofilm formation is initiated when planktonic cells find a surface where they can adhere and take advantage of the nutrients and other advantages.[99] The ability to adhere is a fast process, and even though our transcriptomic analysis gives us information about the adhesion-related genes expression of a mature biofilm, it would also be interesting to explore the transcriptomic variations of genes known to be important for biofilm formation in *C. glabrata* cells during all its developmental process. Thereupon, in an attempt to understand the variation of the level of transcripts at different time points of biofilm development, correspondent to some of the most important adhesins found in this study to be strongly regulated in biofilm cells by Tec1 TF, we chose *CgAED2*, *CgPWP5* and *CgAWP13* genes to be quantified by RT-qPCR. Gene expression was measured in wild-type and *Δtec1* cells after 6 h, 24 h and 48 h of biofilm development (**Figure 27**).

The expression of *CgAED2*, *CgPWP5* and *CgAWP13* was found to increase progressively in the wild-type strain, as the biofilm develops overtime. The results can be interpreted as the growing need for the biofilm cells to attach to each other, as it starts growing and developing the thick cell layers that are characteristic of this species. On the other hand, in the absence of *CgTEC1* expression levels are kept in relatively low levels, even decreasing slightly with time, suggesting that Tec1 is a crucial intervenient in regulating the adhesion phenomenon, gaining importance especially in the later stages of biofilm formation.

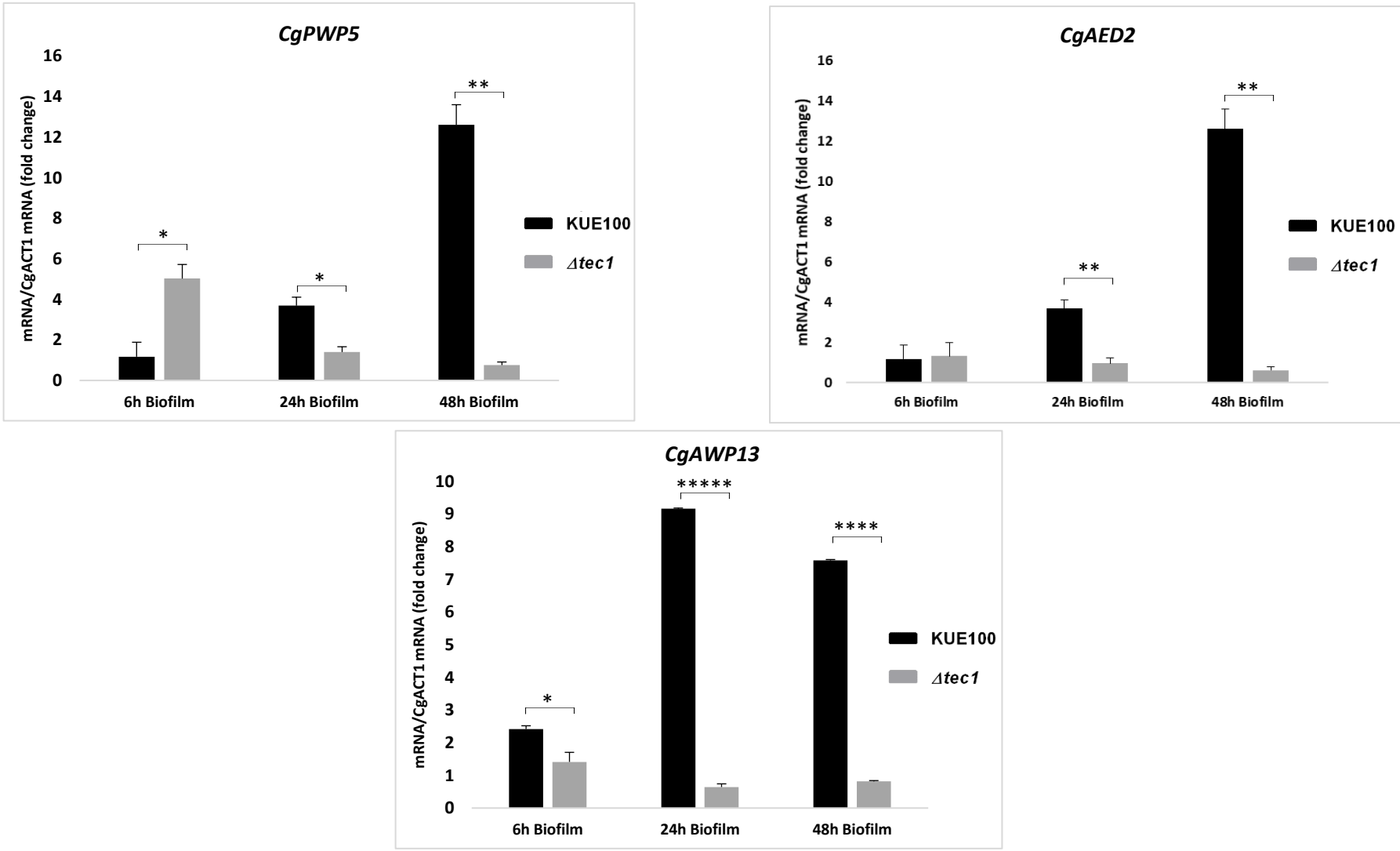


**Figure 27- The deletion of the *CgTEC1* gene leads to a biofilm evolution-related decrease in the expression of the adhesion encoding genes *CgPWP5*, *CgAED2* and *CgAWP13*.** Comparison of the variation of the *CgPWP5*, *CgAED2* and *CgAWP13* transcript levels in wild-type *C. glabrata* KUE100 cells and *Δtec1* deletion mutant cells, after 6 h, 24 h and 48 h of biofilm growth. The presented transcript levels were obtained by quantitative RT-PCR and are *CgPWP; CgAED2; CgAWP13 mRNA / CgACT1 mRNA* levels, relative to the values registered in wild-type cells after the chosen growth times. The indicated values are averages of at least three independent experiments. Error bars represent the corresponding standard deviations. **P*<0,05; ***P*<0,01; ****P*<0,001; *****P*<0,0001; ******P*<0,00001.

3.5.2.2- Tec1 controls the expression of genes related to amino acid and nitrogen metabolism

Another functional category found to be important in biofilm formation is amino acid and nitrogen metabolism, which holds 24 up- and 45 down-regulated genes, in a total of 69 genes controlled by Tec1. This TF appears as repressing, possibly in an indirect fashion, the biosynthesis of some amino acids, namely lysine, arginine, proline, methionine, serine, glycine, valine, leucine, isoleucine, tryptophan, tyrosine, phenylalanine and histidine. On the other hand, Tec1 activates a number of genes involved in glutamate, pyruvate and cysteine biosynthesis (Figure 18). Among the Tec1 regulated genes are *CAGL0B00286g* (*ScCHA1*), *LEU2*, *BAT2*, *CAGL0F01749g* (*CaSHM2*), *CAGL0K00825g* (with no described orthologs in *S. cerevisiae* and *C. albicans*), *MET6*, *CAGL0M12837g* (*ScSER33*), *HOM6*, *CAGL0J07062g* (*CaCAR1*) and *CAGL0K07788g* (*CaLYS2*), which are repressed by Tec1; and *CAGL0L12254g* (*CaALT1*), *GLT1* and *MET15*, which are activated by Tec1. Overall, Tec1 was found to control amino acid metabolism, partially contributing for the accumulation α-oxoacids, in response to nitrogen starvation.

3.5.2.3- Carbon and energy metabolism genes are regulated by Tec1

Wild-type cells showed a shift in energy metabolism during biofilm formation, probably to adapt to the microenvironment of the biofilm, where it is supposed to be lack of nutrients, including glucose. Our RNA-seq data shows that Tec1 is responsible for regulating 53 genes involved in carbon and energy metabolism. These were organized in KEGG PATHWAY software to better understand its impact on carbon metabolism pathways (Figure 19). Within the genes involved in carbon metabolic pathways, Tec1 was found to activate the expression of 7 genes: *ZWF1*, *GND1*, *CAGL0E05610* (*ScPYK2*), *CAGL0H06633* (*ScPCK1*), *CAGL0L03982* (*CaMLS1*), *ACO1*, *CAGL0B04917* (*CaIDP2*); and repress, possibly in an indirect fashion, 1 gene, CAGL0B02717 (*ScACS2*). The great majority of the Tec1 activated genes encode glyoxylate cycle enzymes. Moreover, Tec1 was found to exert a repressing effect over a great number of genes involved in long-chain fatty acid biosynthesis in biofilm cells (Figure 20). According to the information gathered in the PathoYeastract database, only the *C. albicans* orthologs *CIT1*, *CDC19* and *PCK1* were found to be under CaTec1 control in this species, driving us to conclude that Tec1 is not responsible for controlling carbon metabolism for energy production as it seems to happen in *C. glabrata*.

3.5.2.4- Tec1 contributes to decreased ergosterol content in *C. glabrata* biofilms

Ergosterol is the main sterol found in fungi and has been shown to be an important component of the cell membrane of biofilm cells and more recently proven to play a role on biofilm ECM composition.[46]

Tec1 was found, through RNA-seq analysis, to regulate the expression of 7 ergosterol biosynthesis-related genes (**Figure 21**). Tec1 seems to act on decreasing ergosterol biosynthesis through the repression of *CgERG2*, *CgERG8* and *CAGL0L12364g* (ortholog of *CaERG10*) genes in biofilm cells.
In an attempt to confirm these transcriptomic observations, and to uncover the final outcome of the changes in ergosterol biosynthesis genes found to be up- and down- regulated in biofilm cells (Section 3.5.1.4), total ergosterol was extracted from biofilm and planktonic cells and quantified by HPLC. The ergosterol of the mutant cells *Δtec1* was compared to that of the wild-type KUE100 strain (**Figure 28**).

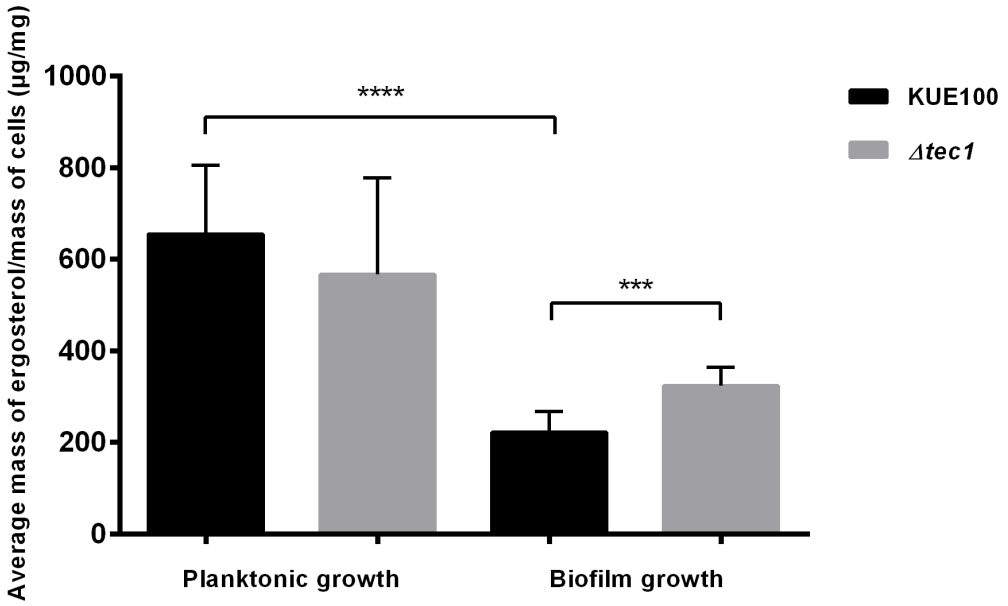


**Figure 28- The ergosterol content in yeast cells is reduced when grown in biofilm and Tec1 is predicted to play a role in ergosterol content reduction in biofilm.** Wild-type and single deletion mutant cells were harvested after 24 h of planktonic or biofilm growth and total ergosterol was extracted and quantified through HPLC. The displayed ergosterol content is the average of at least three independent experiments, standard deviation being represented by the error bars. ****P*<0,001; *****P*<0,0001.

From the ergosterol quantification results it is possible to ascertain that *C. glabrata* cells grown in biofilm suffer a significant reduction (almost 3-fold) of total ergosterol content. Additionally, Tec1 in fact acts on contributing for the reduction of ergosterol biosynthesis, as hypothesized by the RNA-seq data, as the deletion mutant cells displays a 31% increase on ergosterol content in biofilm cells. No significant differences were noted between both strains during planktonic growth.
The reduction of total ergosterol content in 24 h biofilm cells was observed in *C. albicans*, Fox et al. (2015) reported the down-regulation of genes related to ergosterol biosynthesis in mature biofilms.[118] Furthermore, *C. albicans* biofilms were observed to show high levels of ergosterol in early phases of biofilm formation, however this decreased in 50% when biofilms reached mature phase of growth. The same might be happening in *C. glabrata* biofilms.[108,119] Additionally, the low oxygen concentrations that the innermost cells might be subjected to may explain the need of these cells to control ergosterol biosynthesis. In this context, the observed decrease ergosterol content might be a required biofilm formation feature, which is favored by the presence of Tec1.

3.5.2.5- Tec1 controls the expression of genes involved in stress response

Tec1 seems to be determinant of cell defense against stress conditions, as this is the second most attributed biological function to the Tec1 activated genes. Tec1 activates 37 stress response genes, including the biofilm induced *HSP12* and *SSA5* encoding for chaperones involved in heat-shock response; *SOD1*, *CTA1*, *TSA1* and YHB1, encoding oxidative stress response enzymes; and *HAA1*, *HAP5* and *CNA1*, encoding TFs controlling various aspects of stress response.

The genes documented in PathoYeastract to be regulated by Tec1 in *C. albicans* biofilm cells comprise *HSP70* encoding a heat-shock protein, *GAC1* encoding a putative regulatory subunit of serine/threonine phosphoprotein phosphatase 1 involved in activation of heat-shock proteins, *SFL1* encoding a TF that negatively regulates flocculation and *YHB1* acting in nitric oxide scavenging/detoxification, which in our dataset appear as up-regulated by Tec1 in *C. glabrata* biofilm cells. Among the down-regulated genes of our dataset, *SKN7* required for oxidative stress response and *HSP70* encoding a heat-shock protein, were all found as also being regulated by Tec1 in *C. albicans*. Therefore, Tec1 is found in both species to be important in regulation of stress response of cells grown in biofilm.

3.5.2.6- Multidrug resistance genes are transcriptionally regulated by Tec1

Tec1 was also found to activate a subset of 13 MDR genes, including those encoding for the MFS of drug transporters: *TPO1_2*, *TPO3*, *QDR2*, *CAGL0B02079g* (ortholog of *ScAZR1*); and genes belonging to the ABC transporters superfamily, as *CDR1* and *PDH1*. Additionally, other Tec1 activates MDR genes include *CAGL0M10307g* (ortholog of *CaAUR1*) and *CAGL0G05566g* (ortholog of *CaFMP45*), both intervening on sphingolipid biosynthesis and cell wall organization, respectively. These results seem to propose a role for Tec1 on increasing *C. glabrata* cells' resistance to drugs, especially azoles. Yet the same role is not suggested for the CaTec1, as none of the *C. albicans* orthologs of the genes from this group appears to be activated by this TF in cells cultured under biofilm conditions, given by the PathoYeastract database.

### 3.6- Tec1 activated *CgAUR1*, *CgAED2* and *CgSUR2* genes also play a role in biofilm development

Among the Tec1 activated genes up-regulated in biofilm cells, 8 were selected for further analysis for a role in *C. glabrata* biofilm formation, namely *AED2*, *PWP5*, *AWP13* genes encoding adhesins; *BMT1* and *BMT7* encoding beta-mannosyltransferases; *SUR2* gene, related to sphingolipid biosynthesis; *PUP1*, an uncharacterized gene encoding a mitochondria-localized protein and *CAGL0M10307g* (ortholog of *CaAUR1* and *ScAUR1* genes) related to drug resistance. As a first approach about the role of these genes on biofilm development, deletion mutants devoid of each of the mentioned genes, kindly provided by Dr. Hiroji Chibana, Chiba University, Japan, were grown to form biofilms in both RPMI and SDB media and compared to the wild-type KUE100 strain, grown in the same conditions. All deletion mutants tested, except for *Δpup1*, display decreased levels of biofilm formation, when compared to the wild-type population, when cultivated in RPMI medium (**Figure 29 A**). On the other hand, this observation is only confirmed for the *Δaur1* cells in SDB medium (**Figure 29 B**). Indeed, Aur1 appears to be a clear new determinant of biofilm formation in *C. glabrata*. *CgAUR1* (ORF *CAGL0M10307g*), however, remains uncharacterized in this species. In *S. cerevisiae*, Aur1 has been related to antifungal drug resistance, being determinant of Aureobasidin A (AbA) resistance, among other drugs. Genetic approaches allowed to identify *AUR1* gene as required for formation of inositolphosphorylceramide (IPC) in yeast, suggesting that this gene encodes part or all of the IPC synthase, which is essential for fungal sphingolipid biosynthesis.[120] Whether this is the role of *C. glabrata*'s Aur1 and whether IPC synthesis is required for biofilm formation remains uncharted.

Other genes that might deserve further investigations are the *CgAED2* and *CgSUR2* genes, since although they did not show a significant difference in the formed biofilms, compared to the wild-type strain, when grown in SDB medium, their absence was found to affect *C. glabrata* biofilm formation in RPMI medium.

Interestingly, the multidrug resistance transporter encoding genes *CgQDR2*, *CgTPO1_2*[13], found in this study to be activated by Tec1, had been previously shown to be required for biofilm formation, through unknown mechanisms.

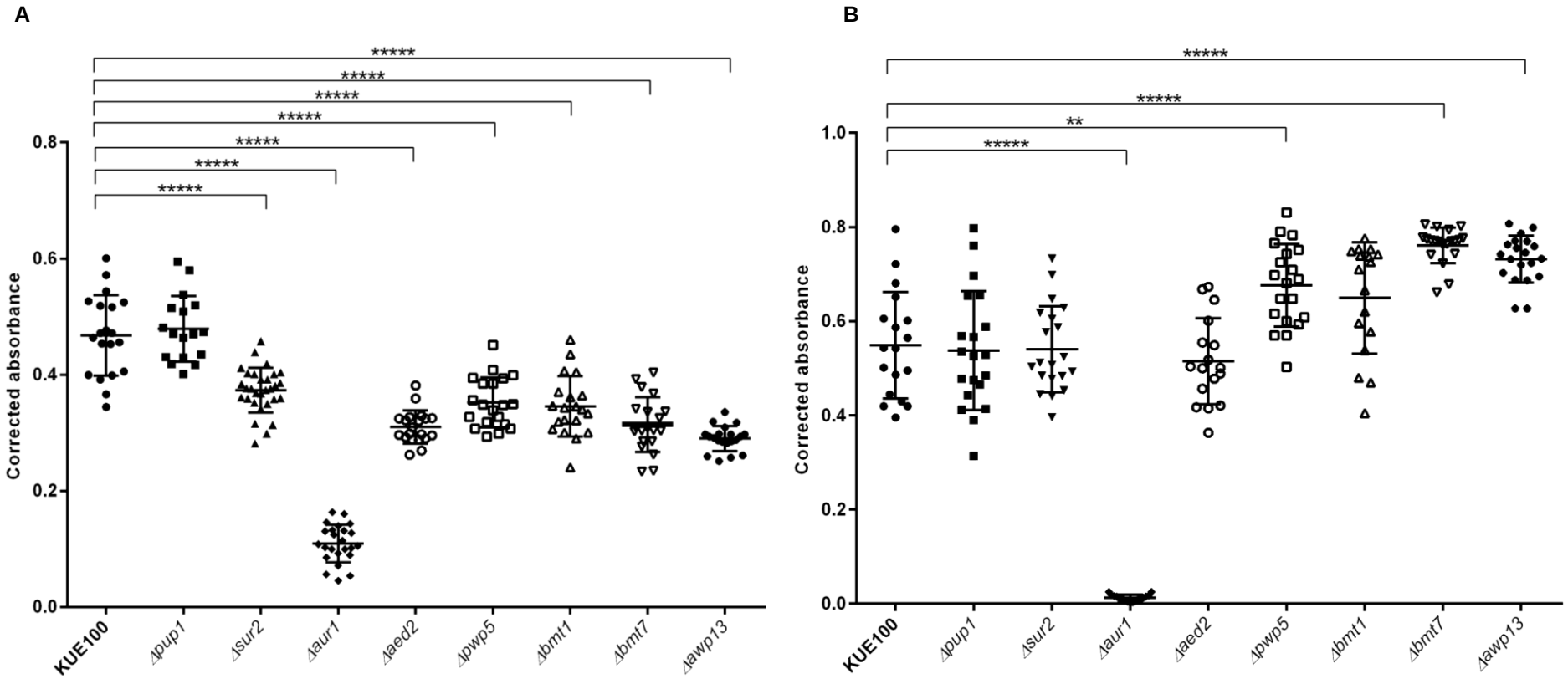


**Figure 29- *CgAUR1* gene plays a role in adherence and biofilm development in RPMI (pH4) (A) and SDB (pH5.6) (B).** Wild-type and the indicated deletion mutant cells were growth for 24 h in microtiter plates, after which cell viability was assessed based on PrestoBlue assay. A scatter dot plot representation of the data is shown, where each dot represents the level of biofilm formed in each sample. The average level of formed biofilm in at least 15 independent experiments is indicated by the black line, standard deviation being represented by the error bars. ****P*<0,001;*****P*<0,0001;******P*<0,00001.

### 3.7- *In silico* prediction of the CgTec1 recognition sequences

Since the nucleotide sequences targeted by Tec1 in *C. glabrata* are still unknown, a search for consensus sequences within the Tec1-activated genes, unveiled in this study, was performed. By resorting to the PathoYeastract database, these upstream regions were obtained and scanned for conserved sequences using the DREME (Discriminative Regular Expression Motif Elicitation) informatic tool (http://meme-suite.org/doc/dreme.html). 25 consensus sequences were obtained with high scores, as illustrated in **Figures A3** and **A4**. Given the high number of predicted motifs, the list was narrowed down to 18 consensus sequences, by both excluding the motifs containing TATA boxes, or long AAA/TTT stretches. To narrow down this list even further, the possible comparison to *C. albicans* and *S. cerevisiae* Tec1 motifs was hypothesized. To do that, however, we needed to check for conservation in the DNA-binding domain of the Tec1 proteins.

Aiming to inspect the possible 3D structure of Tec1, as well as its ligand binding sites and conserved domains, comparing to the Tec1 orthologs in *C. albicans* and *S. cerevisiae*, we sought to understand if we could rely on what is already described about these orthologs' ligand sequences. The I-TASSER (Iterative Threading ASSEmbly Refinement) bioinformatic tool was used to study the possible structures of CgTec1. After retrieving the protein FASTA sequence from the PathoYeastract database, the predicted model given by I-TASSER that presented higher score was obtained (**Figure 30**). For each target, I-TASSER simulations generate a large ensemble of structural conformations, called decoys. To select the final models, I-TASSER uses the SPICKER program to cluster all the decoys based on the pair-wise structure similarity and reports up to five models which corresponds to the five largest structure clusters. The confidence of each model is quantitatively measured by the C-score that is calculated based on the significance of threading template alignments and the convergence parameters of the structure assembly simulations. C-score is typically in the range of [-5, 2], where a C-score of a higher value suggests a model with a higher confidence and vice-versa.

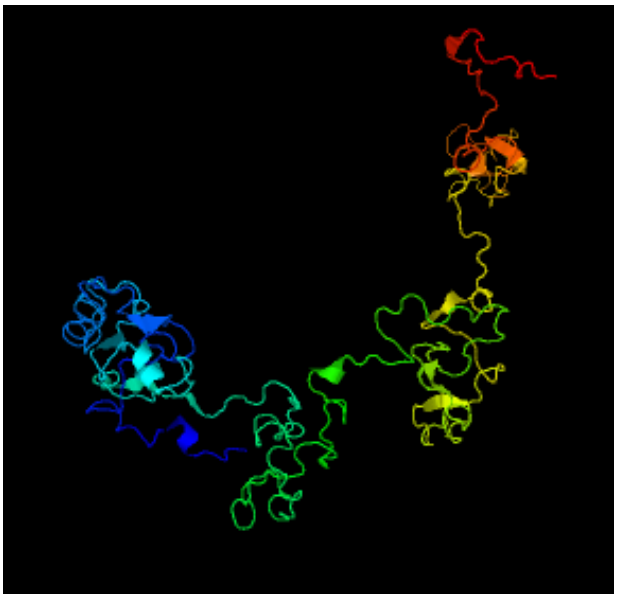

**Figure 30- Top final Tec1 structure model predicted by I-TASSER. The C-score value for the predicted structure was -1.** The structure was obtained in https://zhanglab.ccmb.med.umich.edu/I-TASSER/ with the protein FASTA format sequence of Tec1, retrieved from CGD.

I-TASSER can also be used to predict ligand binding sites in the predicted structure model. Thus, this software provided us biological annotations of the target protein by COFACTOR and COACH based on the I-TASSER structure prediction. While COFACTOR deduces protein functions (ligand-binding sites, Enzyme Commission [EC] and GO) using structure comparison and protein-protein networks, COACH is a meta-server approach that combines multiple function annotation results (on ligand-binding sites) from the COFACTOR, TM-SITE and S-SITE programs. The results are shown in **Figure 31** illustrating the two most confident ligand binding sites predicted for the first model.

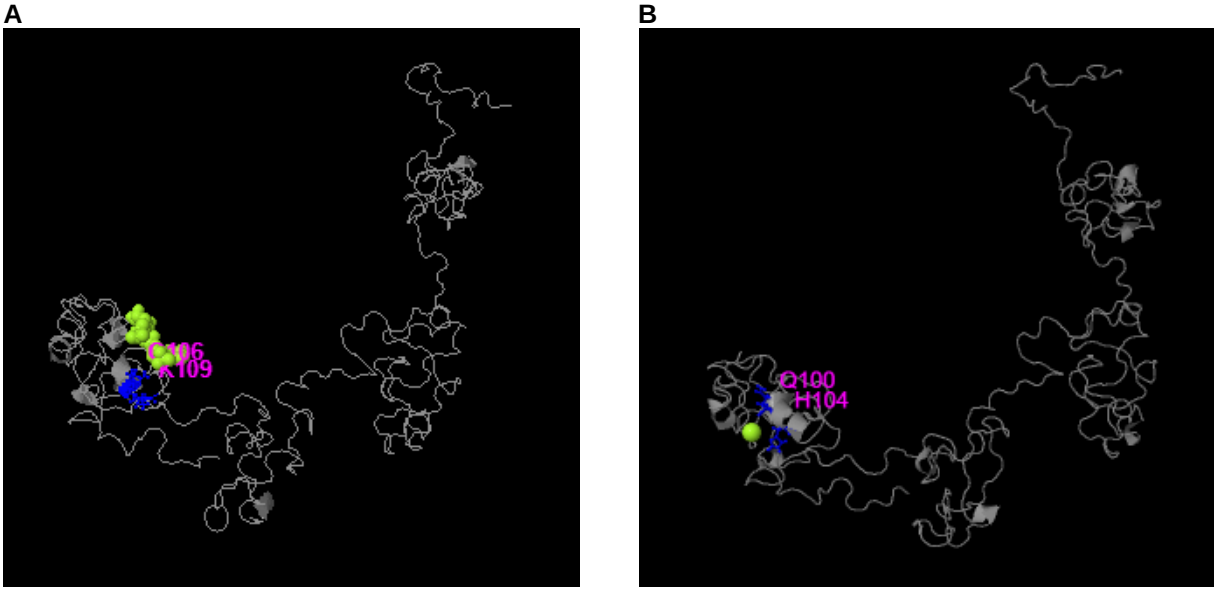


**Figure 31- I-TASSER predicted ligand binding sites of the transcription factor Tec1 predicted model, highlighting the ligand binding site residues Q106 and K109 (A), and Q100 and H104 (B).** The predicted ligand binding residues were obtained in https://zhanglab.ccmb.med.umich.edu/I-TASSER/ with the protein FASTA format sequence of Tec1, retrieved from CGD.

Afterwards, the InterPro database was used to search for conserved domains in Tec1 protein. InterPro recognized a single conserved domain, from residue 35 to residue 115, belonging to TEA/ATTS domain superfamily, responsible for DNA-binding TF activity.

A multiple alignment of the three (*C. glabrata*, *C. albicans* and *S. ceresiviae*) Tec1 orthologs protein sequences, resorting to Clustal Omega (https://www.ebi.ac.uk/Tools/msa/clustalo/), enabled the identification of conserved regions (**Figure 32**). A particularly conserved region was found from residue 48 to residue 109 of *C. glabrata* Tec1 (61 amino acid residues). This is in agreement with the idea that these orthologs share a TEA/ATTS domain and also agrees with the result given by the InterPro database, since these regions are overlapped. Lastly, this region potentially contains the ligand binding site, predicted by I-TASSER to be in residues 106 and 109, a glutamine and a lysine, respectively.


**Figure 32- Multiple sequence alignment of Tec1 from *S. cerevisiae*, *C. albicans* and *C. glabrata* reveals a conserved amino acid sequence of 61 residues from residue 48 to 109 of Tec1 protein sequence in *C. glabrata*.** The alignment was performed in Clustal Omega, a multiple sequence alignment program (https://www.ebi.ac.uk/Tools/msa/clustalo/) using the protein sequences of Tec1 orthologs retrieved in CGD.

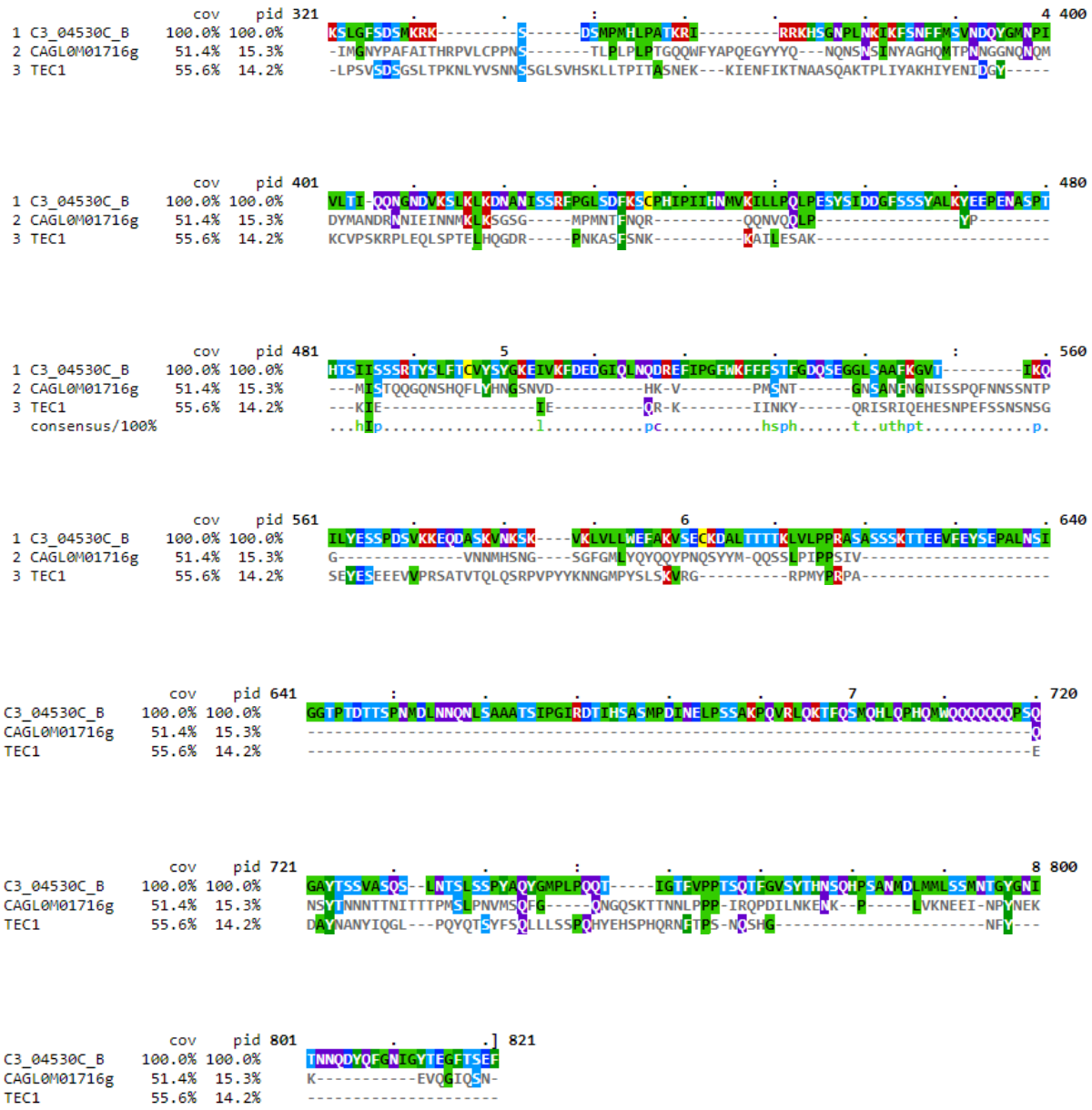

**Figure 32 (continuation)- Multiple sequence alignment of Tec1 from *S. cerevisiae*, *C. albicans* and *C. glabrata* reveals a conserved amino acid sequence of 61 residues from residue 48 to 109 of Tec1 protein sequence in *C. glabrata*.** The alignment was performed in Clustal Omega, a multiple sequence alignment program (https://www.ebi.ac.uk/Tools/msa/clustalo/) using the protein sequences of Tec1 orthologs retrieved in CGD.

With this information, it is possible to hypothesize that *C. glabrata* Tec1 is likely to have recognition sequences similar to those recognized by its orthologs in *S. cerevisiae* and *C. albicans*. Thus, the Tec1 described binding motifs in *S. cerevisiae* and *C. albicans* (retrieved in Yeastract and PathoYeastract databases, respectively) were used to further narrow down the number of *C. glabrata* Tec1 binding motifs (**Table 7**).

The number of consensus regions described for *S. cerevisiae* were found to be 8, contrasting with only 3 for *C. albicans.* Interestingly, the consensus sequences **CATTC**T, **CATTC**C and RM**ATTC**YY from *S. cerevisiae* Tec1 and **CATTC**Y and WR**CATTC**YH from *C. albicans* Tec1 appear to share a core region with each other (**Table 7**). Comparing them with the predicted *C. glabrata* Tec1 recognition sites (**Table 8**), and considering the complementary strands, the most similar sequence appears in motif T(C/G/T)C**CATT**G. Three additional motifs can also be considered (**Table 9**). It seems that the predicted DNA binding sites in *C. glabrata* have diverged from those identified in *C. albicans* and *S. cerevisiae*. However, it must be taken in consideration the evolution of the species and the possible synonymous mutations episodes. Still, this is a field that deserves to be more deeply investigated.

**Table 7- Number of up-regulated genes of the biofilm dataset found to have the sequence of the consensus recognized by Tec1 that are described for *S. cerevisiae* and *C. albicans*, respectively.** The binding motif sequences were obtained in the Yeastract and PathoYeastract databases, respectively and *S. cerevisiae* consensus sequences are represented according to the IUPAC frequency table in Yeastract (Table A3).

| ***S. cerevisiae* consensus** | **Number of genes** |
|---|---|
| TTCTCACATTCTTC | 0 |
| CATTCT | 208 |
| CATTCC | 159 |
| CATTCTT | 84 |
| RMATTCYY | 219 |
| tcRRGAATGTtgxt | 0 |
| VRGAATgt | 84 |
| gRGAATGY | 42 |
| ***C. albicans* consensus** | **Number of genes** |
| WRCATTCYH | 90 |
| CATTCY | 291 |
| AAAAAAAAAAGAAAG | 2 |

**Table 8- Number of up-regulated genes of the biofilm dataset found to have the sequence of the consensus recognized by Tec1 that were retrieved in DREME.** The number of genes was obtained in PathoYeastract database.

| Tec1 predicted consensus | Number of genes |
|---|---|
| GGGGRGGM | 141 |
| GCGATGAS | 104 |
| CYCCCCYC | 162 |
| CACMCRCA | 124 |
| CACAGARR | 152 |
| AGARAGAR | 206 |
| SMAGAGA | 285 |
| CAATGGBA | 96 |
| CAMATACA | 100 |
| CYTCTC | 362 |
| AARGRAAA | 273 |
| CGGGTAM | 72 |
| CGATGSCC | 41 |
| AGAABAGC | 78 |
| CCHCCCC | 211 |
| GCAYAGAA | 73 |
| AGCAMTAC | 61 |
| ACAAGMA | 239 |

**Table 9- Tec1 predicted binding motif candidates. The binding sequences were retrieved in DREME bioinformatic software.** The up-regulated genes were chosen and the upstream sequences were obtained in FASTA format in PathoYeastract database. The best candidates were selected based on their similarities with the most conserved part of Tec1 binding motifs in S. cerevisiae and C. albicans and the number of targeted genes. The sequences are organized by predicted motif / complementary strand.

| Predicted Tec1 binding motifs |
|---|
| CAATGG(C/G/T)A / T(A/C/G)C**CATT**G |
| CA(A/**C**)**AT**A**C**A **/** TGTCT(G/T)TG |
| CGATG(G/C)CC / GG(C/G)**CAT**CG |
| GCGATGA(G/C) / (C/G)T**CAT**CGC |

# 4- Final Discussion

The present thesis describes an in-depth analysis of the involvement of TF Tec1 in *C. glabrata* biofilm formation. Several studies have characterized *Candida* biofilm transcriptomes. Although many different growth conditions and comparison conditions were utilized, there is good overall agreement, especially among many of the most highly induced genes in biofilm formation. Most importantly, these transcriptome studies have provided leads for functional analysis.

In the first part of this work, Tec1 was found to be required for adhesion to human vaginal epithelial cells and for biofilm formation in polystyrene surface. However, the over-expression of *CgTEC1* gene did not result in increased adhesion of *C. glabrata* cells to the human vaginal epithelium cells. Tec1 showed in this study to be more determinant for activating adhesin-encoding genes in later stages of biofilm formation, and considering that the time to which cells were allowed to contact and adhere was 30 min, in the future it would be interesting to evaluate adhesion to the human vaginal epithelium cells for longer time periods. Additionally, the induction of *CgTEC1* expression may not necessarily result in the intensification of adhesion, as it will act in many other cellular biological functions.

Considering that Tec1 is undoubtedly related to hyphal differentiation in *C. albicans*, this feature was analyzed for *C. glabrata* Tec1. The pseudohyphal differentiation was observed to be, at least in part, regulated by Tec1. Despite these findings, the conditions to which the cells were exposed do not reproduce what would be the natural behavior of *C. glabrata* cells *in vivo* and no pseudohyphae differentiation was yet reported to be a natural feature in biofilm formation in this species. Furthermore, Tec1 does not show nuclear accumulation as an activation mechanism for biofilm formation. Thus, the molecular mechanisms underlying Tec1 activation are still to be elucidated.

RNA-seq has been revolutionizing transcriptome profiling with deep-sequencing technologies. With this approach the transcriptome-wide changes of cells undergoing biofilm formation, in relation to planktonic cells, were assessed. This yielded a total of 3070 genes with altered expression, highlighting the multifactorial and complex nature of biofilm formation. The genes with altered expression levels were found to belong to multiple biological functions, but many (17%) remain uncharacterized, making the task of analyzing biofilm formation mechanisms more difficult.

Among the functional groups found to be important in biofilm development, some were highlighted such as adhesion, which included up-regulation of a great number of adhesion-related genes including those encoding for families I (EPA genes), II (PWP genes), III (AED genes) and IV (AWP genes) adhesins. This is in agreement with the key role of cell-substrate and cell-cell adhesion on biofilm establishment and development. Nitrogen and carbon metabolism were also shown to undergo crucial changes, presumably in response to nutrient deprivation. For example, biofilm cells displayed repression of genes encoding enzymes required for amination steps and activation of some required for deamination steps, suggesting that the respective α-oxoacids intermediates are favoring the energetic metabolism. An energetic shift is also induced in these cells observed by activation of glyoxylate cycle related genes. The down-regulation of fatty acid biosynthesis and up-regulation of β-oxidation pathway might be

supplying 2-carbon molecules to this alternative energetic pathway. Furthermore, activation of peroxisomes' assembly is also suggested by the transcriptomics data, reinforcing this hypothesis.

Results regarding the ergosterol biosynthesis pathway were found to be puzzling. Some genes encoding enzymes of this biosynthetic pathway were found to be activated, while others were found to be repressed, with an expected consequent accumulation of intermediate metabolites. Interestingly, however, the overall outcome of these genes was experimentally shown to be a decreased level of ergosterol in *C. glabrata* biofilm cells. Additionally, two orthologs of Tec1 and Efg1 of *C. albicans* encoded by ORFs *CAGL0M01716g* and *CAGL0M0763*, respectively, were also found up-regulated in our *C. glabrata* biofilm cells.

Another functional group found to be important in biofilm formation was stress response, with up-regulation of several TFs, such as *CgYAP6, CgYAP7, CgCAD1* and *CgAP1*, responsible for oxidative and metal stress response, *CgMSN1* and *CgMSN4*, controlling the general stress response, *CgRIM101*, *CgHAA1*, *CgWAR1*, involved in the acid/alkaline stress response, *CgHAC1*, controlling the unfolded protein response and *CgHOT1*, required for the osmotic stress response. This observation suggests a highly regulated response to environmental stress conditions is activated in biofilm cells. Additionally, biofilm cells also displayed increased expression of MDR genes, namely *CgCDR1*, *CgQDR2*, *CgAQR1*, *CgTPO1_2* and *CgTPO3*, with *CgQDR2* and *CgTPO1_2* already shown by our group to be important for biofilm formation. Although biofilm cells have been shown to be particularly resistant to antifungals, this fact might result not only from the overexpression of MDR transporters, but also from the action of the ECM that limits the diffusion of antifungals towards inner biofilm cells.

RNA-seq approach was also used to unveil the role of Tec1 in *C. glabrata* biofilm formation. Tec1 was found to up-regulate ¼ of the activated genes in biofilm cells, suggesting that this is a key regulator of biofilm-induced changes in *C. glabrata*. The observed reduction of biofilm formation and adhesion to vaginal epithelium cells is hypothesized to be due to the high number of adhesion-related genes found to be up-regulated by this TF. The transcript levels of *CgAED2*, *CgPWP5* and *CgAWP13* genes, encoding adhesins, showed further that the action of Tec1 appears to be particularly crucial in later stages of biofilm formation. Among the Tec1 targets studied for a possible role in biofilm formation, Aur1, suggested to play a role in sphingolipid metabolism, was found to be crucial in this process. It will be interesting to assess the mechanism underlying this Tec1 dependent phenotype. Interestingly, Tec1 was also found to affect many other processes that occur during biofilm formation, including increased drug and stress resistance, and carbon and nitrogen metabolism remodeling. Indirectly, Tec1 also appears to inhibit ergosterol biosynthesis in biofilm cells. Interestingly, biofilm cells were found to contain decreased levels of ergosterol when compared to planktonically grown cells, which might be due to low oxygen levels felt by *C. glabrata* cells in the inner parts of the biofilm. As ergosterol is also present in *C. albicans* biofilm matrix[46], it would be interesting to perform a molecular analysis of the *C. glabrata* biofilm ECM, as it could shed more light about the contribution of possible extracellular ergosterol presence in biofilms, as well as for the effect of *CgTEC1* deletion in this context.

Further *in silico* analysis allowed the prediction of Tec1 protein structure and the search for conserved domains revealed the TEA/ATTS domain, which is described to be present in *C. albicans* and *S. cerevisiae* Tec1 orthologs, containing the predicted DNA binding residues. These observations encouraged the analysis of the promoter regions of Tec1 activated genes, which enabled the identification of possible binding sequences for this TF, similar to the ones already described in *S. cerevisiae* and *C. albicans.* The most probable were found to be “CAATGGBA", “CAMATACA”, “CGATGSCC” and “GCGATGAS” (with B=C/G/T, M=A/C and S=G/C).

In this work, Tec1 is strongly suggested to be a key player in biofilm development in *C. glabrata*. **Figure 33** illustrates a model of the main Tec1 induced responses in a biofilm cell.

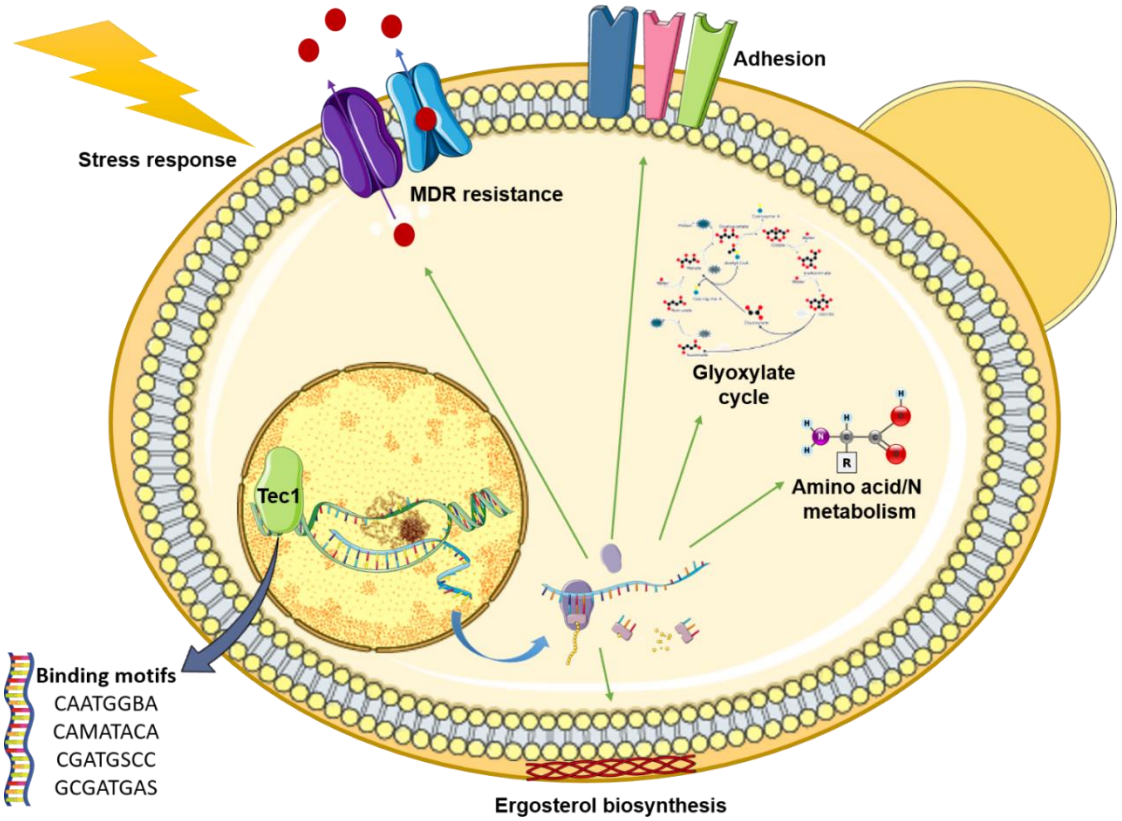


**Figure 33- Hypothetical model of action of Tec1 transcription factor in *C. glabrata* biofilm formation.** Upon biofilm formation initiation, the transcription factor Tec1 is activated and this induces the expression of 487 genes found in this work to be related to key biofilm development-related biological functions. These comprise adhesion, stress and multidrug resistance, the cell wall organization, activation of glyoxylate cycle and amino acid and nitrogen metabolism in response to nutrient deprivation and pseudohyphal growth.

Many studies have focused on the regulatory processes underlying biofilm-induced genes in yeasts, other than *C. glabrata*. Perhaps the most elegant approach was undertaken by Nobile *et al.* (2012), who disclosed a transcriptional regulatory network underlying biofilm formation in *C. albicans*. Tec1 was found in their study to be part of this complex regulatory network. In our work, Tec1 showed to control the expression of 1082 genes, with some genes found to encode for putative TFs (**Figure 34**). Based

on this observation, it is likely that Tec1 is one of the key players in the very complex regulatory network regulating biofilm formation in *C. glabrata*.

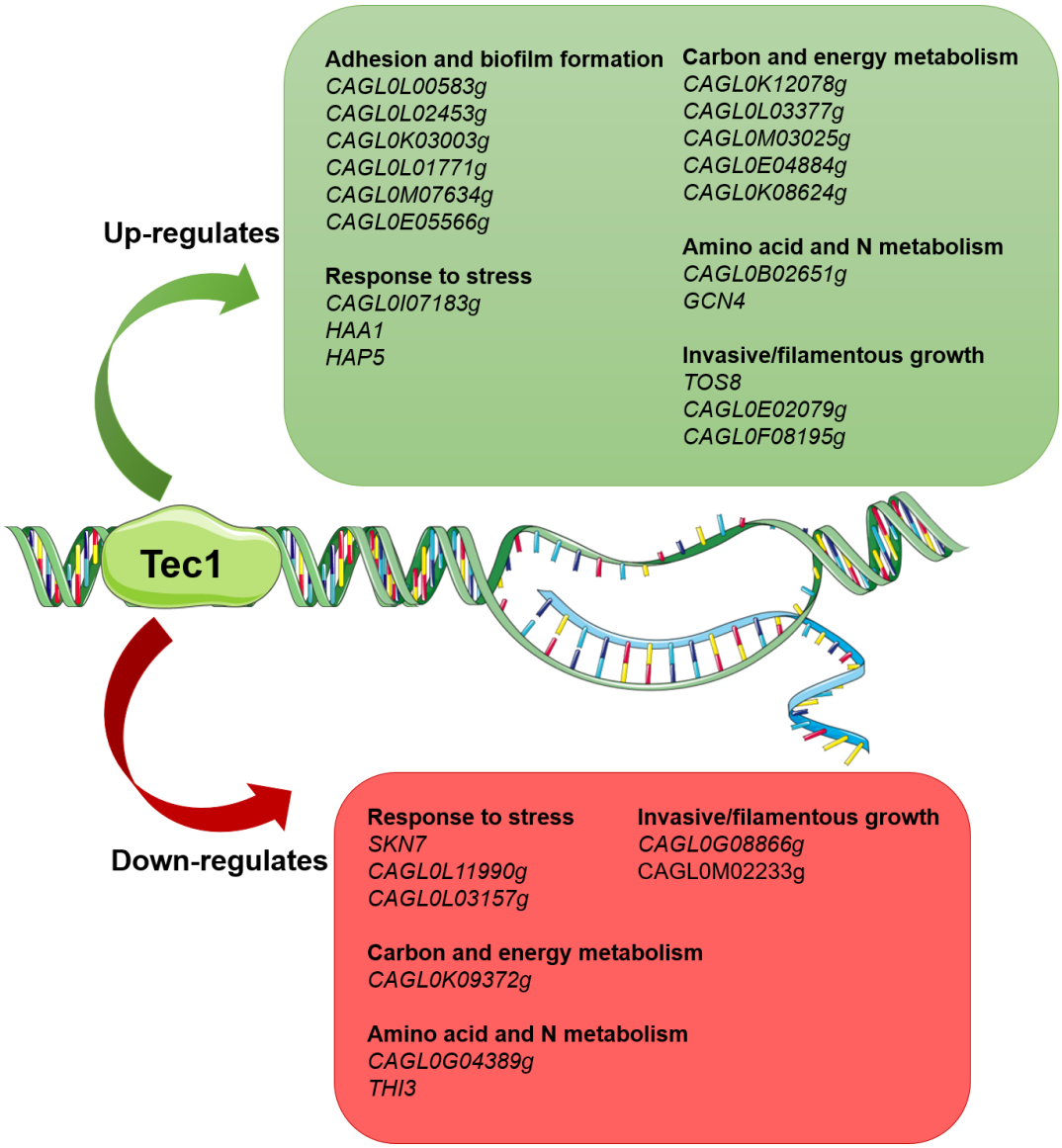


**Figure 34- Differentially expressed transcription factors found in RNA-seq analysis to be regulated by Tec1 in *C. glabrata* 24 h biofilms. *C. glabrata* ORFs directly or indirectly up (green) and downregulated (red) by the transcription factor Tec1.** The ORFs downregulated by Tec1 are those demonstrated to be upregulated in *Δtec1* 24 h biofilm cells, which transcriptome was analyzed through RNA-seq against wild-type *C. glabrata* 24 h biofilm cells.

Despite many open questions, the overall picture obtained with these results revealed the complexity and multifactorial nature of biofilm formation. The importance of Tec1 on regulating this phenomenon in *C. glabrata* is highlighted, placing this TF in a possible new drug target scenario, aiming to develop novel therapies that would prevent and overcome biofilm formation.

# 5- References


1. Underhill, D. M. & Pearlman, E. Immune Interactions with Pathogenic and Commensal Fungi: A Two-Way Street. *Immunity* **43,** 845–58 (2015).
2. Badiee, P. & Hashemizadeh, Z. Opportunistic invasive fungal infections: diagnosis & clinical management. *Indian J. Med. Res.* **139,** 195–204 (2014).
3. Ifrim, D. C. *et al.* Role of Dectin-2 for host defense against systemic infection with *Candida glabrata*. *Infect. Immun.* **82,** 1064–73 (2014).
4. Netea, M. G., Joosten, L. A. B., van der Meer, J. W. M., Kullberg, B.-J. & van de Veerdonk, F. L. Immune defence against *Candida* fungal infections. *Nat. Rev. Immunol.* **15,** 630–42 (2015).
5. Yapar, N. Epidemiology and risk factors for invasive candidiasis. *Ther. Clin. Risk Manag.* **10,** 95–105 (2014).
6. Kullberg, B. J. & Arendrup, M. C. Invasive Candidiasis. *N. Engl. J. Med.* **374,** 794–5 (2016).
7. Lewis, K. Riddle of biofilm resistance. *Antimicrob. Agents Chemother.* **45,** 999–1007 (2001).
8. Merseguel, K. B. *et al.* Genetic diversity of medically important and emerging *Candida* species causing invasive infection. *BMC Infect. Dis.* **15,** 57 (2015).
9. Rodrigues, C. F., Silva, S. & Henriques, M. *Candida glabrata*: a review of its features and resistance. *Eur. J. Clin. Microbiol. Infect. Dis.* **33,** 673–88 (2014).
10. Tam, P., Gee, K., Piechocinski, M. & Macreadie, I. *Candida glabrata*, Friend and Foe. *J. fungi (Basel, Switzerland)* **1,** 277–292 (2015).
11. Glöckner, A. & Cornely, O. A. *Candida glabrata*--unique features and challenges in the clinical management of invasive infections. *Mycoses* **58,** 445–50 (2015).
12. Kaur, R., Domergue, R., Zupancic, M. L. & Cormack, B. P. A yeast by any other name: *Candida glabrata* and its interaction with the host. *Curr. Opin. Microbiol.* **8,** 378–84 (2005).
13. Santos, R. *et al.* The multidrug resistance transporters CgTpo1_1 and CgTpo1_2 play a role in virulence and biofilm formation in the human pathogen *Candida glabrata*. *Cell. Microbiol.* **19,** (2017).
14. Gilbert, A. S., Wheeler, R. T. & May, R. C. Fungal Pathogens: Survival and Replication within Macrophages. *Cold Spring Harb. Perspect. Med.* **5,** a019661 (2014).
15. Riera, M., Mogensen, E., D'Enfert, C. & Janbon, G. New regulators of biofilm development in *Candida glabrata*. *Res. Microbiol.* **163,** 297–307 (2012).
16. Pais, P., Costa, C., Cavalheiro, M., Romão, D. & Teixeira, M. C. Transcriptional Control of Drug Resistance, Virulence and Immune System Evasion in Pathogenic Fungi: A Cross-Species Comparison. *Front. Cell. Infect. Microbiol.* **6,** 131 (2016).
17. Sardi, J. D. C. O. *et al.* Highlights in pathogenic fungal biofilms. *Rev. Iberoam. Micol.* **31,** 22–9
18. Desai, J. V, Mitchell, A. P. & Andes, D. R. Fungal biofilms, drug resistance, and recurrent infection. *Cold Spring Harb. Perspect. Med.* **4,** (2014).
19. d'Enfert, C. & Janbon, G. Biofilm formation in *Candida glabrata*: What have we learnt from

functional genomics approaches? *FEMS Yeast Res.* **16,** fov111 (2016).

20. Chandra, J. & Mukherjee, P. K. *Candida* Biofilms: Development, Architecture, and Resistance. *Microbiol. Spectr.* **3,** (2015).
21. Blankenship, J. R. & Mitchell, A. P. How to build a biofilm: a fungal perspective. *Curr. Opin. Microbiol.* **9,** 588–94 (2006).
22. Seneviratne, C. J., Jin, L. & Samaranayake, L. P. Biofilm lifestyle of *Candida*: a mini review. *Oral Dis.* **14,** 582–90 (2008).
23. Cavalheiro, M. & Teixeira, M. C. *Candida* Biofilms: Threats, Challenges, and Promising Strategies. *Front. Med.* **5,** 28 (2018).
24. Andes, D. *et al.* Development and characterization of an in vivo central venous catheter *Candida albicans* biofilm model. *Infect. Immun.* **72,** 6023–31 (2004).
25. Kucharíková, S. *et al.* In vivo *Candida glabrata* biofilm development on foreign bodies in a rat subcutaneous model. *J. Antimicrob. Chemother.* **70,** 846–56 (2015).
26. Rajendran, R. *et al.* Biofilm formation is a risk factor for mortality in patients with *Candida albicans* bloodstream infection-Scotland, 2012-2013. *Clin. Microbiol. Infect.* **22,** 87–93 (2016).
27. Kraneveld, E. A. *et al.* Identification and differential gene expression of adhesin-like wall proteins in *Candida glabrata* biofilms. *Mycopathologia* **172,** 415–27 (2011).
28. Verstrepen, K. J. & Klis, F. M. Flocculation, adhesion and biofilm formation in yeasts. *Mol. Microbiol.* **60,** 5–15 (2006).
29. De Las Peñas, A. *et al.* Virulence-related surface glycoproteins in the yeast pathogen *Candida glabrata* are encoded in subtelomeric clusters and subject to RAP1- and SIR-dependent transcriptional silencing. *Genes Dev.* **17,** 2245–58 (2003).
30. Modrzewska, B. & Kurnatowski, P. Adherence of *Candida* sp. to host tissues and cells as one of its pathogenicity features. *Ann. Parasitol.* **61,** 3–9 (2015).
31. de Groot, P. W. J., Bader, O., de Boer, A. D., Weig, M. & Chauhan, N. Adhesins in human fungal pathogens: glue with plenty of stick. *Eukaryot. Cell* **12,** 470–81 (2013).
32. Rodrigues, C. F., Rodrigues, M. E., Silva, S. & Henriques, M. *Candida glabrata* Biofilms: How Far Have We Come? *J. fungi (Basel, Switzerland)* **3,** (2017).
33. Cormack, B. P., Ghori, N. & Falkow, S. An adhesin of the yeast pathogen *Candida glabrata* mediating adherence to human epithelial cells. *Science* **285,** 578–82 (1999).
34. Zupancic, M. L. *et al.* Glycan microarray analysis of *Candida glabrata* adhesin ligand specificity. *Mol. Microbiol.* **68,** 547–59 (2008).
35. Desai, C., Mavrianos, J. & Chauhan, N. *Candida glabrata* Pwp7p and Aed1p are required for adherence to human endothelial cells. *FEMS Yeast Res.* **11,** 595–601 (2011).
36. Hirota, K. *et al.* Pathogenic factors in *Candida* biofilm-related infectious diseases. *J. Appl. Microbiol.* **122,** 321–330 (2017).
37. Sudbery, P., Gow, N. & Berman, J. The distinct morphogenic states of *Candida albicans*. *Trends Microbiol.* **12,** 317–24 (2004).

38. Csank, C. & Haynes, K. *Candida glabrata* displays pseudohyphal growth. *FEMS Microbiol. Lett.* **189,** 115–20 (2000).
39. Gagiano, M., Bauer, F. F. & Pretorius, I. S. The sensing of nutritional status and the relationship to filamentous growth in *Saccharomyces cerevisiae*. *FEMS Yeast Res.* **2,** 433–70 (2002).
40. Kern, K., Nunn, C. D., Pichová, A. & Dickinson, J. R. Isoamyl alcohol-induced morphological change in *Saccharomyces cerevisiae* involves increases in mitochondria and cell wall chitin content. *FEMS Yeast Res.* **5,** 43–9 (2004).
41. Cuéllar-Cruz, M., López-Romero, E., Villagómez-Castro, J. C. & Ruiz-Baca, E. *Candida* species: new insights into biofilm formation. *Future Microbiol.* **7,** 755–71 (2012).
42. Vandeputte, P. *et al.* Reduced susceptibility to polyenes associated with a missense mutation in the ERG6 gene in a clinical isolate of *Candida glabrata* with pseudohyphal growth. *Antimicrob. Agents Chemother.* **51,** 982–90 (2007).
43. Araújo, D., Henriques, M. & Silva, S. Portrait of *Candida* Species Biofilm Regulatory Network Genes. *Trends Microbiol.* **25,** 62–75 (2017).
44. Rodrigues, C. F. & Henriques, M. Oral mucositis caused by *Candida glabrata* biofilms: failure of the concomitant use of fluconazole and ascorbic acid. *Ther. Adv. Infect. Dis.* **4,** 10–17 (2017).
45. Flemming, H.-C. & Wingender, J. The biofilm matrix. *Nat. Rev. Microbiol.* **8,** 623–33 (2010).
46. Zarnowski, R. *et al.* Novel entries in a fungal biofilm matrix encyclopedia. *MBio* **5,** e01333-14 (2014).
47. Monteiro, D. R. *et al.* Silver colloidal nanoparticles: effect on matrix composition and structure of *Candida albicans* and *Candida glabrata* biofilms. *J. Appl. Microbiol.* **114,** 1175–83 (2013).
48. Yu, S.-J., Chang, Y.-L. & Chen, Y.-L. Deletion of ADA2 Increases Antifungal Drug Susceptibility and Virulence in *Candida glabrata*. *Antimicrob. Agents Chemother.* **62,** (2018).
49. Kaur, R., Ma, B. & Cormack, B. P. A family of glycosylphosphatidylinositol-linked aspartyl proteases is required for virulence of *Candida glabrata*. *Proc. Natl. Acad. Sci. U. S. A.* **104,** 7628–33 (2007).
50. Alves, C. T. *et al. Candida albicans* promotes invasion and colonisation of *Candida glabrata* in a reconstituted human vaginal epithelium. *J. Infect.* **69,** 396–407 (2014).
51. Pathak, A. K., Sharma, S. & Shrivastva, P. Multi-species biofilm of *Candida albicans* and non-*Candida albicans Candida* species on acrylic substrate. *J. Appl. Oral Sci.* **20,** 70–5 (2012).
52. Castaño, I. *et al.* Telomere length control and transcriptional regulation of subtelomeric adhesins in *Candida glabrata*. *Mol. Microbiol.* **55,** 1246–58 (2005).
53. Iraqui, I. *et al.* The Yak1p kinase controls expression of adhesins and biofilm formation in *Candida glabrata* in a Sir4p-dependent pathway. *Mol. Microbiol.* **55,** 1259–71 (2005).
54. Gow, N. A. R., Brown, A. J. P. & Odds, F. C. Fungal morphogenesis and host invasion. *Curr. Opin. Microbiol.* **5,** 366–71 (2002).
55. Maiti, P. *et al.* Mapping of functional domains and characterization of the transcription factor Cph1 that mediate morphogenesis in *Candida albicans*. *Fungal Genet. Biol.* **83,** 45–57 (2015).

56. Calcagno, A.-M. *et al. Candida glabrata* STE12 is required for wild-type levels of virulence and nitrogen starvation induced filamentation. *Mol. Microbiol.* **50,** 1309–18 (2003).
57. Doedt, T. *et al.* APSES proteins regulate morphogenesis and metabolism in *Candida albicans*. *Mol. Biol. Cell* **15,** 3167–80 (2004).
58. Lohse, M. B., Gulati, M., Johnson, A. D. & Nobile, C. J. Development and regulation of single- and multi-species *Candida albicans* biofilms. *Nat. Rev. Microbiol.* **16,** 19–31 (2018).
59. Kamran, M. *et al.* Inactivation of transcription factor gene ACE2 in the fungal pathogen *Candida glabrata* results in hypervirulence. *Eukaryot. Cell* **3,** 546–52 (2004).
60. Stichternoth, C. & Ernst, J. F. Hypoxic adaptation by Efg1 regulates biofilm formation by *Candida albicans*. *Appl. Environ. Microbiol.* **75,** 3663–72 (2009).
61. Mulhern, S. M., Logue, M. E. & Butler, G. *Candida albicans* transcription factor Ace2 regulates metabolism and is required for filamentation in hypoxic conditions. *Eukaryot. Cell* **5,** 2001–13 (2006).
62. Schwarzmüller, T. *et al.* Systematic phenotyping of a large-scale *Candida glabrata* deletion collection reveals novel antifungal tolerance genes. *PLoS Pathog.* **10,** e1004211 (2014).
63. Song, J. W. *et al.* Expression of CgCDR1, CgCDR2, and CgERG11 in *Candida glabrata* biofilms formed by bloodstream isolates. *Med. Mycol.* **47,** 545–8 (2009).
64. Khakhina, S., Simonicova, L. & Moye-Rowley, W. S. Positive autoregulation and repression of transactivation are key regulatory features of the *Candida glabrata* Pdr1 transcription factor. *Mol. Microbiol.* **107,** 747–764 (2018).
65. Pais, P. *et al.* Membrane Proteome-Wide Response to the Antifungal Drug Clotrimazole in *Candida glabrata*: Role of the Transcription Factor CgPdr1 and the Drug:H+ Antiporters CgTpo1_1 and CgTpo1_2. *Mol. Cell. Proteomics* **15,** 57–72 (2016).
66. Whaley, S. G. *et al.* Jjj1 Is a Negative Regulator of Pdr1-Mediated Fluconazole Resistance in *Candida glabrata*. *mSphere* **3,**
67. Li, Q. Q. *et al.* Sterol uptake and sterol biosynthesis act coordinately to mediate antifungal resistance in *Candida glabrata* under azole and hypoxic stress. *Mol. Med. Rep.* **17,** 6585–6597 (2018).
68. Rodrigues, C. & Henriques, M. Portrait of Matrix Gene Expression in *Candida glabrata* Biofilms with Stress Induced by Different Drugs. *Genes (Basel).* **9,** 205 (2018).
69. Bard, M. *et al.* Sterol uptake in *Candida glabrata*: rescue of sterol auxotrophic strains. *Diagn. Microbiol. Infect. Dis.* **52,** 285–93 (2005).
70. Fonseca, E. *et al.* Effects of fluconazole on *Candida glabrata* biofilms and its relationship with ABC transporter gene expression. *Biofouling* **30,** 447–57 (2014).
71. Nobile, C. J. *et al.* A recently evolved transcriptional network controls biofilm development in *Candida albicans*. *Cell* **148,** 126–38 (2012).
72. Regan, H. *et al.* Negative regulation of filamentous growth in *Candida albicans* by Dig1p. *Mol. Microbiol.* **105,** 810–824 (2017).

73. Daniels, K. J., Srikantha, T., Pujol, C., Park, Y.-N. & Soll, D. R. Role of Tec1 in the development, architecture, and integrity of sexual biofilms of *Candida albicans*. *Eukaryot. Cell* **14,** 228–40 (2015).
74. Sahni, N. *et al.* Tec1 mediates the pheromone response of the white phenotype of *Candida albicans*: insights into the evolution of new signal transduction pathways. *PLoS Biol.* **8,** e1000363 (2010).
75. Glazier, V. E. *et al.* Genetic analysis of the *Candida albicans* biofilm transcription factor network using simple and complex haploinsufficiency. *PLoS Genet.* **13,** e1006948 (2017).
76. Panariello, B. H. D., Klein, M. I., Pavarina, A. C. & Duarte, S. Inactivation of genes TEC1 and EFG1 in *Candida albicans* influences extracellular matrix composition and biofilm morphology. *J. Oral Microbiol.* **9,** 1385372 (2017).
77. van der Felden, J., Weisser, S., Brückner, S., Lenz, P. & Mösch, H.-U. The transcription factors Tec1 and Ste12 interact with coregulators Msa1 and Msa2 to activate adhesion and multicellular development. *Mol. Cell. Biol.* **34,** 2283–93 (2014).
78. Zhang, Q. *et al.* Regulation of filamentation in the human fungal pathogen *Candida tropicalis*. *Mol. Microbiol.* **99,** 528–45 (2016).
79. Chen, K.-H., Miyazaki, T., Tsai, H.-F. & Bennett, J. E. The bZip transcription factor Cgap1p is involved in multidrug resistance and required for activation of multidrug transporter gene CgFLR1 in *Candida glabrata*. *Gene* **386,** 63–72 (2007).
80. Jansen, G., Wu, C., Schade, B., Thomas, D. Y. & Whiteway, M. Drag&Drop cloning in yeast. *Gene* **344,** 43–51 (2005).
81. Jiang, H., Lei, R., Ding, S.-W. & Zhu, S. Skewer: a fast and accurate adapter trimmer for next-generation sequencing paired-end reads. *BMC Bioinformatics* **15,** 182 (2014).
82. Skrzypek, M. S. *et al.* The Candida Genome Database (CGD): incorporation of Assembly 22, systematic identifiers and visualization of high throughput sequencing data. *Nucleic Acids Res.* **45,** D592–D596 (2017).
83. Anders, S. & Huber, W. Differential expression analysis for sequence count data. *Genome Biol.* **11,** R106 (2010).
84. Love, M. I., Huber, W. & Anders, S. Moderated estimation of fold change and dispersion for RNA-seq data with DESeq2. *Genome Biol.* **15,** 550 (2014).
85. Gentleman, R. C. *et al.* Bioconductor: open software development for computational biology and bioinformatics. *Genome Biol.* **5,** R80 (2004).
86. Cherry, J. M. *et al.* Saccharomyces Genome Database: the genomics resource of budding yeast. *Nucleic Acids Res.* **40,** D700-5 (2012).
87. Martin, D. *et al.* GOToolBox: functional analysis of gene datasets based on Gene Ontology. *Genome Biol.* **5,** R101 (2004).
88. Kanehisa, M., Sato, Y., Kawashima, M., Furumichi, M. & Tanabe, M. KEGG as a reference resource for gene and protein annotation. *Nucleic Acids Res.* **44,** D457-62 (2016).

89. Jensen, L. J. *et al.* STRING 8--a global view on proteins and their functional interactions in 630 organisms. *Nucleic Acids Res.* **37,** D412-6 (2009).
90. Monteiro, P. T. *et al.* The PathoYeastract database: an information system for the analysis of gene and genomic transcription regulation in pathogenic yeasts. *Nucleic Acids Res.* **45,** D597–D603 (2017).
91. Bailey, T. L. *et al.* MEME SUITE: tools for motif discovery and searching. *Nucleic Acids Res.* **37,** W202-8 (2009).
92. Yang, J. *et al.* The I-TASSER Suite: protein structure and function prediction. *Nat. Methods* **12,** 7–8 (2015).
93. Finn, R. D. *et al.* InterPro in 2017-beyond protein family and domain annotations. *Nucleic Acids Res.* **45,** D190–D199 (2017).
94. Sievers, F. *et al.* Fast, scalable generation of high-quality protein multiple sequence alignments using Clustal Omega. *Mol. Syst. Biol.* **7,** 539 (2011).
95. Köhrer, K. & Domdey, H. Preparation of high molecular weight RNA. *Methods Enzymol.* **194,** 398–405 (1991).
96. Quellhorst, G., Han, Y. & Blanchard, R. Validating Microarray Data Using R2 RT-PCR. *SABiosciences manuals* (2010).
97. Gong, Ping, Xin Guan, and E. W. A rapid method to extract ergosterol from soil by physical disruption. *Appl. Soil Ecol.* **17,** 285–289 (2001).
98. Dickinson, J. R. Filament formation in *Saccharomyces cerevisiae*--a review. *Folia Microbiol. (Praha).* **53,** 3–14 (2008).
99. Muzny, C. A. & Schwebke, J. R. Biofilms: An Underappreciated Mechanism of Treatment Failure and Recurrence in Vaginal Infections. *Clin. Infect. Dis.* **61,** 601–6 (2015).
100. Lohse, M. B., Gulati, M., Johnson, A. D. & Nobile, C. J. Development and regulation of single- and multi-species *Candida albicans* biofilms. *Nat. Rev. Microbiol.* **16,** 19–31 (2018).
101. Dickinson, J. R. 'Fusel' alcohols induce hyphal-like extensions and pseudohyphal formation in yeasts. *Microbiology* **142 ( Pt 6,** 1391–7 (1996).
102. Vandromme, M., Gauthier-Rouvière, C., Lamb, N. & Fernandez, A. Regulation of transcription factor localization: fine-tuning of gene expression. *Trends Biochem. Sci.* **21,** 59–64 (1996).
103. García-Sánchez, S. *et al. Candida albicans* biofilms: a developmental state associated with specific and stable gene expression patterns. *Eukaryot. Cell* **3,** 536–45 (2004).
104. Nett, J. E., Lepak, A. J., Marchillo, K. & Andes, D. R. Time course global gene expression analysis of an in vivo *Candida* biofilm. *J. Infect. Dis.* **200,** 307–13 (2009).
105. Chandra, J. *et al.* Biofilm formation by the fungal pathogen *Candida albicans*: development, architecture, and drug resistance. *J. Bacteriol.* **183,** 5385–94 (2001).
106. Murillo, L. A. *et al.* Genome-wide transcription profiling of the early phase of biofilm formation by *Candida albicans*. *Eukaryot. Cell* **4,** 1562–73 (2005).
107. Rajendran, R. *et al.* Integrating *Candida albicans* metabolism with biofilm heterogeneity by

transcriptome mapping. *Sci. Rep.* **6,** 35436 (2016).

108. Yeater, K. M. *et al.* Temporal analysis of *Candida albicans* gene expression during biofilm development. *Microbiology* **153,** 2373–85 (2007).
109. Hurtaux, T. *et al.* Evaluation of monovalent and multivalent iminosugars to modulate *Candida albicans* β-1,2-mannosyltransferase activities. *Carbohydr. Res.* **429,** 123–7 (2016).
110. West, L. *et al.* Differential virulence of *Candida glabrata* glycosylation mutants. *J. Biol. Chem.* **288,** 22006–18 (2013).
111. Fabre, E. *et al.* Characterization of the recombinant *Candida albicans* β-1,2-mannosyltransferase that initiates the β-mannosylation of cell wall phosphopeptidomannan. *Biochem. J.* **457,** 347–60 (2014).
112. Jawhara, S. *et al.* Murine model of dextran sulfate sodium-induced colitis reveals *Candida glabrata* virulence and contribution of β-mannosyltransferases. *J. Biol. Chem.* **287,** 11313–24 (2012).
113. Costa, C. *et al. Candida glabrata* drug:H+ antiporter CgQdr2 confers imidazole drug resistance, being activated by transcription factor CgPdr1. *Antimicrob. Agents Chemother.* **57,** 3159–67 (2013).
114. Costa, C. *et al.* The dual role of *candida glabrata* drug:H+ antiporter CgAqr1 (ORF CAGL0J09944g) in antifungal drug and acetic acid resistance. *Front. Microbiol.* **4,** (2013).
115. Costa, C. *et al. Candida glabrata* drug:H+ antiporter CgTpo3 (ORF CAGL0I10384g): role in azole drug resistance and polyamine homeostasis. *J. Antimicrob. Chemother.* **69,** 1767–76 (2014).
116. Ramage, G., Rajendran, R., Sherry, L. & Williams, C. Fungal biofilm resistance. *Int. J. Microbiol.* **2012,** 528521 (2012).
117. Leitão, A. Biofilm formation by the human pathogen *Candida glabrata*: The regulator CgEfg2 and its targets. (Instituto Superior Técnico, 2018).
118. Fox, E. P. *et al.* An expanded regulatory network temporally controls *Candida albicans* biofilm formation. *Mol. Microbiol.* **96,** 1226–39 (2015).
119. Mukherjee, P. K., Chandra, J., Kuhn, D. M. & Ghannoum, M. A. Mechanism of fluconazole resistance in *Candida albicans* biofilms: phase-specific role of efflux pumps and membrane sterols. *Infect. Immun.* **71,** 4333–40 (2003).
120. Heidler, S. A. & Radding, J. A. The AUR1 gene in *Saccharomyces cerevisiae* encodes dominant resistance to the antifungal agent aureobasidin A (LY295337). *Antimicrob. Agents Chemother.* **39,** 2765–9 (1995).

# 6- Annexe

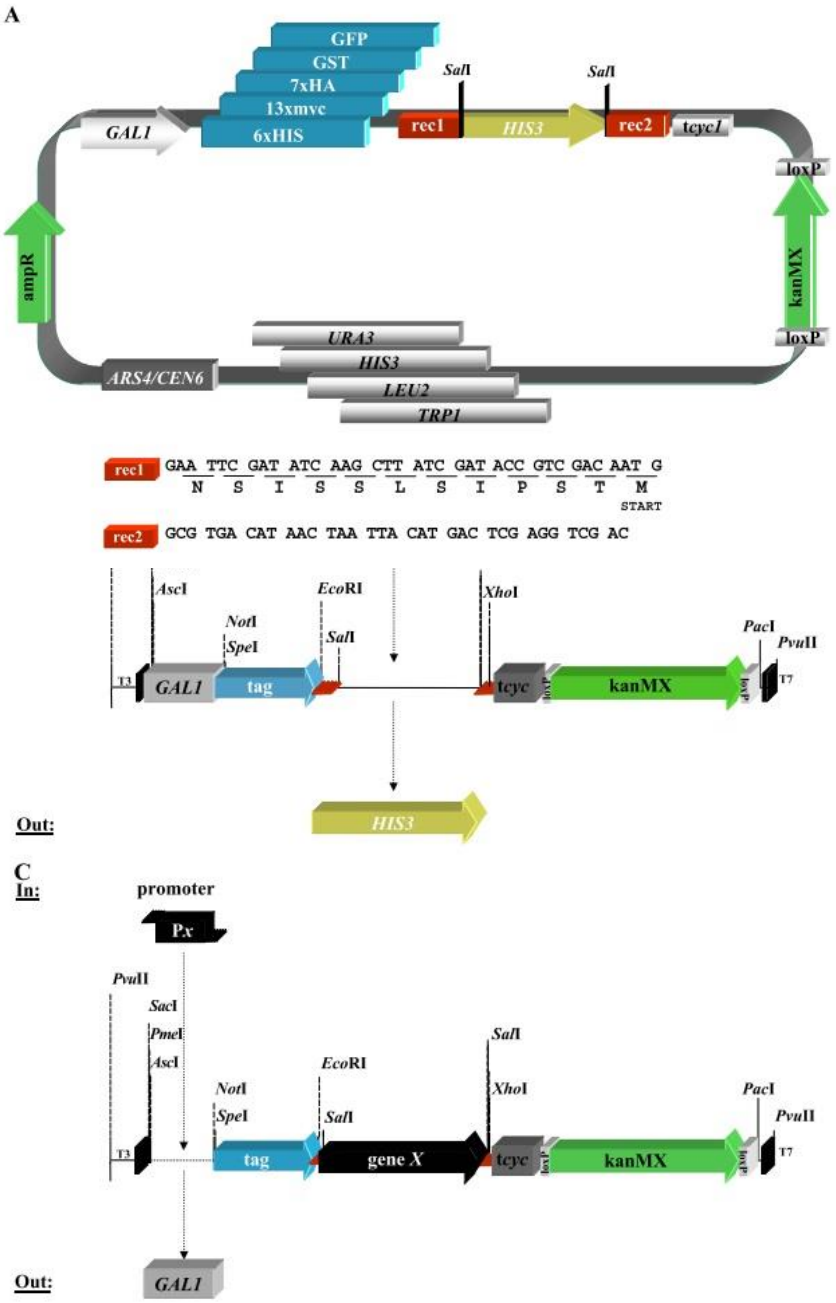


**Figure A1- Schematic representation of the basic pGREG vector system.** (A) The inducible *GAL1*promoter controls the expression of tags or generated fusion proteins. Downstream of the tags a *HIS3* stuffer fragment is located flanked by specific sites for recombination, rec1 and rec2. The vectors contain one of the selectable yeast markers *URA3*, *LEU2*, *TRP1* and *HIS3* as well as an additional KanMX cassette flanked by loxP sites. Sequences of rec1 and rec2 used for the targeted *in vivo* recombination of DNA fragments into the vector, including the translated sequence encoded by the rec1 linker between tag and protein of interest. (B) An example for targeted recombination into pGREG vectors. Gene *X*, flanked by rec1 and rec2 replaces the *HIS3*stuffer fragment by successful gene integration, and a screen for loss of the selection marker identifies potential recombinants. (C) Subsequent replacement of the *GAL1* promoter by other promoters, e.g. the own promoter of gene *X* (P*X*)[80].

molecular probes | invitrogen by life technologies

**Product Information Sheet**

# PrestoBlue™ Cell Viability Reagent Protocol

**Catalog Number: A13261 and A13262** **Literature Part Number: MAN0003232**

Literature Lot Number: V1 Revision date: 11 October 2010

**FAST FACTS**

PrestoBlue™ Cell Viability Reagent is a ready-to-use reagent for rapidly evaluating the viability and proliferation of a wide range of cell types. PrestoBlue™ reagent is quickly reduced by metabolically active cells, providing a quantitative measure of viability and cytotoxicity in as little as 10 minutes. Protect reagent from long term exposure to light and avoid contamination, as this can reduce sensitivity.

| Catalog no. | Amount | Storage and Handling |
|---|---|---|
| A13261 | 25 mL | Store at 4°C, protected from light. Avoid contamination. |
| A13262 | 100 mL | |

## Quick Reference Protocol

1. PrestoBlue™ Cell Viability Reagent is supplied as a 10X solution. Add PrestoBlue™ Reagent directly to cells in culture medium. See below for example volumes:

| Format | Volume of Cells + Media | Volume of PrestoBlue™ Reagent |
|---|---|---|
| Cuvette | 900 µL | 100 µL |
| 96 well plate | 90 µL | 10 µL |
| 384 well plate | 36 µL | 4 µL |

**Note:** Correct for background fluorescence by including control wells containing only cell culture media (no cells) on each plate.

2. Incubate ≥10 minutes at 37° C. Longer incubation times will increase sensitivity of detection. As this is a live cell assay, readings may be taken at multiple time points to determine optimal performance in your lab.

| Format | Recommended Incubation Time |
|---|---|
| Bottom-read fluorescence | 10 minutes – 2 hours |
| Top-read fluorescence | 30 minutes – 2 hours |
| Absorbance | 20 minutes – 2 hours |
| Room temperature incubation | 10 minutes – 2 hours |
| Low cell number (< 5,000 cells/100 µL) | 20 minutes – 24 hours |

3. Read fluorescence or absorbance. Fluorescence is more sensitive than absorbance and is the preferred detection method.

| Format | Excitation | Emission |
|---|---|---|
| General | 540–570 nm | 580–610 nm |
| Fluorescence (Monochrometer) | 560 nm (10 nm bandwidth) | 590 nm (10 nm bandwidth) |
| Fluorescence (Filter) | 535 nm (25 nm bandwidth) | 615 nm (10 nm bandwidth) |
| Absorbance | 570 nm | 600 nm (reference wavelength for normalization) |

4. Calculate and plot the results. Higher fluorescence or absorbance values correlate to greater total metabolic activity.

| Format | Instructions |
|---|---|
| Fluorescence | a. Optional: Average the fluorescence values of the no-cell control wells and subtract from the fluorescence value of each experimental well.<br>b. Plot fluorescence vs. experimental condition (cell number, compound concentration). |
| Absorbance | a. Normalize the 570 nm values to the 600 nm values for the experimental wells.<br>b. Plot the normalized 570 nm absorbance values vs. experimental condition (cell number, compound concentration). |

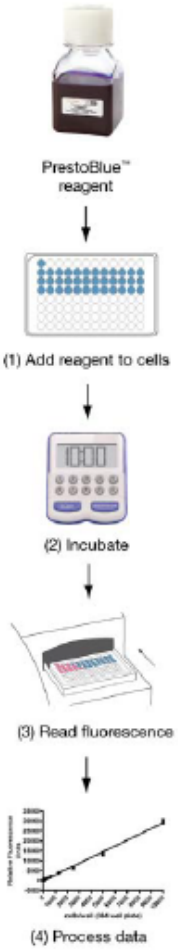


For Technical Support, email probestech@invitrogen.com or phone (800) 438-2209 or (541) 335-0353

Corporate Headquarters • 5791 Van Allen Way • Carlsbad, CA 92008 • Phone: 760 603 7200 • FAX: 760 602 6500 • www.invitrogen.com

**Figure A2- PrestoBlue™ cell viability assay protocol by Invitrogen.** PrestoBlue® is a ready to use cell permeable resazurin-based solution that functions as a cell viability indicator by using the reducing power of living cells to quantitatively measure the proliferation of cells. When added to cells, the PrestoBlue® reagent is modified by the reducing environment of the viable cell and turns red in color, becoming highly fluorescent. This color change can be detected using fluorescence or absorbance measurements.

**Table A1- Gene ID, *S. cerevisiae* orthologous, description and wild-type planktonic vs wild-type biofilm (log2FoldChange) for each differentially expressed gene in the most relevant functional groups.** Full table is provided in supplementary material (CD).

| | Gene ID | Sc orthologous | Description | log2FoldChange |
|---|---|---|---|---|
| Cell wall organization | CAGL0D01034g | PSA1 | GDP-mannose pyrophosphorylase involved in the synthesis of GDP-mannose for protein glycosylation | -4.93594858006695 |
| | CAGL0I06160g | CIS3 | Pir protein family member, putative cell wall component | -4.82148975996513 |
| | CAGL0I04818g | CHS2 | Ortholog(s) have chitin synthase activity | -4.47519652715729 |
| | CAGL0M08756g | EXG2 | Putative exo-1,3-beta-glucanase; predicted GPI-anchor | -4.30761975874411 |
| | CAGL0M03773g | TOS6 | Predicted GPI-linked adhesin-like protein | -4.20169530946103 |
| | CAGL0G08668g | SIM1 | Ortholog(s) have role in fungal-type cell wall organization and endoplasmic reticulum, fungal-type cell wall localization | -4.14430758196996 |
| | CAGL0M08514g | PIR3 | Pir protein family member, putative cell wall component | -4.12752890530874 |
| | CAGL0I06204g | YJL160C | Pir protein family member, putative cell wall component | -4.01975282184051 |
| | CAGL0E04620g | PST1 | Ecm33-family protein with a predicted role in cell wall biogenesis and organization; predicted GPI-anchor | -3.95772286333688 |
| | CAGL0F07601g | CWP2 | GPI-linked cell wall protein | -3.85174628512212 |
| | CAGL0G09449g | CRH1 | Putative glycoside hydrolase; predicted GPI-anchor | -3.66916834753834 |
| | CAGL0M05599g | TOS1 | Ortholog(s) have cell surface, endoplasmic reticulum, extracellular region, fungal-type vacuole, hyphal cell wall localization | -3.51483315562939 |
| | CAGL0M13321g | SVP26 | Ortholog(s) have COPII adaptor activity and role in ER to Golgi vesicle-mediated transport, fungal-type cell wall organization, protein glycosylation, protein retention in Golgi apparatus | -3.18692790048584 |
| | CAGL0A01474g | SCW11 | Ortholog(s) have cell surface, extracellular region, fungal-type cell wall localization | -3.05786625560811 |
| | CAGL0C02101g | KEG1 | Ortholog(s) have role in (1->6)-beta-D-glucan biosynthetic process, chromosome organization and integral component of endoplasmic reticulum membrane localization | -3.02484802403914 |
| | CAGL0M08448g | MCD4 | Ortholog(s) have mannose-ethanolamine phosphotransferase activity and role in ATP transport, GPI anchor biosynthetic process, conidium formation, regulation of growth rate | -3.01924879476438 |
| | CAGL0G00286g | | Putative glycoside hydrolase of the Gas/Phr family; predicted GPI-anchor | -2.98954753774317 |
| | CAGL0M11572g | LCL2 | Ortholog(s) have role in ER-associated ubiquitin-dependent protein catabolic process and fungal-type vacuole localization | -2.92247163646063 |
| | CAGL0L12232g | GAA1 | Ortholog(s) have role in attachment of GPI anchor to protein and GPI-anchor transamidase complex localization | -2.9195676294234 |
| | CAGL0J05236g | LAS21 | Ortholog(s) have mannose-ethanolamine phosphotransferase activity | -2.91543631206463 |
| | CAGL0I00484g | EXG1 | Ortholog(s) have cell adhesion molecule binding, glucan endo-1,6-beta-glucosidase activity, glucan exo-1,3-beta-glucosidase activity | -2.89290396335411 |
| | CAGL0I06182g | HSP150 | Pir protein family member, putative cell wall component | -2.84150618383928 |

| | | | | |
|---|---|---|---|---|
| | CAGL0F01287g | GAS5 | Putative transglycosidase with a predicted role in the elongation of 1,3-beta-glucan | -2.77620336043602 |
| | CAGL0F01485g | TIR4 | Putative GPI-linked cell wall mannoprotein of the Srp1p/Tip1p family | -2.74518440530592 |
| | CAGL0G00814g | CHS5 | Ortholog(s) have small GTPase binding activity | -2.74049186503539 |
| | CAGL0L00979g | TED1 | Ortholog(s) have role in ER to Golgi vesicle-mediated transport and endoplasmic reticulum localization | -2.63188065382928 |
| | CAGL0M05841g | KTR2 | Ortholog(s) have alpha-1,2-mannosyltransferase activity, mannosylphosphate transferase activity, role in cell wall mannoprotein biosynthetic process, protein N-linked glycosylation and Golgi apparatus localization | -2.61792009529716 |
| | CAGL0M05027g | BCH1 | Ortholog(s) have small GTPase binding activity and role in Golgi to plasma membrane transport, fungal-type cell wall chitin biosynthetic process | -2.58497864918708 |
| | CAGL0C01727g | ALG7 | Ortholog(s) have UDP-N-acetylglucosamine-dolichyl-phosphate N-acetylglucosaminephosphotransferase activity | -2.52468164014426 |
| | CAGL0H07403g | KRE2 | Ortholog(s) have alpha-1,2-mannosyltransferase activity | -2.3536307761802 |
| | CAGL0I04532g | MNN2 | Alpha-1,2-mannosyltransferase, involved in protein mannosylation in Golgi | -2.30949816280454 |
| | CAGL0K06281g | GUK1 | Ortholog(s) have guanylate kinase activity, role in GDP biosynthetic process, GMP metabolic process and biofilm matrix, cytoplasm, nucleus localization | -2.26964058049449 |
| | CAGL0M11880g | PER1 | Ortholog(s) have role in GPI anchor biosynthetic process, cellular manganese ion homeostasis and Golgi apparatus, endoplasmic reticulum, fungal-type vacuole membrane localization | -2.23608233653413 |
| | CAGL0G04015g | GPI13 | Ortholog(s) have mannose-ethanolamine phosphotransferase activity | -2.0596719240596 |
| | CAGL0J05544g | END3 | Ortholog(s) have protein binding, bridging activity, role in ascospore wall assembly, endocytosis and cell periphery, mating projection tip localization | -1.90777077081539 |
| | CAGL0A04081g | YLR194C | Predicted GPI-linked cell wall protein | -1.76708368006806 |
| | CAGL0M00220g | PMT4 | Ortholog(s) have dolichyl-phosphate-mannose-protein mannosyltransferase activity | -1.73620420776413 |
| | CAGL0K00979g | PMT6 | Ortholog(s) have role in cellular response to drug, cellular response to neutral pH, cellular response to starvation and filamentous growth of a population of unicellular organisms in response to neutral pH, more | -1.70547182632086 |
| | CAGL0A01452g | CWH41 | Putative glucosidase I; glycoside hydrolase; predicted GPI-anchor | -1.69931077260549 |
| | CAGL0M13453g | GPI16 | Ortholog(s) have GPI-anchor transamidase activity and role in attachment of GPI anchor to protein, conidium formation, fungal-type cell wall organization, fungal-type cell wall polysaccharide biosynthetic process, regulation of growth rate | -1.68410915628385 |
| | CAGL0K12408g | BST1 | Ortholog(s) have phosphatidylinositol deacylase activity | -1.65353589331546 |
| | CAGL0I08459g | RHO1 | Ortholog(s) have GTP binding, GTPase activity, signal transducer activity | -1.60842413609808 |
| | CAGL0G00858g | MID2 | Ortholog(s) have transmembrane signaling receptor activity | -1.54551276440998 |
| | CAGL0B04565g | KTR1 | Ortholog(s) have alpha-1,2-mannosyltransferase activity | -1.53568008957537 |
| | CAGL0G00220g | BGL2 | Ortholog(s) have 1,3-beta-glucanosyltransferase activity, glucan endo-1,3-beta-D-glucosidase activity | -1.27269624912657 |
| | CAGL0E01419g | MKC7 | Putative aspartic protease; predicted GPI-anchor; member of a YPS gene cluster that is required for virulence in mice; induced in response to low pH and high temperature | -1.24871904784173 |
| | CAGL0L03520g | BCK1 | Ortholog(s) have MAP kinase kinase kinase activity | -1.24057376008064 |
| | CAGL0L01243g | GDA1 | Ortholog(s) have guanosine-diphosphatase activity, uridine-diphosphatase activity | -1.235981536971 |

| | | | | |
|---|---|---|---|---|
| | CAGL0B04389g | | Putative class IV chitin synthase; mutants display a significantly thickened cell wall mannoprotein layer; mutants are delayed in cell wall formation during protoplast regeneration | -1.21799419592839 |
| | CAGL0M13827g | FKS3 | Putative 1,3-beta-d-glucan synthase component | -1.17265170712495 |
| | CAGL0I04092g | SHE10 | Ortholog(s) have role in ascospore wall assembly and endoplasmic reticulum localization | -1.17210286421784 |
| | CAGL0C02453g | YPT31 | Ortholog(s) have GTPase activity and role in early endosome to Golgi transport, exocytosis, fungal-type cell wall organization or biogenesis, mitotic cytokinesis, vacuole fusion, non-autophagic | -1.17039109607557 |
| | CAGL0C04235g | GPI18 | Ortholog(s) have dolichyl-phosphate-mannose-glycolipid alpha-mannosyltransferase activity and role in GPI anchor biosynthetic process | -1.09060747245746 |
| | CAGL0J00539g | SLT2 | Mitogen-activated protein kinase with a role in cell wall integrity | -1.07458474052331 |
| | CAGL0K09548g | SMP3 | Ortholog(s) have alpha-1,2-mannosyltransferase activity, dolichyl-phosphate-mannose-glycolipid alpha-mannosyltransferase activity and role in GPI anchor biosynthetic process, fungal-type cell wall biogenesis, plasmid maintenance | -1.05937267507407 |
| | CAGL0G00308g | SCW4 | Putative transglycosidase with a predicted role in the modification of 1,3-beta-glucan | 1.03049120229629 |
| | CAGL0J06182g | SKO1 | bZIP domain-containing protein | 1.06788393036006 |
| | CAGL0H05621g | RLM1 | Putative transcription factor with a predicted role in cell wall integrity | 1.06899210429789 |
| | CAGL0H09592g | | Putative GPI-linked cell wall protein | 1.08630654571261 |
| | CAGL0G01034g | FKS1 | Putative 1,3-beta-glucan synthase component; functionally redundant with Fks2p; "hot spot" mutations in FKS1 confer resistance to echinocandins | 1.13671087959852 |
| | CAGL0K03399g | YPK2 | Ortholog(s) have protein serine/threonine kinase activity, protein serine/threonine kinase inhibitor activity | 1.16616739667233 |
| | CAGL0A02431g | YPS7 | Putative aspartic protease; predicted GPI-anchor; expression induced at high temperature | 1.25976982754294 |
| | CAGL0L03289g | UTH1 | Ortholog(s) have role in fungal-type cell wall biogenesis, fungal-type cell wall organization, mitophagy and cell surface, extracellular region, extrinsic component of mitochondrial inner membrane, fungal-type cell wall localization | 1.26348378688395 |
| | CAGL0I10054g | SKN1 | Ortholog(s) have glucosidase activity, role in (1->6)-beta-D-glucan biosynthetic process, fungal-type cell wall organization, sphingolipid biosynthetic process and integral component of membrane localization | 1.28523441082997 |
| | CAGL0M04169g | KRE1 | Putative cell wall protein with similarity to *S. cerevisiae* Kre1p; predicted role in cell wall biogenesis and organization; predicted GPI-anchor | 1.31750054557928 |
| | CAGL0A04411g | SKT5 | Ortholog(s) have enzyme activator activity and role in barrier septum assembly, cellular protein localization, fungal-type cell wall chitin biosynthetic process, regulation of fungal-type cell wall beta-glucan biosynthetic process | 1.33289782716021 |
| | CAGL0L10670g | ROT1 | Predicted GPI-linked cell wall protein | 1.35595821588016 |
| | CAGL0B02904g | | Beta mannosyltransferase | 1.36614484787957 |
| | CAGL0L01331g | ANP1 | Alpha-1,6-mannosyltransferase with a role in protein N-linked glycosylation in Golgi | 1.39787307487688 |
| | CAGL0B00616g | SPS22 | Ecm33-family protein with a predicted role in cell wall biogenesis and organization; predicted GPI-anchor | 1.44685229159603 |
| | CAGL0J05896g | PGA1 | Ortholog(s) have mannosyltransferase activity, role in GPI anchor biosynthetic process and integral component of endoplasmic reticulum membrane, mannosyltransferase complex, nuclear envelope localization | 1.46780582824048 |
| | CAGL0J03828g | MKK1 | Ortholog(s) have MAP kinase kinase activity, protein tyrosine kinase activity, structural constituent of cell wall activity | 1.51769445991745 |
| | CAGL0B02948g | | Beta mannosyltransferase | 1.66963324741013 |

| | | | | |
|---|---|---|---|---|
| | CAGL0E02255g | ZEO1 | Ortholog(s) have role in fungal-type cell wall organization and extrinsic component of plasma membrane, mitochondrial outer membrane localization | 1.78899510911196 |
| | CAGL0G06072g | ECM14 | Ortholog(s) have endoplasmic reticulum, fungal-type vacuole localization | 1.80587747558472 |
| | CAGL0E05126g | CDC43 | Ortholog(s) have CAAX-protein geranylgeranyltransferase activity, role in glucan biosynthetic process, protein geranylgeranylation and CAAX-protein geranylgeranyltransferase complex, cytosol, nucleus localization | 1.85874617414368 |
| | CAGL0H10120g | YBR056W | Ortholog(s) have glucan endo-1,6-beta-glucosidase activity and role in fungal-type cell wall beta-glucan metabolic process, fungal-type cell wall disassembly involved in conjugation with cellular fusion | 1.86345850277581 |
| | CAGL0H09614g | TIR1 | Putative GPI-linked cell wall protein | 1.8712003512191 |
| | CAGL0K05247g | CSR2 | Ortholog(s) have ubiquitin protein ligase binding activity, role in fungal-type cell wall organization, regulation of transcription from RNA polymerase II promoter and cytosol, nucleus localization | 1.99085652775695 |
| | CAGL0K12980g | | Beta mannosyltransferase | 2.11811102379457 |
| | CAGL0I07249g | BAG7 | Putative GTPase-activating protein involved in cell wall and cytoskeleton homeostasis; gene is upregulated in azole-resistant strain | 2.28345142229744 |
| | CAGL0B00594g | YCL048W-A | Predicted GPI-linked protein | 2.32202602787528 |
| | CAGL0F03883g | GAS3 | Putative glycoside hydrolase of the Gas/Phr family; predicted GPI-anchor | 2.44579153925499 |
| | CAGL0H01661g | SPS2 | Ecm33-family protein with a predicted role in cell wall biogenesis and organization; predicted GPI-anchor | 2.44983280295166 |
| | CAGL0J11462g | YNL190W | Predicted GPI-linked cell wall protein | 2.48250508756196 |
| | CAGL0B02882g | | Beta mannosyltransferase; transmembrane domain protein similar to C. albicans WRY family; gene is downregulated in azole-resistant strain | 2.67134972647007 |
| | CAGL0C03872g | TIR3 | Putative GPI-linked cell wall protein involved in sterol uptake | 2.72420426487234 |
| | CAGL0H07997g | | Protein involved in cell wall beta 1,6-glucan synthesis, similar to Kre9p, | 2.74194393008807 |
| | CAGL0L05434g | NCA3 | Ortholog(s) have role in fungal-type cell wall organization or biogenesis, mitochondrion organization and fungal-type cell wall, fungal-type vacuole localization | 2.8924796867853 |
| | CAGL0G08602g | RPI1 | Ortholog(s) have GTPase regulator activity, role in Ras protein signal transduction, fungal-type cell wall biogenesis, positive regulation of transcription from RNA polymerase II promoter and nucleus localization | 2.89620155616948 |
| | CAGL0G05984g | SPS100 | Ortholog(s) have role in ascospore wall assembly | 2.99469240521345 |
| | CAGL0D00286g | | Beta mannosyltransferase | 3.15181303629568 |
| | CAGL0J06050g | YGP1 | Ortholog(s) have role in cell wall assembly and extracellular region localization | 3.15261108672318 |
| | CAGL0H02563g | HOR7 | Predicted GPI-linked protein | 3.54441087715188 |
| | CAGL0F03003g | HKR1 | Ortholog(s) have osmosensor activity and role in (1->3)-beta-D-glucan biosynthetic process, cellular bud site selection, fungal-type cell wall organization, hyperosmotic response, osmosensory signaling pathway via Sho1 osmosensor | 3.90341026006541 |
| | CAGL0E01595g | GAS4 | Putative glycoside hydrolase of the Gas/Phr family; predicted GPI-anchor | 3.97718252846192 |
| | CAGL0F00891g | LDS2 | Ortholog(s) have role in ascospore wall assembly and ascospore wall, ascus lipid particle, cytoplasm, prospore membrane localization | 4.79146601654687 |
| | CAGL0B02926g | | Beta mannosyltransferase | 5.16840053283222 |
| Re | CAGL0G03795g | SSA2 | Heat shock protein of the HSP70 family | -3.50042939310893 |

| | | | | |
|---|---|---|---|---|
| | CAGL0A02530g | TRR1 | Thioredoxin reductase | -3.40364178913331 |
| | CAGL0A04301g | PTC3 | Ortholog(s) have MAP kinase threonine phosphatase activity, protein serine/threonine phosphatase activity | -3.35254039587457 |
| | CAGL0G01925g | YKR070W | Ortholog(s) have role in hyperosmotic response, response to antibiotic, response to salt stress and mitochondrion localization | -2.79585658309549 |
| | CAGL0F08833g | MSB2 | Putative adhesin-like protein | -2.7259183920443 |
| | CAGL0J09834g | PTC4 | Ortholog(s) have protein serine/threonine phosphatase activity, role in protein dephosphorylation and mitochondrion localization | -2.71617828897327 |
| | CAGL0J02750g | CAJ1 | Ortholog of *S. cerevisiae* : CAJ1, C. albicans SC5314 : C4_05810W_A, C. dubliniensis CD36 : Cd36_45380, C. parapsilosis CDC317 : CPAR2_500650 and Candida tenuis NRRL Y-1498 : CANTEDRAFT_132273 | -2.51486108142404 |
| | CAGL0L00495g | HSC82 | Putative heat shock protein | -2.29757582245609 |
| | CAGL0E04906g | AHA1 | Ortholog(s) have ATPase activator activity, chaperone binding activity, role in cellular response to heat, protein folding and cytosol localization | -2.20186510941179 |
| | CAGL0M09185g | EMC2 | Ortholog(s) have role in protein folding in endoplasmic reticulum and ER membrane protein complex, cell division site, cytosol, mitotic spindle pole body, nucleus localization | -2.18526717776661 |
| | CAGL0E04114g | AFG1 | Ortholog(s) have role in cellular response to oxidative stress, misfolded or incompletely synthesized protein catabolic process, protein import into peroxisome matrix and mitochondrial inner membrane localization | -2.13379058608997 |
| | CAGL0B03685g | | Putative flavodoxin | -2.13142441306128 |
| | CAGL0G07271g | TSA1 | Putative thioredoxin peroxidase; protein differentially expressed in azole resistant strain | -2.08185233653904 |
| | CAGL0F00825g | GSH2 | Putative glutathione synthetase; role in redox homeostasis and detoxification of the cell of metal ions | -2.07803917417526 |
| | CAGL0H08283g | HSP10 | Ortholog(s) have chaperone binding, unfolded protein binding activity, role in chaperone-mediated protein complex assembly, protein import into mitochondrial intermembrane space, protein refolding and mitochondrial matrix localization | -2.01408355613194 |
| | CAGL0D05522g | EMC6 | Ortholog(s) have role in protein folding in endoplasmic reticulum and ER membrane protein complex localization | -1.89650235177832 |
| | CAGL0K05423g | TIP41 | Ortholog(s) have role in TOR signaling and positive regulation of phosphoprotein phosphatase activity, more | -1.86778407916782 |
| | CAGL0J05566g | MKT1 | Ortholog(s) have role in cellular response to DNA damage stimulus, interspecies interaction between organisms and P-body, cytoplasmic stress granule, cytosol, nuclear periphery, polysome localization | -1.84323949579915 |
| | CAGL0J00561g | YHI9 | Ortholog(s) have role in chromatin silencing by small RNA, endoplasmic reticulum unfolded protein response and cytosol, nucleus localization | -1.7468426106686 |
| | CAGL0G04961g | GRX8 | Ortholog(s) have glutathione-disulfide reductase activity and cytoplasm localization | -1.63226322647135 |
| | CAGL0F09097g | SKN7 | Predicted transcription factor, involved in oxidative stress response; required for induction of TRX2, TRR1 and TSA1 transcription under oxidative stress | -1.56776360895858 |
| | CAGL0E02739g | SGT2 | Ortholog(s) have protein complex scaffold activity, role in posttranslational protein targeting to membrane, response to heat and TRC complex, nucleus localization | -1.5663249159307 |
| | CAGL0I04026g | PBP4 | Ortholog(s) have cytoplasmic stress granule, nucleus localization | -1.54308917772077 |
| | CAGL0C04631g | AIM25 | Ortholog(s) have role in cellular response to heat, cellular response to oxidative stress, chronological cell aging, negative regulation of mitophagy and mitochondrion localization | -1.52552088031311 |
| | CAGL0H01815g | CBF1 | Centromere binding factor; basic helix-loop-helix leucine zipper DNA-binding protein; binds in vitro to centromere DNA element I sequence GTCACATG; complements the methionine biosynthesis defect of a Saccharomyces cerevisiae cbf1 mutant | -1.51585754782999 |

| | | | | |
|---|---|---|---|---|
| | CAGL0M10829g | SSK2 | Ortholog(s) have MAP kinase kinase kinase activity, actin binding activity | -1.47662037818126 |
| | CAGL0B02761g | DCR2 | Ortholog(s) have phosphoprotein phosphatase activity and role in negative regulation of endoplasmic reticulum unfolded protein response, protein dephosphorylation, traversing start control point of mitotic cell cycle | -1.4358951930504 |
| | CAGL0M04697g | RDL2 | Ortholog(s) have thiosulfate sulfurtransferase activity and mitochondrion localization | -1.4275007665402 |
| | CAGL0C02233g | MXR1 | Ortholog(s) have L-methionine-(S)-S-oxide reductase activity, peptide-methionine (S)-S-oxide reductase activity and role in L-methionine salvage from methionine sulphoxide, cellular response to hydrogen peroxide | -1.36839783564363 |
| | CAGL0G03597g | SHO1 | *S. cerevisiae* ortholog SHO1 has role in establishment of cell polarity, osmosensory signaling pathway, signal transduction involved in filamentous growth, cellular response to heat; osmosensitivity of CBS138 strain not seen in other strains | -1.31720315917977 |
| | CAGL0M06325g | SMP1 | Ortholog(s) have DNA binding, bending, sequence-specific DNA binding activity, role in positive regulation of transcription from RNA polymerase II promoter in response to osmotic stress and cytoplasm, nucleus localization | -1.28226765630935 |
| | CAGL0H03443g | HSF1 | Ortholog(s) have sequence-specific DNA binding, transcription factor activity, sequence-specific DNA binding activity | -1.28074124867603 |
| | CAGL0C02123g | ERJ5 | Ortholog(s) have role in protein folding and endoplasmic reticulum localization | -1.26769728819215 |
| | CAGL0K06743g | YBP1 | Protein involved in resistance to hydrogen peroxide; *S. cerevisiae* ortholog Ybp1p has role in cellular response to oxidative stress and localizes to cytoplasm | -1.26112912738279 |
| | CAGL0H08195g | STI1 | Ortholog(s) have ATPase inhibitor activity, Hsp70 protein binding, Hsp90 protein binding, mRNA binding activity, role in protein folding, protein targeting to mitochondrion and cytosol, nucleus localization | -1.25446117427624 |
| | CAGL0C02035g | DUG1 | Ortholog(s) have metallodipeptidase activity, omega peptidase activity, role in glutathione catabolic process and biofilm matrix, cytosol, mitochondrion, nucleus, ribosome localization | -1.25008995890291 |
| | CAGL0J02068g | EPS1 | Ortholog(s) have protein disulfide isomerase activity, protein-disulfide reductase (glutathione) activity, unfolded protein binding activity | -1.23863054528179 |
| | CAGL0M06171g | UMP1 | Ortholog(s) have role in cellular response to DNA damage stimulus, proteasome assembly, ubiquitin-dependent protein catabolic process and cytosol, nucleus localization | -1.22601039735976 |
| | CAGL0K03201g | YHL018W | Ortholog(s) have role in ascospore formation, cellular response to biotic stimulus and cellular response to starvation, more | -1.21053696061009 |
| | CAGL0K05813g | GRX2 | Ortholog(s) have glutathione disulfide oxidoreductase activity, glutathione peroxidase activity, glutathione transferase activity and role in glutathione metabolic process, pathogenesis, removal of superoxide radicals | -1.11777408545519 |
| | CAGL0L10956g | RIM20 | Ortholog(s) have role in cellular response to lithium ion, cellular response to neutral pH, entry into host and filamentous growth of a population of unicellular organisms in response to pH, more | -1.09586852543284 |
| | CAGL0H03707g | SIS1 | Ortholog(s) have misfolded protein binding activity | -1.09418941157117 |
| | CAGL0I03322g | ECM10 | Ortholog(s) have role in protein refolding, protein targeting to mitochondrion, spore germination and mitochondrial membrane, mitochondrial nucleoid localization | -1.07223781649004 |
| | CAGL0H04125g | ALO1 | Ortholog(s) have D-arabinono-1,4-lactone oxidase activity | -1.04488701646285 |
| | CAGL0K08756g | YAP5 | bZIP domain-containing protein | -1.02433419772652 |
| | CAGL0I00836g | SIP5 | Ortholog(s) have role in cellular response to glucose starvation and Golgi apparatus, endoplasmic reticulum, fungal-type vacuole membrane localization | -1.01586998706293 |
| | CAGL0D03234g | PSR2 | Ortholog(s) have role in cellular response to salt stress, response to heat and cytosol localization | 1.00113372627324 |
| | CAGL0G02893g | POS5 | Ortholog(s) have NADH kinase activity, role in NADP biosynthetic process, cellular response to oxidative stress and mitochondrial matrix localization | 1.0118937198993 |
| | CAGL0I05038g | PTC2 | Ortholog(s) have MAP kinase threonine phosphatase activity, protein serine/threonine phosphatase activity | 1.02613984593142 |

| | | | | |
|---|---|---|---|---|
| | CAGL0G02101g | ECM4 | Putative omega class glutathione transferase; gene is downregulated in azole-resistant strain | 1.06702911587737 |
| | CAGL0K01177g | PAC10 | Ortholog(s) have tubulin binding activity, role in response to cold, tubulin complex assembly and cytosol, nucleus, polysome, prefoldin complex localization | 1.07691908836272 |
| | CAGL0L10186g | TMC1 | Putative stress-induced protein; gene is upregulated in azole-resistant strain | 1.14471542042427 |
| | CAGL0M06083g | SSE2 | Heat shock protein of HSP70 family | 1.15940715316127 |
| | CAGL0H06567g | SLN1 | Ortholog(s) have histidine phosphotransfer kinase activity, osmosensor activity, phosphorelay response regulator activity, protein histidine kinase activity | 1.16688424233361 |
| | CAGL0M04763g | YOR289W | Ortholog(s) have role in cellular response to drug and cytosol, nucleus localization | 1.22141136502121 |
| | CAGL0H08866g | HOT1 | Putative transcription factor involved in osmostress response; gene is upregulated in azole-resistant strain | 1.23021955183358 |
| | CAGL0F05329g | YDR210W | Ortholog of *S. cerevisiae* : YDR210W and Saccharomyces cerevisiae S288C : YDR210W | 1.23074740147241 |
| | CAGL0H04631g | YAP1 | Protein with a basic leucine zipper (bZip) domain involved in drug resistance and the response to oxidative stress; activates multidrug transporter FLR1 | 1.26784914225026 |
| | CAGL0E05962g | FMP40 | Ortholog(s) have cytosol, mitochondrion, nucleus localization | 1.30268583060988 |
| | CAGL0L11110g | CMP2 | Catalytic subunit of calcineurin, calcium/calmodulin-dependent Ser/Thr-specific protein phosphatase; regulates stress-responding transcription factor Crz1p; involved in thermotolerance, response to ER stress, cell wall integrity, virulence | 1.35111732415506 |
| | CAGL0H10076g | YRO2 | Ortholog(s) have cellular bud, endoplasmic reticulum, mitochondrion, plasma membrane localization | 1.35551336477638 |
| | CAGL0H04367g | WAR1 | Ortholog(s) have sequence-specific DNA binding activity | 1.4285641602271 |
| | CAGL0F03245g | IRE1 | Putative protein kinase and endonuclease required for response to ER stress independently of Hac1p; involved in nonspecific degradation of ER-localized mRNAs but not in unfolded protein response via activation of Hac1p | 1.42958748558098 |
| | CAGL0D05610g | PSR1 | Ortholog(s) have phosphoprotein phosphatase activity, role in cellular response to salt stress, filamentous growth, response to heat and cytosol, plasma membrane localization | 1.44137055807843 |
| | CAGL0K02145g | COM2 | Ortholog(s) have sequence-specific DNA binding activity and role in cellular response to acetate, cellular response to drug, regulation of transcription from RNA polymerase II promoter in response to stress | 1.44383878036487 |
| | CAGL0F03069g | CAD1 | bZIP domain-containing protein | 1.49387105075052 |
| | CAGL0H08129g | DFG16 | Ortholog(s) have role in cellular response to pH, filamentous growth of a population of unicellular organisms in response to pH, pathogenesis, protein processing, pseudohyphal growth, regulation of intracellular pH | 1.52802410418038 |
| | CAGL0F08745g | STF2 | Ortholog(s) have role in cellular response to desiccation and cytoplasm localization | 1.62970064883327 |
| | CAGL0M08404g | TPK3 | Ortholog(s) have cAMP-dependent protein kinase activity and role in Ras protein signal transduction, mitochondrion organization, protein kinase A signaling, protein phosphorylation | 1.63760268427101 |
| | CAGL0G06578g | OCA1 | Ortholog(s) have role in cellular response to oxidative stress and cytoplasm localization | 1.65661330562945 |
| | CAGL0G08151g | GRX3 | Ortholog(s) have 2 iron, 2 sulfur cluster binding, RNA polymerase II activating transcription factor binding, glutathione disulfide oxidoreductase activity | 1.67866010087762 |
| | CAGL0K09834g | NST1 | Ortholog(s) have role in response to salt stress and cytoplasm localization | 1.68007135893622 |
| | CAGL0L02827g | PTP2 | Ortholog(s) have protein tyrosine phosphatase activity | 1.69839482840551 |
| | CAGL0L03630g | GSH1 | Putative gamma glutamylcysteine synthetase, essential for viability; role in glutathione biosynthesis; required to keep the redox homeostasis and to detoxify the cell of metal ions | 1.72495555954918 |

| | | | | |
|---|---|---|---|---|
| | CAGL0H02827g | JEM1 | Ortholog(s) have chaperone binding, unfolded protein binding activity and role in ER-associated ubiquitin-dependent protein catabolic process, karyogamy involved in conjugation with cellular fusion, protein folding in endoplasmic reticulum | 1.75993905697335 |
| | CAGL0I01166g | TRR2 | Thioredoxin reductase (NADPH) | 1.86695712954673 |
| | CAGL0I10582g | YGR127W | Ortholog(s) have role in filamentous growth and intracellular localization | 1.94012033308356 |
| | CAGL0L05258g | SRX1 | Ortholog(s) have sulfiredoxin activity, role in cellular protein localization, cellular response to oxidative stress and cytosol, nucleus localization | 1.95536397728113 |
| | CAGL0H07425g | CNS1 | Ortholog(s) have Hsp70 protein binding, Hsp90 protein binding, ribosome binding activity, role in cellular response to drug, protein folding and cytosol, nucleus localization | 1.97206259332195 |
| | CAGL0E03762g | RIM101 | Ortholog(s) have sequence-specific DNA binding, transcriptional repressor activity, RNA polymerase II core promoter proximal region sequence-specific binding activity | 2.09579515032475 |
| | CAGL0H00935g | YAR1 | Ortholog(s) have unfolded protein binding activity | 2.12429401995742 |
| | CAGL0I05934g | YJL144W | Ortholog(s) have role in cellular response to water deprivation and cytoplasm localization | 2.1511214680126 |
| | CAGL0F06545g | RIM9 | Ortholog(s) have role in ascospore formation, cellular response to alkaline pH, cellular response to lithium ion, cellular response to neutral pH and cellular response to starvation, more | 2.18060575714489 |
| | CAGL0B03509g | RCK2 | Ortholog(s) have protein serine/threonine kinase activity | 2.20509194878687 |
| | CAGL0C04741g | SOD1 | Cytosolic copper-zinc superoxide dismutase | 2.2328449476456 |
| | CAGL0H06611g | ESL1 | Ortholog of *S. cerevisiae* : ESL1, C. albicans SC5314 : C4_01020C_A, C. dubliniensis CD36 : Cd36_41030, C. parapsilosis CDC317 : CPAR2_401340 and Candida tenuis NRRL Y-1498 : CANTEDRAFT_104645 | 2.23407388551108 |
| | CAGL0F07513g | MBR1 | Ortholog(s) have role in aerobic respiration | 2.31486717673838 |
| | CAGL0H04499g | HLJ1 | Ortholog(s) have ATPase activator activity, role in ER-associated ubiquitin-dependent protein catabolic process and endoplasmic reticulum membrane localization | 2.3207447690831 |
| | CAGL0H08580g | | Has domain(s) with predicted FMN binding, iron ion binding, oxidoreductase activity and role in oxidation-reduction process | 2.3290642948095 |
| | CAGL0K10604g | CMK1 | Ortholog(s) have calmodulin-dependent protein kinase activity, role in protein phosphorylation, signal transduction and cytoplasm localization | 2.36925466639635 |
| | CAGL0B00836g | MXR2 | Ortholog(s) have peptide-methionine (R)-S-oxide reductase activity, role in cellular response to oxidative stress and cytosol, mitochondrion, nucleus localization | 2.40996079054349 |
| | CAGL0G08019g | YDR090C | Ortholog(s) have role in cellular response to biotic stimulus, cellular response to starvation and filamentous growth of a population of unicellular organisms in response to biotic stimulus, more | 2.46162849951114 |
| | CAGL0H04037g | GAC1 | Ortholog(s) have heat shock protein binding, protein phosphatase regulator activity and role in glycogen metabolic process, meiotic nuclear division, mitotic spindle assembly checkpoint, response to heat | 2.50413380071585 |
| | CAGL0K00759g | ZPR1 | Protein with similarity to M. musculus zinc finger protein Zpr1p | 2.62068663117656 |
| | CAGL0H07667g | PDE1 | Ortholog(s) have 3',5'-cyclic-AMP phosphodiesterase activity, 3',5'-cyclic-GMP phosphodiesterase activity | 2.64415771469504 |
| | CAGL0E02079g | MSN1 | Ortholog(s) have sequence-specific DNA binding activity | 2.66545147802133 |
| | CAGL0L10560g | SSZ1 | Protein with a predicted role in pleiotropic drug resistance | 2.68569921374983 |
| | CAGL0L04092g | NMA111 | Ortholog(s) have serine-type peptidase activity, role in apoptotic process, cellular lipid metabolic process, cellular response to heat, protein catabolic process and nucleus localization | 2.73541173223969 |
| | CAGL0L06666g | YHB1 | Putative flavohemoglobin, involved in nitric oxide detoxification | 2.77313099207695 |

| | | | | |
|---|---|---|---|---|
| | CAGL0M03663g | RIM21 | Ortholog(s) have role in ascospore formation, cellular response to alkaline pH, cellular response to lithium ion and cellular response to neutral pH, more | 2.78202222073425 |
| | CAGL0D01584g | JID1 | Ortholog(s) have mitochondrion localization | 2.87557812996913 |
| | CAGL0K12540g | HAC1 | bZIP domain-containing transcription factor, activates transcription of genes involved in unfolded protein response; activation does not require cleavage of HAC1 mRNA by Ire1p | 2.87611384311831 |
| | CAGL0E04356g | SOD2 | Ortholog(s) have manganese ion binding, superoxide dismutase activity | 2.9274617438716 |
| | CAGL0F01265g | YAP7 | bZIP domain-containing protein involved in regulation of nitric oxide detoxification | 2.95317447690549 |
| | CAGL0K12144g | FES1 | Putative Hsp70p nucleotide exchange factor; protein abundance decreased in ace2 mutant cells | 3.03245682764208 |
| | CAGL0M13189g | MSN4 | Putative transcription factor similar to *S. cerevisiae* Msn4p; involved in response to oxidative stress | 3.07089329535443 |
| | CAGL0L09339g | HAA1 | Putative transcription factor, involved in regulation of response to acetic acid stress | 3.09819616148218 |
| | CAGL0K10868g | | Putative catalase A; gene is downregulated in azole-resistant strain; regulated by oxidative stress and glucose starvation; protein abundance increased in ace2 mutant cells | 3.1273987349684 |
| | CAGL0H03971g | YCP4 | Ortholog(s) have role in cellular response to oxidative stress, pathogenesis and membrane raft, mitochondrion, plasma membrane localization | 3.1450757175513 |
| | CAGL0K06259g | TSA2 | Thiol-specific antioxidant protein; predicted thioredoxin peroxidase involved in oxidative stress response; protein abundance decreased in ace2 mutant cells | 3.15723604029932 |
| | CAGL0J07502g | YNL234W | Putative protein similar to globins with a heme-binding domain; gene is upregulated in azole-resistant strain | 3.25308834294313 |
| | CAGL0M08800g | YAP6 | bZIP domain-containing protein | 3.30626270021698 |
| | CAGL0K04741g | SSB2 | Heat shock protein of HSP70 family | 3.41306848161002 |
| | CAGL0J00891g | | Putative protein required for growth at low temperature; gene is downregulated in azole-resistant strain | 3.43404518040423 |
| | CAGL0G03289g | SSA4 | Heat shock protein of the HSP70 family | 3.5804695886548 |
| | CAGL0J09966g | YDJ1 | Putative mitochondrial and ER import protein; protein abundance increased in ace2 mutant cells | 3.76561983562898 |
| | CAGL0K03459g | SPG4 | Ortholog of *S. cerevisiae* : SPG4 and Saccharomyces cerevisiae S288C : YMR107W | 4.53911641858522 |
| | CAGL0J04202g | HSP12 | Heat shock protein; gene is upregulated in azole-resistant strain; expression upregulated in biofilm vs planktonic cell culture | 4.57725517268747 |
| | CAGL0L00583g | USV1 | Ortholog(s) have sequence-specific DNA binding, transcription factor activity, sequence-specific DNA binding activity | 4.5907372626125 |
| | CAGL0F07953g | SPG1 | Ortholog(s) have endoplasmic reticulum, mitochondrion localization | 4.82926510946983 |
| | CAGL0G02783g | SHQ1 | Ortholog(s) have unfolded protein binding activity, role in box H/ACA snoRNP assembly and cytosol, nucleoplasm localization | 5.17516707251316 |
| | CAGL0F08195g | MGA1 | Ortholog(s) have sequence-specific DNA binding, transcription factor activity, sequence-specific DNA binding activity | 5.29010363214814 |
| | CAGL0F08217g | YGR250C | Ortholog(s) have mRNA binding activity and cytoplasmic stress granule localization | 5.46519663031966 |
| | CAGL0D00154g | AQY1 | Has domain(s) with predicted transporter activity, role in transport and membrane localization | 7.0175707992169 |
| | CAGL0G05269g | FMP16 | Putative mitochondrial protein; gene is downregulated in azole-resistant strain | 8.96836792746183 |
| | CAGL0E05984g | GRE1 | Ortholog of *S. cerevisiae* : GRE1 and Saccharomyces cerevisiae S288C : YPL223C | 9.87413342381116 |

| | | | | |
|---|---|---|---|---|
| Response to drugs | CAGL0K00737g | SLI1 | Ortholog(s) have N-acetyltransferase activity, role in response to drug and nuclear envelope, plasma membrane localization | -3.46009213750262 |
| | CAGL0E03003g | NAT2 | Ortholog(s) have role in N-terminal peptidyl-methionine acetylation, cellular response to drug and mitochondrion localization | -2.07231668877769 |
| | CAGL0I02552g | STB5 | Predicted sequence-specific DNA binding transcription factor, negative regulator of azole resistance; acts as transcriptional repressor of ATP-binding Cassette (ABC) transporter genes | -1.43746699128384 |
| | CAGL0M01760g | | Multidrug transporter of ATP-binding cassette (ABC) superfamily, involved in resistance to azoles; expression regulated by Pdr1p; increased abundance in azole resistant strains; expression increased by loss of the mitochondrial genome | -1.15119804906066 |
| | CAGL0J04774g | TDA5 | Ortholog(s) have role in response to drug and cytosol, endoplasmic reticulum, mitochondrion localization | -1.11097128908204 |
| | CAGL0J09944g | AQR1 | Plasma membrane drug:H+ antiporter involved in resistance to drugs and acetic acid | 1.02804784342591 |
| | CAGL0I04862g | | Predicted plasma membrane ATP-binding cassette (ABC) transporter, putative transporter involved in multidrug resistance; involved in Pdr1p-mediated azole resistance | 1.04543897830221 |
| | CAGL0L04576g | YRM1 | Ortholog(s) have RNA polymerase II transcription factor activity, sequence-specific DNA binding, sequence-specific DNA binding activity and role in regulation of transcription from RNA polymerase II promoter | 1.06424253697549 |
| | CAGL0M01078g | YDR338C | Ortholog(s) have fungal-type vacuole membrane localization | 1.5718635563175 |
| | CAGL0I08019g | YOL075C | Ortholog(s) have role in cellular response to drug and cell periphery, extrinsic component of fungal-type vacuolar membrane localization | 1.60005425398319 |
| | CAGL0H00440g | YJR124C | Ortholog(s) have fungal-type vacuole membrane localization | 1.75586187397337 |
| | CAGL0B02343g | ATR1 | Putative multidrug efflux pump of major facilitator superfamily; gene is downregulated in azole-resistant strain | 2.01580198869693 |
| | CAGL0B02079g | AZR1 | Ortholog(s) have azole transporter activity, role in asperfuranone biosynthetic process, azole transport and plasma membrane localization | 2.81646712843933 |
| | CAGL0G01122g | YLR346C | Putative protein; gene is upregulated in azole-resistant strain | 2.98342002217262 |
| | CAGL0M05445g | COS111 | Ortholog(s) have role in signal transduction and mitochondrion localization | 3.04009620373924 |
| | CAGL0K03069g | IRC21 | Ortholog(s) have role in response to drug and cytosol, nucleus localization | 3.55461150214479 |
| | CAGL0E03674g | | Putative drug:H+ antiporter, involved in efflux of clotrimazole; required for resistance to clotrimazole and other drugs | 3.58753098506812 |
| | CAGL0L10912g | TPO4 | Ortholog(s) have spermidine transmembrane transporter activity, spermine transmembrane transporter activity, role in spermidine transport, spermine transport and fungal-type vacuole membrane, plasma membrane localization | 3.63271315923149 |
| | CAGL0H10450g | YDL114W | Ortholog(s) have endoplasmic reticulum localization | 4.00524143335671 |
| | CAGL0I10384g | TPO2 | Predicted polyamine transporter of the major facilitator superfamily; required for azole resistance | 4.64338261710025 |
| | CAGL0M01870g | | Putative zinc finger protein; gene is upregulated in azole-resistant strain | 4.83933730317767 |
| | CAGL0G08624g | QDR1 | Drug:H+ antiporter of the Major Facilitator Superfamily, confers imidazole drug resistance, involved in quinidine/multidrug efflux; gene is activated by Pdr1p; upregulated in azole-resistant strain | 5.25389419552867 |
| | CAGL0J00363g | YHK8 | Putative protein of major facilitator superfamily; gene is downregulated in azole-resistant strain | 6.67898449512817 |
| Virulence | CAGL0E01771g | | Putative aspartic protease; predicted GPI-anchor; member of a YPS gene cluster that is required for virulence in mice; gene is downregulated in azole-resistant strain | -3.66347538867643 |
| | CAGL0E01859g | | Putative aspartic protease; predicted GPI-anchor; member of a YPS gene cluster that is required for virulence in mice; induced in response to low pH and high temperature | 1.29347776157894 |

| | | | | |
|---|---|---|---|---|
| | CAGL0E01881g | | Putative aspartic protease; member of a YPS gene cluster that is required for virulence in mice; induced in response to low pH and high temperature | 1.90900835695974 |
| | CAGL0E01727g | | Putative aspartic protease; predicted GPI-anchor; member of a YPS gene cluster that is required for virulence in mice | 3.4464680148029 |
| | CAGL0E01749g | | Putative aspartic protease; member of a YPS gene cluster that is required for virulence in mice; induced in response to low pH and high temperature | 3.79943918914773 |
| **Adhesion and biofilm formation** | CAGL0K09130g | SRL1 | Putative adhesin-like protein | -5.317380929373 |
| | CAGL0L13332g | | Sub-telomerically encoded lectin-like adhesin with a role in cell adhesion; contains multiple tandem repeats; predicted GPI-anchor; belongs to adhesin cluster I | -4.9199580385345 |
| | CAGL0L13299g | | Putative adhesin; belongs to adhesin cluster I | -4.19032202657194 |
| | CAGL0G05896g | DSE2 | Putative adhesin-like protein | -3.78221615282249 |
| | CAGL0E02915g | | Putative adhesin-like protein | -3.69958855463031 |
| | CAGL0G09537g | IES4 | Putative adhesin-like protein | -2.55836734251073 |
| | CAGL0B03399g | | Protein involved in sub-telomeric silencing and regulation of biofilm formation; involved in regulation of telomere length; mutants display increased colonization of mouse kidneys relative to wild-type; required for silencing at MTL3 | -2.4918006069107 |
| | CAGL0L00227g | | Putative adhesin with glycine and serine rich repeats; belongs to adhesin cluster V | -2.10136043878248 |
| | CAGL0G03487g | TMN3 | Ortholog(s) have role in cellular copper ion homeostasis, cellular response to drug, invasive growth in response to glucose limitation, pseudohyphal growth, vacuolar transport and COPI-coated vesicle, Golgi apparatus localization | -2.00699317032467 |
| | CAGL0H00110g | | Adhesin-like protein with internal repeats; predicted GPI-anchor; likely a C-terminal fragment of a single ORF with CAGL0H00132g; belongs to adhesin cluster V | -1.74664544115037 |
| | CAGL0C01133g | | Adhesin-like protein; belongs to adhesin cluster VII; predicted GPI anchor | -1.69653361005933 |
| | CAGL0K00170g | | Putative adhesin-like protein; belongs to adhesin cluster I | -1.27449964771154 |
| | CAGL0E01661g | | Adhesin-like protein with tandem repeats; predicted GPI-anchor; belongs to adhesin cluster III | -1.19666550535911 |
| | CAGL0F09273g | | Putative adhesin-like protein; belongs to adhesin cluster V | 1.00376643232775 |
| | CAGL0I10246g | | Adhesin-like protein with tandem repeats; contains a PA14 domain; belongs to adhesin cluster II | 1.06461007650106 |
| | CAGL0I00220g | | Predicted GPI-linked adhesin-like protein; belongs to adhesin cluster I | 1.06661636964225 |
| | CAGL0J05159g | | Putative adhesin-like protein | 1.09216224132623 |
| | CAGL0J00253g | MTL1 | Putative adhesin-like protein | 1.21215045156334 |
| | CAGL0J11990g | | Putative adhesin-like protein with internal repeats; identified in cell wall extracts by mass spectrometry; ORF appears artificially broken into fragments due to sequencing errors; belongs to adhesin cluster V; predicted GPI anchor | 1.2318423860663 |
| | CAGL0H08844g | DDR48 | Putative adhesin-like protein | 1.47032033932445 |
| | CAGL0A01366g | | Putative adhesin; belongs to adhesin cluster I | 1.66457728491842 |
| | CAGL0K13024g | | Adhesin-like protein required for adherence to endothelial cells; identified in cell wall extracts by mass spectrometry; belongs to adhesin cluster III; predicted GPI anchor; 6 tandem repeats; expressed more in stationary growth phase | 1.70531136817866 |
| | CAGL0E06644g | | Sub-telomerically encoded adhesin with a role in cell adhesion; GPI-anchored cell wall protein; N-terminal ligand binding domain binds to ligands containing a terminal galactose residue; belongs to adhesin cluster I | 1.71570142900477 |

| | | | | |
|---|---|---|---|---|
| | CAGL0I05170g | CST6 | bZIP domain-containing protein involved in regulation of biofilm formation; negatively regulates expression of the EPA6 adhesin independently of Yak1p/Sir4p signaling; regulates carbonic anhydrase Nce103p in response to carbon dioxide | 1.7350955824476 |
| | CAGL0L00157g | | Putative adhesin-like protein; multiple tandem repeats; predicted GPI-anchor; belongs to adhesin cluster III | 1.74550576250933 |
| | CAGL0M00132g | | Putative adhesin-like cell wall protein; belongs to adhesin cluster I | 1.76472681897738 |
| | CAGL0D06226g | | Putative adhesin-like protein | 1.79728021397183 |
| | CAGL0J11891g | | Putative adhesin-like protein; identified in cell wall extracts by mass spectrometry; belongs to adhesin cluster VI | 1.81870612717552 |
| | CAGL0G05808g | YDL211C | Putative adhesin-like protein | 1.88269759498482 |
| | CAGL0A01284g | | Putative adhesin-like protein; belongs to adhesin cluster I | 1.89222333915883 |
| | CAGL0J02552g | | Adhesin-like protein; predicted GPI anchor; belongs to adhesin cluster VI | 2.00663324906419 |
| | CAGL0I11011g | | Putative adhesin; belongs to adhesin cluster V | 2.13026058049217 |
| | CAGL0G10175g | | Adhesin-like protein; identified in cell wall extracts by mass spectrometry; belongs to adhesin cluster IV; predicted GPI anchor | 2.32099571094345 |
| | CAGL0E00231g | | Putative adhesin-like protein; contains tandem repeats and a predicted GPI-anchor; belongs to adhesin cluster III | 2.38134788253228 |
| | CAGL0E06666g | | Epithelial adhesion protein; predicted GPI-anchor; belongs to adhesin cluster I | 2.42580194701581 |
| | CAGL0M07634g | SOK2 | Ortholog(s) have sequence-specific DNA binding, transcription factor activity, sequence-specific DNA binding activity | 2.87792716233405 |
| | CAGL0J02508g | | Adhesin-like protein; identified in cell wall extracts by mass spectrometry; belongs to adhesin cluster VI; predicted GPI anchor | 2.91006446690673 |
| | CAGL0E06688g | | Epithelial adhesion protein; belongs to adhesin cluster I; GPI-anchored | 2.91498409653071 |
| | CAGL0I10200g | | Protein with tandem repeats; putative adhesin-like protein; belongs to adhesin cluster II | 2.94016612610038 |
| | CAGL0J02530g | | Putative adhesion protein; predicted GPI-anchor; belongs to adhesin cluster VI | 2.98507846684666 |
| | CAGL0E00275g | | Putative adhesin; belongs to adhesin cluster I | 3.17800492886771 |
| | CAGL0G04125g | | Protein with similarity to *S. cerevisiae* Sag1 agglutinin, involved in cell adhesion; predicted GPI-anchor | 3.42211001891302 |
| | CAGL0J05984g | AAH1 | Ortholog(s) have adenine deaminase activity, role in adenine catabolic process, cell-abiotic substrate adhesion, hypoxanthine salvage and cytosol, nucleus localization | 3.45083927383838 |
| | CAGL0I07183g | SFL1 | Ortholog(s) have RNA polymerase II core promoter proximal region sequence-specific DNA binding, RNA polymerase II repressing transcription factor binding and RNA polymerase II transcription factor activity, more | 3.52737426267657 |
| | CAGL0M04807g | SNF2 | Component of the chromatin remodelling Swi/Snf complex; involved in regulation of biofilm formation | 3.64839327675781 |
| | CAGL0I10147g | | Protein with 32 tandem repeats; putative adhesin-like protein; belongs to adhesin cluster II | 3.80147539904505 |
| | CAGL0H10626g | | Predicted cell wall adhesin with a role in adhesion; belongs to adhesin cluster III; predicted GPI anchor; contains tandem repeats | 4.41212008796675 |
| | CAGL0K13002g | | Putative adhesin; predicted GPI-anchor; belongs to adhesin cluster III | 4.65623346755426 |
| | CAGL0I10340g | | Cell wall adhesin; predicted GPI anchor; contains tandem repeats; belongs to adhesin cluster II | 5.91704936820502 |
| | CAGL0H07469g | ICS2 | Putative adhesin-like protein | 7.32947972155892 |

| | | | | |
|---|---|---|---|---|
| | CAGL0M01716g | TEC1 | Ortholog(s) have RNA polymerase II core promoter proximal region sequence-specific DNA binding, transcription factor activity and RNA polymerase II transcription factor recruiting, more | 7.98294722373464 |
| Carbon and energy metabolism | CAGL0I01210g | CTM1 | Ortholog(s) have [cytochrome c]-lysine N-methyltransferase activity, role in peptidyl-lysine methylation and cytosol localization | -5.33036610188914 |
| | CAGL0F04719g | GSY2 | Ortholog(s) have glycogen (starch) synthase activity, role in glycogen biosynthetic process and cytoplasm, nucleus localization | -4.93693981327728 |
| | CAGL0K10626g | GSY1 | Ortholog(s) have glycogen (starch) synthase activity, role in glycogen biosynthetic process and mitochondrion localization | -4.88775889749938 |
| | CAGL0H09878g | | Inorganic pyrophosphatase, cytoplasmic | -4.26986158100482 |
| | CAGL0H02695g | GLG1 | Ortholog(s) have glycogenin glucosyltransferase activity and role in glycogen biosynthetic process | -4.22130941846629 |
| | CAGL0C02211g | | Putative glycoside hydrolase of the Crh family; predicted GPI-anchor | -4.04383860784786 |
| | CAGL0L01925g | UGP1 | Putative UDP-glucose pyrophosphorylase; increased protein abundance in azole resistant strain | -3.92078078105673 |
| | CAGL0J08272g | GOR1 | Ortholog(s) have glyoxylate reductase activity, role in glyoxylate catabolic process and cytosol, extracellular region, mitochondrion, nucleus localization | -3.75925584417892 |
| | CAGL0M07447g | YMR027W | Ortholog(s) have phosphatase activity and cytosol, nucleus localization | -3.6949958489745 |
| | CAGL0J04400g | HAP3 | Ortholog(s) have RNA polymerase II core promoter proximal region sequence-specific DNA binding, transcriptional activator activity, RNA polymerase II core promoter proximal region sequence-specific binding activity | -3.69403011197976 |
| | CAGL0J01441g | ADH3 | Ortholog(s) have alcohol dehydrogenase (NAD) activity | -3.54171998659186 |
| | CAGL0F04895g | GPH1 | Ortholog(s) have glycogen phosphorylase activity, role in glycogen catabolic process, response to heat and cell surface, cytoplasm, hyphal cell wall localization | -3.30679805373706 |
| | CAGL0B04367g | SCO1 | Ortholog(s) have copper ion binding activity, role in copper ion transport, protein complex assembly and mitochondrial inner membrane, plasma membrane localization | -3.09505472981869 |
| | CAGL0F06061g | ARA2 | Ortholog(s) have D-arabinose 1-dehydrogenase [NAD(P)+] activity and role in dehydro-D-arabinono-1,4-lactone biosynthetic process | -3.03467213107474 |
| | CAGL0J03212g | ALD5 | Putative mitochondrial aldehyde dehydrogenase (NAD+); protein abundance increased in ace2 mutant cells | -2.96976381155909 |
| | CAGL0H02233g | PPA2 | Ortholog(s) have inorganic diphosphatase activity, role in aerobic respiration and mitochondrion localization | -2.96778136453224 |
| | CAGL0A02816g | YPR1 | Putative 2-methylbutyraldehyde reductase; gene is upregulated in azole-resistant strain | -2.88662012622711 |
| | CAGL0E02629g | ALG6 | Ortholog(s) have dolichyl pyrophosphate Man9GlcNAc2 alpha-1,3-glucosyltransferase activity and role in aerobic respiration, oligosaccharide-lipid intermediate biosynthetic process, protein glycosylation | -2.7398480912941 |
| | CAGL0G07315g | RCF1 | Ortholog(s) have role in mitochondrial respiratory chain complex IV assembly, mitochondrial respiratory chain supercomplex assembly | -2.73413467642301 |
| | CAGL0A03949g | COQ9 | Ortholog(s) have role in ubiquinone-6 biosynthetic process and mitochondrial inner membrane localization | -2.71063649533844 |
| | CAGL0K06831g | PDB1 | Ortholog(s) have pyruvate dehydrogenase (acetyl-transferring) activity and role in acetyl-CoA biosynthetic process from pyruvate, arginine biosynthetic process, glutamine biosynthetic process | -2.57769380281448 |
| | CAGL0M09647g | YMR155W | Ortholog(s) have fungal-type vacuole localization | -2.52497251830234 |
| | CAGL0M12727g | MAM33 | Ortholog(s) have translation activator activity, role in aerobic respiration, penicillin biosynthetic process, positive regulation of mitochondrial translation and mitochondrial matrix localization | -2.50386078342558 |
| | CAGL0J09812g | TPS1 | Ortholog(s) have alpha,alpha-trehalose-phosphate synthase (UDP-forming) activity | -2.48224959091417 |

| | | | | |
|---|---|---|---|---|
| | CAGL0F06941g | PYC1 | Putative pyruvate carboxylase isoform; gene is upregulated in azole-resistant strain | -2.47867638800571 |
| | CAGL0H07579g | HXK2 | Putative hexokinase B | -2.45247066071812 |
| | CAGL0A01133g | MDL2 | Ortholog(s) have role in cellular response to hydrogen peroxide and mitochondrial inner membrane, vacuolar membrane localization | -2.43777496738022 |
| | CAGL0F07469g | RMD9 | Ortholog(s) have mRNA binding activity, role in aerobic respiration, regulation of mRNA stability, translational initiation and extrinsic component of mitochondrial inner membrane localization | -2.42811424850729 |
| | CAGL0H04983g | | Putative mannose-1-phosphate guanyltransferase | -2.37234390620211 |
| | CAGL0J06710g | COQ5 | Ortholog(s) have 2-hexaprenyl-6-methoxy-1,4-benzoquinone methyltransferase activity, role in aerobic respiration, cellular response to drug, ubiquinone biosynthetic process and mitochondrial matrix localization | -2.34080453906774 |
| | CAGL0L01485g | GSF2 | Putative protein of the ER membrane involved in hexose transporter secretion; gene is upregulated in azole-resistant strain | -2.32892335624418 |
| | CAGL0K10296g | IAH1 | Ortholog(s) have hydrolase activity, acting on ester bonds activity | -2.27118106028848 |
| | CAGL0K04411g | LST7 | Ortholog(s) have GTPase activator activity, role in positive regulation of GTPase activity, positive regulation of TORC1 signaling and Lst4-Lst7 complex, cytosol, nucleus, vacuolar membrane localization | -2.18743019033715 |
| | CAGL0I06831g | COX15 | Ortholog(s) have 2 iron, 2 sulfur cluster binding, cytochrome-c oxidase activity, oxidoreductase activity, acting on NAD(P)H, heme protein as acceptor activity and role in heme a biosynthetic process, respiratory electron transport chain | -2.17841185000703 |
| | CAGL0M11242g | YMR226C | Ortholog(s) have carbonyl reductase (NADPH) activity, serine 3-dehydrogenase activity and cytosol, nucleus, ribosome localization | -2.14840798829088 |
| | CAGL0G05335g | TPS2 | Ortholog(s) have trehalose-phosphatase activity | -2.12988250531165 |
| | CAGL0A04829g | HXK1 | Putative hexokinase isoenzyme 2; protein differentially expressed in azole resistant strain | -2.07027841588739 |
| | CAGL0L00847g | CBR1 | Ortholog(s) have cytochrome-b5 reductase activity, acting on NAD(P)H activity and endoplasmic reticulum, mitochondrial outer membrane, nucleus, plasma membrane localization | -2.05595339982095 |
| | CAGL0M03377g | GLC3 | Ortholog(s) have 1,4-alpha-glucan branching enzyme activity, role in glycogen biosynthetic process and cytoplasm localization | -1.98899576068299 |
| | CAGL0L01177g | FRD1 | Putative soluble fumarate reductase | -1.96329863399472 |
| | CAGL0I07601g | COQ3 | Ortholog(s) have 3-demethylubiquinone-6 3-O-methyltransferase activity, hexaprenyldihydroxybenzoate methyltransferase activity and role in ubiquinone biosynthetic process | -1.93635114469347 |
| | CAGL0H05445g | | Glucose-6-phosphate isomerase | -1.92378081899339 |
| | CAGL0D00198g | BDH1 | Ortholog(s) have (R,R)-butanediol dehydrogenase activity, role in butanediol biosynthetic process and cytoplasm localization | -1.91545009399715 |
| | CAGL0L09493g | YIR007W | Ortholog(s) have steryl-beta-glucosidase activity, role in ergosteryl 3-beta-D-glucoside catabolic process and cytosol, fungal-type vacuole membrane localization | -1.90360537484478 |
| | CAGL0A01089g | PBI1 | Has domain(s) with predicted alcohol O-acetyltransferase activity and role in alcohol metabolic process | -1.88424983843073 |
| | CAGL0I02200g | SOL3 | Putative 6-phosphogluconolactonase | -1.87195577233804 |
| | CAGL0C04257g | COQ1 | Ortholog(s) have di-trans,poly-cis-decaprenylcistransferase activity, trans-hexaprenyltranstransferase activity, role in ubiquinone biosynthetic process and decaprenyl diphosphate synthase complex, mitochondrion localization | -1.81763834232928 |
| | CAGL0M00682g | YLR446W | Has domain(s) with predicted ATP binding, glucose binding, hexokinase activity, phosphotransferase activity, alcohol group as acceptor activity | -1.80693662973404 |
| | CAGL0D06138g | HEM2 | Putative porphobilinogen synthase; involved in cadmium tolerance | -1.78559410194321 |

| | | | | |
|---|---|---|---|---|
| | CAGL0H05137g | ALD6 | Ortholog(s) have aldehyde dehydrogenase [NAD(P)+] activity, role in NADPH regeneration, acetate biosynthetic process, response to salt stress and cytosol, mitochondrion localization | -1.7648810138129 |
| | CAGL0K07480g | PGM1 | Putative phosphoglucomutase | -1.73447804828335 |
| | CAGL0M13013g | OAR1 | Ortholog(s) have 3-oxoacyl-[acyl-carrier-protein] reductase (NADPH) activity, role in aerobic respiration, fatty acid metabolic process and mitochondrion localization | -1.7234077622924 |
| | CAGL0K02409g | ATP20 | Ortholog(s) have proton-transporting ATP synthase activity, rotational mechanism activity and role in ATP synthesis coupled proton transport, cristae formation, protein complex oligomerization | -1.71491946411647 |
| | CAGL0C03652g | COQ2 | Ortholog(s) have 4-hydroxybenzoate octaprenyltransferase activity, role in ubiquinone biosynthetic process and integral component of mitochondrial membrane, mitochondrial inner membrane localization | -1.67789156191961 |
| | CAGL0J09394g | YDL124W | Ortholog(s) have alditol:NADP+ 1-oxidoreductase activity, alpha-keto amide reductase activity, alpha-keto ester reductase activity and indole-3-acetaldehyde reductase (NADH) activity, more | -1.66524408985387 |
| | CAGL0E05412g | KRE5 | Ortholog(s) have UDP-glucose:glycoprotein glucosyltransferase activity | -1.66390677091198 |
| | CAGL0I00924g | GLO4 | Ortholog(s) have hydroxyacylglutathione hydrolase activity, role in methylglyoxal catabolic process to D-lactate via S-lactoyl-glutathione and cytosol, mitochondrial matrix, nucleus localization | -1.64385481849013 |
| | CAGL0L07480g | NRG2 | Ortholog(s) have double-stranded DNA binding, sequence-specific DNA binding, transcription factor activity, sequence-specific DNA binding activity | -1.6372443569297 |
| | CAGL0M09581g | ATP1 | F1F0-ATPase complex, F1 alpha subunit | -1.61236150873309 |
| | CAGL0K10274g | CAT5 | Ortholog(s) have 2-octoprenyl-3-methyl-6-methoxy-1,4-benzoquinone hydroxylase activity, role in ubiquinone biosynthetic process and mitochondrial inner membrane localization | -1.60125927854705 |
| | CAGL0K11297g | YDR248C | Ortholog(s) have glucokinase activity, gluconokinase activity, role in D-gluconate catabolic process and cytosol, fungal-type vacuole, nucleus localization | -1.59024962379474 |
| | CAGL0F07315g | SNF4 | Ortholog(s) have AMP binding, AMP-activated protein kinase activity, ATP binding, protein serine/threonine kinase activator activity | -1.57927278033622 |
| | CAGL0E02387g | COQ10 | Ortholog(s) have ubiquinone binding activity, role in cellular respiration, ubiquinone biosynthetic process and mitochondrial inner membrane localization | -1.56852215119546 |
| | CAGL0H00506g | ATP2 | F1F0-ATPase complex, F1 beta subunit; expression upregulated in biofilm vs planktonic cell culture; protein abundance decreased in ace2 mutant cells | -1.53172684097737 |
| | CAGL0E04796g | GTB1 | Ortholog(s) have alpha-1,4-glucosidase activity, role in N-glycan processing, polysaccharide biosynthetic process and endoplasmic reticulum lumen, glucosidase II complex localization | -1.52273971729187 |
| | CAGL0L06974g | YDL086W | Ortholog(s) have mitochondrion localization | -1.5213834575408 |
| | CAGL0J06468g | TSL1 | Ortholog(s) have alpha,alpha-trehalose-phosphate synthase (UDP-forming) activity, enzyme regulator activity, trehalose-phosphatase activity and role in trehalose biosynthetic process | -1.51271621824975 |
| | CAGL0H06853g | | Putative NADP-dependent alcohol dehydrogenase VI; protein abundance increased in ace2 mutant cells | -1.50857576615564 |
| | CAGL0L07722g | PGK1 | Putative 3-phosphoglycerate kinase; protein differentially expressed in azole resistant strain; protein abundance increased in ace2 mutant cells | -1.46096011860188 |
| | CAGL0L05478g | RPE1 | Ortholog(s) have ribulose-phosphate 3-epimerase activity, role in pentose-phosphate shunt and cytosol, nucleus localization | -1.45161040827296 |
| | CAGL0L11374g | DAK1 | Ortholog(s) have glycerone kinase activity, role in cellular response to toxic substance, glycerol catabolic process and cytosol localization | -1.44182364363789 |
| | CAGL0M14047g | ADH6 | Putative NADPH-dependent cinnamyl alcohol dehydrogenase; gene is upregulated in azole-resistant strain | -1.4146929535809 |

| | | | | |
|---|---|---|---|---|
| | CAGL0E05830g | CBP3 | Ortholog(s) have ribosome binding activity and role in mitochondrial respiratory chain complex III assembly, positive regulation of mitochondrial translation | -1.41364747879341 |
| | CAGL0G09977g | GDB1 | Ortholog(s) have 4-alpha-glucanotransferase activity, amylo-alpha-1,6-glucosidase activity, role in glycogen catabolic process and mitochondrion localization | -1.40361855076408 |
| | CAGL0K01705g | GPM2 | Ortholog(s) have cytoplasm localization | -1.39854293405481 |
| | CAGL0L04202g | NRK1 | Ortholog(s) have ribosylnicotinamide kinase activity, role in NAD biosynthesis via nicotinamide riboside salvage pathway, nicotinamide riboside metabolic process and cytosol, fungal-type vacuole, nucleus localization | -1.39735235276345 |
| | CAGL0J05126g | BNA3 | Ortholog(s) have 2-aminoadipate transaminase activity, kynurenine-oxoglutarate transaminase activity, role in kynurenic acid biosynthetic process and cytosol, mitochondrion, nucleus localization | -1.38678777292993 |
| | CAGL0I05632g | PHO91 | Ortholog(s) have glycerol-3-phosphate transmembrane transporter activity, inorganic phosphate transmembrane transporter activity | -1.36487803610109 |
| | CAGL0I01320g | OSM1 | Ortholog(s) have fumarate reductase (NADH) activity, role in FAD metabolic process, protein folding in endoplasmic reticulum and endoplasmic reticulum, mitochondrion localization | -1.36278664656391 |
| | CAGL0I07139g | LSC1 | Ortholog(s) have succinate-CoA ligase (ADP-forming) activity, role in succinyl-CoA metabolic process and mitochondrial nucleoid localization | -1.33638521034808 |
| | CAGL0G09361g | PDX1 | Ortholog(s) have structural molecule activity, role in acetyl-CoA biosynthetic process from pyruvate, filamentous growth, single-species biofilm formation on inanimate substrate and mitochondrial pyruvate dehydrogenase complex localization | -1.32613559779121 |
| | CAGL0J07084g | YPL113C | Ortholog(s) have oxidoreductase activity, acting on the CH-OH group of donors, NAD or NADP as acceptor activity | -1.28659180004284 |
| | CAGL0J10186g | LAT1 | Ortholog(s) have dihydrolipoyllysine-residue acetyltransferase activity, pyruvate dehydrogenase (acetyl-transferring) activity and role in acetyl-CoA biosynthetic process from pyruvate, pyruvate catabolic process | -1.27939253227141 |
| | CAGL0F08107g | LSC2 | Succinate-CoA ligase beta subunit | -1.27030432705812 |
| | CAGL0M10593g | ATP23 | Ortholog(s) have role in mitochondrial protein processing, mitochondrial proton-transporting ATP synthase complex assembly and extrinsic component of mitochondrial inner membrane, mitochondrial intermembrane space localization | -1.25474958473146 |
| | CAGL0H02387g | TPS3 | Putative trehalose-6-phosphate synthase/phosphatase subunit; gene is upregulated in azole-resistant strain | -1.24967787526029 |
| | CAGL0G02651g | FYV10 | Ortholog(s) have ubiquitin-protein transferase activity and role in negative regulation of apoptotic process, negative regulation of gluconeogenesis, proteasome-mediated ubiquitin-dependent protein catabolic process | -1.2484427189604 |
| | CAGL0L03674g | GSM1 | Ortholog(s) have sequence-specific DNA binding, transcription factor activity, sequence-specific DNA binding activity and role in regulation of transcription from RNA polymerase II promoter | -1.232785403374 |
| | CAGL0K06787g | PYC2 | Ortholog(s) have pyruvate carboxylase activity, role in carbon utilization, cellular response to glucose starvation, gluconeogenesis, response to heat and cytosol localization | -1.18488283755551 |
| | CAGL0L02079g | CTP1 | Ortholog(s) have tricarboxylate secondary active transmembrane transporter activity, role in mitochondrial citrate transport, transmembrane transport and mitochondrion, plasma membrane localization | -1.18473238892316 |
| | CAGL0C05511g | PHO13 | Ortholog(s) have alkaline phosphatase activity, magnesium ion binding, phosphoglycolate phosphatase activity, phosphoprotein phosphatase activity | -1.17893387580813 |
| | CAGL0L12078g | PDA1 | Ortholog(s) have pyruvate dehydrogenase (acetyl-transferring) activity and role in acetyl-CoA biosynthetic process from pyruvate, carbon utilization, pseudohyphal growth, pyruvate catabolic process | -1.17892429066159 |
| | CAGL0F05423g | COQ4 | Ortholog(s) have role in ubiquinone biosynthetic process and mitochondrial inner membrane localization | -1.16538713374206 |
| | CAGL0C04455g | | F1F0-ATPase complex, F1 delta subunit; protein abundance decreased in ace2 mutant cells | -1.15904863760199 |
| | CAGL0H00847g | HUT1 | Ortholog(s) have UDP-galactose transmembrane transporter activity, role in UDP-galactose transmembrane transport, UDP-glucose transport and endoplasmic reticulum localization | -1.15503697134818 |

| | | | | |
|---|---|---|---|---|
| | CAGL0H05489g | ATP4 | Ortholog(s) have proton-transporting ATP synthase activity, rotational mechanism, proton-transporting ATPase activity, rotational mechanism activity and role in ATP synthesis coupled proton transport, protein complex oligomerization | -1.15155446488165 |
| | CAGL0L00869g | PKP1 | Ortholog(s) have pyruvate dehydrogenase (acetyl-transferring) kinase activity, role in carbon utilization, cellular response to drug, peptidyl-serine phosphorylation and mitochondrion localization | -1.14052024464065 |
| | CAGL0H06699g | GUT2 | Ortholog(s) have glycerol-3-phosphate dehydrogenase activity, role in NADH oxidation, glycerol metabolic process, replicative cell aging and integral component of mitochondrial outer membrane, plasma membrane localization | -1.12970859662113 |
| | CAGL0G09339g | XKS1 | Ortholog(s) have xylulokinase activity, role in xylulose catabolic process and cytosol, nucleus localization | -1.12704977835688 |
| | CAGL0I07447g | ITR2 | Ortholog(s) have myo-inositol transmembrane transporter activity, role in carbohydrate import across plasma membrane, myo-inositol transport and Golgi apparatus, fungal-type vacuole membrane, plasma membrane localization | -1.11569059050838 |
| | CAGL0A01804g | HXT1 | Ortholog(s) have fructose transmembrane transporter activity, pentose transmembrane transporter activity, role in glucose transport, mannose transport and plasma membrane localization | -1.10068014885913 |
| | CAGL0L12210g | CSF1 | Ortholog(s) have role in fermentation, protein maturation and mitochondrion localization | -1.09054016088277 |
| | CAGL0F03685g | COX10 | Ortholog(s) have role in heme a biosynthetic process and mitochondrion localization | -1.0871551382694 |
| | CAGL0I07645g | RFC4 | Putative fructose 1,6-bisphosphate aldolase; protein differentially expressed in azole resistant strain | -1.08393218740443 |
| | CAGL0I02486g | ENO2 | Putative enolase I; protein abundance increased in azole resistant strain and in ace2 mutant cells | -1.05713043693647 |
| | CAGL0K05775g | SDH7 | Ortholog(s) have role in carbon utilization, mitochondrial respiratory chain complex II assembly, regulation of gluconeogenesis and mitochondrial intermembrane space localization | -1.04401002497514 |
| | CAGL0K09702g | YNL134C | Putative stress-induced alcohol dehydrogenase; gene is upregulated in azole-resistant strain; protein differentially expressed in azole resistant strain | -1.03550270721848 |
| | CAGL0H08327g | | Putative triose-phosphate isomerase; protein abundance decreased in ace2 mutant cells | -1.03506013061719 |
| | CAGL0B01727g | YDR109C | Has domain(s) with predicted phosphotransferase activity, alcohol group as acceptor activity and role in carbohydrate metabolic process | -1.03061450853889 |
| | CAGL0H05819g | INA17 | Ortholog(s) have role in mitochondrial proton-transporting ATP synthase complex assembly and INA complex localization | -1.02449121870405 |
| | CAGL0J03080g | RGI1 | Ortholog(s) have role in energy reserve metabolic process and cell periphery, cytoplasm, nucleus localization | -1.02014236825239 |
| | CAGL0H06259g | PSK1 | Significant homology to PAS domain containing protein kinase | 1.01100833127426 |
| | CAGL0I06094g | FBP26 | Ortholog(s) have fructose-2,6-bisphosphate 2-phosphatase activity, role in glucose metabolic process and cytoplasm localization | 1.08896920404514 |
| | CAGL0I03190g | RIP1 | Putative ubiquinol-Cytochrome c reductase iron-sulfur protein | 1.094568729477 |
| | CAGL0K01507g | GPR1 | Ortholog(s) have G-protein coupled receptor activity, glucose binding activity | 1.10302896046683 |
| | CAGL0J02904g | GIP2 | Ortholog(s) have protein phosphatase regulator activity, role in glycogen metabolic process, protein dephosphorylation and protein phosphatase type 1 complex localization | 1.1061133769621 |
| | CAGL0F04213g | PET9 | Ortholog(s) have ATP:ADP antiporter activity and role in ADP transport, aerobic respiration, anaerobic respiration, apoptotic process, heme transport, mitochondrial ATP transmembrane transport, response to oxidative stress | 1.1507643564195 |
| | CAGL0B03421g | HAP1 | Ortholog(s) have RNA polymerase II core promoter proximal region sequence-specific DNA binding, transcriptional activator activity, RNA polymerase II core promoter proximal region sequence-specific binding activity | 1.15896112307864 |
| | CAGL0J04268g | | Ortholog(s) have acetate CoA-transferase activity, acetyl-CoA hydrolase activity, succinyl-CoA hydrolase activity, role in propionate metabolic process, methylcitrate cycle, response to acetate and glyoxysome, mitochondrion localization | 1.21245770103251 |

| | | | | |
|---|---|---|---|---|
| | CAGL0G01100g | YLR345W | Ortholog(s) have cytosol localization | 1.21551518836857 |
| | CAGL0F05071g | ECI1 | Ortholog(s) have dodecenoyl-CoA delta-isomerase activity, role in fatty acid beta-oxidation, filamentous growth and peroxisome localization | 1.23365098213276 |
| | CAGL0K09900g | HAP5 | Ortholog(s) have DNA binding, RNA polymerase II core promoter proximal region sequence-specific DNA binding, transcription factor activity, sequence-specific DNA binding activity | 1.23482672920464 |
| | CAGL0G05379g | GCR2 | Ortholog(s) have RNA polymerase II activating transcription factor binding, transcription factor activity, RNA polymerase II transcription factor binding activity | 1.23535270740674 |
| | CAGL0A02475g | ATP22 | Ortholog(s) have translation regulator activity, role in positive regulation of mitochondrial translation, proton-transporting ATP synthase complex biogenesis and mitochondrial inner membrane localization | 1.2418893348767 |
| | CAGL0C01397g | PFK26 | Ortholog(s) have 6-phosphofructo-2-kinase activity and role in fructose 2,6-bisphosphate metabolic process | 1.25567117732328 |
| | CAGL0C01771g | YBR241C | Ortholog(s) have fungal-type vacuole membrane localization | 1.25952755678971 |
| | CAGL0L03740g | RKI1 | Ortholog(s) have ribose-5-phosphate isomerase activity, role in pentose-phosphate shunt, pyridoxine biosynthetic process and cytoplasm, nucleus localization | 1.29131888838633 |
| | CAGL0L10758g | PFK2 | Putative 6-phosphofructokinase, beta subunit; protein abundance increased in ace2 mutant cells | 1.29905303243074 |
| | CAGL0M10439g | NTH1 | Ortholog(s) have alpha,alpha-trehalase activity, calcium ion binding activity, role in ascospore formation, cellular response to desiccation, trehalose catabolic process involved in cellular response to stress and cytosol localization | 1.31187820569354 |
| | CAGL0M03025g | CAT8 | Ortholog(s) have RNA polymerase II core promoter proximal region sequence-specific DNA binding, transcriptional activator activity, RNA polymerase II core promoter proximal region sequence-specific binding activity | 1.31222433656185 |
| | CAGL0C01325g | COX5B | Ortholog(s) have cytochrome-c oxidase activity, nitrite reductase (NO-forming) activity, role in mitochondrial electron transport, cytochrome c to oxygen and mitochondrial respiratory chain complex IV localization | 1.3426047030126 |
| | CAGL0D04774g | ANT1 | Ortholog(s) have adenine nucleotide transmembrane transporter activity, role in ATP transport, fatty acid beta-oxidation, peroxisome organization and glyoxysome, integral component of peroxisomal membrane localization | 1.3625574719621 |
| | CAGL0I02838g | AZF1 | Ortholog(s) have RNA polymerase II core promoter proximal region sequence-specific DNA binding, transcriptional activator activity, RNA polymerase II core promoter proximal region sequence-specific binding activity | 1.37615834233354 |
| | CAGL0L11088g | YOR283W | Ortholog(s) have phosphatase activity, role in dephosphorylation and cytosol, nucleus localization | 1.37962741427276 |
| | CAGL0K01683g | GPD1 | Putative cytoplasmic glycerol-3-phosphate dehydrogenase (NAD+); protein abundance increased in ace2 mutant cells | 1.42085260142231 |
| | CAGL0F05863g | SDH4 | Ortholog(s) have succinate dehydrogenase (ubiquinone) activity, role in cellular respiration and mitochondrion, plasma membrane localization | 1.44076547662088 |
| | CAGL0J05522g | SAL1 | Ortholog(s) have ATP:ADP antiporter activity, calcium ion binding activity, role in ADP transport, ATP transport, mitochondrial transport and mitochondrion localization | 1.45863889081302 |
| | CAGL0B03663g | CIT2 | Ortholog(s) have citrate (Si)-synthase activity and mitochondrion, peroxisome localization | 1.49282439145504 |
| | CAGL0L06160g | COX4 | Ortholog(s) have cytochrome-c oxidase activity, zinc ion binding activity and role in aerobic respiration, mitochondrial electron transport, cytochrome c to oxygen | 1.55636636085759 |
| | CAGL0C03267g | FPS1 | Glycerol transporter; involved in flucytosine resistance; double fps1/fps2 mutant accumulates glycerol, has constitutive cell wall stress, is hypersensitive to caspofungin in vitro and in vivo | 1.56323599417653 |
| | CAGL0I00418g | OLE1 | Ortholog(s) have electron carrier activity, stearoyl-CoA 9-desaturase activity | 1.57300583247989 |
| | CAGL0C05027g | YAT1 | Ortholog(s) have role in acetate catabolic process, alcohol metabolic process, carnitine metabolic process, cellular respiration and cytosol, mitochondrion localization | 1.57918499796651 |

| | | | | |
|---|---|---|---|---|
| | CAGL0K10736g | CYB2 | Ortholog(s) have L-lactate dehydrogenase (cytochrome) activity and glyoxysome, mitochondrial intermembrane space, nucleus localization | 1.62306010849198 |
| | CAGL0M01672g | YDR387C | Ortholog(s) have fungal-type vacuole membrane localization | 1.62787998159312 |
| | CAGL0L11000g | HEM4 | Ortholog(s) have uroporphyrinogen-III synthase activity, role in heme biosynthetic process and cytosol, nucleus localization | 1.63199873900826 |
| | CAGL0J06380g | INH1 | Ortholog(s) have ATPase inhibitor activity, role in negative regulation of ATPase activity and mitochondrion, nucleus localization | 1.63991748004544 |
| | CAGL0E04884g | ADR1 | Ortholog(s) have RNA polymerase II activating transcription factor binding, RNA polymerase II core promoter proximal region sequence-specific DNA binding and TFIIB-class transcription factor binding, more | 1.65604004032286 |
| | CAGL0L06204g | COX13 | Ortholog(s) have cytochrome-c oxidase activity, enzyme regulator activity, role in aerobic respiration, mitochondrial respiratory chain supercomplex assembly and mitochondrial respiratory chain complex IV, plasma membrane localization | 1.65898264927418 |
| | CAGL0D00748g | COX9 | Ortholog(s) have cytochrome-c oxidase activity, role in mitochondrial electron transport, cytochrome c to oxygen and mitochondrial respiratory chain complex IV, plasma membrane localization | 1.72353091151863 |
| | CAGL0J09020g | SNF3 | Putative plasma membrane high affinity glucose sensor, required for growth under glucose-limiting conditions | 1.80409794932428 |
| | CAGL0M03399g | UBC8 | Ortholog(s) have ubiquitin-protein transferase activity | 1.80452832008205 |
| | CAGL0M12551g | RGI2 | Ortholog(s) have role in energy reserve metabolic process and cytoplasm localization | 1.80970797213519 |
| | CAGL0I05148g | DLD1 | D-lactate ferricytochrome C oxidoreductase | 1.82435176232555 |
| | CAGL0M05907g | OAF3 | Ortholog(s) have role in cellular response to oleic acid, negative regulation of transcription from RNA polymerase II promoter and mitochondrion, nucleus localization | 1.82681116779904 |
| | CAGL0J07150g | PIP2 | Ortholog(s) have RNA polymerase II core promoter proximal region sequence-specific DNA binding, transcriptional activator activity, RNA polymerase II core promoter proximal region sequence-specific binding activity | 1.88590857642869 |
| | CAGL0J00429g | COX6 | Cytochrome c oxidase subunit VI | 1.90808491247709 |
| | CAGL0H03663g | IDP3 | Ortholog(s) have isocitrate dehydrogenase (NADP+) activity, role in fatty acid beta-oxidation and mitochondrion, peroxisomal importomer complex, peroxisome localization | 1.92826897012088 |
| | CAGL0E01287g | KGD2 | Ortholog(s) have role in 2-oxoglutarate metabolic process, mitochondrial genome maintenance and mitochondrial nucleoid, mitochondrial oxoglutarate dehydrogenase complex localization | 1.96156603554924 |
| | CAGL0E01705g | MDH2 | Ortholog(s) have L-malate dehydrogenase activity, role in gluconeogenesis, protein import into peroxisome matrix and cytosol, nuclear periphery localization | 2.01144074257658 |
| | CAGL0K12210g | YMC2 | Ortholog(s) have organic acid transmembrane transporter activity, role in mitochondrial transport, transmembrane transport and mitochondrion localization | 2.0197038525926 |
| | CAGL0G01969g | SIS2 | Ortholog(s) have phosphopantothenoylcysteine decarboxylase activity, protein phosphatase inhibitor activity and role in regulation of mitotic cell cycle, response to salt stress | 2.05250069306249 |
| | CAGL0J09680g | HEM3 | Ortholog(s) have hydroxymethylbilane synthase activity, role in heme biosynthetic process, pathogenesis and cytoplasm, nucleus localization | 2.10232577407213 |
| | CAGL0B02607g | HEM1 | 5-aminolevulinate synthase | 2.10433773893009 |
| | CAGL0I05390g | SKS1 | Ortholog(s) have protein serine/threonine kinase activity | 2.12701243999776 |
| | CAGL0G02717g | SGA1 | Ortholog(s) have glucan 1,4-alpha-glucosidase activity, role in glycogen catabolic process and Golgi apparatus, endoplasmic reticulum, fungal-type vacuole, prospore membrane localization | 2.14297574063744 |
| | CAGL0J08910g | | Has domain(s) with predicted hydrolase activity, hydrolyzing O-glycosyl compounds activity and role in carbohydrate metabolic process | 2.16556741314198 |

| | | | | |
|---|---|---|---|---|
| | CAGL0H02491g | COX7 | Ortholog(s) have cytochrome-c oxidase activity, role in mitochondrial electron transport, cytochrome c to oxygen and mitochondrial respiratory chain complex IV, plasma membrane localization | 2.21684737936907 |
| | CAGL0E02035g | MCH4 | Ortholog(s) have cell periphery, fungal-type vacuole membrane localization | 2.23460340921839 |
| | CAGL0G09064g | YIG1 | Ortholog(s) have role in glycerol biosynthetic process and cytosol, nucleus localization | 2.24753334256839 |
| | CAGL0L09108g | PDH1 | Ortholog(s) have role in propionate metabolic process and mitochondrial outer membrane localization | 2.25098963048328 |
| | CAGL0G08712g | KGD1 | Ortholog(s) have mitochondrial nucleoid, mitochondrial oxoglutarate dehydrogenase complex localization | 2.29749884184322 |
| | CAGL0C05137g | GPD2 | Putative glycerol 3-phosphate dehydrogenase; protein differentially expressed in azole resistant strain | 2.36359561397995 |
| | CAGL0I07227g | IDH2 | Putative isocitrate dehydrogenase | 2.39380695444479 |
| | CAGL0A01045g | FUM1 | Ortholog(s) have fumarate hydratase activity, role in fumarate metabolic process, tricarboxylic acid cycle and cytosol, mitochondrial matrix localization | 2.40913530425009 |
| | CAGL0K12100g | HEM13 | Putative coproporphyrinogen III oxidase; protein differentially expressed in azole resistant strain | 2.44758806243918 |
| | CAGL0M12430g | GPP1 | Putative DL-glycerol phosphatase | 2.58844665107726 |
| | CAGL0L00649g | ACS1 | Acetyl-coenzyme A synthetase | 2.60395021965805 |
| | CAGL0G06380g | GDS1 | Ortholog(s) have role in aerobic respiration and mitochondrion, nucleus localization | 2.62448032044803 |
| | CAGL0G02673g | | Ortholog(s) have isocitrate dehydrogenase (NAD+) activity, role in isocitrate metabolic process, tricarboxylic acid cycle and cytoplasm localization | 2.62706839532198 |
| | CAGL0D06424g | ACO1 | Putative aconitate hydratase | 2.68111732329094 |
| | CAGL0E03916g | GUT1 | Ortholog(s) have glycerol kinase activity and mitochondrion localization | 2.77654593483029 |
| | CAGL0F08085g | MPC3 | Ortholog(s) have pyruvate transmembrane transporter activity, role in mitochondrial pyruvate transmembrane transport and mitochondrial membrane, plasma membrane localization | 2.82399793195561 |
| | CAGL0L10043g | STD1 | Ortholog(s) have protein kinase activator activity | 2.99617725597648 |
| | CAGL0L09273g | ICL2 | Ortholog(s) have isocitrate lyase activity, methylisocitrate lyase activity, role in propionate catabolic process, 2-methylcitrate cycle and mitochondrial matrix localization | 3.03972542851034 |
| | CAGL0A03740g | | Ortholog(s) have role in fatty acid beta-oxidation, long-chain fatty acid catabolic process and peroxisome localization | 3.07926357628974 |
| | CAGL0C04323g | NTH2 | Ortholog(s) have alpha,alpha-trehalase activity, role in trehalose catabolic process and mitochondrion localization | 3.09891554059377 |
| | CAGL0F00913g | PSK2 | Ortholog(s) have protein serine/threonine kinase activity | 3.14526303316394 |
| | CAGL0F08261g | ENO1 | Ortholog(s) have high molecular weight kininogen binding, phosphopyruvate hydratase activity | 3.22593243875289 |
| | CAGL0G01540g | NCE103 | Beta carbonic anhydrase with a predicted role in non-classical protein export; upregulated in azole-resistant strain; enzyme activity increased by amines and amino acids; protein abundance decreased in ace2 cells | 3.29908839848988 |
| | CAGL0E05566g | TYE7 | Ortholog(s) have sequence-specific DNA binding, transcription factor activity, sequence-specific DNA binding activity | 3.33808094742989 |
| | CAGL0A01628g | MIG1 | Transcriptional regulatory protein | 3.36838011331985 |
| | CAGL0H03993g | CIT1 | Ortholog(s) have citrate (Si)-synthase activity, role in acetyl-CoA catabolic process, tricarboxylic acid cycle and glyoxysome, mitochondrion localization | 3.38012458051265 |
| | CAGL0L09086g | CIT3 | Ortholog(s) have 2-methylcitrate synthase activity, citrate (Si)-synthase activity, role in propionate catabolic process, 2-methylcitrate cycle, tricarboxylic acid cycle and mitochondrion localization | 3.63917078302804 |

| | | | | |
|---|---|---|---|---|
| | CAGL0K08624g | HAP4 | Ortholog(s) have RNA polymerase II activating transcription factor binding, transcriptional activator activity, RNA polymerase II core promoter proximal region sequence-specific binding activity | 3.76643365356462 |
| | CaglfMp09 | | Mitochondrially encoded subunit a of the F0 sector of mitochondrial F1F0 ATP synthase | 3.77062548608441 |
| | CAGL0I00748g | NDE1 | Ortholog(s) have NADH dehydrogenase activity, role in NADH oxidation, chronological cell aging, glycolytic fermentation to ethanol and mitochondrion, plasma membrane localization | 3.90883436114502 |
| | CaglfMp04 | | Subunit I of cytochrome c oxidase, which is the terminal member of the mitochondrial inner membrane electron transport chain; one of 3 mitochondrially-encoded subunits; gene contains three Group I introns encoding putative endonucleases | 3.962282654772 |
| | CAGL0K12254g | VID24 | Ortholog(s) have role in negative regulation of gluconeogenesis, proteasome-mediated ubiquitin-dependent protein catabolic process, protein catabolic process in the vacuole, protein targeting to vacuole | 4.33731944409932 |
| | CaglfMp11 | | Subunit II of cytochrome c oxidase, which is the terminal member of the mitochondrial inner membrane electron transport chain; genomic sequence has a frameshift causing truncation of 25 codons relative to other yeast COX2 genes | 4.3469484010141 |
| | CAGL0C03223g | SDH2 | Putative iron-sulfur protein subunit of succinate dehydrogenase; gene is downregulated in azole-resistant strain | 4.54672679284782 |
| | CAGL0J00451g | | Putative glyceraldehyde-3-phosphate dehydrogenase; protein differentially expressed in azole resistant strain; expression downregulated in biofilm vs planktonic cell culture | 4.57079071101978 |
| | CAGL0K07007g | YBR238C | Ortholog(s) have mRNA binding activity and role in aerobic respiration, filamentous growth of a population of unicellular organisms in response to neutral pH, single-species biofilm formation on inanimate substrate | 4.66656647190834 |
| | CaglfMp10 | | Subunit c of the F0 sector of mitochondrial inner membrane F1-F0 ATP synthase, encoded on the mitochondrial genome | 4.73977192459119 |
| | CAGL0J03058g | ICL1 | Ortholog(s) have isocitrate lyase activity, role in acetate catabolic process, carbon utilization, fatty acid catabolic process, glyoxylate cycle, pathogenesis and cytosol, glyoxysome, peroxisomal matrix localization | 5.01276937936376 |
| | CAGL0L03982g | MLS1 | Ortholog(s) have malate synthase activity, role in acetate catabolic process, carbon utilization, fatty acid catabolic process, glyoxylate cycle and cytosol, glyoxysome, peroxisomal matrix localization | 5.20694348338948 |
| | CAGL0A02321g | HXT5 | Ortholog(s) have fructose transmembrane transporter activity, glucose transmembrane transporter activity, mannose transmembrane transporter activity and role in fructose import across plasma membrane, glucose import across plasma membrane | 5.25471347748214 |
| | CAGL0L07766g | ADY2 | Ortholog(s) have acetate transmembrane transporter activity, ammonium transmembrane transporter activity and role in ammonium transport, nitrogen utilization, plasma membrane acetate transport | 5.63086064682298 |
| | CAGL0B04917g | IDP2 | S-adenosylmethionine synthetase | 5.65510661756844 |
| | CAGL0M09020g | SFC1 | Ortholog(s) have succinate:fumarate antiporter activity, role in acetate catabolic process, carbon utilization, fatty acid catabolic process, fumarate transport, succinate transport and mitochondrion, plasma membrane localization | 5.66073115079483 |
| | CAGL0H04939g | FBP1 | Ortholog(s) have fructose 1,6-bisphosphate 1-phosphatase activity, role in gluconeogenesis, reactive oxygen species metabolic process and cytosol, periplasmic space localization | 5.89507575048193 |
| | CAGL0F06809g | YVH1 | Ortholog(s) have protein tyrosine phosphatase activity | 5.97051934791296 |
| | CAGL0B04213g | RGC1 | Ortholog(s) have role in positive regulation of glycerol transport and cytoplasm localization | 6.66405274070384 |
| | CAGL0K12078g | NRG1 | Ortholog(s) have RNA polymerase II core promoter proximal region sequence-specific DNA binding, RNA polymerase II repressing transcription factor binding and transcriptional repressor activity, more | 8.11789418466999 |
| | CAGL0H06633g | | Putative phosphoenolpyruvate carboxykinase; gene is downregulated in azole-resistant strain | 8.62662179393254 |
| | CAGL0K10428g | IGD1 | Ortholog(s) have enzyme inhibitor activity, role in negative regulation of glycogen catabolic process and cytoplasm localization | 9.24575845348038 |
| | CAGL0A01826g | HXT3 | Ortholog(s) have glucose transmembrane transporter activity and plasma membrane localization | 10.0639954458794 |

| | | | | |
|---|---|---|---|---|
| **Aminoacid metabolism** | CAGL0I04994g | MET6 | 5-methyltetrahydropteroyltriglutamate homocysteine methyltransferase; protein abundance increased in ace2 mutant cells | -4.0214546434684 |
| | CAGL0J08415g | SAM2 | S-adenosylmethionine synthetase | -3.78486042329185 |
| | CAGL0H06369g | CYS3 | Ortholog(s) have cystathionine gamma-lyase activity, role in cysteine biosynthetic process via cystathionine, methionine biosynthetic process, transsulfuration and cytoplasm, nucleus localization | -3.32033485451651 |
| | CAGL0D03036g | AVT1 | Ortholog(s) have L-glutamine transmembrane transporter activity, L-isoleucine transmembrane transporter activity, L-tyrosine transmembrane transporter activity | -3.26377674026584 |
| | CAGL0B03839g | MET3 | Ortholog(s) have sulfate adenylyltransferase (ATP) activity | -3.13614590451067 |
| | CAGL0H10538g | YDL119C | Ortholog(s) have glycine transmembrane transporter activity, role in glycine import and mitochondrion localization | -3.01891746990778 |
| | CAGL0J07062g | CAR1 | Ortholog(s) have arginase activity, manganese ion binding, ornithine carbamoyltransferase inhibitor activity, zinc ion binding activity | -2.98492514064968 |
| | CAGL0M12386g | MMF1 | Ortholog(s) have role in isoleucine biosynthetic process, mitochondrial genome maintenance, mitochondrial translation and mitochondrial matrix localization | -2.92755143071168 |
| | CAGL0F01749g | SHM2 | Putative serine hydroxymethyltransferase; protein differentially expressed in azole resistant strain | -2.73790819203374 |
| | CAGL0K00825g | | Has domain(s) with predicted phosphatase activity, phosphoserine phosphatase activity and role in L-serine biosynthetic process, metabolic process | -2.4840800776844 |
| | CAGL0C05247g | MET22 | Protein serine/threonine phosphatase; protein abundance increased in ace2 mutant cells | -2.23856227908517 |
| | CAGL0M00176g | BAT2 | Ortholog(s) have L-isoleucine transaminase activity, L-leucine transaminase activity, L-valine transaminase activity | -2.20134585708139 |
| | CAGL0E05104g | LYS5 | Ortholog(s) have enzyme activator activity, holo-[acyl-carrier-protein] synthase activity and role in peptidyl-serine phosphopantetheinylation, protein-cofactor linkage | -2.1423333192964 |
| | CAGL0I06578g | YER152C | Ortholog(s) have 2-aminoadipate transaminase activity and cytoplasm, nucleus localization | -2.07133544255096 |
| | CAGL0E06468g | AVT3 | Ortholog(s) have L-arginine transmembrane transporter activity, L-glutamine transmembrane transporter activity and L-histidine transmembrane transporter activity, more | -2.05633506875369 |
| | CAGL0H06963g | YML096W | Ortholog(s) have cytosol, nucleus localization | -2.0548574214268 |
| | CAGL0K07788g | LYS2 | Ortholog(s) have L-aminoadipate-semialdehyde dehydrogenase activity, role in lysine biosynthetic process via aminoadipic acid, negative regulation of lysine biosynthetic process via aminoadipic acid and cytosol localization | -1.70758708667761 |
| | CAGL0M00330g | HOM6 | Ortholog(s) have homoserine dehydrogenase activity, role in homoserine biosynthetic process, methionine biosynthetic process, threonine biosynthetic process and cytoplasm, nucleus localization | -1.70580323195828 |
| | CAGL0H04587g | AVT5 | Ortholog of *S. cerevisiae* : AVT5 and Saccharomyces cerevisiae S288C : YBL089W | -1.60118682609174 |
| | CAGL0M12837g | SER33 | Ortholog(s) have alpha-ketoglutarate reductase activity, phosphoglycerate dehydrogenase activity, role in serine family amino acid biosynthetic process and cytosol localization | -1.56514555025844 |
| | CAGL0H03795g | | 3-isopropylmalate dehydrogenase | -1.42678768524774 |
| | CAGL0M06897g | YNL024C | Ortholog(s) have cytoplasm localization | -1.42132368004034 |
| | CAGL0F00693g | PRO2 | Putative gamma-glutamyl phosphate reductase; suppressor mutation (pro2-4) allows inviable gsh1 mutant to grow in the absence of glutathione | -1.41964862077859 |
| | CAGL0E02497g | PFA4 | Ortholog(s) have palmitoyltransferase activity, role in protein palmitoylation and endoplasmic reticulum localization | -1.4183143032284 |
| | CAGL0E03157g | CYS4 | Ortholog(s) have cystathionine beta-synthase activity, mRNA binding activity | -1.40820887106364 |

| | | | | |
|---|---|---|---|---|
| | CAGL0J04554g | | Has domain(s) with predicted catalytic activity, pyridoxal phosphate binding, transaminase activity and role in biosynthetic process, cellular amino acid metabolic process | -1.24395391481492 |
| | CAGL0M00880g | CAR2 | Putative ornithine aminotransferase; protein abundance increased in ace2 mutant cells | -1.2424437350713 |
| | CAGL0M06017g | TYR1 | Ortholog(s) have prephenate dehydrogenase (NADP+) activity, role in tyrosine biosynthetic process and cytosol localization | -1.23078330244765 |
| | CAGL0M00374g | MET5 | Ortholog(s) have sulfite reductase (NADPH) activity and role in hydrogen sulfide biosynthetic process, sulfate assimilation, sulfur amino acid biosynthetic process | -1.22956696526985 |
| | CAGL0M12188g | GCV3 | Ortholog(s) have glycine dehydrogenase (decarboxylating) activity, role in glycine catabolic process, one-carbon metabolic process, protein lipoylation and mitochondrion localization | -1.22839283859559 |
| | CAGL0D06402g | MET17 | O-acetyl homoserine sulfhydrylase (OAHSH), ortholog of *S. cerevisiae* MET17; required for utilization of inorganic sulfate as sulfur source; able to utilize cystine as a sulfur source while *S. cerevisiae* met15 mutants are unable to do so | -1.2113972740513 |
| | CAGL0F07029g | MET13 | Ortholog(s) have methylenetetrahydrofolate reductase (NAD(P)H) activity, role in methionine biosynthetic process, one-carbon metabolic process and mitochondrion localization | -1.19349094006509 |
| | CAGL0I09130g | PTR3 | Ortholog(s) have role in response to amino acid and extrinsic component of plasma membrane localization | -1.08183763008772 |
| | CAGL0J02398g | HIS6 | Ortholog(s) have 1-(5-phosphoribosyl)-5-[(5-phosphoribosylamino)methylideneamino]imidazole-4-carboxamide isomerase activity, role in histidine biosynthetic process and cytosol, nucleus localization | 1.00410478175018 |
| | CAGL0H07249g | | Putative deoxyhypusine synthase | 1.02607279583854 |
| | CAGL0G04741g | LEU4 | Ortholog(s) have 2-isopropylmalate synthase activity, role in cellular response to drug, leucine biosynthetic process and mitochondrion localization | 1.04463317351726 |
| | CAGL0C04917g | CPA2 | Ortholog(s) have carbamoyl-phosphate synthase (glutamine-hydrolyzing) activity, role in arginine biosynthetic process and carbamoyl-phosphate synthase complex, mitochondrion localization | 1.0498389827676 |
| | CAGL0L12562g | MET31 | Ortholog(s) have RNA polymerase II transcription factor activity, sequence-specific transcription regulatory region DNA binding, core promoter proximal region sequence-specific DNA binding activity | 1.05699236589768 |
| | CAGL0L12254g | ALT1 | Ortholog(s) have L-alanine:2-oxoglutarate aminotransferase activity, role in alanine biosynthetic process, alanine catabolic process, cellular response to drug, chronological cell aging and cytosol, mitochondrion, nucleus localization | 1.07275671977553 |
| | CAGL0H02871g | ARG2 | Ortholog(s) have acetyl-CoA:L-glutamate N-acetyltransferase activity, role in ornithine biosynthetic process and mitochondrial matrix, mitochondrial membrane localization | 1.08843395313659 |
| | CAGL0J02794g | ISD11 | Ortholog(s) have cysteine desulfurase activity, role in iron-sulfur cluster assembly and L-cysteine desulfurase complex, extrinsic component of mitochondrial inner membrane, mitochondrial matrix, nucleus localization | 1.11962381152287 |
| | CAGL0K09328g | THR4 | Threonine synthase | 1.15550100353212 |
| | CAGL0L12012g | TMT1 | Ortholog(s) have trans-aconitate 3-methyltransferase activity and cytosol localization | 1.20606486846359 |
| | CAGL0B03993g | ILV3 | Ortholog(s) have dihydroxy-acid dehydratase activity, role in branched-chain amino acid biosynthetic process and mitochondrion localization | 1.22020876385941 |
| | CAGL0L07546g | BAP3 | Ortholog(s) have amino acid transmembrane transporter activity, role in amino acid transport, transmembrane transport and endoplasmic reticulum, mitochondrion localization | 1.22952694045111 |
| | CAGL0J09504g | MET12 | Ortholog(s) have methylenetetrahydrofolate reductase (NAD(P)H) activity and role in methionine biosynthetic process, one-carbon metabolic process | 1.28960532293764 |
| | CAGL0I05126g | ILV1 | Ortholog(s) have L-threonine ammonia-lyase activity, role in isoleucine biosynthetic process, threonine catabolic process, valine biosynthetic process and mitochondrion localization | 1.30720416782128 |
| | CAGL0D03190g | MEU1 | Ortholog(s) have S-methyl-5-thioadenosine phosphorylase activity, mRNA binding activity, role in L-methionine salvage from methylthioadenosine, glutamate biosynthetic process and cytosol, extracellular region, nucleus localization | 1.32004230050483 |

| | | | | |
|---|---|---|---|---|
| | CAGL0B04455g | AVT4 | Ortholog(s) have L-glutamine transmembrane transporter activity, L-isoleucine transmembrane transporter activity, L-tyrosine transmembrane transporter activity and role in amino acid transmembrane export from vacuole | 1.32414026941432 |
| | CAGL0J08162g | LYP1 | Ortholog(s) have basic amino acid transmembrane transporter activity, role in basic amino acid transport and mitochondrion localization | 1.34310476495657 |
| | CAGL0H07051g | ASP1 | Ortholog(s) have asparaginase activity, role in asparagine catabolic process and Golgi apparatus localization | 1.34949817107234 |
| | CAGL0B00286g | CHA1 | Ortholog(s) have L-serine ammonia-lyase activity, L-threonine ammonia-lyase activity, role in L-serine catabolic process, threonine catabolic process and mitochondrial nucleoid localization | 1.45285870793707 |
| | CAGL0I09009g | HIS2 | Ortholog(s) have histidinol-phosphatase activity, role in histidine biosynthetic process and cytosol, nucleus localization | 1.47286149853851 |
| | CAGL0F03025g | ARO80 | Ortholog(s) have RNA polymerase II transcription factor activity, sequence-specific DNA binding, sequence-specific DNA binding activity | 1.47861063255175 |
| | CAGL0L02035g | MAE1 | Ortholog(s) have malate dehydrogenase (decarboxylating) (NAD+) activity, role in cellular amino acid metabolic process, malate metabolic process, pyruvate metabolic process and cytosol, mitochondrion localization | 1.49398366984289 |
| | CAGL0D01892g | AAT2 | Ortholog(s) have L-aspartate:2-oxoglutarate aminotransferase activity, role in aspartate biosynthetic process and cytosol, extracellular region, nucleus, peroxisome localization | 1.51078603226565 |
| | CAGL0D02178g | | Has domain(s) with predicted role in amino acid transport, transmembrane transport and integral component of membrane, membrane localization | 1.52500659872788 |
| | CAGL0H06875g | ARG81 | Ortholog(s) have transcription cofactor activity | 1.57206887411114 |
| | CAGL0L02475g | GCN4 | bZIP domain-containing protein | 1.6026164656022 |
| | CAGL0A01199g | DIP5 | Putative dicarboxylic amino acid permease | 1.60270753461759 |
| | CAGL0A02508g | YPQ2 | Ortholog(s) have basic amino acid transmembrane transporter activity, role in basic amino acid transmembrane export from vacuole and integral component of fungal-type vacuolar membrane localization | 1.60361433488069 |
| | CAGL0I06116g | SSY5 | Ortholog(s) have serine-type endopeptidase activity, role in protein processing, response to amino acid and extrinsic component of plasma membrane localization | 1.61200071884697 |
| | CAGL0M04059g | PHA2 | Ortholog(s) have prephenate dehydratase activity, role in L-phenylalanine biosynthetic process and cytosol, nucleus localization | 1.63543789362685 |
| | CAGL0B04961g | DPH5 | Ortholog(s) have diphthine synthase activity, role in peptidyl-diphthamide biosynthetic process from peptidyl-histidine and cytosol, nucleus localization | 1.64754260118761 |
| | CAGL0J08184g | ALP1 | Ortholog(s) have basic amino acid transmembrane transporter activity, role in basic amino acid transport and endoplasmic reticulum localization | 1.64819152715892 |
| | CAGL0G06688g | MET4 | bZIP domain-containing protein | 1.75571277255088 |
| | CAGL0K08668g | MET28 | bZIP domain-containing protein | 1.782776383295 |
| | CAGL0F06501g | ARG7 | Ortholog(s) have acetyl-CoA:L-glutamate N-acetyltransferase activity, glutamate N-acetyltransferase activity, role in ornithine biosynthetic process and mitochondrial matrix localization | 1.81736619529013 |
| | CAGL0L01089g | GLT1 | Ortholog(s) have glutamate synthase (NADH) activity, role in glutamate biosynthetic process and cytosol, mitochondrion localization | 1.82772836595289 |
| | CAGL0L00781g | MET30 | Ortholog(s) have protein binding, bridging, ubiquitin binding activity | 1.84118979247331 |
| | CAGL0M04499g | PUT1 | Ortholog(s) have proline dehydrogenase activity, role in proline catabolic process to glutamate and mitochondrion localization | 1.96161271037474 |

| | | | | |
|---|---|---|---|---|
| | CAGL0I07689g | YPQ1 | Ortholog(s) have basic amino acid transmembrane transporter activity, role in basic amino acid transmembrane export from vacuole and endoplasmic reticulum, integral component of fungal-type vacuolar membrane localization | 1.96703225372005 |
| | CAGL0H00396g | LEU3 | Ortholog(s) have sequence-specific DNA binding, transcriptional activator activity, RNA polymerase II core promoter proximal region sequence-specific binding and transcriptional repressor activity, more | 2.02895594947929 |
| | CAGL0K05753g | GNP1 | Ortholog(s) have L-proline transmembrane transporter activity, role in amino acid transport, transmembrane transport and cell periphery, cellular bud neck, endoplasmic reticulum, mitochondrion localization | 2.11545117707654 |
| | CAGL0M00154g | | Plasma membrane high affinity cystine specific transporter; present only in pathogenic yeasts; confers the ability to utilize cystine as a sulfur source | 2.19469454877938 |
| | CAGL0J08316g | MET2 | Ortholog(s) have homoserine O-acetyltransferase activity, role in homoserine metabolic process, methionine biosynthetic process, regulation of DNA methylation and cytosol localization | 2.20509682539814 |
| | CAGL0H01441g | PRO1 | Ortholog(s) have glutamate 5-kinase activity, role in proline biosynthetic process, ribophagy and cytoplasm localization | 2.2348761804304 |
| | CAGL0L09691g | PUT3 | Ortholog(s) have RNA polymerase II core promoter proximal region sequence-specific DNA binding, transcriptional activator activity, RNA polymerase II core promoter proximal region sequence-specific binding activity | 2.28786446269165 |
| | CAGL0K05357g | GLN1 | Ortholog(s) have glutamate-ammonia ligase activity, role in ammonia assimilation cycle, cellular response to nitrogen starvation, glutamine biosynthetic process and cytosol, nuclear periphery localization | 2.35539997038103 |
| | CAGL0M11440g | CHA4 | Ortholog(s) have sequence-specific DNA binding, transcription factor activity, sequence-specific DNA binding activity and role in cellular amino acid catabolic process, positive regulation of transcription, DNA-templated | 2.40668906749162 |
| | CAGL0B01507g | ARG8 | Ortholog(s) have N2-acetyl-L-ornithine:2-oxoglutarate 5-aminotransferase activity, role in arginine biosynthetic process and mitochondrial matrix, nucleus localization | 2.43404901761206 |
| | CAGL0L06710g | RTC2 | Ortholog(s) have basic amino acid transmembrane transporter activity | 2.48270207181007 |
| | CAGL0L03267g | GAP1 | Ortholog(s) have L-proline transmembrane transporter activity, polyamine transmembrane transporter activity and role in amino acid transmembrane transport, polyamine transport, regulation of nitrogen utilization | 2.52202746507813 |
| | CAGL0E05632g | PUT4 | Ortholog(s) have L-proline transmembrane transporter activity, role in gamma-aminobutyric acid transport, proline transport and Golgi apparatus, endoplasmic reticulum localization | 2.56217403496147 |
| | CAGL0F07777g | ALD3 | Putative aldehyde dehydrogenase; expression upregulated in biofilm vs planktonic cell culture | 2.66287875757591 |
| | CAGL0I04730g | HMT1 | Putative hnRNP arginine N-methyltransferase | 2.82901469820248 |
| | CAGL0A03102g | ARO10 | Ortholog(s) have phenylpyruvate decarboxylase activity | 3.09821478846691 |
| | CAGL0I10791g | | Ortholog(s) have ornithine carbamoyltransferase activity, role in arginine biosynthetic process via ornithine, asexual sporulation and mitochondrial matrix localization | 3.16545271328103 |
| | CAGL0J11484g | DUG3 | Component of the Dug1p-Dug2p-Dug3p complex involved in glutathione degradation; required for glutathione utilization in C. glabrata when glutathione import is enabled by expression of the *S. cerevisiae* Opt1p transporter | 3.25372315162536 |
| | CAGL0L02937g | HIS3 | Putative imidazoleglycerol-phosphate dehydratase | 3.28943728706016 |
| | CAGL0E04312g | STP2 | Ortholog(s) have RNA polymerase II core promoter proximal region sequence-specific DNA binding, transcriptional activator activity, RNA polymerase II core promoter proximal region sequence-specific binding activity | 3.72053745735121 |
| | CAGL0I05500g | PRS2 | Ortholog(s) have ribose phosphate diphosphokinase activity, role in 5-phosphoribose 1-diphosphate biosynthetic process, cytokinesis, fungal-type cell wall organization and cytosol, ribose phosphate diphosphokinase complex localization | 3.89628640486045 |
| | CAGL0C04565g | JJJ3 | Ortholog(s) have ferrous iron binding activity, role in peptidyl-diphthamide biosynthetic process from peptidyl-histidine and cytosol, nucleus localization | 3.90963175266395 |
| | CAGL0K10362g | ORT1 | Ortholog(s) have L-ornithine transmembrane transporter activity, role in arginine biosynthetic process, mitochondrial ornithine transport and mitochondrial envelope localization | 4.01214707843081 |

| | | | | |
|---|---|---|---|---|
| | CAGL0H08393g | BAP2 | Ortholog(s) have amino acid transmembrane transporter activity, role in amino acid transport, transmembrane transport and endoplasmic reticulum localization | 4.10604407467508 |
| | CAGL0I09592g | CPA1 | Ortholog(s) have carbamoyl-phosphate synthase (glutamine-hydrolyzing) activity, role in arginine biosynthetic process and carbamoyl-phosphate synthase complex, cytoplasmic stress granule localization | 4.57872709384522 |
| | CAGL0G02761g | DPH1 | Ortholog(s) have role in peptidyl-diphthamide biosynthetic process from peptidyl-histidine and cytosol, nucleus localization | 4.77550276955705 |
| | CAGL0F00407g | LIA1 | Ortholog(s) have deoxyhypusine monooxygenase activity | 5.26584724701059 |
| | CAGL0K12518g | AGX1 | Ortholog(s) have alanine-glyoxylate transaminase activity, role in glycine biosynthetic process, by transamination of glyoxylate and biofilm matrix, cytosol, mitochondrion localization | 5.33656717848359 |
| **Ergosterol biosynthesis** | CAGL0L12364g | ERG10 | Ortholog(s) have acetyl-CoA C-acetyltransferase activity, role in ergosterol biosynthetic process and cytosol, nucleus localization | -3.5024462453419 |
| | CAGL0L10714g | ERG2 | C-8 sterol isomerase | -3.41466569849143 |
| | CAGL0F03993g | ERG8 | Ortholog(s) have phosphomevalonate kinase activity | -2.82697058325284 |
| | CAGL0L13134g | YLR072W | Ortholog(s) have sterol transporter activity, role in intracellular sterol transport and ER-mitochondrion membrane contact site, mitochondrion, nucleus-vacuole junction, vacuole-mitochondrion membrane contact site localization | -2.80397605939125 |
| | CAGL0M07095g | ERG9 | Squalene synthase (farnesyl-diphosphate farnesyl transferase); catalyzes the first step in sterol biosynthesis | -2.73196787663871 |
| | CAGL0I02970g | ERG24 | Ortholog(s) have delta14-sterol reductase activity and role in cellular response to drug, ergosterol biosynthetic process, filamentous growth of a population of unicellular organisms in response to biotic stimulus, pathogenesis | -2.10444847628514 |
| | CAGL0J10780g | OSH3 | Ortholog(s) have lipid binding, sterol transporter activity | -1.99644111557889 |
| | CAGL0J05918g | NSG2 | Ortholog(s) have unfolded protein binding activity, role in sterol biosynthetic process and endoplasmic reticulum localization | -1.69544884293426 |
| | CAGL0A00429g | ERG4 | Putative C24 sterol reductase | -1.5135169049815 |
| | CAGL0F07865g | UPC2 | Putative Zn(2)-Cys(6) binuclear cluster transcriptional regulator of ergosterol biosynthesis | -1.37460610107039 |
| | CAGL0F08437g | SAY1 | Ortholog(s) have steryl deacetylase activity, role in response to toxic substance, sterol deacetylation and cell periphery, endoplasmic reticulum lumen, integral component of membrane, lipid particle localization | -1.2791317310716 |
| | CAGL0M11506g | ERG27 | Ortholog(s) have 3-keto sterol reductase activity, role in cellular response to drug, ergosterol biosynthetic process and endoplasmic reticulum membrane, lipid particle, mitochondrial outer membrane localization | -1.11737700998649 |
| | CAGL0E04158g | DET1 | Ortholog(s) have acid phosphatase activity, role in dephosphorylation, intracellular sterol transport and cytoplasm, nucleus localization | 1.20864980605541 |
| | CAGL0F03861g | ERG12 | Ortholog(s) have mevalonate kinase activity and role in ergosterol biosynthetic process, farnesyl diphosphate biosynthetic process, mevalonate pathway, isopentenyl diphosphate biosynthetic process, mevalonate pathway | 1.36526684938095 |
| | CAGL0K08030g | NVJ2 | Ortholog(s) have lipid binding activity and endoplasmic reticulum, nucleus-vacuole junction, plasma membrane, ribosome localization | 1.53670306351194 |
| | CAGL0H03245g | SCY1 | Ortholog(s) have role in negative regulation of TORC1 signaling and clathrin-coated vesicle, cytosol localization | 1.54293130325004 |
| | CAGL0C02981g | ARE1 | Putative acyl-CoA:sterol acyltransferase involved in sterol esterification; gene is upregulated in azole-resistant strain | 1.68822539298711 |
| | CAGL0G07667g | PRY1 | Ortholog(s) have cholesterol binding, magnesium ion binding activity, role in sterol transport and endoplasmic reticulum, extracellular region, fungal-type vacuole, nuclear envelope localization | 1.95634431995384 |
| | CAGL0K12716g | YFL040W | Ortholog(s) have fungal-type vacuole, prospore membrane localization | 1.99372419149826 |
| | | | | |

| | | | | |
|---|---|---|---|---|
| | CAGL0D05566g | YEH1 | Ortholog(s) have sterol esterase activity, role in sterol metabolic process and integral component of membrane, lipid particle localization | 2.31163207256448 |
| | CAGL0F01419g | AUS1 | ATP-binding cassette transporter involved in sterol uptake | 2.76242433481335 |
| | CAGL0M10571g | ARE2 | Ortholog(s) have ergosterol O-acyltransferase activity, role in ergosterol metabolic process and endoplasmic reticulum localization | 2.90024272069978 |
| | CAGL0F03267g | YHR080C | Ortholog(s) have sterol binding activity and cortical endoplasmic reticulum, mitochondrion, ribosome localization | 3.46964840259323 |
| | CAGL0F01793g | ERG3 | Delta 5,6 sterol desaturase; C-5 sterol desaturase; predicted transmembrane domain and endolasmic reticulum (ER) binding motif; gene used for molecular typing of C. glabrata strain isolates | 3.47626736236227 |
| | CAGL0K04477g | ERG25 | Ortholog(s) have C-4 methylsterol oxidase activity, role in ergosterol biosynthetic process and endoplasmic reticulum membrane, plasma membrane localization | 3.67303558615778 |
| | CAGL0D05940g | ERG1 | Squalene epoxidase with a role in ergosterol synthesis; involved in growth under conditions of low oxygen tension | 3.79853432844869 |
| | CAGL0E04334g | ERG11 | Putative cytochrome P-450 lanosterol 14-alpha-demethylase; target enzyme of azole antifungal drugs; increased protein abundance in azole resistant strain | 4.01040685430362 |
| | CAGL0I04246g | SUT1 | Putative transcription factor involved in sterol uptake; gene is upregulated in azole-resistant strain | 4.12842345098001 |
| | CAGL0L03828g | CYB5 | Ortholog(s) have electron carrier activity, role in ergosterol biosynthetic process and endoplasmic reticulum membrane localization | 4.59450135562817 |
| | CAGL0F05137g | PRY2 | Ortholog(s) have sterol binding activity, role in pathogenesis, sterol transport and cell surface, endoplasmic reticulum, extracellular region, fungal-type vacuole localization | 8.18637995390137 |
| **Nitrogen metabolism** | CAGL0I08283g | PRO3 | Putative gamma-glutamyl phosphate reductase | -2.70573683827508 |
| | CAGL0K06809g | YBR220C | Ortholog(s) have Golgi apparatus localization | -2.66057923292623 |
| | CAGL0K08558g | GFA1 | Ortholog(s) have glutamine-fructose-6-phosphate transaminase (isomerizing) activity | -2.35655047867919 |
| | CAGL0H03399g | HNM1 | Ortholog(s) have (R)-carnitine transmembrane transporter activity, choline transmembrane transporter activity, ethanolamine transmembrane transporter activity | -2.1033692435427 |
| | CAGL0G05291g | PAA1 | Ortholog(s) have aralkylamine N-acetyltransferase activity, diamine N-acetyltransferase activity, role in chromatin organization and cytoplasm localization | -1.85060893871946 |
| | CAGL0D03982g | PUT2 | Ortholog(s) have 1-pyrroline-5-carboxylate dehydrogenase activity, role in glutamate biosynthetic process, hyphal growth, proline catabolic process to glutamate and cytosol, mitochondrial matrix localization | -1.74773418239312 |
| | CAGL0M05533g | | Ortholog(s) have role in nitrogen compound metabolic process | -1.62591855573303 |
| | CAGL0F06743g | DAL81 | Ortholog(s) have RNA polymerase II transcription coactivator activity involved in preinitiation complex assembly, RNA polymerase II transcription factor activity and sequence-specific DNA binding, more | -1.31889806404833 |
| | CAGL0H02607g | | Ortholog(s) have adenosylmethionine decarboxylase activity, role in spermidine biosynthetic process, spermine biosynthetic process and cytosol, nucleus localization | 1.03421798634557 |
| | CAGL0D04928g | MEP3 | Ortholog(s) have ammonium transmembrane transporter activity, role in ammonium transport, nitrogen utilization and endoplasmic reticulum, plasma membrane localization | 1.03528774369177 |
| | CAGL0D00484g | SPE1 | Ortholog(s) have ornithine decarboxylase activity and role in DNA biosynthetic process, nuclear division, pantothenate biosynthetic process, putrescine biosynthetic process, spermidine biosynthetic process, spore germination | 1.08577045378889 |
| | CAGL0D04026g | UGA1 | Ortholog(s) have 4-aminobutyrate transaminase activity, pyridoxal phosphate binding activity and role in cellular amide catabolic process, gamma-aminobutyric acid catabolic process, glutamate metabolic process | 1.18265474232705 |

| | | | | |
|---|---|---|---|---|
| | CAGL0E00759g | ARG82 | Ortholog(s) have inositol tetrakisphosphate 3-kinase activity, inositol tetrakisphosphate 6-kinase activity and inositol-1,3,4,5,6-pentakisphosphate kinase activity, more | 1.6769674885383 |
| | CAGL0J06028g | MEP2 | Ortholog(s) have high-affinity secondary active ammonium transmembrane transporter activity, methylammonium transmembrane transporter activity | 1.72659995742323 |
| | CAGL0J07392g | URE2 | Protein with an N-terminal prion domain and a C-terminal domain that regulates nitrogen catabolism; complements *S. cerevisiae* ure2 mutant for nitrogen regulation but does not form [URE3] prion when expressed in *S. cerevisiae* | 1.83358674019464 |
| | CAGL0C02277g | GLN3 | Putative zinc finger transcription factor with a predicted role in nitrogen catabolite repression | 1.87106806474486 |
| | CAGL0G01210g | NIT3 | Putative nitrilase; protein abundance increased in ace2 mutant cells | 1.9095717102486 |
| | CAGL0J10274g | MKS1 | Ortholog(s) have role in mitochondria-nucleus signaling pathway, negative regulation of transcription from RNA polymerase II promoter, regulation of nitrogen utilization, regulation of pseudohyphal growth and cytoplasm localization | 1.93858350257218 |
| | CAGL0K03157g | DUR3 | Putative plasma membrane polyamine transporter | 2.29936950917728 |
| | CAGL0H02585g | GAD1 | Ortholog(s) have glutamate decarboxylase activity, role in cellular response to oxidative stress, glutamate catabolic process and cytoplasm localization | 2.42475233179812 |
| | CAGL0I10747g | MEP1 | Ortholog(s) have ammonium transmembrane transporter activity, role in ammonium transport, nitrogen utilization and endoplasmic reticulum localization | 2.42906659512049 |
| | CAGL0H09152g | PTK1 | Ortholog(s) have role in polyamine transport | 2.4549969080211 |
| | CAGL0C04191g | UGA2 | Ortholog(s) have succinate-semialdehyde dehydrogenase [NAD(P)+] activity and role in cellular response to oxidative stress, gamma-aminobutyric acid catabolic process, glutamate decarboxylation to succinate | 2.71634066207462 |
| | CAGL0A03212g | ATO3 | Ortholog(s) have ammonium transmembrane transporter activity, role in ammonium transport, nitrogen utilization, transmembrane transport and mitochondrion, plasma membrane localization | 3.27534661976074 |
| | CAGL0K07634g | GAT1 | Ortholog(s) have sequence-specific DNA binding, transcription factor activity, RNA polymerase II transcription factor binding and transcriptional activator activity, more | 3.7891813814905 |
| | CAGL0I00902g | GAT2 | Has domain(s) with predicted sequence-specific DNA binding, transcription factor activity, sequence-specific DNA binding, zinc ion binding activity and role in regulation of transcription, DNA-templated | 4.05001506475768 |
| | CAGL0M03465g | ATO2 | Ortholog(s) have acetate transmembrane transporter activity, ammonium transmembrane transporter activity and role in ammonium transport, nitrogen utilization, plasma membrane acetate transport | 5.83367161094676 |
| | CAGL0I08613g | | Putative plasma membrane polyamine transporter | 6.03995603496322 |
| **Lipid metabolism** | CAGL0I05940g | SFH5 | Ortholog(s) have phosphatidylinositol transporter activity | -4.69222589410956 |
| | CAGL0H08712g | | Has domain(s) with predicted phosphatidylinositol binding activity and role in cell communication | -4.55393839199683 |
| | CAGL0F00363g | OPI3 | Ortholog(s) have phosphatidyl-N-dimethylethanolamine N-methyltransferase activity, phosphatidyl-N-methylethanolamine N-methyltransferase activity and role in cleistothecium development, phosphatidylcholine biosynthetic process | -4.51373898029842 |
| | CAGL0H07513g | IFA38 | Predicted ketoreductase involved in production of very long chain fatty acid for sphingolipid biosynthesis; mutants show reduced sensitivity to caspofungin and increased sensitivity to micafungin | -4.09703523070487 |
| | CAGL0D00528g | FAS1 | Ortholog(s) have 3-hydroxyacyl-[acyl-carrier-protein] dehydratase activity, [acyl-carrier-protein] S-acetyltransferase activity and [acyl-carrier-protein] S-malonyltransferase activity, more | -3.83341976535918 |
| | CAGL0L08184g | ELO2 | Predicted fatty acid elongase with role in sphingolipid biosynthetic process; mutants show reduced sensitivity to caspofungin and increased sensitivity to micafungin | -3.79385201965775 |
| | CAGL0G08085g | DNF2 | Ortholog(s) have phospholipid-translocating ATPase activity | -3.74513130615385 |

| | | | | |
|---|---|---|---|---|
| | CAGL0I04070g | SLC1 | Ortholog(s) have 1-acylglycerol-3-phosphate O-acyltransferase activity, role in glycerophospholipid biosynthetic process and endoplasmic reticulum, lipid particle, plasma membrane localization | -3.66591138657971 |
| | CAGL0E06138g | | Ortholog(s) have fatty acid synthase activity, role in palmitic acid biosynthetic process, response to pH and fatty acid synthase complex, glyoxysome localization | -3.64691376621933 |
| | CAGL0L10780g | HFA1 | Ortholog(s) have acetyl-CoA carboxylase activity, role in fatty acid biosynthetic process and cytosol, fungal-type vacuole membrane, mitochondrion localization | -3.64036404426526 |
| | CAGL0D06446g | STT4 | Ortholog(s) have 1-phosphatidylinositol 4-kinase activity, role in invasive filamentous growth, macroautophagy, mitophagy, phosphatidylinositol phosphorylation and cytosol, mitochondrion, plasma membrane localization | -3.59978097420172 |
| | CAGL0M06237g | EHT1 | Ortholog(s) have alcohol O-butanoyltransferase activity, serine hydrolase activity, short-chain carboxylesterase activity and role in medium-chain fatty acid biosynthetic process, medium-chain fatty acid catabolic process | -3.58904798721431 |
| | CAGL0F01111g | OPI10 | Ortholog(s) have role in inositol metabolic process and cytosol, nuclear envelope localization | -3.57680320561404 |
| | CAGL0M04367g | CKI1 | Ortholog(s) have choline kinase activity, ethanolamine kinase activity, role in phosphatidylcholine biosynthetic process, phosphatidylethanolamine biosynthetic process and cytosol, nucleus localization | -3.49251764025582 |
| | CAGL0D04950g | LOA1 | Ortholog(s) have lysophosphatidic acid acyltransferase activity, role in cellular triglyceride homeostasis, lipid particle organization, protein targeting to vacuole and Golgi apparatus, endoplasmic reticulum, lipid particle localization | -3.46121874270333 |
| | CAGL0G09955g | DPM1 | Ortholog(s) have dolichyl-phosphate beta-D-mannosyltransferase activity | -3.20652782137942 |
| | CAGL0I06050g | INO1 | Putative inositol 1-phosphate synthase; regulated by the transcriptional activators Ino2p and Ino4p; protein differentially expressed in azole resistant strain | -3.02157259855269 |
| | CAGL0J02970g | CEM1 | Ortholog(s) have mitochondrion localization | -2.94330290386579 |
| | CAGL0H01309g | DPL1 | Ortholog(s) have sphinganine-1-phosphate aldolase activity and role in calcium-mediated signaling, cellular response to starvation, sphingolipid metabolic process | -2.87573528137651 |
| | CAGL0I09812g | DGK1 | Ortholog(s) have diacylglycerol kinase activity, role in phosphatidic acid biosynthetic process and integral component of endoplasmic reticulum membrane localization | -2.85807071280038 |
| | CAGL0B03443g | MCP2 | Ortholog(s) have role in lipid homeostasis, mitochondrion organization and integral component of mitochondrial membrane, mitochondrial inner membrane localization | -2.84288439633924 |
| | CAGL0G06270g | DRS2 | Ortholog(s) have phospholipid-translocating ATPase activity | -2.82432991976222 |
| | CAGL0G04851g | ELO3 | Predicted fatty acid elongase involved in production of very long chain fatty acids for sphingolipid biosynthesis; mutants show reduced sensitivity to caspofungin and increased sensitivity to micafungin | -2.49208104651747 |
| | CAGL0L03564g | PHS1 | Ortholog(s) have 3-hydroxyacyl-CoA dehydratase activity, enoyl-CoA hydratase activity and role in fatty acid elongation, sphingolipid biosynthetic process, vacuolar transport | -2.47769474143168 |
| | CAGL0J06226g | PSD1 | Ortholog(s) have phosphatidylserine decarboxylase activity | -2.43055423683523 |
| | CAGL0H06501g | VAC14 | Ortholog(s) have protein binding, bridging activity | -2.41927297268398 |
| | CAGL0D04290g | YKL091C | Ortholog(s) have phosphatidylcholine binding, phosphatidylinositol binding activity and nucleus localization | -2.31442408651216 |
| | | | | |
| | CAGL0F03817g | YMR210W | Ortholog(s) have acylglycerol lipase activity and role in medium-chain fatty acid biosynthetic process, triglyceride metabolic process | -2.29032696278064 |
| | CAGL0F07535g | YJU3 | Ortholog(s) have acylglycerol lipase activity, serine hydrolase activity, role in triglyceride metabolic process and endoplasmic reticulum, lipid particle, mitochondrial outer membrane, plasma membrane localization | -2.23741376238888 |
| | CAGL0J04664g | | Has domain(s) with predicted phosphopantetheine binding activity and role in fatty acid biosynthetic process | -2.2199643763732 |

| | | | | |
|---|---|---|---|---|
| | CAGL0L10450g | ALG8 | Ortholog(s) have dolichyl pyrophosphate Glc1Man9GlcNAc2 alpha-1,3-glucosyltransferase activity, role in oligosaccharide-lipid intermediate biosynthetic process, protein N-linked glycosylation and endoplasmic reticulum membrane localization | -2.21669200500419 |
| | CAGL0I04642g | FAT1 | Ortholog(s) have long-chain fatty acid transporter activity, very long-chain fatty acid-CoA ligase activity and role in long-chain fatty acid import, very long-chain fatty acid metabolic process | -2.20461116645502 |
| | CAGL0K02959g | NEM1 | Ortholog(s) have phosphoprotein phosphatase activity and role in negative regulation of phospholipid biosynthetic process, nuclear envelope organization, positive regulation of phosphatidate phosphatase activity, protein dephosphorylation | -2.19955644425495 |
| | CAGL0E01309g | EKI1 | Ortholog(s) have choline kinase activity, ethanolamine kinase activity, role in phosphatidylcholine biosynthetic process, phosphatidylethanolamine biosynthetic process and cytoplasm localization | -2.07936110744195 |
| | CAGL0K00583g | ELO1 | Ortholog(s) have fatty acid elongase activity, role in fatty acid elongation, unsaturated fatty acid and endoplasmic reticulum localization | -2.07331553157356 |
| | CAGL0J04378g | RFT1 | Ortholog(s) have role in glycolipid translocation and endoplasmic reticulum membrane localization | -2.07050370461231 |
| | CAGL0K03509g | HFD1 | Putative mitochondrial fatty aldehyde dehydrogenase; gene is upregulated in azole-resistant strain | -2.05617054420638 |
| | CAGL0K02739g | LAG1 | Ortholog(s) have sphingosine N-acyltransferase activity and role in ceramide biosynthetic process, filamentous growth of a population of unicellular organisms, replicative cell aging, unidimensional cell growth | -2.04064976193598 |
| | CAGL0G05071g | LCB2 | Ortholog(s) have serine C-palmitoyltransferase activity, role in cellular response to drug, sphingolipid biosynthetic process and SPOTS complex localization | -1.95698955456568 |
| | CAGL0L04642g | ALE1 | Ortholog(s) have 1-acylglycerol-3-phosphate O-acyltransferase activity, 1-acylglycerophosphocholine O-acyltransferase activity, role in glycerophospholipid biosynthetic process and endoplasmic reticulum, ribosome localization | -1.9214573673819 |
| | CAGL0A02926g | VPS74 | Ortholog(s) have enzyme binding, phosphatidylinositol-4-phosphate binding activity | -1.91306131362312 |
| | CAGL0H05599g | YDC1 | Ortholog(s) have dihydroceramidase activity, role in ceramide biosynthetic process, ceramide catabolic process and endoplasmic reticulum, fungal-type vacuole membrane localization | -1.88396938134478 |
| | CAGL0M10769g | ALG12 | Ortholog(s) have alpha-1,6-mannosyltransferase activity, role in dolichol-linked oligosaccharide biosynthetic process, protein glycosylation and endoplasmic reticulum localization | -1.85943476853283 |
| | CAGL0H05005g | CSR1 | Ortholog(s) have phosphatidylinositol transporter activity | -1.84985939020359 |
| | CAGL0K04103g | CAX4 | Ortholog(s) have dolichyldiphosphatase activity, role in lipid biosynthetic process, protein N-linked glycosylation and integral component of endoplasmic reticulum membrane localization | -1.81588254772196 |
| | CAGL0K05621g | TGL5 | Ortholog(s) have lysophosphatidic acid acyltransferase activity, triglyceride lipase activity, role in triglyceride mobilization and lipid particle localization | -1.79540872617069 |
| | CAGL0I00330g | SCS3 | Ortholog(s) have role in phospholipid biosynthetic process and endoplasmic reticulum localization | -1.77393135431386 |
| | CAGL0J02134g | INP51 | Ortholog(s) have phosphatidylinositol-4,5-bisphosphate 5-phosphatase activity | -1.75456439943902 |
| | CAGL0M09933g | FLD1 | Ortholog(s) have role in lipid particle organization and cortical endoplasmic reticulum, integral component of endoplasmic reticulum membrane localization | -1.75073182156186 |
| | CAGL0K05005g | ALG9 | Ortholog(s) have glycolipid mannosyltransferase activity, role in dolichol-linked oligosaccharide biosynthetic process, protein glycosylation and endoplasmic reticulum localization | -1.73023550585352 |
| | CAGL0C04895g | YMR1 | Ortholog(s) have mRNA binding, phosphatidylinositol-3-phosphatase activity, role in phosphatidylinositol dephosphorylation and cytosol localization | -1.61557516116061 |
| | CAGL0J08437g | LPP1 | Ortholog(s) have phosphatidate phosphatase activity, role in phospholipid metabolic process and membrane localization | -1.59520606316524 |
| | CAGL0L03432g | GWT1 | Ortholog(s) have glucosaminyl-phosphotidylinositol O-acyltransferase activity and role in GPI anchor biosynthetic process | -1.56258206256449 |

| | | | | |
|---|---|---|---|---|
| | CAGL0M05621g | CSH1 | Ortholog(s) have mannosyltransferase activity, role in mannosyl-inositol phosphorylceramide biosynthetic process and cis-Golgi network membrane, fungal-type vacuole, trans-Golgi network membrane localization | -1.55730914923831 |
| | CAGL0D04972g | TAZ1 | Ortholog(s) have 1-acylglycerophosphocholine O-acyltransferase activity | -1.48086319906318 |
| | CAGL0M13673g | LIP1 | Ortholog(s) have sphingosine N-acyltransferase activity, role in ceramide biosynthetic process and acyl-CoA ceramide synthase complex, endoplasmic reticulum membrane, nuclear envelope localization | -1.44956390722231 |
| | CAGL0M05731g | ALG2 | Ortholog(s) have GDP-Man:Man1GlcNAc2-PP-Dol alpha-1,3-mannosyltransferase activity, glycolipid 6-alpha-mannosyltransferase activity, role in oligosaccharide-lipid intermediate biosynthetic process and endoplasmic reticulum localization | -1.44699730100933 |
| | CAGL0D06270g | ALG13 | Ortholog(s) have N-acetylglucosaminyldiphosphodolichol N-acetylglucosaminyltransferase activity and role in dolichol-linked oligosaccharide biosynthetic process | -1.41459326371561 |
| | CAGL0H01089g | INM2 | Ortholog(s) have inositol monophosphate 1-phosphatase activity and role in inositol phosphate dephosphorylation | -1.39403112534275 |
| | CAGL0G08690g | AYR1 | Ortholog(s) have acylglycerone-phosphate reductase activity, triglyceride lipase activity and role in phosphatidic acid biosynthetic process, triglyceride catabolic process | -1.38453147453073 |
| | CAGL0K02805g | | Predicted inositolphosphorylceramide (IPC) synthase, catalyzes the essential step in sphingolipid biosynthesis; potential antifungal drug target | -1.33908203874673 |
| | CAGL0H04477g | DNF3 | Ortholog(s) have phospholipid-translocating ATPase activity and role in intracellular protein transport, phospholipid translocation, response to pheromone involved in conjugation with cellular fusion | -1.33842083226551 |
| | CAGL0K00297g | SAC1 | Ortholog(s) have phosphatidylinositol-3,5-bisphosphate 5-phosphatase activity, phosphatidylinositol-3-phosphatase activity, phosphatidylinositol-4-phosphate phosphatase activity | -1.30193674259375 |
| | CAGL0I04334g | LCB3 | Ortholog(s) have sphingosine-1-phosphate phosphatase activity, role in calcium-mediated signaling and endoplasmic reticulum localization | -1.27976664650108 |
| | CAGL0G02145g | YKR078W | Ortholog(s) have phosphatidylinositol-3-phosphate binding activity and cytoplasm localization | -1.26167054253282 |
| | CAGL0B04631g | INP53 | Ortholog(s) have calcium ion binding, inositol-1,2,4,5,6-pentakisphosphate 5-phosphatase activity and inositol-1,2,4,5-tetrakisphosphate 5-phosphatase activity, more | -1.22485660034333 |
| | CAGL0E03201g | CHO2 | Ortholog(s) have phosphatidylethanolamine N-methyltransferase activity, role in phosphatidylcholine biosynthetic process and cell periphery, endoplasmic reticulum membrane localization | -1.20053023834647 |
| | CAGL0L04554g | LCB4 | Ortholog(s) have D-erythro-sphingosine kinase activity, role in calcium-mediated signaling, sphingolipid metabolic process and Golgi apparatus, cortical endoplasmic reticulum, plasma membrane localization | -1.19183332836704 |
| | CAGL0F03773g | EFR3 | Ortholog(s) have role in establishment of protein localization to plasma membrane and mitochondrion, plasma membrane localization | -1.17746877270177 |
| | CAGL0K01837g | TSC13 | Ortholog(s) have oxidoreductase activity, role in very long-chain fatty acid metabolic process and endoplasmic reticulum membrane, mitochondrion localization | -1.12746375385476 |
| | CAGL0L12892g | SFK1 | Ortholog(s) have role in actin cytoskeleton organization, inositol lipid-mediated signaling, vacuole organization and plasma membrane localization | -1.10884571109239 |
| | CAGL0I08745g | PSD2 | Ortholog(s) have phosphatidylserine decarboxylase activity | -1.00412950732114 |
| | CAGL0M11462g | ICT1 | Ortholog(s) have lysophosphatidic acid acyltransferase activity and role in phosphatidic acid biosynthetic process | -1.00320386542666 |
| | CAGL0C05269g | INP54 | Ortholog(s) have phosphatidylinositol-4,5-bisphosphate 5-phosphatase activity, role in phosphatidylinositol dephosphorylation and endoplasmic reticulum, fungal-type vacuole membrane localization | 1.12110493160737 |
| | CAGL0C03509g | FPK1 | Ortholog(s) have protein serine/threonine kinase activity and role in positive regulation of phospholipid translocation, protein autophosphorylation, response to pheromone involved in conjugation with cellular fusion | 1.21846667092965 |

| | | | | |
|---|---|---|---|---|
| | CAGL0F06831g | MGA2 | Ortholog(s) have role in cellular response to cold, chromatin silencing at silent mating-type cassette and mRNA stabilization, more | 1.31582322124482 |
| | CAGL0M03157g | IRS4 | Ortholog(s) have role in autophagy, cellular response to starvation, chromatin silencing at rDNA, fungal-type cell wall organization, inositol lipid-mediated signaling and mitochondrion, pre-autophagosomal structure localization | 1.4376899807651 |
| | CAGL0K05995g | LCB5 | Putative sphingoid long-chain base kinase; gene is upregulated in azole-resistant strain | 1.47320492098283 |
| | CAGL0H06787g | POT1 | Ortholog(s) have acetyl-CoA C-acyltransferase activity, mRNA binding activity, role in fatty acid beta-oxidation and glyoxysome, mitochondrial intermembrane space, peroxisomal matrix localization | 1.49327035158848 |
| | CAGL0G02365g | TGL4 | Ortholog(s) have calcium-independent phospholipase A2 activity, lysophosphatidic acid acyltransferase activity, sterol esterase activity, triglyceride lipase activity | 1.60841436305704 |
| | CAGL0J09196g | SRF1 | Ortholog(s) have role in positive regulation of catalytic activity and cell periphery, fungal-type vacuole localization | 1.80065525183447 |
| | CAGL0D03960g | BRL1 | Ortholog(s) have role in lipid homeostasis, mRNA export from nucleus, nuclear envelope organization and endoplasmic reticulum, integral component of membrane, nuclear envelope localization | 1.87629163549534 |
| | CAGL0K07458g | YPK1 | Ortholog(s) have protein serine/threonine kinase activity | 1.98583017441957 |
| | CAGL0D00418g | FAT3 | Ortholog(s) have role in long-chain fatty acid transport and cell periphery, mitochondrion localization | 2.02115629992392 |
| | CAGL0J11770g | PLB1 | Putative phospholipase B; predicted GPI-anchor | 2.0675581416745 |
| | CAGL0L00561g | SSO1 | Ortholog(s) have SNAP receptor activity, phosphatidic acid binding, phosphatidylinositol-3,4-bisphosphate binding, phosphatidylinositol-3,5-bisphosphate binding, phosphatidylinositol-4,5-bisphosphate binding activity | 2.14919819837545 |
| | CAGL0H01177g | DPP1 | Ortholog(s) have diacylglycerol diphosphate phosphatase activity, phosphatidate phosphatase activity and role in farnesol biosynthetic process, phospholipid metabolic process | 2.23221227178473 |
| | CAGL0C04279g | RER2 | Ortholog(s) have dehydrodolichyl diphosphate synthase activity and role in ER to Golgi vesicle-mediated transport, dolichol biosynthetic process, protein glycosylation | 2.2640250102595 |
| | CAGL0H01375g | SUR2 | Predicted sphinganine hydroxylase with role in sphingolipid biosynthesis; mutants show reduced sensitivity to caspofungin and increased sensitivity to micafungin | 2.30841411189982 |
| | CAGL0K07293g | FAA4 | Ortholog(s) have long-chain fatty acid-CoA ligase activity and role in long-chain fatty acid import, long-chain fatty-acyl-CoA metabolic process, sphingoid long-chain base transport | 2.32194183960331 |
| | CAGL0A00341g | MPO1 | Ortholog(s) have role in sphingoid catabolic process and endoplasmic reticulum localization | 2.42048034648307 |
| | CAGL0C03289g | YBT1 | Putative ABC transporter involved in bile acid transport; gene is upregulated in azole-resistant strain | 2.4839376620687 |
| | CAGL0G08316g | ARV1 | Lipid transporter involved in sterol trafficking and transport of glycosylphosphatidylinositol and sphingolipid precursors | 2.48873097235758 |
| | CAGL0M10307g | AUR1 | Ortholog(s) have inositol phosphoceramide synthase activity and role in cellular response to drug, inositolphosphoceramide metabolic process, sphingolipid biosynthetic process | 2.53415287897849 |
| | CAGL0E02321g | PLB3 | Putative phospholipase B; predicted GPI-anchor | 2.74593069629897 |
| | CAGL0M08552g | PMP3 | Ortholog(s) have phosphatidic acid binding, phosphatidylinositol-3,5-bisphosphate binding, phosphatidylinositol-3-phosphate binding, sphingolipid binding activity | 2.89209487015534 |
| | CAGL0M07700g | SEC59 | Ortholog(s) have dolichol kinase activity, role in dolichyl monophosphate biosynthetic process and endoplasmic reticulum membrane localization | 2.99113567794769 |
| | CAGL0A01243g | GIT1 | Has domain(s) with predicted transmembrane transporter activity, role in transmembrane transport and integral component of membrane localization | 3.07713324835091 |
| | CAGL0G05313g | IPT1 | Ortholog(s) have transferase activity, transferring phosphorus-containing groups activity | 3.13429457965559 |

| | | | | |
|---|---|---|---|---|
| | CAGL0G08195g | UPS2 | Ortholog(s) have role in cardiolipin metabolic process, cell-abiotic substrate adhesion, cristae formation, negative regulation of phosphatidylcholine biosynthetic process, phosphatidylethanolamine metabolic process, phospholipid transport | 3.25334107754382 |
| | CAGL0H04543g | SCS22 | Ortholog(s) have role in endoplasmic reticulum membrane organization, phospholipid biosynthetic process, regulation of phosphatidylinositol dephosphorylation and cytosol localization | 3.27264711587291 |
| | CAGL0L09383g | SUT2 | Ortholog(s) have sequence-specific DNA binding activity | 3.31857738176565 |
| | CAGL0F03399g | SCS7 | Ortholog(s) have fatty acid alpha-hydroxylase activity, role in mannosyl-inositol phosphorylceramide metabolic process and endoplasmic reticulum, membrane localization | 3.35629749251716 |
| | CAGL0L02167g | FOX2 | Ortholog(s) have 3-hydroxyacyl-CoA dehydrogenase activity, 3-hydroxybutyryl-CoA epimerase activity, enoyl-CoA hydratase activity | 3.36281683748434 |
| | CAGL0M07315g | SUR1 | Ortholog(s) have mannosyltransferase activity, role in glycosphingolipid biosynthetic process, mannosyl-inositol phosphorylceramide metabolic process, pathogenesis and fungal-type vacuole membrane localization | 3.44798366938066 |
| | CAGL0M05995g | PET10 | Ortholog(s) have lipid particle localization | 3.49670606387067 |
| | CAGL0H09460g | FAA2 | Ortholog(s) have long-chain fatty acid-CoA ligase activity, medium-chain fatty acid-CoA ligase activity, very long-chain fatty acid-CoA ligase activity and role in long-chain fatty acid metabolic process | 3.55378406029287 |
| | CAGL0J04004g | MCP1 | Ortholog(s) have role in lipid homeostasis, mitochondrion organization and integral component of mitochondrial membrane, mitochondrial outer membrane localization | 3.59970873804449 |
| | CAGL0L04686g | CLD1 | Ortholog(s) have phospholipase A2 activity, role in cardiolipin acyl-chain remodeling and Golgi apparatus, endoplasmic reticulum, mitochondrial inner membrane localization | 3.6254364356395 |
| | CAGL0L10142g | RSB1 | Putative sphingolipid flippase; gene is upregulated in azole-resistant strain | 3.76825811940204 |
| | CAGL0C04939g | YJR107W | Has domain(s) with predicted triglyceride lipase activity and role in lipid metabolic process | 3.84274562317944 |
| | CAGL0E05654g | PGC1 | Ortholog(s) have phosphatidylglycerol phospholipase C activity, role in cell-abiotic substrate adhesion, phosphatidylglycerol catabolic process and lipid particle, mitochondrion localization | 4.52965931280271 |
| | CAGL0H07271g | IPK1 | Ortholog(s) have inositol pentakisphosphate 2-kinase activity, role in inositol phosphate biosynthetic process, nuclear-transcribed mRNA catabolic process, non-stop decay and nucleus localization | 4.62627398792635 |

**Table A2- Gene ID, *S. cerevisiae* orthologous, description and wild-type biofilm vs *Δtec1* biofilm (log2FoldChange) for each differentially expressed gene in the most relevant functional groups.** Full table is provided in supplementary material (CD).

| | Gene ID | Sc orthologous | Description | log2FoldChange |
|---|---|---|---|---|
| Lipid metabolism | CAGL0A01870g | | Has domain(s) with predicted integral component of membrane localization | -3.88091301462576 |
| | CAGL0H08778g | PUF2 | Ortholog(s) have mRNA binding activity, role in nuclear-transcribed mRNA catabolic process, deadenylation-dependent decay and cytoplasm localization | -2.44615314403765 |
| | CAGL0J04004g | MCP1 | Ortholog(s) have role in lipid homeostasis, mitochondrion organization and integral component of mitochondrial membrane, mitochondrial outer membrane localization | -1.89986939579236 |
| | CAGL0H01375g | SUR2 | Predicted sphinganine hydroxylase with role in sphingolipid biosynthesis; mutants show reduced sensitivity to caspofungin and increased sensitivity to micafungin | -1.75308205145561 |
| | CAGL0J11770g | PLB1 | Putative phospholipase B; predicted GPI-anchor | -1.74036585587461 |
| | CAGL0A00341g | MPO1 | Ortholog(s) have role in sphingoid catabolic process and endoplasmic reticulum localization | -1.67386118804836 |
| | CAGL0K08030g | NVJ2 | Ortholog(s) have lipid binding activity and endoplasmic reticulum, nucleus-vacuole junction, plasma membrane, ribosome localization | -1.63823922558717 |
| | CAGL0C05269g | INP54 | Ortholog(s) have phosphatidylinositol-4,5-bisphosphate 5-phosphatase activity, role in phosphatidylinositol dephosphorylation and endoplasmic reticulum, fungal-type vacuole membrane localization | -1.52938178123045 |
| | CAGL0M09713g | YIM1 | Putative protein involved in DNA damage response; gene is upregulated in azole-resistant strain | -1.47774476394915 |
| | CAGL0K07458g | YPK1 | Ortholog(s) have protein serine/threonine kinase activity | -1.36720022175466 |
| | CAGL0F03113g | SNX41 | Ortholog(s) have phosphatidylinositol-3-phosphate binding activity, role in retrograde transport, endosome to Golgi and cytosol, endosome localization | -1.2163867012699 |
| | CAGL0G05313g | IPT1 | Ortholog(s) have transferase activity, transferring phosphorus-containing groups activity | -1.20475968449519 |
| | CAGL0I09328g | TSC10 | Ortholog(s) have 3-dehydrosphinganine reductase activity, role in 3-keto-sphinganine metabolic process, sphingolipid biosynthetic process and endoplasmic reticulum, lipid particle, mitochondrial outer membrane localization | -1.12636063070738 |
| | CAGL0A04103g | UPS1 | Ortholog(s) have phosphatidic acid transporter activity and role in cardiolipin metabolic process, phospholipid translocation, positive regulation of phosphatidylcholine biosynthetic process | -1.100231559034 |
| | CAGL0K07293g | FAA4 | Ortholog(s) have long-chain fatty acid-CoA ligase activity and role in long-chain fatty acid import, long-chain fatty-acyl-CoA metabolic process, sphingoid long-chain base transport | -1.04068854324073 |
| | CAGL0J06952g | IDI1 | Ortholog(s) have isopentenyl-diphosphate delta-isomerase activity, role in farnesyl diphosphate biosynthetic process and cytosol, nucleus localization | 1.03903858140228 |
| | CAGL0D04290g | YKL091C | Ortholog(s) have phosphatidylcholine binding, phosphatidylinositol binding activity and nucleus localization | 1.04651137950607 |
| | CAGL0I04334g | LCB3 | Ortholog(s) have sphingosine-1-phosphate phosphatase activity, role in calcium-mediated signaling and endoplasmic reticulum localization | 1.06990755158683 |

| | | | | |
|---|---|---|---|---|
| | CAGL0M06237g | EHT1 | Ortholog(s) have alcohol O-butanoyltransferase activity, serine hydrolase activity, short-chain carboxylesterase activity and role in medium-chain fatty acid biosynthetic process, medium-chain fatty acid catabolic process | 1.0808538550145 |
| | CAGL0I00330g | SCS3 | Ortholog(s) have role in phospholipid biosynthetic process and endoplasmic reticulum localization | 1.08556437888662 |
| | CAGL0I09746g | SLY41 | Ortholog(s) have phosphoenolpyruvate transmembrane transporter activity, role in ER to Golgi vesicle-mediated transport, phosphoenolpyruvate transmembrane import into Golgi lumen and Golgi apparatus, endoplasmic reticulum localization | 1.09254809538777 |
| | CAGL0F07535g | YJU3 | Ortholog(s) have acylglycerol lipase activity, serine hydrolase activity, role in triglyceride metabolic process and endoplasmic reticulum, lipid particle, mitochondrial outer membrane, plasma membrane localization | 1.10480195143474 |
| | CAGL0I00462g | HRI1 | Ortholog(s) have role in cotranslational protein targeting to membrane and cytosol, endoplasmic reticulum membrane localization | 1.12026965245375 |
| | CAGL0B01947g | INO2 | Transcriptional regulator involved in de novo inositol biosynthesis; activator of INO1 gene expression; mutants unable to grow in the absence of inositol | 1.17626591465989 |
| | CAGL0G08085g | DNF2 | Ortholog(s) have phospholipid-translocating ATPase activity | 1.29334662458254 |
| | CAGL0C02717g | SPO7 | Ortholog(s) have phosphoprotein phosphatase activity and role in negative regulation of phospholipid biosynthetic process, nuclear envelope organization, positive regulation of phosphatidate phosphatase activity, protein dephosphorylation | 1.33164381511703 |
| | CAGL0M04367g | CKI1 | Ortholog(s) have choline kinase activity, ethanolamine kinase activity, role in phosphatidylcholine biosynthetic process, phosphatidylethanolamine biosynthetic process and cytosol, nucleus localization | 1.38034873985515 |
| | CAGL0K04103g | CAX4 | Ortholog(s) have dolichyldiphosphatase activity, role in lipid biosynthetic process, protein N-linked glycosylation and integral component of endoplasmic reticulum membrane localization | 1.39994600548092 |
| | CAGL0I00418g | OLE1 | Ortholog(s) have electron carrier activity, stearoyl-CoA 9-desaturase activity | 1.41239265640741 |
| | CAGL0I06050g | INO1 | Putative inositol 1-phosphate synthase; regulated by the transcriptional activators Ino2p and Ino4p; protein differentially expressed in azole resistant strain | 1.49527197951874 |
| | CAGL0E01309g | EKI1 | Ortholog(s) have choline kinase activity, ethanolamine kinase activity, role in phosphatidylcholine biosynthetic process, phosphatidylethanolamine biosynthetic process and cytoplasm localization | 1.50037733456484 |
| | CAGL0L00847g | CBR1 | Ortholog(s) have cytochrome-b5 reductase activity, acting on NAD(P)H activity and endoplasmic reticulum, mitochondrial outer membrane, nucleus, plasma membrane localization | 1.53794065012536 |
| | CAGL0K02959g | NEM1 | Ortholog(s) have phosphoprotein phosphatase activity and role in negative regulation of phospholipid biosynthetic process, nuclear envelope organization, positive regulation of phosphatidate phosphatase activity, protein dephosphorylation | 1.62596274815806 |
| | CAGL0H07513g | IFA38 | Predicted ketoreductase involved in production of very long chain fatty acid for sphingolipid biosynthesis; mutants show reduced sensitivity to caspofungin and increased sensitivity to micafungin | 1.81485554834466 |
| | CAGL0L04642g | ALE1 | Ortholog(s) have 1-acylglycerol-3-phosphate O-acyltransferase activity, 1-acylglycerophosphocholine O-acyltransferase activity, role in glycerophospholipid biosynthetic process and endoplasmic reticulum, ribosome localization | 1.82752052652897 |
| | CAGL0J02970g | CEM1 | Ortholog(s) have mitochondrion localization | 1.85551622605975 |
| | CAGL0H09878g | | Inorganic pyrophosphatase, cytoplasmic | 1.92341385536309 |
| | CAGL0L08184g | ELO2 | Predicted fatty acid elongase with role in sphingolipid biosynthetic process; mutants show reduced sensitivity to caspofungin and increased sensitivity to micafungin | 1.98779625357107 |
| | CAGL0H03399g | HNM1 | Ortholog(s) have (R)-carnitine transmembrane transporter activity, choline transmembrane transporter activity, ethanolamine transmembrane transporter activity | 2.44970030301462 |
| | CAGL0D00528g | FAS1 | Ortholog(s) have 3-hydroxyacyl-[acyl-carrier-protein] dehydratase activity, [acyl-carrier-protein] S-acetyltransferase activity and [acyl-carrier-protein] S-malonyltransferase activity, more | 2.63652789314031 |

| | | | | |
|---|---|---|---|---|
| | CAGL0E06138g | | Ortholog(s) have fatty acid synthase activity, role in palmitic acid biosynthetic process, response to pH and fatty acid synthase complex, glyoxysome localization | 2.6868833625579 |
| | CAGL0I05940g | SFH5 | Ortholog(s) have phosphatidylinositol transporter activity | 2.94323266571164 |
| | CAGL0I04070g | SLC1 | Ortholog(s) have 1-acylglycerol-3-phosphate O-acyltransferase activity, role in glycerophospholipid biosynthetic process and endoplasmic reticulum, lipid particle, plasma membrane localization | 3.00073831928014 |
| | CAGL0H08712g | | Has domain(s) with predicted phosphatidylinositol binding activity and role in cell communication | 3.66985249965408 |
| | CAGL0L10780g | HFA1 | Ortholog(s) have acetyl-CoA carboxylase activity, role in fatty acid biosynthetic process and cytosol, fungal-type vacuole membrane, mitochondrion localization | 3.76906082568599 |
| **Ergosterol biosynthesis** | CAGL0M10571g | ARE2 | Ortholog(s) have ergosterol O-acyltransferase activity, role in ergosterol metabolic process and endoplasmic reticulum localization | -2.60663182064951 |
| | CAGL0F01419g | AUS1 | ATP-binding cassette transporter involved in sterol uptake | -2.3393541054118 |
| | CAGL0J02684g | ERG28 | Ortholog(s) have protein binding, bridging activity, role in ergosterol biosynthetic process and endoplasmic reticulum membrane localization | -1.31670788879883 |
| | CAGL0L03828g | CYB5 | Ortholog(s) have electron carrier activity, role in ergosterol biosynthetic process and endoplasmic reticulum membrane localization | -1.07531271060378 |
| | CAGL0L10714g | ERG2 | C-8 sterol isomerase | 1.31011806705941 |
| | CAGL0F03993g | ERG8 | Ortholog(s) have phosphomevalonate kinase activity | 1.33568136741782 |
| | CAGL0L12364g | ERG10 | Ortholog(s) have acetyl-CoA C-acetyltransferase activity, role in ergosterol biosynthetic process and cytosol, nucleus localization | 1.97093105005441 |
| **Response to drugs** | CAGL0M04763g | YOR289W | Ortholog(s) have role in cellular response to drug and cytosol, nucleus localization | -2.3565797510508 |
| | CAGL0G05566g | FMP45 | Ortholog(s) have role in ascospore formation, cellular response to drug, fungal-type cell wall organization | -2.13837310415967 |
| | CAGL0F02717g | PDR15 | Multidrug transporter, predicted plasma membrane ATP-binding cassette (ABC) transporter; regulated by Pdr1p; involved in fluconazole resistance | -2.07054320251719 |
| | CAGL0M08552g | PMP3 | Ortholog(s) have phosphatidic acid binding, phosphatidylinositol-3,5-bisphosphate binding, phosphatidylinositol-3-phosphate binding, sphingolipid binding activity | -1.62202886134619 |
| | CAGL0G01122g | YLR346C | Putative protein; gene is upregulated in azole-resistant strain | -1.43906480940674 |
| | CAGL0E03674g | | Putative drug:H+ antiporter, involved in efflux of clotrimazole; required for resistance to clotrimazole and other drugs | -1.29736540476397 |
| | CAGL0F03069g | CAD1 | bZIP domain-containing protein | -1.24666448543314 |
| | CAGL0M10307g | AUR1 | Ortholog(s) have inositol phosphoceramide synthase activity and role in cellular response to drug, inositolphosphoceramide metabolic process, sphingolipid biosynthetic process | -1.20003281154036 |
| | CAGL0I10384g | TPO2 | Predicted polyamine transporter of the major facilitator superfamily; required for azole resistance | -1.17908308657211 |
| | CAGL0G08624g | QDR1 | Drug:H+ antiporter of the Major Facilitator Superfamily, confers imidazole drug resistance, involved in quinidine/multidrug efflux; gene is activated by Pdr1p; upregulated in azole-resistant strain | -1.15485871518729 |
| | CAGL0I08503g | MET16 | Ortholog(s) have phosphoadenylyl-sulfate reductase (thioredoxin) activity and role in cellular response to drug, sulfate assimilation, phosphoadenylyl sulfate reduction by phosphoadenylyl-sulfate reductase (thioredoxin) | -1.09903950178777 |
| | CAGL0B02079g | AZR1 | Ortholog(s) have azole transporter activity, role in asperfuranone biosynthetic process, azole transport and plasma membrane localization | -1.05766730560832 |

| | | | | |
|---|---|---|---|---|
| | CAGL0L04466g | SEY1 | Ortholog(s) have GTPase activity and role in cellular response to drug, endoplasmic reticulum inheritance, endoplasmic reticulum membrane fusion, hexose transport, pathogenesis | -1.04759909061909 |
| | CAGL0M01738g | SPT7 | Ortholog(s) have structural molecule activity, role in cellular response to drug, conjugation with cellular fusion, histone acetylation, protein complex assembly and SAGA complex, SLIK (SAGA-like) complex, mitochondrion localization | 1.07981805114753 |
| | CAGL0B02343g | ATR1 | Putative multidrug efflux pump of major facilitator superfamily; gene is downregulated in azole-resistant strain | 1.16107209562374 |
| | CAGL0J09944g | AQR1 | Plasma membrane drug:H+ antiporter involved in resistance to drugs and acetic acid | 1.35059902981903 |
| | CAGL0L00869g | PKP1 | Ortholog(s) have pyruvate dehydrogenase (acetyl-transferring) kinase activity, role in carbon utilization, cellular response to drug, peptidyl-serine phosphorylation and mitochondrion localization | 1.71624380620693 |
| | CAGL0C05555g | GUD1 | Ortholog(s) have guanine deaminase activity, role in cellular response to drug and cytosol localization | 1.78498661748683 |
| **Response to stress** | CAGL0G05269g | FMP16 | Putative mitochondrial protein; gene is downregulated in azole-resistant strain | -2.86252551572596 |
| | CAGL0G03289g | SSA4 | Heat shock protein of the HSP70 family | -2.42527058598609 |
| | CAGL0C04741g | SOD1 | Cytosolic copper-zinc superoxide dismutase | -2.37027164196275 |
| | CAGL0J08613g | YVC1 | Ortholog(s) have calcium activated cation channel activity, calcium channel activity, potassium channel activity, sodium channel activity, voltage-gated ion channel activity | -2.26292293318458 |
| | CAGL0K12958g | | Putative stress-induced alcohol dehydrogenase; gene is upregulated in azole-resistant strain | -2.02495576305155 |
| | CAGL0J06820g | RNY1 | Ortholog(s) have endoribonuclease activity, role in RNA catabolic process, apoptotic process, cell morphogenesis and cytosol, extracellular region, fungal-type vacuole localization | -1.93947147757128 |
| | CAGL0F07953g | SPG1 | Ortholog(s) have endoplasmic reticulum, mitochondrion localization | -1.88589620810547 |
| | CAGL0E05984g | GRE1 | Ortholog of *S. cerevisiae* : GRE1 and Saccharomyces cerevisiae S288C : YPL223C | -1.88393227059029 |
| | CAGL0L02431g | | Has domain(s) with predicted role in cell redox homeostasis | -1.87676632120402 |
| | CAGL0K10868g | | Putative catalase A; gene is downregulated in azole-resistant strain; regulated by oxidative stress and glucose starvation; protein abundance increased in ace2 mutant cells | -1.78141159201152 |
| | CAGL0H06611g | ESL1 | Ortholog of *S. cerevisiae* : ESL1, C. albicans SC5314 : C4_01020C_A, C. dubliniensis CD36 : Cd36_41030, C. parapsilosis CDC317 : CPAR2_401340 and Candida tenuis NRRL Y-1498 : CANTEDRAFT_104645 | -1.71832180038471 |
| | CAGL0G02101g | ECM4 | Putative omega class glutathione transferase; gene is downregulated in azole-resistant strain | -1.62581374762683 |
| | CAGL0F05709g | ATC1 | Ortholog(s) have role in bipolar cellular bud site selection, cellular cation homeostasis and cytoplasm, nucleus localization | -1.57029709466553 |
| | CAGL0H03971g | YCP4 | Ortholog(s) have role in cellular response to oxidative stress, pathogenesis and membrane raft, mitochondrion, plasma membrane localization | -1.54976963945856 |
| | CAGL0D00660g | YDL073W | Ortholog(s) have MAP-kinase scaffold activity and role in negative regulation of MAP kinase activity, osmosensory signaling pathway via Sho1 osmosensor | -1.53745197353433 |
| | CAGL0G08151g | GRX3 | Ortholog(s) have 2 iron, 2 sulfur cluster binding, RNA polymerase II activating transcription factor binding, glutathione disulfide oxidoreductase activity | -1.5256951353135 |
| | CAGL0J04202g | HSP12 | Heat shock protein; gene is upregulated in azole-resistant strain; expression upregulated in biofilm vs planktonic cell culture | -1.49683229124089 |
| | CAGL0H04037g | GAC1 | Ortholog(s) have heat shock protein binding, protein phosphatase regulator activity and role in glycogen metabolic process, meiotic nuclear division, mitotic spindle assembly checkpoint, response to heat | -1.46441647552877 |
| | CAGL0F03003g | HKR1 | Ortholog(s) have osmosensor activity and role in (1->3)-beta-D-glucan biosynthetic process, cellular bud site selection, fungal-type cell wall organization, hyperosmotic response, osmosensory signaling pathway via Sho1 osmosensor | -1.45826808448714 |

| | | | | |
|---|---|---|---|---|
| | CAGL0D06600g | KNS1 | Ortholog(s) have protein serine/threonine kinase activity, protein tyrosine kinase activity and role in negative regulation of transcription from RNA polymerase III promoter, peptidyl-serine phosphorylation, protein autophosphorylation | -1.3715423921649 |
| | CAGL0I07183g | SFL1 | Ortholog(s) have RNA polymerase II core promoter proximal region sequence-specific DNA binding, RNA polymerase II repressing transcription factor binding and RNA polymerase II transcription factor activity, more | -1.36675159534605 |
| | CAGL0M10439g | NTH1 | Ortholog(s) have alpha,alpha-trehalase activity, calcium ion binding activity, role in ascospore formation, cellular response to desiccation, trehalose catabolic process involved in cellular response to stress and cytosol localization | -1.35745282316783 |
| | CAGL0F08217g | YGR250C | Ortholog(s) have mRNA binding activity and cytoplasmic stress granule localization | -1.3277130652816 |
| | CAGL0M04675g | RDL1 | Ortholog(s) have thiosulfate sulfurtransferase activity and endoplasmic reticulum, mitochondrial outer membrane localization | -1.29254212990473 |
| | CAGL0M13651g | PRC1 | Ortholog(s) have serine-type carboxypeptidase activity, role in phytochelatin biosynthetic process and endoplasmic reticulum, extracellular region, fungal-type vacuole localization | -1.26785852242602 |
| | CAGL0L09339g | HAA1 | Putative transcription factor, involved in regulation of response to acetic acid stress | -1.26418948968026 |
| | CAGL0F06545g | RIM9 | Ortholog(s) have role in ascospore formation, cellular response to alkaline pH, cellular response to lithium ion, cellular response to neutral pH and cellular response to starvation, more | -1.26003255816952 |
| | CAGL0E00803g | HSP42 | Putative small cytosolic stress-induced chaperone; gene is upregulated in azole-resistant strain | -1.20999224353021 |
| | CAGL0F07513g | MBR1 | Ortholog(s) have role in aerobic respiration | -1.1906261449888 |
| | CAGL0L05258g | SRX1 | Ortholog(s) have sulfiredoxin activity, role in cellular protein localization, cellular response to oxidative stress and cytosol, nucleus localization | -1.1139309342028 |
| | CAGL0K06259g | TSA2 | Thiol-specific antioxidant protein; predicted thioredoxin peroxidase involved in oxidative stress response; protein abundance decreased in ace2 mutant cells | -1.11295228321097 |
| | CAGL0L10890g | YTM1 | Ortholog(s) have role in cellular response to biotic stimulus, cellular response to starvation and chromosome organization, more | -1.11212606700758 |
| | CAGL0F09075g | SCH9 | Ortholog(s) have protein serine/threonine kinase activity | -1.05380615755593 |
| | CAGL0K09900g | HAP5 | Ortholog(s) have DNA binding, RNA polymerase II core promoter proximal region sequence-specific DNA binding, transcription factor activity, sequence-specific DNA binding activity | -1.04030140369281 |
| | CAGL0L11110g | CMP2 | Catalytic subunit of calcineurin, calcium/calmodulin-dependent Ser/Thr-specific protein phosphatase; regulates stress-responding transcription factor Crz1p; involved in thermotolerance, response to ER stress, cell wall integrity, virulence | -1.00490746352909 |
| | CAGL0I04048g | | Ortholog(s) have fructose 1,6-bisphosphate 1-phosphatase activity, role in carbon utilization, cellular response to glucose starvation, glycerol catabolic process and cytosol, nucleus localization | -1.00273688734617 |
| | CAGL0L06666g | YHB1 | Putative flavohemoglobin, involved in nitric oxide detoxification | -1.00029493140007 |
| | CAGL0G00946g | | Has domain(s) with predicted thiol oxidase activity and role in oxidation-reduction process | 1.08533681359678 |
| | CAGL0F09097g | SKN7 | Predicted transcription factor, involved in oxidative stress response; required for induction of TRX2, TRR1 and TSA1 transcription under oxidative stress | 1.09453823780125 |
| | CAGL0B03509g | RCK2 | Ortholog(s) have protein serine/threonine kinase activity | 1.10694212209907 |
| | CAGL0L10538g | PAN5 | Ortholog(s) have cytosol, nucleus localization | 1.11148781501821 |
| | CAGL0E04114g | AFG1 | Ortholog(s) have role in cellular response to oxidative stress, misfolded or incompletely synthesized protein catabolic process, protein import into peroxisome matrix and mitochondrial inner membrane localization | 1.11571238378917 |
| | CAGL0K08492g | YPF1 | Ortholog(s) have aspartic endopeptidase activity, intramembrane cleaving activity and role in cellular response to starvation, proteolysis involved in cellular protein catabolic process | 1.14949847461296 |

| | | | | |
|---|---|---|---|---|
| | CAGL0C02321g | PHM8 | Ortholog(s) have lysophosphatidic acid phosphatase activity, nucleotidase activity and role in cellular response to phosphate starvation, nucleotide catabolic process, response to carbon starvation, triglyceride homeostasis | 1.18187737489927 |
| | CAGL0M11704g | AHP1 | Putative thiol-specific peroxiredoxin; alkyl hydroperoxide reductase; protein differentially expressed in azole resistant strain; expression upregulated in biofilm vs planktonic cell culture; protein abundance decreased in ace2 mutant cells | 1.23931434133212 |
| | CAGL0A03784g | TIM18 | Ortholog(s) have protein channel activity and role in apoptotic process, cellular response to oxidative stress, protein import into mitochondrial inner membrane, response to arsenic-containing substance, response to osmotic stress | 1.24891173105336 |
| | CAGL0L11990g | GRX4 | Ortholog(s) have RNA polymerase II activating transcription factor binding, disulfide oxidoreductase activity | 1.25751405713217 |
| | CAGL0L00495g | HSC82 | Putative heat shock protein | 1.26076762114484 |
| | CAGL0I08855g | TRS65 | Ortholog(s) have Rab guanyl-nucleotide exchange factor activity, role in intra-Golgi vesicle-mediated transport, protein complex assembly and TRAPPII protein complex, trans-Golgi network localization | 1.26896227056989 |
| | CAGL0H01199g | GCN2 | Ortholog(s) have eukaryotic translation initiation factor 2alpha kinase activity, tRNA binding activity | 1.32880773328243 |
| | CAGL0L07304g | GET3 | Ortholog(s) have ATPase activity, guanyl-nucleotide exchange factor activity, unfolded protein binding activity | 1.4911596213114 |
| | CAGL0A02530g | TRR1 | Thioredoxin reductase | 1.53449280723124 |
| | CAGL0G01925g | YKR070W | Ortholog(s) have role in hyperosmotic response, response to antibiotic, response to salt stress and mitochondrion localization | 1.56582880376081 |
| | CAGL0L03157g | DAL80 | Ortholog(s) have RNA polymerase II transcription factor activity, sequence-specific DNA binding, sequence-specific DNA binding activity | 1.64546001845417 |
| | CAGL0K01265g | PRP38 | Ortholog(s) have role in cellular response to biotic stimulus, cellular response to starvation and filamentous growth of a population of unicellular organisms in response to biotic stimulus, more | 1.71664880013701 |
| | CAGL0H06523g | PAN6 | Ortholog(s) have pantoate-beta-alanine ligase activity, role in pantothenate biosynthetic process and cytosol, nucleus localization | 2.01284928501794 |
| | CAGL0K05137g | ATH1 | Ortholog(s) have alpha,alpha-trehalase activity and role in cellular response to desiccation, cellular response to ethanol, cellular response to freezing, pathogenesis, trehalose catabolic process | 2.07316422295874 |
| | CAGL0F03553g | DAP1 | Putative heme-binding protein involved in regulation of cytochrome P450, Erg11p; required for growth under iron starvation | 2.11811147019201 |
| | CAGL0G03795g | SSA2 | Heat shock protein of the HSP70 family | 2.14502062700479 |
| | CAGL0L01551g | SUR7 | Ortholog(s) have role in ascospore formation, cellular response to biotic stimulus, cellular response to chemical stimulus, cellular response to glucose starvation and cellular response to neutral pH, more | 2.19937081935591 |
| | CAGL0M07293g | PDR12 | Putative ABC transporter of weak organic acids; gene is downregulated in azole-resistant strain | 2.87444296073841 |
| **Cell wall organization** | CAGL0G05984g | SPS100 | Ortholog(s) have role in ascospore wall assembly | -2.4284908690557 |
| | CAGL0I07249g | BAG7 | Putative GTPase-activating protein involved in cell wall and cytoskeleton homeostasis; gene is upregulated in azole-resistant strain | -2.13772974350001 |
| | CAGL0F00891g | LDS2 | Ortholog(s) have role in ascospore wall assembly and ascospore wall, ascus lipid particle, cytoplasm, prospore membrane localization | -2.11910445373268 |
| | CAGL0C03872g | TIR3 | Putative GPI-linked cell wall protein involved in sterol uptake | -2.10649440452375 |
| | CAGL0F03883g | GAS3 | Putative glycoside hydrolase of the Gas/Phr family; predicted GPI-anchor | -2.08118221694821 |

| | | | | |
|---|---|---|---|---|
| | CAGL0K05247g | CSR2 | Ortholog(s) have ubiquitin protein ligase binding activity, role in fungal-type cell wall organization, regulation of transcription from RNA polymerase II promoter and cytosol, nucleus localization | -2.04699414866645 |
| | CAGL0H10120g | YBR056W | Ortholog(s) have glucan endo-1,6-beta-glucosidase activity and role in fungal-type cell wall beta-glucan metabolic process, fungal-type cell wall disassembly involved in conjugation with cellular fusion | -1.80834653196511 |
| | CAGL0F00869g | RRT8 | Ortholog(s) have role in ascospore wall assembly and ascospore wall, lipid particle, prospore membrane localization | -1.72145130156897 |
| | CAGL0B02882g | | Beta mannosyltransferase; transmembrane domain protein similar to C. albicans WRY family; gene is downregulated in azole-resistant strain | -1.66649015744415 |
| | CAGL0H09614g | TIR1 | Putative GPI-linked cell wall protein | -1.6470678295455 |
| | CAGL0I10516g | YGR130C | Ortholog(s) have role in fungal-type cell wall organization, pathogenesis and cytoplasm, eisosome, integral component of plasma membrane, membrane raft localization | -1.56652690608562 |
| | CAGL0J06050g | YGP1 | Ortholog(s) have role in cell wall assembly and extracellular region localization | -1.54393046391714 |
| | CAGL0H09592g | | Putative GPI-linked cell wall protein | -1.51461410946931 |
| | CAGL0K12980g | | Beta mannosyltransferase | -1.48360421690155 |
| | CAGL0F07579g | CWP1 | Putative GPI-linked cell wall protein | -1.3701435791406 |
| | CAGL0B02948g | | Beta mannosyltransferase | -1.34826061077687 |
| | CAGL0E02255g | ZEO1 | Ortholog(s) have role in fungal-type cell wall organization and extrinsic component of plasma membrane, mitochondrial outer membrane localization | -1.33579451568817 |
| | CAGL0F01859g | OSW2 | Ortholog(s) have role in ascospore wall assembly and cytoplasm, prospore membrane localization | -1.29664186486439 |
| | CAGL0D00286g | | Beta mannosyltransferase | -1.27989693282127 |
| | CAGL0J11462g | YNL190W | Ortholog(s) have GTPase regulator activity, role in Ras protein signal transduction, fungal-type cell wall biogenesis, positive regulation of transcription from RNA polymerase II promoter and nucleus localization | -1.1755019753622 |
| | CAGL0G08602g | RPI1 | Ortholog(s) have GTPase regulator activity, role in Ras protein signal transduction, fungal-type cell wall biogenesis, positive regulation of transcription from RNA polymerase II promoter and nucleus localization | -1.1304704139168 |
| | CAGL0G06072g | ECM14 | Ortholog(s) have endoplasmic reticulum, fungal-type vacuole localization | -1.11591600988049 |
| | CAGL0D01276g | OPY2 | Ortholog(s) have role in establishment of protein localization to plasma membrane, fungal-type cell wall biogenesis, mitotic cell cycle G1 arrest in response to pheromone and osmosensory signaling pathway, more | -1.07425259201139 |
| | CAGL0K12408g | BST1 | Ortholog(s) have phosphatidylinositol deacylase activity | 1.0039656579656 |
| | CAGL0G00220g | BGL2 | Ortholog(s) have 1,3-beta-glucanosyltransferase activity, glucan endo-1,3-beta-D-glucosidase activity | 1.09216049864001 |
| | CAGL0B03905g | GPI14 | Ortholog(s) have mannosyltransferase activity, role in GPI anchor biosynthetic process, fungal-type cell wall organization, hyphal growth and glycosylphosphatidylinositol-mannosyltransferase I complex localization | 1.0960042527466 |
| | CAGL0F01463g | TIR2 | Putative GPI-linked cell wall mannoprotein of the Srp1p/Tip1p family | 1.12221284302969 |
| | CAGL0F01287g | GAS5 | Putative transglycosidase with a predicted role in the elongation of 1,3-beta-glucan | 1.16050128625682 |
| | CAGL0E05412g | KRE5 | Ortholog(s) have UDP-glucose:glycoprotein glucosyltransferase activity | 1.18019570129626 |
| | CAGL0C05577g | ADY3 | Ortholog(s) have role in ascospore wall assembly, ascospore-type prospore membrane assembly, mitochondrion inheritance and prospore membrane leading edge, spindle pole body localization | 1.19392200334493 |
| | CAGL0L12232g | GAA1 | Ortholog(s) have role in attachment of GPI anchor to protein and GPI-anchor transamidase complex localization | 1.35448191452692 |

| | | | | |
|---|---|---|---|---|
| | CAGL0L07370g | QRI1 | Ortholog(s) have UDP-N-acetylglucosamine diphosphorylase activity, role in UDP-N-acetylglucosamine biosynthetic process and cytosol, nucleus localization | 1.36154860762885 |
| | CAGL0C02101g | KEG1 | Ortholog(s) have role in (1->6)-beta-D-glucan biosynthetic process, chromosome organization and integral component of endoplasmic reticulum membrane localization | 1.41190160633075 |
| | CAGL0A04411g | SKT5 | Ortholog(s) have enzyme activator activity and role in barrier septum assembly, cellular protein localization, fungal-type cell wall chitin biosynthetic process, regulation of fungal-type cell wall beta-glucan biosynthetic process | 1.41822665286383 |
| | CAGL0I04818g | CHS2 | Ortholog(s) have chitin synthase activity | 1.4595598037469 |
| | CAGL0F07601g | CWP2 | GPI-linked cell wall protein | 1.49964111377883 |
| | CAGL0C02211g | | Putative glycoside hydrolase of the Crh family; predicted GPI-anchor | 1.60637947827916 |
| | CAGL0M08756g | EXG2 | Putative exo-1,3-beta-glucanase; predicted GPI-anchor | 1.64564157621726 |
| | CAGL0D01034g | PSA1 | GDP-mannose pyrophosphorylase involved in the synthesis of GDP-mannose for protein glycosylation | 2.16918641553043 |
| | CAGL0M08514g | PIR3 | Pir protein family member, putative cell wall component | 2.28044147585019 |
| | CAGL0L05434g | NCA3 | Ortholog(s) have role in fungal-type cell wall organization or biogenesis, mitochondrion organization and fungal-type cell wall, fungal-type vacuole localization | 2.56519947015104 |
| | CAGL0G08668g | SIM1 | Ortholog(s) have role in fungal-type cell wall organization and endoplasmic reticulum, fungal-type cell wall localization | 3.35462360703946 |
| | CAGL0I06160g | CIS3 | Pir protein family member, putative cell wall component | 3.46161409831653 |
| **Adhesion and biofilm formation** | CAGL0K13002g | | Putative adhesin; predicted GPI-anchor; belongs to adhesin cluster III | -2.57134078544503 |
| | CAGL0I10340g | | Cell wall adhesin; predicted GPI anchor; contains tandem repeats; belongs to adhesin cluster II | -2.4444537915958 |
| | CAGL0H10626g | | Predicted cell wall adhesin with a role in adhesion; belongs to adhesin cluster III; predicted GPI anchor; contains tandem repeats | -2.32995390294082 |
| | CAGL0L00583g | USV1 | Ortholog(s) have sequence-specific DNA binding, transcription factor activity, sequence-specific DNA binding activity | -2.29318880554299 |
| | CAGL0L02453g | MIT1 | Ortholog(s) have sequence-specific DNA binding, transcription factor activity, sequence-specific DNA binding activity | -2.04678290411291 |
| | CAGL0K07007g | YBR238C | Ortholog(s) have mRNA binding activity and role in aerobic respiration, filamentous growth of a population of unicellular organisms in response to neutral pH, single-species biofilm formation on inanimate substrate | -1.80763597643238 |
| | CAGL0M04807g | SNF2 | Component of the chromatin remodelling Swi/Snf complex; involved in regulation of biofilm formation | -1.73848420535382 |
| | CAGL0J09922g | SUN4 | Ortholog(s) have glucan endo-1,3-beta-D-glucosidase activity | -1.65420943709638 |
| | CAGL0K03003g | MOT3 | Ortholog(s) have RNA polymerase II activating transcription factor binding and RNA polymerase II core promoter proximal region sequence-specific DNA binding, more | -1.6027834745932 |
| | CAGL0J02530g | | Putative adhesion protein; predicted GPI-anchor; belongs to adhesin cluster VI | -1.59168581282626 |
| | CAGL0L01771g | PHD1 | Ortholog(s) have sequence-specific DNA binding, transcription factor activity, sequence-specific DNA binding activity | -1.51763089124678 |
| | CAGL0G04125g | | Protein with similarity to *S. cerevisiae* Sag1 agglutinin, involved in cell adhesion; predicted GPI-anchor | -1.48221733406149 |
| | CAGL0A01366g | | Putative adhesin; belongs to adhesin cluster I | -1.44963273561852 |
| | CAGL0M07634g | SOK2 | Ortholog(s) have sequence-specific DNA binding, transcription factor activity, sequence-specific DNA binding activity | -1.44233119307216 |
| | CAGL0A01284g | | Putative adhesin-like protein; belongs to adhesin cluster I | -1.41956628914455 |

| | | | | |
|---|---|---|---|---|
| | CAGL0K10164g | SED1 | Predicted GPI-linked protein; putative adhesin-like protein | -1.40415612643359 |
| | CAGL0K13024g | | Adhesin-like protein required for adherence to endothelial cells; identified in cell wall extracts by mass spectrometry; belongs to adhesin cluster III; predicted GPI anchor; 6 tandem repeats; expressed more in stationary growth phase | -1.38137124457619 |
| | CAGL0E05566g | TYE7 | Ortholog(s) have sequence-specific DNA binding, transcription factor activity, sequence-specific DNA binding activity | -1.30159812112794 |
| | CAGL0H08844g | DDR48 | Putative adhesin-like protein | -1.10912618657301 |
| | CAGL0K00110g | | Putative adhesin; identified in cell wall extracts by mass spectrometry; belongs to adhesin cluster V; predicted GPI-anchor | 1.20652472796853 |
| | CAGL0E06666g | | Epithelial adhesion protein; predicted GPI-anchor; belongs to adhesin cluster I | 1.29023503519476 |
| | CAGL0G09537g | IES4 | Putative adhesin-like protein | 1.51937315305889 |
| | CAGL0M08448g | MCD4 | Ortholog(s) have mannose-ethanolamine phosphotransferase activity and role in ATP transport, GPI anchor biosynthetic process, conidium formation, regulation of growth rate | 1.58416869192494 |
| | CAGL0M09086g | BUD4 | Ortholog(s) have GTP binding, cell adhesion molecule binding activity | 1.62491137006138 |
| | CAGL0F08833g | MSB2 | Putative adhesin-like protein | 1.64420919976671 |
| | CAGL0M05599g | TOS1 | Ortholog(s) have cell surface, endoplasmic reticulum, extracellular region, fungal-type vacuole, hyphal cell wall localization | 1.87514214795963 |
| | CAGL0I00484g | EXG1 | Ortholog(s) have cell adhesion molecule binding, glucan endo-1,6-beta-glucosidase activity, glucan exo-1,3-beta-glucosidase activity | 2.53390309171756 |
| | CAGL0E06644g | | Sub-telomerically encoded adhesin with a role in cell adhesion; GPI-anchored cell wall protein; N-terminal ligand binding domain binds to ligands containing a terminal galactose residue; belongs to adhesin cluster I | 2.5784581997599 |
| | CAGL0M03773g | TOS6 | Predicted GPI-linked adhesin-like protein | 2.9283532093881 |
| | CAGL0K09130g | SRL1 | Putative adhesin-like protein | 3.05425320841327 |
| **Carbon and energy metabolism** | CAGL0A01826g | HXT3 | Ortholog(s) have glucose transmembrane transporter activity and plasma membrane localization | -4.232052320438 |
| | CAGL0K10428g | IGD1 | Ortholog(s) have enzyme inhibitor activity, role in negative regulation of glycogen catabolic process and cytoplasm localization | -3.71261565298922 |
| | CAGL0K12078g | NRG1 | Ortholog(s) have RNA polymerase II core promoter proximal region sequence-specific DNA binding, RNA polymerase II repressing transcription factor binding and transcriptional repressor activity, more | -3.11039130707329 |
| | CAGL0H06633g | | Putative phosphoenolpyruvate carboxykinase; gene is downregulated in azole-resistant strain | -2.05778891511583 |
| | CAGL0M08800g | YAP6 | bZIP domain-containing protein | -2.03062615849952 |
| | CAGL0K03421g | PGM2 | Ortholog(s) have phosphoglucomutase activity | -1.6794662408765 |
| | CAGL0L03377g | SIP4 | Ortholog(s) have RNA polymerase II core promoter proximal region sequence-specific DNA binding, transcriptional activator activity, RNA polymerase II core promoter proximal region sequence-specific binding activity | -1.64120667493773 |
| | CAGL0E05148g | AMS1 | Ortholog(s) have alpha-mannosidase activity, role in oligosaccharide catabolic process and cytosol, fungal-type vacuole membrane localization | -1.61219043573685 |
| | CAGL0F04851g | NCA2 | Ortholog(s) have role in aerobic respiration, mRNA metabolic process and mitochondrial outer membrane localization | -1.57898277163458 |
| | CAGL0M13343g | GND1 | 6-phosphogluconate dehydrogenase | -1.57698015974231 |
| | CAGL0M09020g | SFC1 | Ortholog(s) have succinate:fumarate antiporter activity, role in acetate catabolic process, carbon utilization, fatty acid catabolic process, fumarate transport, succinate transport and mitochondrion, plasma membrane localization | -1.55254700114783 |

| | | | | |
|---|---|---|---|---|
| | CAGL0A02321g | HXT5 | Ortholog(s) have fructose transmembrane transporter activity, glucose transmembrane transporter activity, mannose transmembrane transporter activity and role in fructose import across plasma membrane, glucose import across plasma membrane | -1.5506559242774 |
| | CAGL0M12551g | RGI2 | Ortholog(s) have role in energy reserve metabolic process and cytoplasm localization | -1.49113781692603 |
| | CAGL0E05610g | PYK2 | Ortholog(s) have pyruvate kinase activity, role in canonical glycolysis, pyruvate biosynthetic process and cytosol, mitochondrion localization | -1.4449638204429 |
| | CAGL0B04917g | IDP2 | S-adenosylmethionine synthetase | -1.44242698613362 |
| | CAGL0J02904g | GIP2 | Ortholog(s) have protein phosphatase regulator activity, role in glycogen metabolic process, protein dephosphorylation and protein phosphatase type 1 complex localization | -1.44221003324356 |
| | CAGL0M03025g | CAT8 | Ortholog(s) have RNA polymerase II core promoter proximal region sequence-specific DNA binding, transcriptional activator activity, RNA polymerase II core promoter proximal region sequence-specific binding activity | -1.30241462277849 |
| | CAGL0D01100g | | Has domain(s) with predicted 6-phosphofructo-2-kinase activity, ATP binding, catalytic activity and role in fructose 2,6-bisphosphate metabolic process, fructose metabolic process | -1.29170991172458 |
| | CAGL0E04884g | ADR1 | Ortholog(s) have RNA polymerase II activating transcription factor binding, RNA polymerase II core promoter proximal region sequence-specific DNA binding and TFIIB-class transcription factor binding, more | -1.26263626385715 |
| | CAGL0H03993g | CIT1 | Ortholog(s) have citrate (Si)-synthase activity, role in acetyl-CoA catabolic process, tricarboxylic acid cycle and glyoxysome, mitochondrion localization | -1.25106899775399 |
| | CAGL0C05027g | YAT1 | Ortholog(s) have role in acetate catabolic process, alcohol metabolic process, carnitine metabolic process, cellular respiration and cytosol, mitochondrion localization | -1.23963539248718 |
| | CAGL0A01628g | MIG1 | Transcriptional regulatory protein | -1.2004704562178 |
| | CAGL0L09086g | CIT3 | Ortholog(s) have 2-methylcitrate synthase activity, citrate (Si)-synthase activity, role in propionate catabolic process, 2-methylcitrate cycle, tricarboxylic acid cycle and mitochondrion localization | -1.19847900018678 |
| | CAGL0C05137g | GPD2 | Putative glycerol 3-phosphate dehydrogenase; protein differentially expressed in azole resistant strain | -1.19355840202909 |
| | CAGL0L03982g | MLS1 | Ortholog(s) have malate synthase activity, role in acetate catabolic process, carbon utilization, fatty acid catabolic process, glyoxylate cycle and cytosol, glyoxysome, peroxisomal matrix localization | -1.17025513337122 |
| | CAGL0J07612g | ZWF1 | Glucose-6-phosphate 1-dehydrogenase | -1.16464735429344 |
| | CAGL0J09020g | SNF3 | Putative plasma membrane high affinity glucose sensor, required for growth under glucose-limiting conditions | -1.14814751650483 |
| | CAGL0D06424g | ACO1 | Putative aconitate hydratase | -1.11318008616815 |
| | CAGL0K03289g | YMR099C | Aldose 1-epimerase | -1.09548850322841 |
| | CAGL0K12254g | VID24 | Ortholog(s) have role in negative regulation of gluconeogenesis, proteasome-mediated ubiquitin-dependent protein catabolic process, protein catabolic process in the vacuole, protein targeting to vacuole | -1.0668888645204 |
| | CAGL0K08624g | HAP4 | Ortholog(s) have RNA polymerase II activating transcription factor binding, transcriptional activator activity, RNA polymerase II core promoter proximal region sequence-specific binding activity | -1.02648316387289 |
| | CAGL0K10296g | IAH1 | Ortholog(s) have hydrolase activity, acting on ester bonds activity | 1.02466866814021 |
| | CAGL0L09108g | PDH1 | Ortholog(s) have role in propionate metabolic process and mitochondrial outer membrane localization | 1.0255908833549 |
| | CAGL0M13013g | OAR1 | Ortholog(s) have 3-oxoacyl-[acyl-carrier-protein] reductase (NADPH) activity, role in aerobic respiration, fatty acid metabolic process and mitochondrion localization | 1.06808652780803 |

| | | | | |
|---|---|---|---|---|
| | CAGL0L07480g | NRG2 | Ortholog(s) have double-stranded DNA binding, sequence-specific DNA binding, transcription factor activity, sequence-specific DNA binding activity | 1.11806091394874 |
| | CAGL0K08756g | YAP5 | bZIP domain-containing protein | 1.14776118921033 |
| | CAGL0B04059g | TES1 | Ortholog(s) have acyl-CoA hydrolase activity, role in fatty acid beta-oxidation and glyoxysome, mitochondrion localization | 1.1651747128677 |
| | CAGL0F06897g | YIR035C | Putative protein with alcohol dehydrogenase domain; gene is downregulated in azole-resistant strain | 1.16540657076476 |
| | CAGL0A01804g | HXT1 | Ortholog(s) have fructose transmembrane transporter activity, pentose transmembrane transporter activity, role in glucose transport, mannose transport and plasma membrane localization | 1.22052995938921 |
| | CAGL0J01441g | ADH3 | Ortholog(s) have alcohol dehydrogenase (NAD) activity | 1.25564397456201 |
| | CAGL0B02717g | | Ortholog(s) have role in acetate catabolic process, carbon utilization and cytosol, extracellular region, nucleus localization | 1.31382814719432 |
| | CAGL0K06787g | PYC2 | Ortholog(s) have pyruvate carboxylase activity, role in carbon utilization, cellular response to glucose starvation, gluconeogenesis, response to heat and cytosol localization | 1.43183332104089 |
| | CAGL0H06699g | GUT2 | Ortholog(s) have glycerol-3-phosphate dehydrogenase activity, role in NADH oxidation, glycerol metabolic process, replicative cell aging and integral component of mitochondrial outer membrane, plasma membrane localization | 1.49238955147697 |
| | CAGL0K09372g | MIG2 | Ortholog(s) have RNA polymerase II core promoter proximal region sequence-specific DNA binding, transcriptional repressor activity, RNA polymerase II core promoter proximal region sequence-specific binding activity | 1.57939295228499 |
| | CAGL0L02079g | CTP1 | Ortholog(s) have tricarboxylate secondary active transmembrane transporter activity, role in mitochondrial citrate transport, transmembrane transport and mitochondrion, plasma membrane localization | 1.60769661985165 |
| | CAGL0J07084g | YPL113C | Ortholog(s) have oxidoreductase activity, acting on the CH-OH group of donors, NAD or NADP as acceptor activity | 1.80041022369914 |
| | CAGL0E01529g | PFK27 | Ortholog(s) have role in fructose 2,6-bisphosphate metabolic process, regulation of glycolytic process | 1.96593226959918 |
| | CAGL0M00682g | YLR446W | Has domain(s) with predicted ATP binding, glucose binding, hexokinase activity, phosphotransferase activity, alcohol group as acceptor activity | 2.03265265239099 |
| | CAGL0H06853g | | Putative NADP-dependent alcohol dehydrogenase VI; protein abundance increased in ace2 mutant cells | 2.04020308802061 |
| | CAGL0J08272g | GOR1 | Ortholog(s) have glyoxylate reductase activity, role in glyoxylate catabolic process and cytosol, extracellular region, mitochondrion, nucleus localization | 2.05345742335879 |
| | CAGL0E05280g | | Putative methylglyoxal reductase (NADPH-dependent) | 2.19519426325537 |
| | CAGL0I07117g | THI80 | Ortholog(s) have thiamine diphosphokinase activity, role in thiamine diphosphate biosynthetic process and cytoplasm localization | 2.61571962340388 |
| | CAGL0A01782g | HXT4 | Ortholog(s) have glucose transmembrane transporter activity, pentose transmembrane transporter activity and plasma membrane localization | 2.96018916343664 |
| **Nitrogen metabolism** | CAGL0M03465g | ATO2 | Ortholog(s) have ammonium transmembrane transporter activity and role in ammonium transport, nitrogen utilization, plasma membrane acetate transport | -2.90347880573075 |
| | CAGL0C04191g | UGA2 | Ortholog(s) have succinate-semialdehyde dehydrogenase [NAD(P)+] activity and role in cellular response to oxidative stress, gamma-aminobutyric acid catabolic process, glutamate decarboxylation to succinate | -2.02719534405534 |
| | CAGL0H02585g | GAD1 | Ortholog(s) have glutamate decarboxylase activity, role in cellular response to oxidative stress, glutamate catabolic process and cytoplasm localization | -1.50087322150751 |
| | CAGL0I08613g | | Putative plasma membrane polyamine transporter | -1.45150569006885 |
| | CAGL0A03212g | ATO3 | Ortholog(s) have ammonium transmembrane transporter activity, role in ammonium transport, nitrogen utilization, transmembrane transport and mitochondrion, plasma membrane localization | -1.17970132768684 |

| | | | | |
|---|---|---|---|---|
| | CAGL0G05698g | GDH2 | Ortholog(s) have glutamate dehydrogenase (NAD+) activity, role in nitrogen compound metabolic process and cytosol, mitochondrion localization | -1.05051188026314 |
| | CAGL0G04389g | GZF3 | Ortholog(s) have RNA polymerase II transcription factor activity, sequence-specific DNA binding, sequence-specific DNA binding activity | 1.12334659327785 |
| | CAGL0J06028g | MEP2 | Ortholog(s) have high-affinity secondary active ammonium transmembrane transporter activity, methylammonium transmembrane transporter activity | 1.61956632733007 |
| | CAGL0K03157g | DUR3 | Putative plasma membrane polyamine transporter | 2.40446361386073 |
| | CAGL0M05533g | | Ortholog(s) have role in nitrogen compound metabolic process | 2.77171967699491 |
| **Aminoacid metabolism** | CAGL0M00154g | MET14 | Plasma membrane high affinity cystine specific transporter; present only in pathogenic yeasts; confers the ability to utilize cystine as a sulfur source | -2.60447381729524 |
| | CAGL0L02321g | ALT1 | Ortholog(s) have adenylylsulfate kinase activity, role in sulfate assimilation, phosphoadenylyl sulfate reduction by phosphoadenylyl-sulfate reductase (thioredoxin), sulfur amino acid metabolic process and cytosol, nucleus localization | -2.39611257730056 |
| | CAGL0L12254g | TMT1 | Ortholog(s) have L-alanine:2-oxoglutarate aminotransferase activity, role in alanine biosynthetic process, alanine catabolic process, cellular response to drug, chronological cell aging and cytosol, mitochondrion, nucleus localization | -1.98742680219027 |
| | CAGL0L12012g | MET1 | Ortholog(s) have trans-aconitate 3-methyltransferase activity and cytosol localization | -1.86445107901382 |
| | CAGL0G01903g | MET28 | Ortholog(s) have uroporphyrin-III C-methyltransferase activity, role in cellular response to drug, methionine biosynthetic process, siroheme biosynthetic process and nucleus localization | -1.61769833739376 |
| | CAGL0K08668g | MET32 | bZIP domain-containing protein | -1.47156823413963 |
| | CAGL0B02651g | CIA2 | Ortholog(s) have RNA polymerase II activating transcription factor binding, RNA polymerase II transcription factor activity and sequence-specific transcription regulatory region DNA binding, more | -1.40200691165499 |
| | CAGL0L13046g | MET17 | Ortholog(s) have role in iron-sulfur cluster assembly and cytosol, nucleus localization | -1.33353770603314 |
| | CAGL0D06402g | PUT1 | O-acetyl homoserine sulfhydrylase (OAHSH), ortholog of *S. cerevisiae* MET17; required for utilization of inorganic sulfate as sulfur source; able to utilize cystine as a sulfur source while *S. cerevisiae* met15 mutants are unable to do so | -1.28537357460474 |
| | CAGL0M04499g | GLT1 | Ortholog(s) have proline dehydrogenase activity, role in proline catabolic process to glutamate and mitochondrion localization | -1.27967447734024 |
| | CAGL0L01089g | ARG82 | Ortholog(s) have glutamate synthase (NADH) activity, role in glutamate biosynthetic process and cytosol, mitochondrion localization | -1.276247926315 |
| | CAGL0E00759g | ATG22 | Ortholog(s) have inositol tetrakisphosphate 3-kinase activity, inositol tetrakisphosphate 6-kinase activity and inositol-1,3,4,5,6-pentakisphosphate kinase activity, more | -1.18229254326338 |
| | CAGL0B00770g | MET10 | Ortholog(s) have L-amino acid transmembrane transporter activity, role in L-alpha-amino acid transmembrane transport, amino acid transmembrane export from vacuole and integral component of fungal-type vacuolar membrane localization | -1.17442043547571 |
| | CAGL0D05280g | MET2 | Ortholog(s) have sulfite reductase (NADPH) activity, role in sulfate assimilation and cytosol, sulfite reductase complex (NADPH) localization | -1.0994575163465 |
| | CAGL0J08316g | GCN4 | Ortholog(s) have homoserine O-acetyltransferase activity, role in homoserine metabolic process, methionine biosynthetic process, regulation of DNA methylation and cytosol localization | -1.09047239594702 |
| | CAGL0L02475g | MUP1 | bZIP domain-containing protein | -1.06750116669523 |
| | CAGL0K04367g | ERS1 | Ortholog(s) have L-methionine secondary active transmembrane transporter activity, role in cysteine transport, methionine import and fungal-type vacuole, plasma membrane localization | -1.04951686320713 |
| | CAGL0M06985g | MMF1 | Ortholog(s) have L-cystine transmembrane transporter activity, role in L-cystine transport and endosome, fungal-type vacuole, plasma membrane localization | -1.04646729071837 |

| | | | | |
|---|---|---|---|---|
| | CAGL0M12386g | MDE1 | Ortholog(s) have role in isoleucine biosynthetic process, mitochondrial genome maintenance, mitochondrial translation and mitochondrial matrix localization | 1.00471038848141 |
| | CAGL0M07876g | TRP2 | Ortholog(s) have methylthioribulose 1-phosphate dehydratase activity, role in L-methionine salvage from methylthioadenosine and cytosol, nucleus localization | 1.01277565069223 |
| | CAGL0I05016g | CHA1 | Putative anthranilate synthase component I; protein abundance increased in ace2 mutant cells | 1.01583246171347 |
| | CAGL0B00286g | AVT3 | Ortholog(s) have L-serine ammonia-lyase activity, L-threonine ammonia-lyase activity, role in L-serine catabolic process, threonine catabolic process and mitochondrial nucleoid localization | 1.02749317463127 |
| | CAGL0E06468g | LYS2 | Ortholog(s) have L-arginine transmembrane transporter activity, L-glutamine transmembrane transporter activity and L-histidine transmembrane transporter activity, more | 1.03208774387992 |
| | CAGL0K07788g | YNL010W | Ortholog(s) have L-aminoadipate-semialdehyde dehydrogenase activity, role in lysine biosynthetic process via aminoadipic acid, negative regulation of lysine biosynthetic process via aminoadipic acid and cytosol localization | 1.04141125567219 |
| | CAGL0H03641g | LYS4 | Ortholog(s) have cytosol, nucleus localization | 1.04436251715346 |
| | CAGL0K10978g | LEU1 | Ortholog(s) have homoaconitate hydratase activity, role in lysine biosynthetic process via aminoadipic acid and mitochondrion localization | 1.05456856631133 |
| | CAGL0A00363g | THI3 | Ortholog(s) have 3-isopropylmalate dehydratase activity, role in leucine biosynthetic process and cytoplasmic stress granule, cytosol localization | 1.0630939115761 |
| | CAGL0L06842g | | Ortholog(s) have RNA polymerase II activating transcription factor binding activity and role in positive regulation of thiamine biosynthetic process, positive regulation of transcription from RNA polymerase II promoter | 1.09218352148726 |
| | CAGL0F00253g | LYS9 | Ortholog(s) have anthranilate synthase activity, indole-3-glycerol-phosphate lyase activity, phosphoribosylanthranilate isomerase activity, role in tryptophan biosynthetic process and cytosol localization | 1.09961004124095 |
| | CAGL0C03443g | YDR341C | Putative saccharopine dehydrogenase | 1.13295817374004 |
| | CAGL0A01760g | LYS12 | Ortholog(s) have arginine-tRNA ligase activity, role in arginyl-tRNA aminoacylation and mitochondrion localization | 1.15807898840074 |
| | CAGL0G02585g | AVT1 | Homo-isocitrate dehydrogenase | 1.17395646318957 |
| | CAGL0D03036g | | Ortholog(s) have L-glutamine transmembrane transporter activity, L-isoleucine transmembrane transporter activity, L-tyrosine transmembrane transporter activity | 1.17498170520533 |
| | CAGL0L00759g | MET7 | ATP phosphoribosyltransferase; protein abundance increased in ace2 mutant cells | 1.21492418647115 |
| | CAGL0J03762g | SER33 | Ortholog(s) have tetrahydrofolylpolyglutamate synthase activity, role in one-carbon metabolic process, regulation of DNA methylation and cytosol, endoplasmic reticulum, mitochondrion, nucleus localization | 1.22194628367429 |
| | CAGL0M12837g | GCV3 | Ortholog(s) have alpha-ketoglutarate reductase activity, phosphoglycerate dehydrogenase activity, role in serine family amino acid biosynthetic process and cytosol localization | 1.23312336580641 |
| | CAGL0M12188g | YML096W | Ortholog(s) have glycine dehydrogenase (decarboxylating) activity, role in glycine catabolic process, one-carbon metabolic process, protein lipoylation and mitochondrion localization | 1.27048715521375 |
| | CAGL0H06963g | HIS4 | Ortholog(s) have cytosol, nucleus localization | 1.28555339758936 |
| | CAGL0B00902g | BTN2 | Phosphoribosyl-AMP cyclohydrolase; phosphoribosyl-ATP pyrophosphatase; histidinol dehydrogenase | 1.30758651048495 |
| | CAGL0I10010g | TYR1 | Ortholog(s) have SNARE binding, chaperone binding activity and role in amino acid transport, intracellular protein transport, protein folding, protein localization to nucleus, regulation of pH, retrograde transport, endosome to Golgi | 1.35966735365373 |
| | CAGL0M06017g | | Ortholog(s) have prephenate dehydrogenase (NADP+) activity, role in tyrosine biosynthetic process and cytosol localization | 1.44393307615847 |
| | CAGL0K12232g | YER152C | Ortholog(s) have chorismate mutase activity, role in aromatic amino acid family biosynthetic process, sporocarp development involved in sexual reproduction and cytosol, nucleus localization | 1.44433115598287 |

| | | | | |
|---|---|---|---|---|
| | CAGL0I06578g | YHR112C | Ortholog(s) have 2-aminoadipate transaminase activity and cytoplasm, nucleus localization | 1.45876073146387 |
| | CAGL0I01276g | | Ortholog(s) have cytoplasm, nucleus localization | 1.47674234139642 |
| | CAGL0J04554g | | Has domain(s) with predicted catalytic activity, pyridoxal phosphate binding, transaminase activity and role in biosynthetic process, cellular amino acid metabolic process | 1.48185475498012 |
| | CAGL0K00825g | CPA2 | Has domain(s) with predicted phosphatase activity, phosphoserine phosphatase activity and role in L-serine biosynthetic process, metabolic process | 1.50827514503853 |
| | CAGL0C04917g | YHR033W | Ortholog(s) have carbamoyl-phosphate synthase (glutamine-hydrolyzing) activity, role in arginine biosynthetic process and carbamoyl-phosphate synthase complex, mitochondrion localization | 1.55237598117665 |
| | CAGL0D03894g | | Putative gamma-glutamyl phosphate reductase | 1.59886618433546 |
| | CAGL0H03795g | | 3-isopropylmalate dehydrogenase | 1.6290212027599 |
| | CAGL0G01254g | MET6 | Putative aromatic aminotransferase I | 1.69629476401586 |
| | CAGL0I04994g | YMR226C | 5-methyltetrahydropteroyltriglutamate homocysteine methyltransferase; protein abundance increased in ace2 mutant cells | 1.80207914112461 |
| | CAGL0M11242g | PDC6 | Ortholog(s) have carbonyl reductase (NADPH) activity, serine 3-dehydrogenase activity and cytosol, nucleus, ribosome localization | 1.80795537396487 |
| | CAGL0G02937g | LYS5 | Ortholog(s) have pyruvate decarboxylase activity and role in L-phenylalanine catabolic process, aromatic amino acid family catabolic process to alcohol via Ehrlich pathway, ethanol metabolic process, tryptophan catabolic process | 1.89366541168894 |
| | CAGL0E05104g | CAR1 | Ortholog(s) have enzyme activator activity, holo-[acyl-carrier-protein] synthase activity and role in peptidyl-serine phosphopantetheinylation, protein-cofactor linkage | 1.93104094436889 |
| | CAGL0J07062g | ARG1 | Ortholog(s) have arginase activity, manganese ion binding, ornithine carbamoyltransferase inhibitor activity, zinc ion binding activity | 2.00569785395304 |
| | CAGL0C05115g | BAT2 | Argininosuccinate synthetase | 2.07529356340749 |
| | CAGL0M00176g | HOM6 | Ortholog(s) have L-isoleucine transaminase activity, L-leucine transaminase activity, L-valine transaminase activity | 2.07756796676369 |
| | CAGL0M00330g | SHM2 | Ortholog(s) have homoserine dehydrogenase activity, role in homoserine biosynthetic process, methionine biosynthetic process, threonine biosynthetic process and cytoplasm, nucleus localization | 2.09972245429369 |
| | CAGL0F01749g | | Putative serine hydroxymethyltransferase; protein differentially expressed in azole resistant strain | 2.20419047481663 |

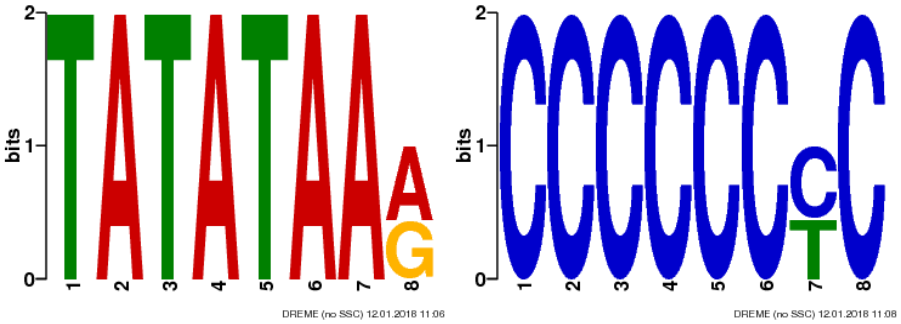


**Figure A3- Consensus sequences retrieved by DREME bioinformatic software, predicted do be recognized by Tec1 TF in the differentially expressed genes in *C. glabrata* planktonic cells.** The up-regulated genes were chosen and the upstream sequences were obtained in FASTA format in PathoYeastract database.

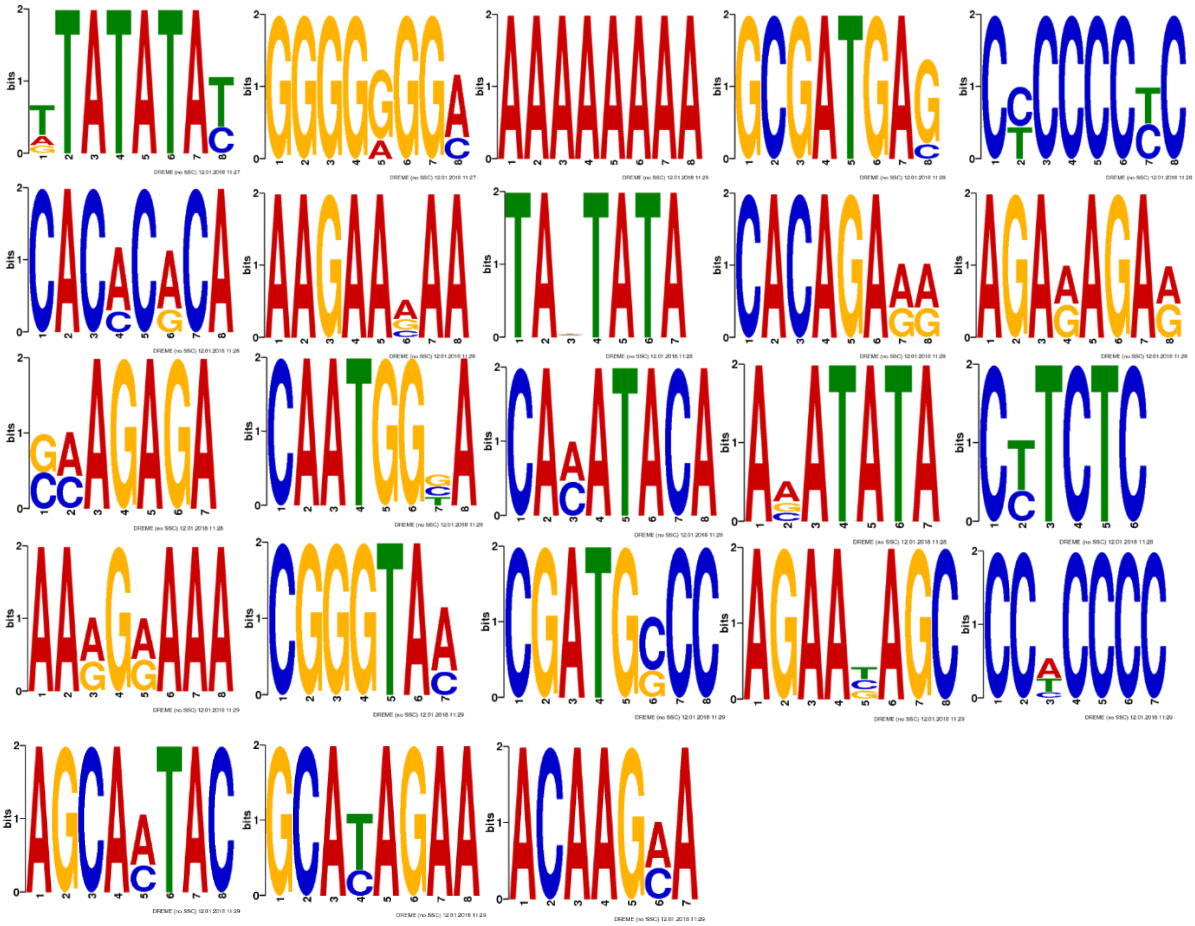

**Figure A4- Consensus sequences retrieved by DREME bioinformatic software, predicted do be recognized by Tec1 TF in the differentially expressed genes in C. glabrata biofilm cells.** The up-regulated genes were chosen and the upstream sequences were obtained in FASTA format in PathoYeastract database.

**Table A3- IUPAC frequency table.** Consensus sequences *of ScTEC1* binding sites were obtained in SGD (https://www.yeastgenome.org/) and were represented according to the following IUPAC frequency table.

| IUPAC frequency table | | | | |
|---|---|---|---|---|
| | A | C | G | T |
| A | 1 | 0 | 0 | 0 |
| C | 0 | 1 | 0 | 0 |
| G | 0 | 0 | 1 | 0 |
| T | 0 | 0 | 0 | 1 |
| W | 1/2 | 0 | 0 | 1/2 |
| S | 0 | 1/2 | 1/2 | 0 |
| R | 1/2 | 0 | 1/2 | 0 |
| Y | 0 | 1/2 | 0 | 1/2 |
| M | 1/2 | 1/2 | 0 | 0 |
| K | 0 | 0 | 1/2 | 1/2 |
| B | 0 | 1/3 | 1/3 | 1/3 |
| D | 1/3 | 0 | 1/3 | 1/3 |
| H | 1/3 | 1/3 | 0 | 1/3 |
| V | 1/3 | 1/3 | 1/3 | 0 |
| N | 1/4 | 1/4 | 1/4 | 1/4 |
| x | 1/4 | 1/4 | 1/4 | 1/4 |
| a | 1/2 | 1/6 | 1/6 | 1/6 |
| c | 1/6 | 1/2 | 1/6 | 1/6 |
| g | 1/6 | 1/6 | 1/2 | 1/6 |
| t | 1/6 | 1/6 | 1/6 | 1/2 |